UNIVERSITÀ
DEGLI STUDI
FIRENZE

PhD IN
CHEMICAL SCIENCES

CYCLE XXX

COORDINATOR Prof. PIERO BAGLIONI

DEVELOPMENT AND APPLICATION OF TARGETED AND UNTARGETED LC-MS/MS METHODS FOR METABOLOMICS STUDIES: FROM VEGETAL TO BIOLOGICAL MATRIXES.

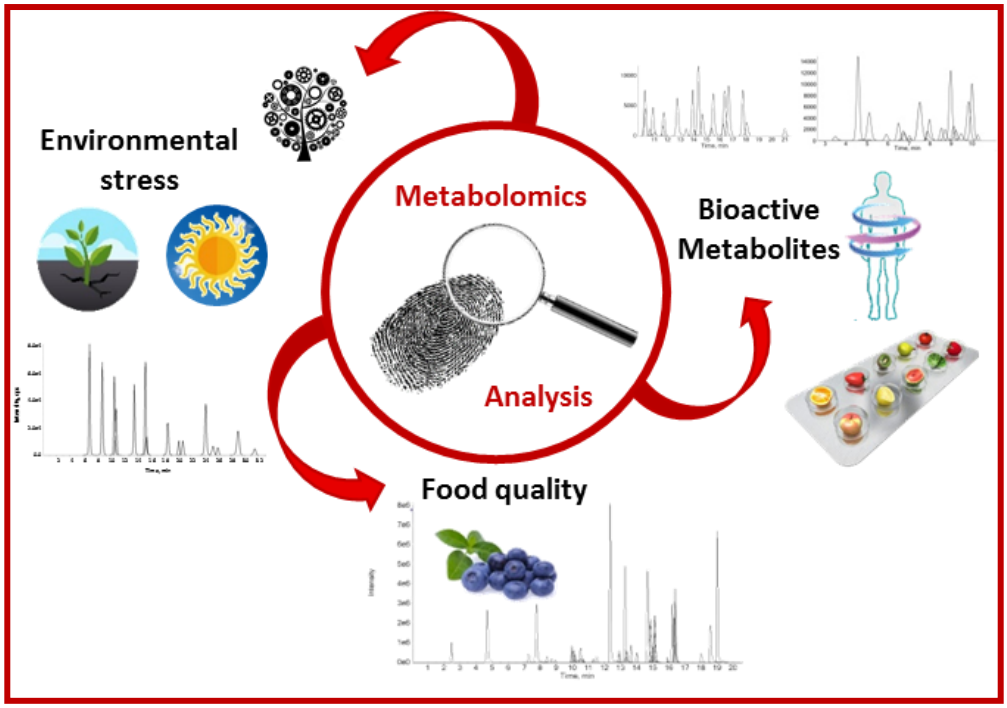

PhD Candidate
Dr. Claudia Ancillotti

Tutor
Dr. Massimo Del Bubba

UNIVERSITÀ
DEGLI STUDI
FIRENZE

PhD IN
CHEMICAL SCIENCES

CYCLE XXX

COORDINATOR Prof. PIERO BAGLIONI

DEVELOPMENT AND APPLICATION OF TARGETED AND UNTARGETED LC-MS/MS METHODS FOR METABOLOMICS STUDIES: FROM VEGETAL TO BIOLOGICAL MATRIXES

Academic discipline CHIM/01

PhD Candidate
Dr. Claudia Ancillotti

Tutor
Dr. Massimo Del Bubba

Coordinator
Prof. Piero Baglioni

Academic years 2014/2017

Index

Chapter 1. General Introduction 7

1.1 Polyphenols 8

1.2 Role of polyphenols in plants and fruits 12

1.2.1 Polyphenols as markers of plant exposure to stress 13

1.2.2 Polyphenols in food science 13

1.3 Functional polyphenol-based foods for human health 15

1.4 Metabolomics approaches for polyphenol investigation 17

1.5 Outline of the thesis 19

Chapter 2. Changes in polyphenol and sugar concentrations in wild type and genetically modified *Nicotiana langsdorffii* Weinmann in response to water and heat stress 27

Chapter 3. Polyphenolic profiles and antioxidant and antiradical activity of Italian berries from *Vaccinium myrtillus* L. and *Vaccinium uliginosum* L. subsp. *gaultherioides* (Bigelow) S.B. Young 85

Chapter 4. Liquid chromatographic/electrospray ionization quadrupole/time of flight tandem mass spectrometric study of polyphenolic composition of different *Vaccinium* berry species and their comparative evaluation 127

Chapter 5. Untargeted metabolomics study for the comparative evaluation of plasma and urinary phenolic metabolites after acute ingestion of *Vaccinium myrtillus* and *Vaccinium corymbosum* berries 195

Chapter 6. Conclusions 249

Chapter 1

General introduction

1.1 Polyphenols

Polyphenols represent the biggest group of phytochemicals generally occurring as glycosides at different concentrations in fruits and vegetables (1). The main classification of phenolic compounds is done according to the aglycone, namely as a function of the number of phenol rings and the structural elements that bind these rings (2).

Among the wide variety of chemical structures, the two main polyphenol classes are represented by phenolic acids and flavonoids (3). Phenolic acids can be further divided into benzoic and cinnamic acid derivatives based on C1-C6 and C3-C6 backbones, respectively (Figure 1).

Benzoic acids

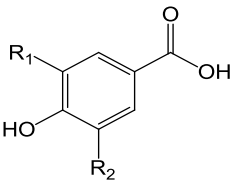

R_1= H, R_2=H **Hydroxybenzoic acid**
R_1= H, R_2=OH **Protocatechuic acid**
R_1= OH, R_2=OH **Gallic acid**
R_1= H, R_2=OCH_3 **Vanillic acid**
R_1= OCH_3, R_2=OCH_3 **Syringic acid**

Cinnamic acids

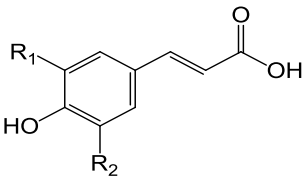

R_1= H, R_2=H **p-Coumaric acid**
R_1= H, R_2=OH **Caffeic acid**
R_1= H, R_2=OCH_3 **Ferulic acid**
R_1= OCH_3, R_2=OCH_3 **Sinapic acid**

Figure 1. Structure of benzoic and hydroxycinnamic acids.

Hydroxycinnamic acids are widely present in fruits, vegetables, coffee, wine and olive oil, mainly in esterified form with organic acids or sugars. For example, caffeic acid is widely present in plant-derived foods as chlorogenic acid (the ester of caffeic acid with quinic acid) (4).

Flavonoids share the general structure C6-C3-C6 (Figure 2) consisting of two aromatic rings (A and B) linked together by three carbon atoms that form an

oxygenated heterocycle (chromane ring C). On the basis of variations in this chromane ring, flavonoids can be further divided into different sub-groups: anthocyanidins, flavanols, flavones, flavanones, flavonols and chalcones (3).

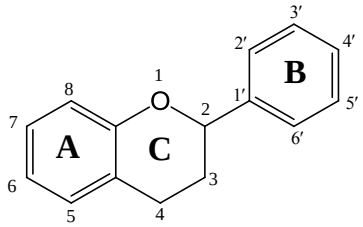

Figure 2. Flavonoid backbone.

Anthocyanins are natural pigments responsible for red, purple and blue colours of some flowers and fruits (e.g. mallow and small berries). They are constituted by anthocyanidins (aglycones) that can be linked to a wide variety of sugar moieties (e.g. glucoside, arabinoside, diglucoside) in different binding positions (5). The most common anthocyanidins are pelargonidin, cyanidin, peonidin, delphinidin, petunidin and malvidin (Figure 3). In solution anthocyanins can be found in different chemical forms depending on the pH and they are characterized by a positive charge at pH < 3 (6).

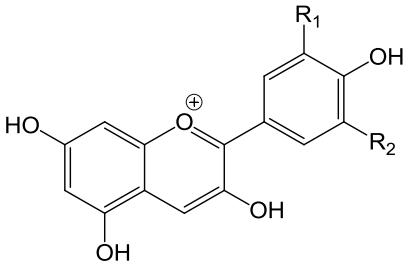

R_1= H, R_2=H **Pelargonidin**
R_1= H, R_2=OH **Cyanidin**
R_1= OH, R_2=OH **Delphinidin**
R_1= H, R_2=OCH_3 **Peonidin**
R_1= OH, R_2=OCH_3 **Petunidin**
R_1= OCH_3, R_2=OCH_3 **Malvidin**

Figure 3. Structure of the most common anthocyanidins.

Among the other flavonoids, flavanols are specifically characterized by the absence of double bond between C2 and C3, as well as C4 carbonyl in ring C (Figure 4). (+)-Catechin and (−)-epicatechin are the two monomeric flavanol frequently found in fruits (e.g. grapes, apple and blueberries) (7). Furthermore, monomeric flavanols and their gallate derivatives (e.g. gallocatechins reported in Figure 4) are also the major flavonoids in tea leaves (8).

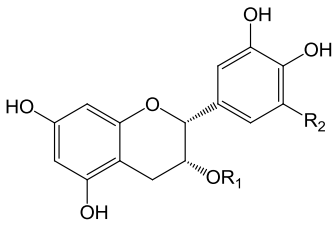

R_1= H, R_2=H **(-) Epicatechin**
R_1= gallyl, R_2=H **(-) Epicatechin gallate**
R_1= H, R_2=OH **(-) Epigallocatechin**
R_1= gallyl, R_2=OH **(-) Epigallocatechin gallate**

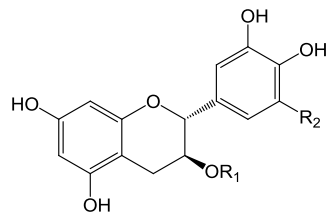

R_1= H, R_2=H **(+) Catechin**
R_1= gallyl, R_2=H **(+) Catechin gallate**
R_1= H, R_2=OH **(+) Gallocatechin**
R_1= gallyl, R_2=OH **(+) Gallocatechin gallate**

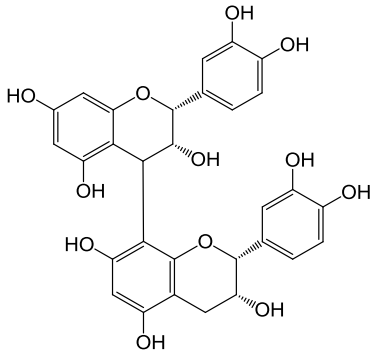

Procyanidin B2

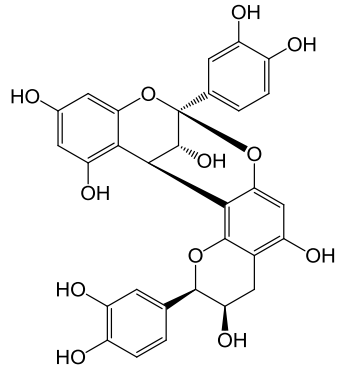

Procyanidin A2

Figure 4. Examples of flavanol structures: the monomers (+)-catechin and (-)-epicatechin, the gallocatechins derivatives and procyanidin B2 and A2.

Catechin and epicatechin can form oligomers and polymers generally called proanthocyanidins since the acid hydrolysis of the polymeric chains produces

anthocyanidins. Depending on the interflavanoid bond type, oligomeric proanthocyanidins can resulted in A-type structure, in which monomers are linked through C2–O–C7 (e.g. procyanidin A2, Figure 4) or C2–O–C5 bonding. Moreover, a B-type structure characterized by C4→C6 (e.g. procyanidin B2, in Figure 4) or C4→C8 linkages can also be present (9).

Flavones and their 3-hydroxy derivatives (i.e. flavonols) including their glycosides, methoxides and other acylated products on all three rings, represent one of the largest subgroup of polyphenols in food(3). In this regard, the dietary flavonoid intake has been estimated to be largely consisting of only three flavonols (i.e. quercetin, myricetin, and kaempferol) and two flavones (i.e. apigenin and luteolin) (10).

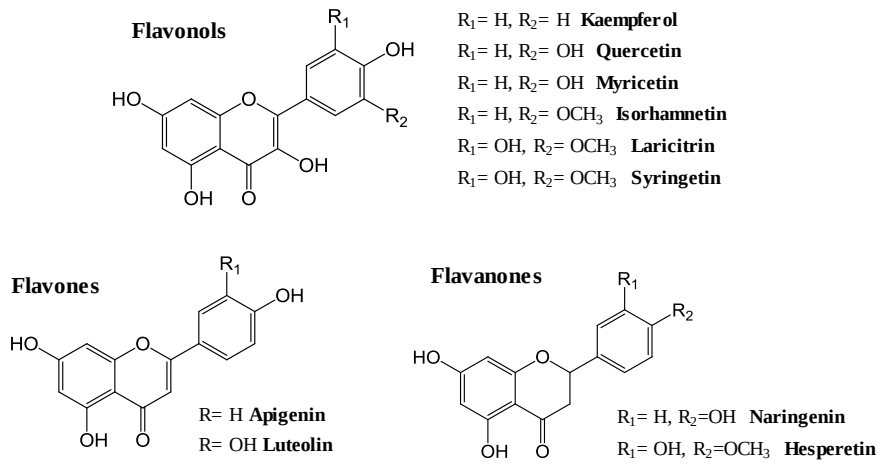

Figure 5. Structures of flavonols, flavones and flavanones widely present in vegetal foods.

Chalcones are open-chain flavonoids in which aromatic rings are linked by a three-carbon enone moiety (Figures 6). They are abundant in fruits (e.g., citruses and apples), vegetables (e.g., tomatoes, and potatoes) and various

plants, many of which have been used for centuries in traditional herbal medicine (11).

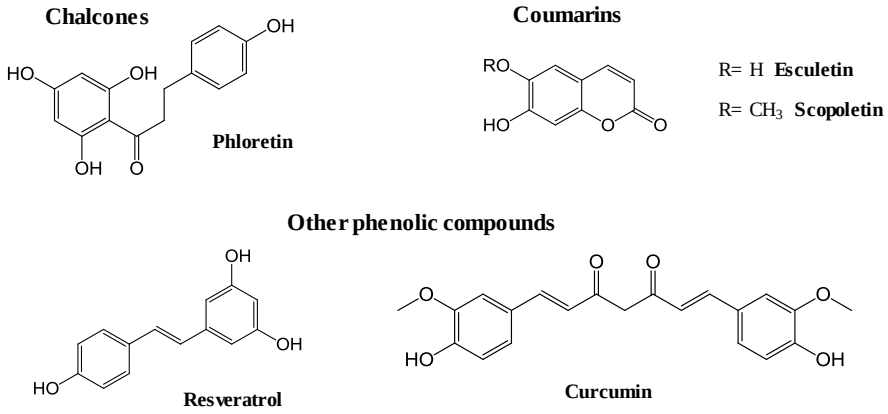

Figure 6. Typical structure of chalcones (phloretin), coumarins (esculetin and scopoletin) and other phenolic compounds (resveratrol and curcumin) found in plant-based foods.

Finally, phenolic compounds belonging to other classes, such as coumarins and stilbenes are considered bioactive compounds, widely determined in plant-based foods. For example, resveratrol and curcumin (Figure 6) were found in wine and turmeric, respectively (12, 13).

1.2 Role of polyphenols in plants and fruits

The study of polyphenols in vegetal matrixes (i.e. plant tissues and fruits) can represent a powerful tool in many field of application, such as environmental and food sciences. In fact, the polyphenol biosynthesis in plants depends on many factors, mainly associated to genetics and environmental factors, such as altitude and solar exposure, as well as the presence of biotic and abiotic stresses (14-17). Therefore, the relation between the polyphenolic profile of a plant, its genetics, as well as the characteristics of its growing environment, could be used for investigating different topics, some of which are taken into consideration in the present thesis and are following briefly introduced.

1.2.1 Polyphenols as markers of plant exposure to stress

The influence of environmental conditions on polyphenols biosynthesis could be applied in studies focused on the evaluation of possible impacts on plants of the environmental pollution and climate changes. In fact, polyphenols are plant secondary metabolites acting in the defence strategy towards different kinds of abiotic stress (18-20).

For example, phenolic compounds are involved in plant response related to heavy metal exposure due to both their redox and metal-chelating properties (21). Therefore, plant models have been frequently studied in order to demonstrate the role of polyphenols in plant response to abiotic stresses, such as metal exposure (22). In this regard, the plant model *Nicotiana langsdorfii*, wild type and modified for the insertion of *gr* and *rolC* genes, has been studied after the exposure to hexavalent chromium (19). An up-regulation of the investigated polyphenols was observed as a response of chromium exposure, and the genetically modified organism resulted more tolerant to the chromium presence in respect to the wild type ones. Interestingly, the higher resistance of genetically modified plants have been suggested to be related to the polyphenol up-regulation caused by gene insertion (19). This result confirmed the key-role of polyphenols in the monitoring of plant response to heavy metal exposure constituting an important type of abiotic stress.

Consequently, the metabolic shift of polyphenols could be useful also for the investigation of other abiotic stresses, such as water deficit and heat stresses. Indeed, the study of over/under expression of polyphenols could represent a tool for estimating plant resistance to climate changes, thus providing useful information in the field of agriculture.

1.2.2 Polyphenols in food science

The relation between polyphenol biosynthesis and plant genetics allows to consider the polyphenolic profile as the typical fingerprint of a vegetal system

and to discriminate among plant species characterized by a strong genetic similarity. This identification tool results particularly important in chemotaxonomic studies in which plant, characterized by a very similar phenotype, are identified based on differences in biochemical composition (23). In this regard, the study of polyphenolic profile as species fingerprint can be applied to the analysis of fruits and vegetables with different purposes. Indeed, metabolomics has been frequently applied to food science in order to assess food quality (24).

Furthermore, food science widely focused on the analysis of bioactive compounds because of the possibility of disease prevention through the assumption of specific foods, called "functional foods" (25). In this regard, polyphenols are considered bioactive compounds due to their healthy attributes, such as anti-inflammatory (26), antihypertensive (27), anti-microbial (28) and anti-cancer properties (29, 30).

Among fruits, small berries (e.g. strawberry, blueberry and raspberry) represent an abundant source of phenolic compounds in human diet (2). In detail, fruits belonging to *Vaccinium myrtillus* species are considered functional foods (31). Nevertheless, other *Vaccinium* species exhibited different polyphenolic profiles, as well as a diverse polyphenol content (32, 33). In this case, metabolomics analysis can be applied to food science in order to discriminate fruits belonging to different species using polyphenolic profile, also contributing to explain the nutraceutical properties of investigated berries.

This kind of approach can also be used for the comparison between the polyphenolic profile of a fruit and its transformed products (e.g. juices) in order to assess the preservation of bioactive compounds during the processing and storage. Moreover, some rich-polyphenol fruits were used for the preparation of supplement, due to their nutraceutical values. In these cases, the analysis of transformed products can confirm the declared concentration

of bioactive compounds and evidence if some fruits with a lower nutraceutical value has been added.

Finally, for some fruits (e.g. persimmon) also the post-harvest treatment can influence polyphenol biosynthesis and this aspect should be taken into account for estimating the fruit quality (34).

1.3 Functional polyphenol-based foods for human health

Polyphenols represent a class of bioactive compounds well-known for their strong antioxidant power due to their chemical structure. In fact, the highly conjugated system with multiple hydroxyl groups make these compounds good electron or hydrogen atom donors, neutralizing free radicals (35). Due to these features polyphenols seem to be able to limit the oxidative stress strictly related to an over-production of reactive oxygen species (ROS). It has been suggested that the oxidative stress is closely related to persistent inflammatory states which in turn are linked to many chronic disease, such as cardiovascular and neurodegenerative pathologies and cancer (36).

For these reasons, functional polyphenol-based foods are increasingly studied in order to characterize their composition and obtain important information on their role in protecting human health.

The clinical effect of polyphenols against a particular disease may be preliminarily evaluated by *in vitro* studies using commercial cell cultures.

Following this approach, extracts of small fruits have been tested in numerous studies involving various pathologies. In detail, *in vitro* studies have been conducted to evaluate the antiproliferative activity of small fruit extracts against various cellular cancer lines. For example, bilberry extracts showed antiproliferative activity and apoptosis induction in different colon cancer cell lines (37, 38). Similarly, polyphenols extracted from strawberry and raspberry fruits inhibited the growth of cell lines of the mouth, colon and prostate cancer (39, 40).

However, studies regarding the functional food *V. myrtillus* and prostate cancerous cells are absent in literature. In this regard, our research team performed preliminary *in vitro* studies of *V. myrtillus* extract on two cell lines of prostate cancer with different biological aggressiveness. The cancer cell lines, tested in the study together with the healthy prostate cells, are LNCaP and DU145, androgen-dependent and androgen-independent, respectively. The preliminary results are very promising because the *V. myrtillus* extract appears to inhibit the growth of cancer cells at different dilutions as a function of the aggressiveness degree. In addition, at the dilution level working against LNCaP cells, no toxicity has been evidenced for healthy prostate cells. Moreover, even if at dilution working for DU145 cells inhibition a toxicity was reported also for healthy prostate cells, these results are considered encouraging. In fact, also the synthesized substances as antitumor (chemotherapeutic) are usually more toxic for healthy cells than cancerous ones.

In addition to the aforementioned *in vitro* studies, also some clinical trials investigating the effectiveness of polyphenol-based functional foods in patients affected by different kind of cancer have shown interesting result (41). More in detail, as regards small berry supplements, the chemopreventive properties of an anthocyanin-rich *V. myrtillus* extract has been suggested in a pilot study with patients affected by colon cancer (42). All these evidences suggested the use of small berries, in particular *Vaccinium* ones, as functional foods in the prevention or treatment of specific diseases. In this regard, the first step necessary to understand the action mechanism of polyphenols as bioactive compounds is the identification of metabolites responsible of biological activity in human body. For this aim, literature studies were carried out by the investigation of polyphenols fate in biological fluids (e.g. serum and urine) after the administration of small berries to human or animals (43-48).

However, the absorption, distribution, metabolism and elimination (ADME) of the most abundant *Vaccinium* berry polyphenols, i.e. anthocyanins, have been scarcely understood (49) and this class of compounds was considered low bioavailable until recently. Nevertheless, recent studies suggested that other metabolites, not yet identified, could be responsible for the healthy properties evidenced by clinical trials (49, 50).

Due to this lack of information, the biofluids analysis of volunteers after the assumption of polyohenol-based functional food, such as *Vaccinium* berries, should be performed using a comprehensive metabolomics approach in order to discover new polyphenol metabolites.

1.4 Metabolomics approaches for polyphenol investigation

For all the purposes mentioned in the previous chapters, the analysis of polyphenols in a biological system (i.e. plant tissues, fruits or biofluids) is essential. A biological matrix is a very complex system, in which polyphenols are present with many other compound classes, such as sugars for plants and fruits and protein for serum samples. This aspect constituted an analytical challenge that can be overcome by the use of clean-up step (e.g. removing of protein and phospholipids in serum samples) and the choice of a very selective analytical methods that must be able to differentiate the selected class of analytes from other interfering compounds.

In the field of metabolomics, nuclear magnetic resonance (NMR) and mass spectrometry (MS) techniques are the most popular method (51). NMR spectroscopy is quantitative without the need of sample preparation (52) but the sensitivity is lower in respect to MS techniques (53).

On the other hand, mass spectrometry when coupled with liquid chromatography (LC) provides an excellent approach that can offer a sensitivity and specificity platform for metabolomics research (51). For this

reason, the LC-MS technique was chosen for the development of the methods used in the present work.

Two different LC-MS metabolomics approach can be applied to the polyphenols investigation of a biological system: targeted and untargeted approach. Targeted analysis focus the research on a set of selected metabolites of which commercial standards are often available. Standards compounds are used for parameter optimization and for the calibration curve because the aim of targeted approach is the quantification of specific metabolites in the investigated biological samples. The mass spectrometer used for this analysis is often a triple quadrupole with the multiple reaction monitoring (MRM) method that select for each compound the two most abundant mass fragments and used them for the quantification of analytes in real samples (54).

On the other hand, the untargeted metabolomics studies allow a more comprehensive evaluation of polyphenol profiles aiming to the simultaneous detection of many analytes. The resulting data set included thousands of metabolite signals, and among these, few are finally identified as candidate biomarkers (55). Thus, in the untargeted metabolomics approach, the LC-MS analysis is directly on the real samples and the data elaboration is the longest analysis step. For this approach, high resolution mass spectrometers are used and many software for data processing and data analysis are necessary (56). In detail, three fundamental steps must be performed after the LC-MS analysis because for each sample a lot of information were acquired. The first step is "data processing" in order to avoid instrumental artefacts and identify all signals caused only by true ions. In this step, also alignment was performed in order to correct retention time differences between runs. In the second step relevant feature (that are identified with a unique mass/charge ratio and retention time) are evidenced using statistical approaches that can be based on univariate or multivariate analysis (57). Then, the last step is the identification of the significant features evidenced in the previous steps.

Compound identification was based on the accurate mass and isotopic profile evaluation, as well as on the fragmentation spectra of parent ions. According to metabolomics guidelines, four levels of identification were distinguished. In detail, level I corresponds to identified compounds through the comparison with an authentic standard, level II corresponds to putatively annotated compounds (e.g. without chemical reference standards, based upon physicochemical properties and/or spectral similarity with spectral libraries), level III corresponds to putatively characterized compound classes (e.g. based upon characteristic physicochemical properties of a chemical class of compounds, or by spectral similarity to known compounds of a chemical class) and level IV represents the unknown compounds (58).

1.5 Outline of the thesis

In the present work, LC-MS and LC-MS/MS methods have been developed and applied for the analysis of polyphenols in different biological system (i.e. plant tissues, fruits and biofluids). For this purpose, both targeted and untargeted approaches were applied for metabolomics analysis in different field, from environmental to food science and clinical researches.

Firstly, a targeted metabolomics approach was applied for the investigation of polyphenols in shoot and root of the plant model *Nicotiana langsdorffii* (wild type and genetically modified) after the exposure to water and heat stress (Chapter 2).

As regard food analysis, the polyphenolic composition of fruits from *V. myrtillus* L. and *V. uliginosum* L. subsp. *gaultherioides* was studied using a LC-MS/MS targeted approach in order to quantify the most abundant anthocyanins and polyphenols of these two berries species (Chapter 3).

Then, an untargeted metabolomics study was performed using the LC-HRMS methods for the comparative evaluation of polyphenol composition of

different *Vaccinium* berry species with the aim of obtaining the comprehensive polyphenolic profile of the investigated fruits (Chapter 4).

Finally, an untargeted metabolomics approach was applied to the analysis of serum and urine of healthy volunteers after assumption of *V. myrtillus* and *V. corymbosum* supplements in order to identify new polyphenol metabolites in human body (Chapter 5).

The results obtaining in this research work are summarized in Chapter 6.

Reference

1. Sakakibara H, Honda Y, Nakagawa S, Ashida H, Kanazawa K. Simultaneous determination of all polyphenols in vegetables, fruits, and teas. Journal of Agricultural and Food Chemistry. 2003;51(3):571-81.
2. Manach C, Scalbert A, Morand C, Rémésy C, Jiménez L. Polyphenols: food sources and bioavailability. The American journal of clinical nutrition. 2004;79(5):727-47.
3. Tsao R. Chemistry and biochemistry of dietary polyphenols. Nutrients. 2010;2(12):1231-46.
4. Nardini M, Cirillo E, Natella F, Scaccini C. Absorption of phenolic acids in humans after coffee consumption. Journal of Agricultural and Food Chemistry. 2002;50(20):5735-41.
5. Castañeda-Ovando A, Pacheco-Hernández MdL, Páez-Hernández ME, Rodríguez JA, Galán-Vidal CA. Chemical studies of anthocyanins: A review. Food Chemistry. 2009;113(4):859-71.
6. Lee J, Durst RW, Wrolstad RE. Determination of total monomeric anthocyanin pigment content of fruit juices, beverages, natural colorants, and wines by the pH differential method: collaborative study. Journal of AOAC international. 2005;88(5):1269-78.
7. Tsao R, Yang R, Young JC, Zhu H. Polyphenolic profiles in eight apple cultivars using high-performance liquid chromatography (HPLC). Journal of agricultural and food chemistry. 2003;51(21):6347-53.
8. Si W, Gong J, Tsao R, Kalab M, Yang R, Yin Y. Bioassay-guided purification and identification of antimicrobial components in Chinese green tea extract. Journal of Chromatography A. 2006;1125(2):204-10.
9. Dixon RA, Xie DY, Sharma SB. Proanthocyanidins–a final frontier in flavonoid research? New phytologist. 2005;165(1):9-28.
10. Aherne SA, O'Brien NM. Dietary flavonols: chemistry, food content, and metabolism. Nutrition. 2002;18(1):75-81.

11. Orlikova B, Tasdemir D, Golais F, Dicato M, Diederich M. Dietary chalcones with chemopreventive and chemotherapeutic potential. Genes & nutrition. 2011;6(2):125-47.
12. Aggarwal BB, Kumar A, Bharti AC. Anticancer potential of curcumin: preclinical and clinical studies. Anticancer research. 2003;23(1/A):363-98.
13. Kopp P. Resveratrol, a phytoestrogen found in red wine. A possible explanation for the conundrum of the'French paradox'? European Journal of Endocrinology. 1998;138(6):619-20.
14. Åkerström A, Jaakola L, Bång U, Jäderlund A. Effects of latitude-related factors and geographical origin on anthocyanidin concentrations in fruits of Vaccinium myrtillus L.(bilberries). Journal of agricultural and food chemistry. 2010;58(22):11939-45.
15. Bruni R, Sacchetti G. Factors affecting polyphenol biosynthesis in wild and field grown St. John's Wort (Hypericum perforatum L. Hypericaceae/Guttiferae). Molecules. 2009;14(2):682-725.
16. Jovančević M, Balijagić J, Menković N, Scaron K, Zdunić G, Janković T, et al. Analysis of phenolic compounds in wild populations of bilberry (Vaccinium myrtillus L.) from Montenegro. Journal of Medicinal Plants Research. 2011;5(6):910-4.
17. Lamperi L, Chiuminatto U, Cincinelli A, Galvan P, Giordani E, Lepri L, et al. Polyphenol levels and free radical scavenging activities of four apple cultivars from integrated and organic farming in different Italian areas. Journal of agricultural and food chemistry. 2008;56(15):6536-46.
18. Ahuja I, de Vos RC, Bones AM, Hall RD. Plant molecular stress responses face climate change. Trends in plant science. 2010;15(12):664-74.
19. Del Bubba M, Ancillotti C, Checchini L, Ciofi L, Fibbi D, Gonnelli C, et al. Chromium accumulation and changes in plant growth, selected phenolics and sugars of wild type and genetically modified Nicotiana langsdorffii. Journal of hazardous materials. 2013;262:394-403.
20. Yildiz- Aktas L, Dagnon S, Gurel A, Gesheva E, Edreva A. Drought Tolerance in Cotton: Involvement of Non- enzymatic ROS- Scavenging Compounds. Journal of agronomy and crop science. 2009;195(4):247-53.
21. Lavid N, Schwartz A, Yarden O, Tel-Or E. The involvement of polyphenols and peroxidase activities in heavy-metal accumulation by epidermal glands of the waterlily (Nymphaeaceae). Planta. 2001;212(3):323-31.
22. Fuoco R, Bogani P, Capodaglio G, Del Bubba M, Abollino O, Giannarelli S, et al. Response to metal stress of Nicotiana langsdorffii plants wild-type and transgenic for the rat glucocorticoid receptor gene. Journal of plant physiology. 2013;170(7):668-75.
23. Siracusa L, Patanè C, Avola G, Ruberto G. Polyphenols as chemotaxonomic markers in Italian "long-storage" tomato genotypes. Journal of agricultural and food chemistry. 2011;60(1):309-14.

24. Cevallos-Cevallos JM, Reyes-De-Corcuera JI, Etxeberria E, Danyluk MD, Rodrick GE. Metabolomic analysis in food science: a review. Trends in Food Science & Technology. 2009;20(11):557-66.
25. European Commission, Functional Foods. In: Directorate-General for Research FcF, editor. Brussels, Belgium2010. p. 1-28.
26. Kim J, Lee K, Lee H. Polyphenols suppress and modulate inflammation: possible roles in health and disease. Polyphenols in human health and disease San Diego, CA: Elsevier Inc p. 2014:1289-307.
27. Rodrigo R, Gil D, Miranda-Merchak A, Kalantzidis G. Antihypertensive role of polyphenols. Advances in clinical chemistry. 2012;58:225.
28. Daglia M. Polyphenols as antimicrobial agents. Current opinion in biotechnology. 2012;23(2):174-81.
29. Paller C, Ye X, Wozniak P, Gillespie B, Sieber P, Greengold R, et al. A randomized phase II study of pomegranate extract for men with rising PSA following initial therapy for localized prostate cancer. Prostate cancer and prostatic diseases. 2013;16(1):50.
30. Wang L-S, Stoner GD. Anthocyanins and their role in cancer prevention. Cancer letters. 2008;269(2):281-90.
31. Beccaro G, Mellano M, Botta R, Chiabrando V, Bounous G, editors. Phenolic and anthocyanin content and antioxidant activity in fruits of bilberry (Vaccinium myrtillus L.) and of highbush blueberry (V. corymbosum L.) cultivars in North Western Italy. VIII International Symposium on Vaccinium Culture 715; 2004.
32. Giovanelli G, Buratti S. Comparison of polyphenolic composition and antioxidant activity of wild Italian blueberries and some cultivated varieties. Food Chemistry. 2009;112(4):903-8.
33. Prencipe FP, Bruni R, Guerrini A, Rossi D, Benvenuti S, Pellati F. Metabolite profiling of polyphenols in Vaccinium berries and determination of their chemopreventive properties. Journal of pharmaceutical and biomedical analysis. 2014;89:257-67.
34. Del Bubba M, Giordani E, Pippucci L, Cincinelli A, Checchini L, Galvan P. Changes in tannins, ascorbic acid and sugar content in astringent persimmons during on-tree growth and ripening and in response to different postharvest treatments. Journal of Food Composition and Analysis. 2009;22(7):668-77.
35. Zhang H, Tsao R. Dietary polyphenols, oxidative stress and antioxidant and anti-inflammatory effects. Current Opinion in Food Science. 2016;8:33-42.
36. Reuter S, Gupta SC, Chaturvedi MM, Aggarwal BB. Oxidative stress, inflammation, and cancer: how are they linked? Free Radical Biology and Medicine. 2010;49(11):1603-16.
37. Aaby K, Grimmer S, Holtung L. Extraction of phenolic compounds from bilberry (Vaccinium myrtillus L.) press residue: Effects on phenolic

composition and cell proliferation. LWT-Food Science and Technology. 2013;54(1):257-64.
38. Yi W, Fischer J, Krewer G, Akoh CC. Phenolic compounds from blueberries can inhibit colon cancer cell proliferation and induce apoptosis. Journal of agricultural and food chemistry. 2005;53(18):7320-9.
39. Seeram NP, Adams LS, Hardy ML, Heber D. Total cranberry extract versus its phytochemical constituents: antiproliferative and synergistic effects against human tumor cell lines. Journal of agricultural and food chemistry. 2004;52(9):2512-7.
40. Zhang Y, Seeram NP, Lee R, Feng L, Heber D. Isolation and identification of strawberry phenolics with antioxidant and human cancer cell antiproliferative properties. Journal of agricultural and food chemistry. 2008;56(3):670-5.
41. Thomasset SC, Berry DP, Garcea G, Marczylo T, Steward WP, Gescher AJ. Dietary polyphenolic phytochemicals—promising cancer chemopreventive agents in humans? A review of their clinical properties. International Journal of Cancer. 2007;120(3):451-8.
42. Thomasset S, Berry DP, Cai H, West K, Marczylo TH, Marsden D, et al. Pilot study of oral anthocyanins for colorectal cancer chemoprevention. Cancer prevention research. 2009;2(7):625-33.
43. Cooke DN, Thomasset S, Boocock DJ, Schwarz M, Winterhalter P, Steward WP, et al. Development of analyses by high-performance liquid chromatography and liquid chromatography/tandem mass spectrometry of bilberry (Vaccinium myrtilus) anthocyanins in human plasma and urine. Journal of agricultural and food chemistry. 2006;54(19):7009-13.
44. Edirisinghe I, Banaszewski K, Cappozzo J, Sandhya K, Ellis CL, Tadapaneni R, et al. Strawberry anthocyanin and its association with postprandial inflammation and insulin. British journal of nutrition. 2011;106(6):913-22.
45. Hollands W, Brett GM, Dainty JR, Teucher B, Kroon PA. Urinary excretion of strawberry anthocyanins is dose dependent for physiological oral doses of fresh fruit. Molecular nutrition & food research. 2008;52(10):1097-105.
46. Kalt W, Liu Y, McDonald JE, Vinqvist-Tymchuk MR, Fillmore SA. Anthocyanin metabolites are abundant and persistent in human urine. Journal of agricultural and food chemistry. 2014;62(18):3926-34.
47. Mazza G, Kay CD, Cottrell T, Holub BJ. Absorption of anthocyanins from blueberries and serum antioxidant status in human subjects. Journal of agricultural and food chemistry. 2002;50(26):7731-7.
48. McGhie TK, Ainge GD, Barnett LE, Cooney JM, Jensen DJ. Anthocyanin glycosides from berry fruit are absorbed and excreted unmetabolized by both humans and rats. Journal of Agricultural and Food Chemistry. 2003;51(16):4539-48.

49. Lila MA, Burton-Freeman B, Grace M, Kalt W. Unraveling anthocyanin bioavailability for human health. Annual review of food science and technology. 2016;7:375-93.
50. Williamson G, Clifford MN. Colonic metabolites of berry polyphenols: the missing link to biological activity? British Journal of Nutrition. 2010;104(S3):S48-S66.
51. Lu W, Bennett BD, Rabinowitz JD. Analytical strategies for LC–MS-based targeted metabolomics. Journal of Chromatography B. 2008;871(2):236-42.
52. Lewis IA, Schommer SC, Hodis B, Robb KA, Tonelli M, Westler WM, et al. Method for determining molar concentrations of metabolites in complex solutions from two-dimensional 1H− 13C NMR spectra. Analytical chemistry. 2007;79(24):9385-90.
53. Want EJ, Cravatt BF, Siuzdak G. The expanding role of mass spectrometry in metabolite profiling and characterization. Chembiochem. 2005;6(11):1941-51.
54. Roberts LD, Souza AL, Gerszten RE, Clish CB. Targeted metabolomics. Current protocols in molecular biology. 2012:30.2. 1-.2. 24.
55. Gorrochategui E, Jaumot J, Lacorte S, Tauler R. Data analysis strategies for targeted and untargeted LC-MS metabolomic studies: overview and workflow. TrAC Trends in Analytical Chemistry. 2016;82:425-42.
56. Katajamaa M, Orešič M. Data processing for mass spectrometry-based metabolomics. Journal of chromatography A. 2007;1158(1):318-28.
57. Sumner LW, Urbanczyk-Wochniak E, Broeckling CD. Metabolomics data analysis, visualization, and integration. Plant bioinformatics: methods and protocols. 2007:409-36.
58. Sumner LW, Amberg A, Barrett D, Beale MH, Beger R, Daykin CA, et al. Proposed minimum reporting standards for chemical analysis. Metabolomics. 2007;3(3):211-21.

Chapter 2

Changes in polyphenol and sugar concentrations in wild type and genetically modified *Nicotiana langsdorffii* Weinmann in response to water and heat stress

Claudia Ancillotti
Patrizia Bogani
Stefano Biricolti
Elisa Calistri
Leonardo Checchini
Lorenzo Ciofi
Cristina Gonnelli
Massimo Del Bubba

Plant Physiology and Biochemistry 97 (2015) 52–61

Abstract

In this study wild type *Nicotiana langsdorffii* plants were genetically transformed by the insertion of the rat gene (*gr*) encoding the glucocorticoid receptor or the *rolC* gene and exposed to water and heat stress. Water stress was induced for 15 days by adding 20% PEG 6000 in the growth medium, whereas the heat treatment was performed at 50°C for 2 h, after that a re-growing capability study was carried out. The plant response to stress was investigated by determining electrolyte leakage, dry weight biomass production and water content. These data were evaluated in relation to antiradical activity and concentrations of total polyphenols, selected phenolic compounds and some soluble sugars, as biochemical indicators of metabolic changes due to gene insertion and/or stress treatments.

As regards the water stress, the measured physiological parameters evidenced an increasing stress level in the order *rolC* < *gr* < WT plants (e.g. about 100% and 50% electrolyte leakage increase in WT and *gr* samples, respectively) and complied with the biochemical pattern, which consisted in a general decrease of antiradical activity and phenolics, together with an increase in sugars.

As regard heat stress, electrolyte leakage data were only in partial agreement with the re-growing capability study. In fact, according to this latter evaluation, *gr* was the genotype less affected by the heat shock. In this regard, sugars and especially phenolic compounds are informative of the long-term effects due to heat shock treatment.

Keywords: carbohydrates, glucocorticoid receptor, heat stress, phenolics, *rolC*, transgenic plants, water stress

1 Introduction

Ongoing climate change represents a current phenomenon that produces significant alterations in temperatures and rainfall in different areas of the planet (Niu et al., 2014). These climate change occurrences deeply impact on all aspects of the architecture of plants, exposing such organisms to various abiotic stress. Water deficit and elevated global temperature are two of the most important environmental stress factors involved with climate change, that induce stress conditions in plants (Ahuja et al., 2010).

Water and heat stress have the common effect to increase radicals and reactive oxygen species (ROS) (Łabanowska et al., 2013; Qu et al., 2013; Edreva et al., 1998); furthermore, they result in changed primary and secondary plant metabolism (Macedo, 2012), besides morphological alterations (Patakas, 2012) and, in the case of crops, also a reduced yield (Macedo, 2012). The up-regulation and down-regulation of specific primary and secondary metabolites represent a defence mechanism to better tolerate these stress and a number of them can be investigated in order to assess the stress conditions of plants. Among the various secondary metabolites occurring in plants, polyphenols are commonly involved in the defence mechanism towards different abiotic stress, including those related to water deficit and exposure to high temperatures (Sanchez-Rodríguez et al., 2011; Yildiz-Aktas et al., 2009; Wahid et al., 2007), due to their properties of hydrogen donors and singlet oxygen quenchers (Łabanowska et al., 2013).

As regards primary metabolites involved in plant response to the above-mentioned stress, soluble sugars do not only function as metabolic and structural resources of plant cells, but also play important roles in cell responses to different kinds of stress, including water deficit (Rosa et al., 2009) and heat exposure (Huve et al., 2006).

Among the different approaches developed to understand molecular and physiological mechanisms that plants oppose to environmental stress

conditions, the genetic engineering of abiotic stress tolerance in plants is one of the most currently used (Cabello et al., 2014; Cvikrova et al., 2013; Al-Quraan et al., 2010).

The recent advances in "omics" technologies (Yuan et al., 2008; Rhee and Mutwil, 2013) have been very useful to identify different stress responsive molecules with a role in the metabolite regulatory networks during the response to abiotic stress (Urano et al., 2010; Cramer et al., 2011; Prabha et al., 2014).

As far as water and heat stress are concerned, the establishment of model plants, for the most part *Arabidopsis thaliana* and *Nicotiana tabacum*, transgenic for regulatory elements such as kinases and transcription factors (Cabello et al., 2014, 2012; Hussain et al., 2011; Tripathi et al., 2014; Yokotani et al., 2013) or genes coding for antioxidant enzymes, heat-shock proteins, osmolytes, enzymes involved in the membrane fluidity and in radical and ROS homeostasis (Chamoli and Verma, 2014; Mittler et al., 2011; Suzuki et al., 2012), revealed that plant response to stress is very complex, involving multiple metabolic pathways that interact to increase levels of stress tolerance (Kotak et al., 2007; Grover et al., 2013).

Recently, also *Nicotiana langsdorffii* has been proposed for investigating the influence of gene insertions on the response to abiotic stress. More in detail, the effects of the introduction of the rat gene (*gr*) encoding the glucocorticoid receptor and the *rolC* gene from *Agrobacterium rhizogenes* on the hormonal network and primary and secondary metabolism, as well as on the sensitivity to selected abiotic stress, were investigated (Scalabrin et al., 2015; Giannarelli et al., 2010; Fuoco et al., 2013; Del Bubba et al., 2013; Bogani et al., 2015).

The interest in *rolC* gene stems from its well-assessed role in the modification of the plant hormonal pattern and the activation of plant defence response to biotic and abiotic stress. In fact, the integration of *rolC* gene from *Agrobacterium rhizogenes* has been clearly demonstrated to

increase cytokinin activity, inducing strong phenotypic modifications of the plant habitus, irrespective to the driving promoter (Estruch et al., 1991; Schmuelling et al., 1993; Fladung and Ballvora, 1992). Furthermore, the enhancement of some secondary metabolites such as tropane alkaloids (Bonhomme et al., 2000) and anthraquinones (Bulgakov et al., 2002; Shkryl et al., 2008) has been observed. It should also be noted that the *rolC* insertion has been reported to enhance the tolerance level to both abiotic and biotic stress (Del Bubba et al., 2013; Bulgakov, 2008; Bulgakov et al., 2008).

As regards the *gr* gene, in our laboratories the transformation of *N. langsdorffii* and *Nicotiana glauca* led to significant phenotypic alterations. Such modifications were attributed to a different phytohormone composition pattern, such as the increase in the auxin/cytokinin ratio (Giannarelli et al., 2010) and the concentration of abscisic acid and salicylic acid (Fuoco et al., 2013). Moreover, *gr* insertion in *N. langsdorffii* conferred a significant resistance to the presence of hexavalent chromium in the growth medium, together with a good metal-accumulation capacity (Del Bubba et al., 2013). In that paper a significant modification of carbohydrate and shikimate phenolic metabolisms in response to Cr(VI) stress was also evidenced. The *gr* overexpression in *N. tabacum* also increased resistance to biotic stress by nematodes, through a greater production of different secondary metabolites (Irdani et al., 2003).

Based on the above-reported considerations, in this paper the following aims were pursued.

1. The evaluation of *gr* and *rolC* engineered *N. langsdorffii* response to water and heat stress, compared to wild type plants, according to the determination of electrolyte leakage, root and shoot biomass production and water content as reference physiological parameters of the health status of plants (Bajji et al., 2002; Barcelo and Poschenrieder, 1990). Recovery of

plants after exposure to heat stress was also studied as indicator of stress injury and level of tolerance to stress conditions, in accordance with findings reported in literature (Bajji et al., 2002).

2. The investigation of the possible role of radical scavenging activity (RSA) and concentrations of some selected soluble sugars, total polyphenols (TP) and various phenolic compounds synthesized within the shikimate pathway for evaluating the plant response to water deficit and heat treatment.

2 Materials and methods

2.1 Reagents and materials

Linsmaier & Skoog (LS) growth medium, naphthalen acetic acid (NAA), N-6-benzylaminopurine (BAP), kanamycin, carbenicillin, 3-O-caffeoylquinic acid (chlorogenic acid), 4-O-caffeoylquinic acid (cryptochlorogenic acid), 5-O-caffeoylquinic acid (neochlorogenic acid), 1,5-dicaffeoylquinic acid, caffeic acid, p-coumaric acid, ferulic acid, scopoletin, esculetin, raffinose, glucose, fructose and sucrose standards were supplied by SigmaeAldrich (St. Louis, MO, USA); LC-MS grade methanol, acetonitrile and water and LC-grade acetic acid were purchased from Panreac (Barcelona, Spain). Folin-Ciocalteu (F-C) reagent, 2,2-diphenyl-1-picrylhydrazyl (DPPH) radical, sodium carbonate, sodium fluoride, sodium hypochlorite, hydrochloric acid and formic acid were obtained from Merck (Darmstadt, Germany). Ultrapure water was obtained from a Millipore (Billerica, MA, USA) MilliQ system. Polytetrafluoroethylene (PTFE) membranes (porosity 0.2 mm) for the filtration of the extracts before HPLC analysis were obtained from Sartorius (Goettingen, Germany). Solid phase extraction (Estruch et al., 1991) Bond Elut C18 were purchased from Agilent Technologies (Santa Clara, CA, USA).

2.2 Transformation and propagation of *N. langsdorffii* plants

Transgenic *gr N. langsdorffii* primary plants (T0) were obtained by the Horsch leaf disc transformation (Horsch et al., 1985) of *N. langsdorffii* with an *Agrobacterium* strain harbouring the binary vector pTI18 (see Fig. 1) (Irdani et al., 2003, 1998, 2010) as described by Giannarelli and co-workers (Giannarelli et al., 2010).

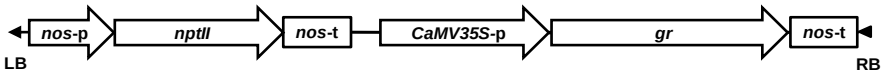

Figure 1. Schematic construct cassette encompassing the T-DNA contained in the LBA4404 *Agrobacterium* strain used for plant transformation.

T0 plants transgenic for the *rolC* gene of *A. rhizogenes* were generated by the transformation of *N. langsdorffii* with the pBin19 vector containing a 1858 bp fragment of pRi1855 T-DNA comprising the *rolC* transcription unit (Cardarelli et al., 1987) as described by Bogani and colleagues (Bogani et al., 2012). Then, ten *gr* T0 and four *rolC* T0 independent transgenic plants were transferred to a containment greenhouse and allowed to self-pollinate at a temperature ranging from 18 to 24 °C, until T1 seeds production. Harvested T1 seeds from each independent transgenic line were surface sterilized with 5% (w/w) sodium hypochlorite aqueous solution for 20 min, washed three times with Milli-Q water (Millipore) and placed on Petri dishes containing LS medium supplemented with 100 mg L^{-1} of kanamycin sulphate (the transformation selection agent). Petri dishes were incubated in a growth chamber at 24 ± 1 °C with a photoperiod of 16 h of light (1500 lux) and 80% relative humidity. T1 seedlings were maintained in these conditions through further transfers onto fresh medium at growth intervals of 30 days each.

The null-segregants from T1 seeds were used as isogenic WT plants; these plants were grown under the same experimental conditions with the only exception of the selective agent in the culture medium.

2.3 Molecular analysis of transformed N. langsdorffii plants (see Appendix S1 in Supplementary Material for full details)

2.3.1 DNA isolation

Genomic DNA was isolated from young leaves of micropropagated plants of each transgenic line and from WT *N. langsdorffii* using the Macherey-Nagel (Düren, Germany) "Nucleospin Plant" kit according to the manufacturer's instructions.

2.3.2 Transgene copy number

The copy number of transgenes was assessed on ten (*gr*) and four (*rolC*) independent lines, using a real-time PCR technique based on the TaqMan® chemistry (Heid et al., 1996), establishing a standard quantification curve (Hoebeeck, 2007) for calculating PCR efficiency and interpolating unknown sample quantities. In nine out of ten investigated gr lines, copy number varied from a single hemizygous copy to two copies per haploid genome, whereas in one case three copies were found.

The *rolC* transgene was found to be present as one single copy in three transgenic lines, while three copies were found in one line.

2.3.3 RNA extraction

Total RNA from leaves of transgenic and WT *N. langsdorffii* plantlets was extracted following the instructions of the Macherey-Nagel ‘‘Nucleospin RNA Plant’’ kit.

2.3.4 Real time RT-PCR

One µg of total RNA was reverse transcribed and amplified in a real-time PCR system for the quantitative expression analysis of *gr* and *rolC* genes.
As regards the *gr* transcription profiles, amounts of gr-mRNA/µg RNA ranged from 0.081 to 0.49 pg/µg RNA in *gr*5 and *gr*9 transgenic lines, respectively.
For single copy *rolC* transgenic lines, expression levels ranged from 0.0025 to 0.014 pg rolC-mRNA/µgRNA, whereas the three-copies line showed the lowest level of expression (0.0018 pg rolC-mRNA/µgRNA).

2.3.5 Reverse-transcription PCR

RT-PCR for the analysis of transgene expression was performed with the “Transcriptor One-Step RT-PCR” Kit (Roche Diagnostics, Milan, Italy) following the manufacturer's instructions. RT-PCR amplification of *rolC* and *gr* transgene was performed using primers described by Bettini and colleagues (Bettini et al., 2010) and Giannarelli and co-workers (Giannarelli et al., 2010).

2.4 Electrolyte leakage (see Appendix S2 in supplementary material for full experimental details)

Electrolyte leakage was determined according to Bogani and coworkers (Bogani et al., 2015). Briefly, thirty leaf discs were collected from randomly picked plants, and placed in three test tubes (10 per tube) containing 5 mL

of 1 M sucrose solution. After equilibration for 30 min at a given temperature, the electrical conductivity was measured. Leaf discs were then frozen at - 80 °C and finally equilibrated at 25 °C before measuring again total conductivity.

2.5 Plant exposure to water and heat stress

Ten individuals from untransformed and transgenic plants randomly chosen from the T1 selfed progeny, the latter being representative of the integration of *gr* and *rolC* transgenes, were used for the experimental treatments.

Polyethyleneglycol (PEG 6000) was used to induce water stress according to van der Weele and co-workers (van der Weele et al., 2000) and 20% PEG was chosen as mimicking severe drought condition, in accordance with various literature reports (Bajji et al., 2000; Khalid et al., 2010; Tejavathi, 2010). To induce water stress, plants were subcultured for 15 days on 50 mL LS medium conditioned with 50 mL of 20% PEG 6000 solution.

Thermal stress was induced by mean the heat shock method, similarly to what is reported in literature (Edreva et al., 1998; Kuznetsov and Shevyakova, 1997; Moriwaki et al., 1999). More in detail, all plant genotypes were grown on LS medium and maintained in a SANYO incubator, mod. MIR-153 (Richmond Scientific Ltd, Chorley, Great Britain) at 50 °C for 2 h prior further analyses.

These experimental conditions were chosen on the basis of electrolyte leakage data found in wild type plants (Bajji et al., 2002). Electrolyte leakage was also determined on WT, *gr* and *rolC* plants exposed to the heat stress and the corresponding controls, with the purpose of evaluating the water stress and the heat stress levels occurring in the different genotypes.

2.6 Handling of plant material

Roots and shoots of WT and transgenic plants, exposed or not to water and heat stress (ten plants for each treatment) were separately collected, washed and carefully dried with blotting paper and finally at 40 °C for 10 min; then the plants were weighted, thus obtaining the fresh weight (FW). Plant organs were finally frozen in liquid nitrogen, lyophilised and weighted for determining the dry weight (Gutierrez et al., 1995). Water content percent (WP) was calculated as reported in the Appendix S3 of the Supplementary Material. Roots and shoots were stored at -20 °C until analysis.

2.7 Chemical analysis (see Appendix S4 in supplementary material for full details)

2.7.1 Total polyphenols

TP were spectrophotometrically determined at λ = 740 nm on the plant extract with the FolineCiocalteau (F-C) method using chlorogenic acid as the reference standard.

2.7.2 RSA

Antiradical activity was spectrophotometrically determined by monitoring the absorbance decrease (λ = 517 nm) of 0.1 mM DPPH solutions containing different amount of root/shoot extract.

2.7.3 Phenolic compounds

The determination of phenolic compounds belonging to the shikimate pathway was performed by liquid chromatography (HPLC) coupled with tandem mass spectrometry (MS/MS) on the evaporated plant extracts.

2.7.4 Soluble sugars

The determination of glucose, fructose and sucrose in plant extracts was performed by HPLC coupled with evaporative light scattering detector (ELSD), after clean-up on a C18 SPE cartridge.

2.8 Statistical analysis

Linear univariate correlations between variables were investigated by the least square method, using Microsoft® Office Excel 2007 (Microsoft Corporation, Redmond, WA, USA).

One-way analysis of variance, Dunnett T3 nonparametric test and Principal Component Analysis (PCA) were performed on the original data, at the 99% probability level ($P \leq 0.01$), by using the statistical package SPSS, version 17.0 for Windows (SPSS Inc., Chicago, IL, USA).

3 Results and discussions

Table 1 illustrates mean data and standard deviations of DW biomass and water content of the investigated samples, whereas electrolyte leakage data were shown in Fig. 2. The appearance of WT, *gr* and *rolC N. langsdorffii* plants, both untreated and exposed to water and heat stress, together with the re-growing capability of the three genotypes in response to this latter stress, are shown in Fig. 3 and in Fig. 4, respectively. Finally, all the chemical parameters were reported in Table 2.

Table 1. Mean values ± standard deviation (n = 10) of dry weight biomass (DW, g per plant) and percentage of water content (WC%) of shoot and root of wild type (WT), *gr* and *rolC* genetically modified *Nicotiana langsdorffii*, untreated and exposed to water stress (WS) and heat stress (HS). Within untreated samples, *gr* or *rolC* values statistically different ($P \leq 0.01$, according to the Dunnett T3 nonparametric test) from the corresponding control (i.e. WT) are in bold character. Within the same genotype, values of water stress or heat stress samples statistically different ($P \leq 0.01$, according to the Dunnett T3 nonparametric test) from the corresponding control (i.e. the untreated sample) are in bold character.

	DW	**WC%**
Shoot		
WT	1.41±0.14	91.5±0.7
WT-WS	**1.11±0.06**	**89.1±0.6**
WT-HS	1.22±0.17	**89.0±0.5**
Gr	**0.58±0.05**	**94.1±0.5**
gr-WS	0.66±0.06	**91.3±1.0**
gr-HS	0.59±0.12	92.8±1.1
rolC	**0.47±0.06**	**94.5±1.6**
rolC-WS	0.59±0.06	92.6±1.0
rolC-HS	0.41±0.05	93.8±0.5
Root		
WT	0.126±0.009	93.1±0.8
WT-WS	**0.100±0.011**	**83.6±1.6**
WT-HS	0.113±0.013	86.8±4.2
Gr	**0.068±0.009**	**80.7±3.0**
gr-WS	**0.025±0.005**	81.4±4.0
gr-HS	0.062±0.017	83.9±5.2
rolC	**0.016±0.004**	93.5±1.5
rolC-WS	0.023±0.005	93.0±1.4
rolC-HS	0.020±0.005	92.1±1.5

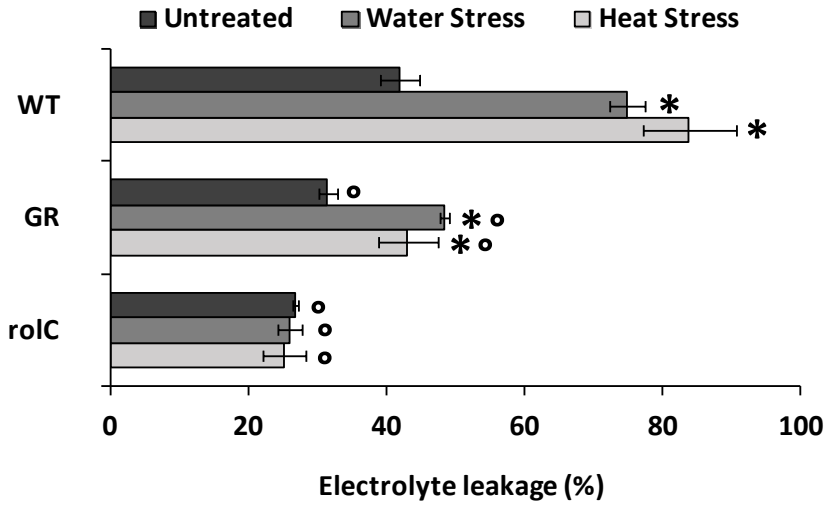

Figure 2. Mean percentages (n = 5) of electrolyte leakage measured at 25 °C on leaf tissues of wild type and genetically modified *Nicotiana langsdorffii*, both untreated and exposed to water stress and heat stress, in respect to data obtained after tissue freezing (see Appendix S2 in Supporting information for full experimental details). WT = *N. langsdorffii* wild type; GR = *N. langsdorffii* modified for *gr* insertion; rolC = *N. langsdorffii* modified for *rolC* insertion. Error bars represent standard deviations. Rectangular bars labelled with the star (*) or the circle (○) indicate the following statistically significant differences ($P \leq 0.01$, according to the Dunnett T3 nonparametric test): (*) within the same genotype, water stress or heat stress samples vs. the untreated sample; (○) within the same stress condition, *GR* or *rolC* vs. WT.

3.1 Effects of gene insertion

3.1.1 Plant appearance and health status parameters

In accordance with findings previously obtained (Giannarelli et al., 2010; Del Bubba et al., 2013; Bogani et al., 2015), plant morphology was clearly affected by gene insertion and a smaller size of the genetically modified plants compared to WT organisms was observed (Fig. 3A-C).

Shoot and root DW biomass data were in agreement with visual observations, being both the above-ground and the underground biomass significantly higher in WT than in *gr* and *rolC* plants (Table 1). Water

content was slightly higher in *gr* and *rolC* shoot than in WT one, whereas a much lower water percentage was observed in untreated *gr* roots than inWT and *rolC* ones (Table 1), in agreement with data previously obtained (Fuoco et al., 2013; Del Bubba et al., 2013).

Electrolyte leakage data (Fig. 2) were found to be significantly different according to the genotype investigated, being the ionic release in the order WT > *gr* > *rolC*. In agreement with this finding, a higher ion leakage was recently reported in WT than in *gr* leaves also by Bogani and co-workers (Bogani et al., 2015).

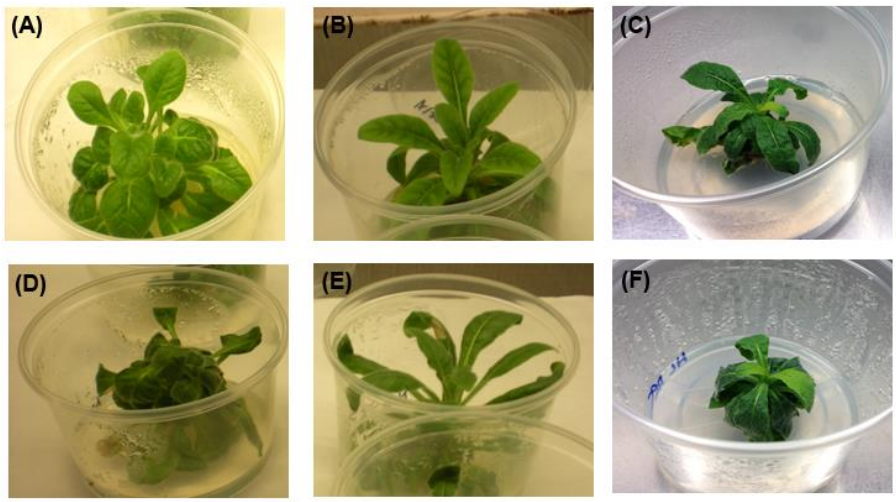

Figure 3. Effect of water stress on wild type and genetically modified *N. langsdorffii* plants, as induced by the growth for 15 days on LS medium containing 20% PEG 6000. (A) Untreated *N. langsdorffii* wild type; (B) untreated *N. langsdorffii gr*; (C) untreated *N. langsdorffii rolC*; (D) water-stressed *N. langsdorffii* wild type; (E) water-stressed *N. langsdorffii gr*; (F) water-stressed *N. langsdorffii rolC*.

3.1.2 Chemical parameters and RSA

The insertion of either *gr* or *rolC* genes produced a significant increase of TP in both shoot and root, compared to WT plants; the increment was particularly evident in shoot, especially for *gr* samples, in which a two-fold TP concentration was observed (Table 2). RSA data followed a trend similar to that of TP, either for shoot or root and a statistically significant linear correlation was found between them (R^2 = 0.93, P<<0.01 and R^2 = 0.96, P<<0.01, for root and shoot, respectively), indicating the large contribution of polyphenols to the whole antiradical activity of plant extracts, as measured by the DPPH method.

As a general finding, among the selected phenolic compounds, chlorogenic acid was by far the most abundant, both in shoot and root, followed by cryptochlorogenic acid and scopoletin, whereas the other phenolic compounds were generally present at much lower concentrations and their relative abundance varied, depending on the genetic modification and the plant organ investigated (Table 2). An increasing trend of most individual phenolic concentrations was found in transformed plants, compared to WT. The main differences between WT and *gr* transformed plants were found for chlorogenic acid and cryptochlorogenic acid in both root and shoot; also caffeic acid significantly increased in *gr* aerial tissues, whereas in root a significant concentration augment was found for scopoletin. Plant transformation with *rolC* gene produced an analogous increment of phenolic compounds in root, whereas in shoot only chlorogenic acid significantly increased as a result of the gene insertion.

Table 2 - Mean values ± standard deviation (n=5) of total polyphenols (TP, mg chlorogenic acid equivalent g-1 DW), radical scavenging activity (RSA, µg DPPH inhibited µg-1 DW), p-coumaric acid (COU, mg kg-1 DW), caffeic acid (CAF, mg kg-1 DW), chlorogenic acid (CHL, mg kg-1 DW), cryptochlorogenic acid (CRY, mg kg-1 DW), neochlorogenic acid (NEO, mg kg-1 DW), ferulic acid (FER, mg kg-1 DW), esculetin (ESC, mg kg-1 DW), scopoletin (SCO, mg kg-1 DW), sucrose (SUC, mg g-1 DW), glucose (GLU, mg g-1 DW), fructose (FRU, mg g-1 DW) in shoot and root of wild type (WT), gr and rolC genetically modified *Nicotiana* langsdorffii, untreated and exposed to water stress (WS) and heat stress (HS). Within untreated samples, gr or rolC values statistically different (P≤0.01, according to the Dunnett T3 nonparametric test) from the corresponding control (i.e. WT) are in bold character. Within the same genotype, values of water stress or heat stress samples statistically different (P≤0.01, according to the Dunnett T3 nonparametric test) from the corresponding control (i.e. the untreated sample) are in bold character.

	TP	**RSA**	**COU**	**CAF**	**CHL**	**CRY**	**NEO**	**FER**	**ESC**	**SCO**	**SUC**	**GLU**	**FRU**
Shoot													
WT	21.5±0.3	0.052±0.004	0.19±0.03	4.4±0.7	582±99	29.7±5.6	2.5±0.6	0.47±0.20	1.2±0.3	17.3±1.9	15.8±2.6	29.3±3.0	41.7±5.4
WT-WS	**19.7±0.4**	**0.033±0.001**	0.17±0.01	3.3±1.0	**358±42**	**17.3±1.2**	2.0±0.2	0.41±0.05	1.5±0.6	66.9±30.0	21.4±2.1	**44.1±2.7**	41.1±3.4
WT-HS	25.2±2.5	**0.092±0.014**	**6.88±1.32**	4.1±0.5	**5755±300**	**159.7±12.6**	**6.3±1.0**	**2.12±0.40**	**<LOD**	**8.7±2.0**	18.9±3.3	25.4±3.4	**25.3±3.2**
gr	**40.7±1.3**	**0.173±0.003**	0.15±0.04	**10.3±1.6**	**4704±291**	**105.5±16.8**	**7.2±1.2**	0.50±0.16	**0.6±0.1**	18.7±1.8	**24.1±2.6**	25.8±2.0	39.1±3.8
gr-WS	38.6±0.7	**0.113±0.002**	0.13±0.01	9.7±2.7	**2065±215**	**39.0±3.0**	6.7±0.3	0.45±0.05	**1.9±0.5**	**114.3±38.9**	**43.3±1.9**	**33.3±0.6**	42.9±2.2
gr-HS	**19.7±2.3**	**0.064±0.014**	**10.58±3.36**	**4.1±1.7**	**3506±596**	101.3±39.7	**4.2±1.2**	**2.65±0.44**	**<LOD**	**65.9±19.7**	**16.8±1.0**	22.7±2.0	**23.2±2.4**
rolC	**27.9±1.7**	**0.076±0.002**	0.27±0.07	5.3±0.3	**2736±238**	39.9±2.5	2.5±0.5	0.42±0.13	0.9±0.1	24.1±3.2	**33.2±4.5**	**47.3±5.3**	**62.0±6.1**
rolC-WS	26.3±0.6	0.068±0.004	0.24±0.04	**0.7±0.1**	**1613±136**	**14.9±0.9**	2.1±0.2	0.37±0.04	0.5±0.1	**7.4±2.8**	41.3±2.8	**68.2±3.2**	69.8±1.7
rolC-HS	**22.6±1.4**	0.077±0.007	**11.12±4.18**	5.1±0.8	**4589±788**	**103.7±2.9**	**4.0±0.6**	**5.13±0.63**	**<LOD**	**47.3±10.6**	**14.8±2.1**	**24.0±4.3**	**22.8±3.8**

Table 2 (continued)

	TP	RSA	COU	CAF	CHL	CRY	NEO	FER	ESC	SCO	SUC	GLU	FRU
Root													
WT	17.0±0.4	0.046±0.006	0.36±0.04	0.9±0.4	464±107	10.8±3.4	2.3±0.7	1.2±0.2	0.31±0.08	38.8±12.3	26.3±3.9	17.1±1.6	27.6±2.8
WT-WS	**14.0±0.2**	**0.029±0.004**	0.30±0.16	0.8±0.2	305±43	6.3±0.4	2.0±0.2	1.0±0.3	0.51±0.12	45.0±3.9	32.1±4.6	**27.0±2.2**	26.6±4.2
WT-HS	**9.0±0.9**	**0.019±0.003**	0.24±0.21	1.1±0.4	446±142	17.2±10.9	1.6±1.1	2.0±0.8	**<LOD**	**2.2±0.7**	**13.7±2.4**	15.4±1.8	**13.1±2.8**
gr	**20.0±0.6**	**0.085±0.005**	**0.14±0.03**	2.6±1.3	**1630±94**	**38.7±6.2**	4.0±0.5	0.6±0.2	0.53±0.09	**83.4±10.0**	**50.3±4.1**	21.0±1.8	31.3±3.3
gr-WS	19.5±0.5	**0.070±0.003**	0.10±0.04	2.2±0.5	**1291±75**	**23.1±2.5**	3.7±0.6	0.5±0.1	0.82±0.20	**124.4±11.9**	56.6±2.0	**31.4±3.1**	32.8±1.7
gr-HS	**12.8±2.1**	**0.035±0.008**	1.53±0.98	1.7±0.5	**568±148**	29.1±14.0	5.7±2.1	2.4±1.1	**<LOD**	**9.1±2.8**	**9.2±0.7**	17.2±2.7	**13.3±4.0**
rolC	18.7±0.7	**0.073±0.007**	**0.84±0.16**	**3.6±0.9**	**1607±133**	**37.6±7.2**	3.6±0.6	1.7±0.2	**0.72±0.09**	**93.9±18.7**	**46.8±3.5**	**34.2±3.9**	**40.1±3.5**
rolC-WS	17.6±0.4	0.068±0.005	0.62±0.13	**1.5±0.4**	**1247±75**	**18.0±2.5**	3.3±0.5	1.4±0.3	0.79±0.19	85.6±5.5	48.6±4.6	**49.9±2.3**	44.3±4.1
rolC-HS	**10.9±0.6**	**0.035±0.003**	**1.30±0.10**	2.1±0.1	1764±236	74.4±15.5	**7.2±0.7**	**2.8±0.2**	**<LOD**	**6.1±2.8**	**9.9±0.7**	**12.3±0.8**	**10.7±0.8**

A different relative abundance of the investigated sugars was found in above-ground and underground plant organs, being fructose the most abundant sugar in shoot and sucrose in root. The insertion of *rolC* gene caused a statistically significant increase of all sugars investigated, in either root or shoot, whereas in both parts of *gr* modified plants, the only significant augment was observed for sucrose (Table 2).

The different phytohormone pattern determined in WT and *gr N. langsdorffii* has been proposed as plausible explanation of metabolic shifts in transgenic plants (Giannarelli et al., 2010; Fuoco et al., 2013). Changes in phytohormone balance, already reported in *rolC* transformed organisms, including *N. tabacum* (Prinsen et al., 1994), could also be invoked as possible explanation of the higher abundance of phenolic metabolites observed herein in *rolC* modified *N. langsdorffii*.

The general increase observed for carbohydrate concentrations, as a consequence of both *gr* and especially *rolC* gene insertions, highlighted the broad effects of these genetic modifications, indicating their possible influence also on the primary metabolism of *N. langsdorffii*. In fact, changed carbohydrate metabolism and alterations of their source/sink relationship have been reported in plants expressing *rolC*, and in these plants the leaf concentrations of glucose and fructose were found to be higher than in untransformed plants (Christensen and Mueller, 2009).

The higher values of TP, RSA and most individual phenolic compounds found in *rolC* and especially *gr* transformed plants, strongly suggest a potentially better response of genetically modified plants to abiotic stress conditions. In fact, abiotic stress usually causes an increase of radicals, including ROS, in the cell metabolism, against which phenolic compounds can efficiently act (Łabanowska et al., 2013; Bulgakov et al., 2013). In this regard, also the increase in sugar concentrations, found in *gr* and above all *rolC* organisms, indicate a higher response potential of transformed plants than WT ones, against stress phenomena involving the formation of free

radicals. In fact, a stabilization role towards these reactive species has been demonstrated for simple carbohydrates, such as glucose, fructose and sucrose (Łabanowska et al., 2013; Gray and Mower, 1991).

3.2 Effects of water stress

3.2.1 Plant appearance and health status parameters

Fig. 3 illustrates the effect on WT and transgenic *N. langsdorffii* plants of the exposure to the water stress, as induced by plant growth for 15 days on LS medium containing 20% PEG 6000. Water stress had a clear wilting effect only on untransformed plants (Fig. 3A and D), whereas *gr* modified plants (Fig. 3B and E) and those transformed via *rolC* insertion (Fig. 3C and E) did not show any visual stress symptom.

Electrolyte leakage was found to be significantly higher in treated WT and *gr* plants, compared to their corresponding control samples (Fig. 2). The ion release was particularly enhanced in water stressed WT plants, being it almost doubled in samples exposed to 20% PEG 6000 in the growth medium, while in *gr* samples the ion leakage increase was of about 50%. Conversely, for *rolC* modified plants no change in the ion release was observed for samples exposed to the water stress, compared to the untreated ones.

The effect of the water deficit on WT plants was also highlighted by biomass data (Table 1); in fact, both shoot and root showed a statistically significant DW decrease. The presence of PEG 6000 in the growth medium produced a statistically significant decrease of root biomass also in *gr* samples, whereas shoot was not influenced by the stress. Interestingly, water deficit did not affect the biomass of *rolC* transformed plants, neither in shoot nor in root, thus highlighting a different response to this stress as a consequence of this gene insertion, compared to WT and *gr* plants.

The exposure to hydric stress did not produce any great variation of water content, compared to untreated samples; however, a statistically significant effect was observed for shoot and especially root of WT plants, as well as for the aerial part of *gr* samples. On the contrary, in *rolC* plant organs, no statistically significant effect was highlighted.

The variations observed in dry biomass and water content in response to water stress were in agreement with the results obtained by Tejavathi (Tejavathi, 2010), who evidenced a much higher decrease in biomass production than in water content of in vitro cultured *Macrotyloma uniflorum* plants, treated with different percentages of PEG, as induction tool of water stress.

The combined evaluation of the plant appearance and the reference physiological parameters of the health status of plants, clearly highlighted the presence in WT plants of a high-level stress condition due to the water deficit induced by 20% PEG 6000 in the growth medium. Conversely, for *rolC* transformed plants, the aforementioned parameters suggested the absence of a stress situation. The status of plants modified for *gr* gene insertion and exposed to water stress, might be considered as intermediate between WT and *rolC* conditions. In fact, for *gr* modified organisms, in spite of very similar visual aspects of untreated samples and those exposed to PEG, the release of ions determined in foliar tissues of transformed plants exposed to the water deficit was much higher than the corresponding control. Thus, in *gr* shoot a significant alteration of the cell membrane stability was evidenced. However, the ion leakage was statistically lower than that determined in WT. Also the different DW trend observed in *gr* plants, compared to WT ones, strongly suggested that the stress level suffered by the former was lower than that undergone by the latter. In this regard, it should be remarked that the common response mechanism to the water deficit, besides the direct reduction of the underground biomass, is the chemical root-to-shoot signaling, causing the decrease of leaf growth

(Schachtman and Goodger, 2008). Therefore, according to the above-mentioned considerations, the stress level suffered by the genotypes investigated owing to the presence of PEG in the growth medium should be in the following increasing order: *rolC* < *gr* < WT, and both WT and *gr* genotypes can be considered as sensitive to this stress. Interestingly, similar conclusions were drawn on the relative stress status of these genotypes exposed to hexavalent chromium (Del Bubba et al., 2013).

3.2.2 Chemical parameters and RSA

Water stress gave rise to a general, albeit small, decrease of TP concentration either in shoot or root; the concentration change was statistically significant only in WT samples, irrespective of the plant organ considered.

RSA data evidenced a pattern quite similar to the one found for TP and as previously observed, a significant linear correlation was found between the two parameters with R^2 values higher than 0.91 ($P<<0.01$) for both underground and above-ground tissues. However, the decrease of the antiradical activity was found to be significant in shoot and root, of both WT and *gr* genotypes, whereas no changes were highlighted for *rolC* plants. Thus, RSA seems to better interpret the tolerant and sensitive conditions evidenced by ion leakage data for *rolC* and WT or *gr* genotypes, respectively. The RSA decrease observed in WT and *gr* plants in response to the PEG treatment, as well as the TP decline in water-stressed WT samples, were in agreement with the higher utilization of antiradical compounds in response to the commonly observed augment of free radicals under water deficit conditions (Łabanowska et al., 2013).

The concentration trend of phenolic compounds belonging to the shikimate pathway was in good agreement with TP profiles, being them reduced in most cases in response to water stress, both in shoot and root, and

irrespective of the genotype considered. A general down-regulation of the shikimate pathway in response to water deficit was also evidenced by Sanchez-Rodríguez et al. (Sanchez-Rodríguez et al., 2011). Noteworthy exceptions to the decreasing trend of phenolic concentrations were represented by coumarins (i.e. esculetin and especially scopoletin), which showed an increase in WT and above all *gr* samples, being the augment in the latter genotype in most cases statistically significant (Table 2). Conversely, in *rolC* samples, scopoletin and esculetin showed a decrease in shoot and a quite constant concentration in root.

The complex set of information obtained from phenolic secondary metabolism data is in agreement with literature studies that reported different phenolic profiles in response to water deficit, depending on the species analyzed and even within the same species as a function of the more or less sensitive/tolerant genotype under investigation. Furthermore, erratic trends were found for different individual phenolics in the same genotype. For example, a significant decrease of TP was evidenced by Tejavathi (Tejavathi, 2010) on in vitro plants of *Macrotyloma uniflorum* L. as a function of the increase of PEG percentage in the growing medium (i.e. with increasing water deficit in plant), that is in experimental conditions very similar to those adopted in our study. Decreasing trends of TP, individual phenolic compounds and DPPH antiradical activity were also observed in one tolerant and one sensitive cultivar of *Gossypium hirsutum* L. cultivated in vivo under water deficit conditions (Yildiz-Aktas et al., 2009). Conversely, TP were found to increase in other tolerant and sensitive genotypes of *G. hirsutum* cultivated in vivo with decreasing the watering level (Shah et al., 2011), evidencing again the complex response of plant phenolic metabolism to the drought stress. This complexity was also highlighted by the results reported by Sanchez-Rodríguez and colleagues, who found either increasing or decreasing trends for selected hydroxycinnamic acids and flavonoids, in leaves of different *Lycopersicon*

esculentum cultivars grown in vivo, in response to the decrease of the irrigation degree (Sanchez-Rodríguez et al., 2011). It should also be remarked that in the same study an erratic trend of phenolic compounds in response to the increase of water stress was also found within the same cultivar. The increase in coumarins observed in WT and *gr* transformed organisms, but not in *rolC*, could be interpreted as a further indication of a higher level of stress suffered by WT and *gr* genotypes, compared to *rolC*. In fact, even though esculetin and scopoletin (together with other coumarins) are considered plant secondary metabolites commonly involved in the response to biotic stress (Schenke et al., 2011), they can also be triggered by abiotic stress, since they display radical scavenging properties toward ROS (Bourgaud et al., 2006). It could be therefore hypothesized that a possible plant response mechanism was the increase of coumarins at the expense of phenolic acids, as proposed by Gutierrez and colleagues for *Helianthus annuus* under water stress induced by sucrose (Gutierrez et al., 1995).

A general increasing trend was found for sugar concentrations in both shoot and root of plants exposed to water stress, compared to the untreated ones. More in detail, glucose was interested by a statistically significant raise in all plant organs of the investigated genotypes, whereas for sucrose and, above all, fructose, the increasing trend was less important, being it in most cases statistically not significant. This trend was in general agreement with many literature studies in which a carbohydrate augment was determined in leaves or root of different species of plants exposed to water stress (Bajji et al., 2000; Khalid et al., 2010; Sanchez et al., 1998; Sasaki et al., 1998). The much higher increment observed for sucrose and especially glucose, the latter always showing statistically significant increase in response to the water stress, could be explained on the basis of their different role in plant metabolism. In fact, sucrose and particularly glucose, act as osmolites to maintain cell homeostasis, while fructose is not related to the

osmoprotection (Rosa et al., 2009). In this regard, it should be mentioned the work of Kameli and Losel (Kameli and Losel,1995), who highlighted a much larger contribution of glucose to the osmotic adjustment, compared to sucrose and fructose, in wheat leaves exposed to water stress. Thus, the much higher glucose concentrations found in either shoot or root of water-stressed *rolC* plants might confirm the better response capacity to water stress of this genotype. Moreover, according to Gray and Mower and Łabanowska and co-workers, the general higher abundance of soluble sugars in *rolC* transformed plants than in the other genotypes could be a source of a higher contribution to ROS scavenging (Łabanowska et al., 2013; Gray and Mower, 1991).

3.3 Effects of heat stress

3.3.1 Plant appearance and health status parameters

The exposure to 50 °C for two hours did not affect the plant appearance, irrespective of the plant genotype considered; however, a very different visual status was highlighted when the plants exposed to the heat stress were monitored after they were replaced at 25 °C for three weeks. In fact, plants modified for *rolC* (Fig. 3C and F) and especially *gr* gene insertion (Fig. 3B and E) showed a re-growth capability much higher than WT samples, most leaves of which were chlorotic and in some cases also wilted (Fig. 3A and D).

Electrolyte leakage data showed a picture quite similar to the one previously discussed for the water stress; in fact, for *rolC* no increase in the ion release was observed in response to the heat treatment, whereas values statistically higher in heat-stressed WT and *gr* plants than in the corresponding untreated samples, were determined. More in detail, the heat shock

treatment gave rise to a much higher augment of the mean ion release in WT (≈100%) than in *gr* (≈35%) leaves.

As expected on the basis of the low exposure time, the DW biomass was not affected by the heat exposure; moreover, no appreciable differences in response to the heat stress were observed also for water content, with the sole exception of WT shoot, for which the biomass decrease was however only about 2.5%. A greater reduction of the mean value of DW (approximately 6%) was observed in WT root, but the high standard deviation found in this case made the difference statistically insignificant. Therefore, among the physiological parameters determined herein as references of the plant health status, electrolyte leakage was the only one that showed statistically significant differences in response to the heat-shock. In particular, as previously observed for the hydric stress, the effect increased in the order *rolC* < *gr* << WT, being the first not statistically affected by the thermal treatment (Fig. 2).

The much higher electrolyte leakage found in WT leaves, compared to the other investigated genotypes, suggested a greater cell membrane impairment in shoot of untransformed plants.

With reference to the magnitude of stress suffered by transformed genotypes, it is interesting to note that, based on re-growth findings (Fig. 4) a different picture of the stress level suffered by *gr* and *rolC* plants is evidenced. In particular, *gr* plants were definitely not affected in their growth after the heat treatment, whereas the growth of *rolC* samples was much less influenced than that of WT organisms during the re-growing recovery period at 25 °C.

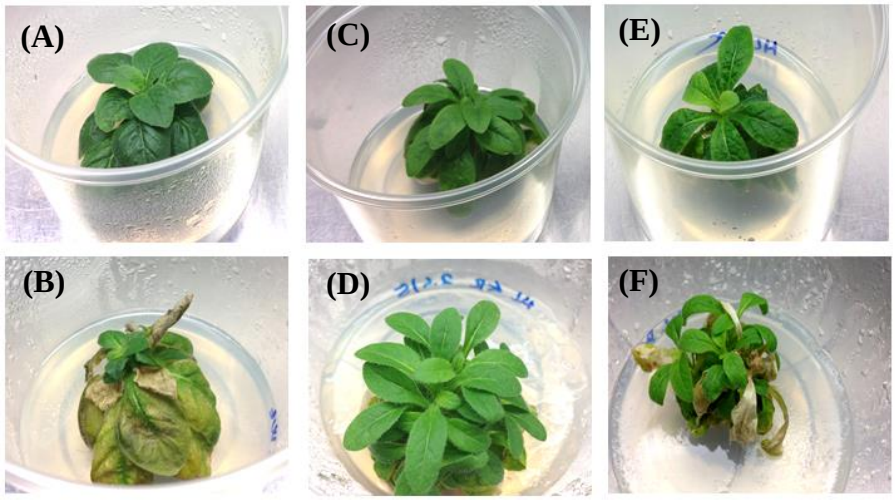

Figure 4. Re-growing capability of wild type and genetically modified *Nicotiana langsdorffii* plants in response to the heat stress (2 h at 50 °C) and after three weeks of recovering to standard temperature growth conditions. (A) Heat treated *N. langsdorffii* wild type; (B) heat treated and recovered *N. langsdorffii* wild type; (C) heat treated *N. langsdorffii gr*; (D) heat treated and recovered *N. langsdorffii gr*; (E) heat treated *N. langsdorffii rolC*; (F) heat treated and recovered *N. langsdorffii rolC*.

3.3.2 Chemical parameters and RSA

In root of all genotypes investigated a similar TP decrease was observed, whereas in shoot different trends were highlighted. In fact, in *gr* shoot a much higher TP decrease was evidenced, compared to *rolC*, whereas for WT shoot a slight increase was observed.

RSA values determined in shoot and root of WT, *gr* and *rolC* plants undergone to heat treatment followed trends very similar to those previously discussed for TP. Accordingly, statistically significant linear correlations were found yet again between the two parameters ($R^2 = 0.72$, $P<<0.01$ and $R^2 = 0.96$, $P<<0.01$, for root and shoot respectively).

The effect of heat treatments on the overall polyphenol biosynthesis was reported in literature for shoot of different species of plants, such as

Phaseolus vulgaris L. (Edreva et al., 1998), *Cucumis sativus* L. (Khan et al., 2012), *N. tabacum* L. (Ivanov et al., 2001) and *L. esculentum* L. (Rivero et al., 2001), whereas no data were reported for root. In these studies a general increase of TP was determined in response to the heat stress, in contrast to data obtained in our research for *gr* and *rolC* plants, as well as WT roots. This trend has been generally attributed to (i) an increase of activity of phenylalanine ammonia-lyase (PAL) that convert phenylalanine in transcinnamic acid, the precursor of polyphenols belonging to shikimate pathway, and (ii) the inhibition of polyphenol oxidase (PPO) and peroxidase (POD) that catalyse the oxidation of polyphenols and phenolic compounds (Wahid et al., 2007). However, plant response is strongly influenced by the exposure length and temperature value adopted for inducing the stress condition. In fact, in most of the aforementioned studies, in which TP increased as a consequence of the heat treatment, temperatures of 35-45 °C and exposure periods ranging from several days to weeks, were used to induce the heat stress, whereas, in our study, plants underwent a thermal shock at 50 °C for 2 h. Therefore, the different experimental conditions, with particular reference to the exposure period at high temperature, could be responsible of the diverse trends found. It should also be underlined that PPO activity is strongly influenced by the plant species, as well as the genotype under investigation, and regarding this latter aspect both increasing and decreasing PPO activity trends in response to heat shock treatments performed at 50 °C for 2 h were observed (Kayani et al., 2011). Furthermore, Moriwaki and co-workers (Moriwaki et al., 1999) reported that a heat shock treatment carried out at 44 °C for 5 h produced a decrease of PAL activity in *Nicotiana plumbaginifolia* shoot suggesting a possible reason of the TP decrease in plants sensitive to the heat stress. It is also noteworthy that for tobacco plants exposed to the temperature of 45 °C for 5 h during a 24 h cycle, a decrease of TP after the first cycle of treatment was observed, followed by a strong increase of polyphenol concentrations in the

later 72-168 h (Ivanov et al., 2001). Based on this last consideration, the different trends observed for both TP and RSA in shoot of the sensitive genotypes (i.e. WT and *gr*), in response to the heat treatment, should not be considered as surprising.

Different trends were observed in our study for phenolic compounds deriving directly from the shikimate pathway, depending on the genetic modification, the plant organ and the compound taken into account, evidencing one more time the complex response of plant phenolic metabolism to abiotic stress (Table 2). Some general considerations can be however attempted, in order to summarise the effects of the heat treatment. The increase observed for all genotypes, especially in shoot, for p-coumaric acid, which is the common precursor of phenolic substances deriving from shikimic acid, may represent a clear indicator of the metabolic shift due to the heat treatment. The more intense response observed in shoot for p-coumaric acid, as well as other phenolics, agreed with the stress application mode, which is reasonably sensed with a greater extent by aerial tissues. Interestingly, significant differences in the metabolic shifts of chlorogenic acids in response to the heat treatment were observed in shoot, downstream the p-coumaric acid biosynthesis, since their concentrations decreased in *gr* and raised in *rolC* and, especially, WT tissues.

The concentration increase of some phenolics observed in *rolC* plants was in contrast with the decrease of TP observed in the same samples, but agreed with literature data concerning long-term treatment experiments that, as above-mentioned, highlighted a net up-regulation of phenolic biosynthesis in response to the heat (Wahid et al., 2007; Ivanov et al., 2001; Rivero et al., 2001). The different profiles observed in response to the treatment with high temperatures for individual phenolic compounds and TP, could be linked to a more rapid metabolic response of the shikimate pathway, compared to the biosynthesis of more complex polyphenols. It should be however noted that the general net increase of phenolic

compounds is in contrast with electrolyte leakage data that suggested a tolerant behaviour of the *rolC* genotype. In this regard, it is important to mention that, according to the previously described re-growth findings (Fig. 4), *gr* plants seem to be not affected by the heat treatment, whereas the growth of *rolC* samples was much less influenced than that of WT organisms during the re-growing recovery period at 25 °C. Based on these findings, it seems that the particular trend of TP, RSA and individual phenolics found in WT, rather than in *rolC* and especially *gr* samples could represent a metabolic indication of the different re-growing capabilities.

A general decreasing trend was found for sugar concentrations in response to the heat treatment, even though the extent of decrease depended on the compound, the plant organ and, above all, the genotype examined (Table 2). More in detail, in shoot of WT plants the heat shock induced a significant decrease only for fructose, whereas sucrose and glucose were not significantly affected by the treatment. In root the decrease of fructose concentration was confirmed and also a statistically significant decline of sucrose concentration was highlighted. For *gr* plants, the trend of sugars in response to the heat treatment was quite similar to the one observed in WT samples, with the only exception of the statistically significant decrease of sucrose in shoot. Finally, a statistically significant concentration decrease was observed for all the investigated sugars in both shoot and root of plants modified for *rolC* gene insertion.

The observed decline in sugar concentrations, strongly differentiated the response to the heat stress from the one due to the water deficit. Our data were in agreement with literature results obtained on *Agrostis stolonifera* L. (Liu and Huang, 2000) and *Nicotiana sylvestris* L. (Kuznetsov and Shevyakova, 1997). In particular, it should be noted that the heat stress conditions employed in the latter study (40 °C for 5 h) were very similar to those adopted in our investigation. Interestingly, the general decline in sucrose concentrations mainly observed in *gr* and *rolC* plants is in

agreement with the findings of Scalabrin and coworkers, who evidenced a higher increase of trichome-specific *Nicotiana* acylsucroses in the aforementioned transformed genotypes than in WT plants, suggesting a defense role of carbohydrates against heat stress (Scalabrin et al., 2015).

4 Conclusions

The insertion of *rolC* and above all *gr* genes induced a basal up-regulation of the phenolic secondary metabolism that may contribute to a better plant response against free radicals produced in consequence of exposure to abiotic stress.

Actually, *gr* and *rolC* plants were more tolerant than WT organisms to water and heat stress. In particular, the *rolC* gene insertion conferred the best response capacity against water stress, whereas *gr* transformed organisms had the highest tolerance to the heat stress. In this regard it should be remarked that the greater resistance observed in this study for *gr* and *rolC* plants was in agreement with the enhanced tolerance observed in a previous research for genetically transformed *N. langsdorffii* exposed to hexavalent chromium (Del Bubba et al., 2013).

According to the present and previous results concerning *N. langsdorffii* genetically modified with the *gr* gene (Del Bubba et al., 2013), the transformation of other plant species could be worth of future investigations, focusing on their practical applications.

The significant changes observed in phenolic and sugar concentrations after exposure to water deficit and heat treatment confirmed the very complex plant metabolic response to these abiotic stress, elsewhere evidenced, as well (Scalabrin et al., 2015).

Data concerning soluble sugars and especially phenolic compounds were informative of the stress condition suffered by plants during the abiotic stress, particularly for the long-term effects due to heat shock treatment.

Under this point of view, transgenic *N. langsdorffii* seems to represent an interesting tool for better elucidating the metabolic pathway involved in the plant response to abiotic stress. Our results confirmed the role of metabolomics, and especially of metabolomic analysis of phenols, to understand some important effects of plant exposure to stress factors.

5 Contributions

Patrizia Bogani planned and performed the transformation experiments to produce plants for stress treatments, and contributed to the genetic analyses and manuscript preparation. Elisa Calistri performed the stress experiments. Stefano Biricolti and Cristina Gonnelli performed physiological analyses and contributed to the genetic analyses and manuscript preparation.
Claudia Ancillotti performed the analysis of sugars, antiradical/antioxidant activity and total polyphenols. Lorenzo Ciofi and Leonardo Checchini performed the analysis of individual phenolics. Massimo Del Bubba performed the statistical elaboration of the data and wrote most of the manuscript.

Acknowledgements

This work was supported by the PRIN grant from the Italian Ministry of Education, University and Research (MIUR) (PRIN 2009 protocol 20098TN4CY).

References

Ahuja, I., de Vos, R.C.H., Bones, A.M., Hall, R.D., 2010. Plant molecular stress responses face climate change. Trends Plant Sci. 15, 664-674.

Al-Quraan, N.A., Locy, R.D., Singh, N.K., 2010. Expression of calmodulin genes in wild type and calmodulin mutants of Arabidopsis thaliana under heat stress. Plant Physiol. Biochem. 48, 697-702.

Bajji, M., Lutts, S., Kinet, J.M., 2000. Physiological changes after exposure to and recovery from polyethylene glycol-induced water deficit in roots and leaves of durum wheat (Triticum durum Desf.) cultivars differing in drought resistance. J. Plant Physiol. 157, 100-108.

Bajji, M., Kinet, J.-M., Lutts, S., 2002. The use of the electrolyte leakage method for assessing cell membrane stability as a water stress tolerance test in durum wheat,. Plant Growth Regul. 36, 61-70.

Barcelo, J., Poschenrieder, C., 1990. Plant water relations as affected by heavy metal stress: a review. J. Plant Nutr. 13, 1-37.

Bettini, P., Baraldi, R., Rapparini, F., Melani, L., Mauro, M.L., Bindi, D., Buiatti, M., 2010. The insertion of the Agrobacterium rhizogenes *rolC* gene in tomato (*Solanum lycopersicum* L.) affects plant architecture and endogenous auxin and abscisic acid levels,. Sci. Hortic. Amst. Neth. 123, 323-328.

Bogani, P., Intrieri, M.C., Buiatti, M., 2012. Genetic and epigenetic factors in the control of dedifferentiation/tumourisation in *Nicotiana* species and hybrids. Plant Biosyst. e Int. J. Deal. All Aspects Plant Biol. 146, 511-521.

Bogani, P., Calistri, E., Biricolti, S., Castiglione, M.R., Turrini, A., Giovannetti, M., Buiatti, M., 2015. The rat glucocorticoid receptor integration in *Nicotiana* langsdorffii genome affects plant responses to abiotic stresses and to arbuscular mycorrhizal symbiosis,. Plant Biotechnol. Rep. 9, 209-220.

Bonhomme, V., Laurain-Mattar, D., Fliniaux, M.A., 2000. Effects of the rol C Gene on hairy Root: Induction development and tropane alkaloid production by Atropa belladonna. J. Nat. Prod. 63, 1249-1252.

Bourgaud, F., Hehn, A., Larbat, R., Doerper, S., Gontier, E., Kellner, S., Matern, U., 2006. Biosynthesis of coumarins in plants: a major pathway still to be unraveled for cytochrome P450 enzymes. Phytochem. Rev. 5, 293-308.

Bulgakov, V.P., 2008. Functions of rol genes in plant secondary metabolism. Biotechnol. Adv. 26, 318-324.

Bulgakov, V.P., Tchernoded, G.K., Mischenko, N.P., Khodakovskaya, M.V., Glazunov, V.P., Radchenko, S.V., Zvereva, E.V., Fedoreyev, S.A., Zhuravlev, Y.N., 2002. Effect of salicylic acid, methyl jasmonate, ethephon and cantharidin on anthraquinone production by Rubia cordifolia callus cultures transformed with the rolB and rolC genes. J. Biotechnol. 97, 213-221.

Bulgakov, V.P., Aminin, D.L., Shkryl, Y.N., Gorpenchenko, T.Y., Veremeichik, G.N., Dmitrenok, P.S., Zhuravlev, Y.N., 2008. Suppression of reactive oxygen species and enhanced stress tolerance in Rubia cordifolia cells expressing the rolC oncogene. Mol. Plant-Microbe Interact. 21, 1561-1570.

Bulgakov, V.P., Shkryl, Y.N., Veremeichik, G.N., Gorpenchenko, T.Y., Vereshchagina, Y.V., 2013. Recent advances in the understanding of agrobacterium rhizogenes-derived genes and their effects on stress resistance and plant metabolism. Adv. Biochem. Eng. Biotechnol. 134, 1-22.

Cabello, J.V., Arce, A.L., Chan, R.L., 2012. The homologous HD-Zip I transcription factors HaHB1 and AtHB13 confer cold tolerance via the induction of pathogenesis-related and glucanase proteins,. Plant J. 69, 141-153.

Cabello, J.V., Lodeyro, A.F., Zurbriggen, M.D., 2014. Novel perspectives for the engineering of abiotic stress tolerance in plants. Curr. Opin. Biotechnol. 26, 62-70.

Cardarelli, M., Mariotti, D., Pomponi, M., Spano, L., Capone, I., Costantino, P., 1987. Agrobacterium rhizogenes T-DNA genes capable of inducing hairy root phenotype. Mol. Gen. Genet. 209, 475-480.

Chamoli, S., Verma, A.K., 2014. Targeting of metabolic pathways for genetic engineering to Combat abiotic stress tolerance in crop plants. In: Gaur, R.K., Sharma, P. (Eds.), Approaches to Plant Stress and Their Management, Springer India, pp. 23-37.

Christensen, B., Mueller, R., 2009. Kalanchoe blossfeldiana transformed with rol genes exhibits improved postharvest performance and increased ethylene tolerance. Postharvest Biol. Technol. 51, 399-406.

Cramer, G., Urano, K., Delrot, S., Pezzotti, M., Shinozaki, K., 2011. Effects of abiotic stress on plants: a systems biology perspective. BMC Plant Biol. 11, 163.

Cvikrova, M., Gemperlova, L., Martincova, O., Vankova, R., 2013. Effect of drought and combined drought and heat stress on polyamine metabolism in prolineover-producing tobacco plants. Plant Physiol. Biochem. 73, 7-15.

Del Bubba, M., Ancillotti, C., Checchini, L., Ciofi, L., Fibbi, D., Gonnelli, C., Mosti, S., 2013. Chromium accumulation and changes in plant growth, selected phenolics and sugars of wild type and genetically modified *Nicotiana langs*dorffii. J. Hazard. Mater. 262, 394-403.

Edreva, A., Yordanov, I., Kardjieva, R., Gesheva, E., 1998. Heat shock responses of bean plants: involvement of free radicals, antioxidants and free radical/active oxygen scavenging systems. Biol. Plant. 41, 185-191.

Estruch, J.J., Chriqui, D., Grossmann, K., Schell, J., Spena, A., 1991. The plant oncogene rolC is responsible for the release of cytokinins from glucoside conjugates,. EMBO J. 10, 2889-2895.

Fladung, M., Ballvora, A., 1992. Further characterization of rollC transgenic tetraploid potato clones, and influence of daylength and level of rolC expression on yield parameters. Plant Breed. 109, 18-27.

Fuoco, R., Bogani, P., Capodaglio, G., Del Bubba, M., Abollino, O., Giannarelli, S., Spiriti, M.M., Muscatello, B., Doumett, S., Turetta, C., Zangrando, R., Zelano, V., Buiatti, M., 2013. Response to metal stress of *Nicotiana langsdorffii* plants wildtype and transgenic for the rat glucocorticoid receptor gene. J. Plant Physiol. 170, 668-675.

Giannarelli, S., Muscatello, B., Bogani, P., Spiriti, M.M., Buiatti, M., Fuoco, R., 2010. Comparative determination of some phytohormones in wild-type and genetically modified plants by gas chromatographyemass spectrometry and high performance liquid chromatography/tandem mass spectrometry. Anal. Biochem. 398, 60-68.

Gray, J., Mower, H.F., 1991. The role of simple carbohydrates in the suppression of hydroxyl free radicals in ·γ-irradiated papaya juice,. Food Chem. 41, 293-301.

Grover, A., Mittal, D., Negi, M., Lavania, D., 2013. Generating high temperature tolerant transgenic plants: Achievements and challenges. Plant Sci. 205-206, 38-47.

Gutierrez, M.-C., Parry, A., Tena, M., Jorrin, J., Edwards, R., 1995. Abiotic elicitation of coumarin phytoalexins in sunflower. Phytochemistry 38, 1185-1191.

Heid, C.A., Stevens, J., Livak, K.J., Williams, P.M., 1996. Real time quantitative PCR. Genome Res. 6, 986-994.

Hoebeeck, J., 2007. Real-time quantitative PCR as an alternative to Southern blot or fluorescence in situ hybridization for detection of

gene copy number changes. In: Hilario, E., Mackay, J. (Eds.), Protocols for Nucleic Acid Analysis by Nonradioactive Probes. Humana Press Inc., Totowa, pp. 205-226.

Horsch, R., Simple, A., Method, General, 1985. For transferring genes into plants. Science 227, 1229-1231.

Hussain, S., Hussain, M.A., Kayani, M., Amjad, S., 2011. Transcription factors as tools to engineer enhanced drought stress tolerance in plants. Biotechnol. Prog. 27, 297-306.

Huve, K., Huve, I., Bichele, M., Tobias, U.L.O., Niinemets, K., 2006. Huve, heat sensitivity of photosynthetic electron transport varies during the day due to changes in sugars and osmotic potential. Plant Cell Environ. 29, 212-228.

Irdani, T., Bogani, P., Mengoni, A., Mastromei, G., Buiatti, M., 1998. Construction of a new vector conferring methotrexate resistance in *Nicotiana tabacum* plants. Plant Mol. Biol. 37, 1079-1084.

Irdani, T., Caroppo, S., Ambrogioni, L., 2003. Response of *Nicotiana tabacum* plants overexpressing a glucocorticoid receptor to Meloidogyne incognita (Nematoda tylenchila) infestation. Redia 86, 4.

Irdani, T., Pastorelli, R., Scotto, C., Bogani, P., 2010. a nuclear steroid receptor expressed in tobacco: gene-regulation and effects on plant development. J. Biotechnol. 150, 475. Suppl.

Ivanov, S., Konstantinova, T., Parvanova, D., Todorova, D., Djilianov, D., Alexieva, V., 2001. Effect of high temperatures on the growth, free proline content and some antioxidants in tobacco plants. Comptes Rendus l'Acad. Bulg. Sci. 54, 71.

Kameli, A., L€osel, D.M., 1995. Contribution of carbohydrates and other solutes to osmotic adjustment in wheat leaves under water stress. J. Plant Physiol. 145, 363-366.

Kayani, W.K., Abdul Majid, S., Mahmood, T., Naqvi, S., Waheed, A., 2011. Effect of temperature stress on polyphenol oxidase activity in grains of some wheat cultivars. Pak. J. Bot. 43, 1011-1020.

Khalid, K.A., Teixeira da Silva, J.A., Cai, W., 2010. Water deficit and polyethylene glycol 6000 affects morphological and biochemical characters of Pelargonium odoratissimum (L.). Sci. Hortic. 125, 159-166.

Khan, A., Hamayun, M.,Waqas, M., Kang, S.-M., Kim, Y.-H., Kim, D.-H., Lee, I.-J., 2012. Exophiala sp.LHL08 association gives heat stress tolerance by avoiding oxidative damage to cucumber plants. Biol. Fertil. Soils 48, 519-529.

Kotak, S., Larkindale, J., Lee, U., von Koskull-D€oring, P., Vierling, E., Scharf, K.-D., 2007. Complexity of the heat stress response in plants. Curr. Opin. Plant Biol. 10, 310-316.

Kuznetsov, V.V., Shevyakova, N.I., 1997. Stress responses of tobacco cells to high temperature and salinity. Proline accumulation and phosphorylation of polypeptides. Physiol. Plant. 100, 320-326.

Łabanowska, M., Filek, M., Kurdziel, M., Bidzinska, E., Miszalski, Z., Hartikainen, H., 2013. EPR spectroscopy as a tool for investigation of differences in radical status in wheat plants of various tolerances to osmotic stress induced by NaCl and PEG-treatment. J. Plant Physiol. 170, 136-145.

Liu, X., Huang, B., 2000. Carbohydrate accumulation in relation to heat stress tolerance in two creeping bentgrass cultivars. J. Am. Soc. Hortic. Sci. 125, 442-447.

Macedo, A., 2012. Abiotic stress responses in plants: metabolism to productivity. In: Ahmad, P., Prasad, M.N.V. (Eds.), Abiotic Stress Responses in Plants, Springer New York, pp. 41-61.

Mittler, R., Mittler, S., Vanderauwera, N., Suzuki, G., Miller, V., Tognetti, K., Vandepoele, M., Gollery, V., Shulaev, F., Van Breusegem, R.,

2011. Mittler, ROS signaling: the new wave? Trends Plant Sci. 16, 300-309.

Moriwaki, M., Moriwaki, T., Yamakawa, T., Washino, T., Kodama, Y., Igarashi, M., 1999., Suppressed phenylalanine ammonia-lyase activity after heat shock in transgenic *Nicotiana plumbaginifolia* containing an Arabidopsis HSP18.2-Parsley PAL2 chimera gene. J. Biosci. Bioeng. 87, 588-593.

Niu, S., Luo, Y., Li, D., Cao, S., Xia, J., Li, J., Smith, M.D., 2014. Plant growth and mortality under climatic extremes: an overview. Environ. Exp. Bot. 98, 13-19.

Patakas, A., 2012. Abiotic stress-induced morphological and anatomical changes in plants. In: Ahmad, P., Prasad, M.N.V. (Eds.), Abiotic Stress Responses in Plants, Springer New York, pp. 21-39.

Prabha, R., Singh, D.P., Keshri, V., Sharma, A.K., 2014. Bioinformatics resources for the management of biological information on plant responses towards stresses. In: Approaches to Plant Stress and Their Management, Springer, pp. 365-382.

Prinsen, E., Chriqui, D., Vilaine, F., Tepfer, M., Onckelen, H.V., 1994. Endogenous phytohormones in tobacco plants transformed with Agrobacterium rhizogenes pRi TL-DNA genes. J. Plant Physiol. 144, 80-85.

Qu, A.-L., Ding, Y.-F., Jiang, Q., Zhu, C., 2013. Molecular mechanisms of the plant heat stress response. Biochem. Biophys. Res. Commun. 432, 203-207.

Rhee, S.Y., Mutwil, M., 2013. Towards revealing the functions of all genes in plants. Trends Plant Sci. 19 (4), 212-221.

Rivero, R.M., Ruiz, J.M., Garcıa, P.C., Lopez-Lefebre, L.R., Sanchez, E., Romero, L., 2001. Resistance to cold and heat stress: accumulation of phenolic compounds in tomato and watermelon plants. Plant Sci. 160, 315-321.

Rosa, M., Rosa, C., Prado, G., Podazza, R., Interdonato, J., Gonzalez, M., Hilal, F., 2009. Soluble sugars: metabolism, sensing and abiotic stress: a complex network in the life of plants,. Plant Signal. Behav. 4, 388-393.

Sanchez, F.J., Manzanares, M.A., de Andres, E.F., Tenorio, J.L., Ayerbe, L., 1998. Turgor maintenance, osmotic adjustment and soluble sugar and proline accumulation in 49 pea cultivars in response to water stress. Field Crops Res. 59, 225-235.

Sanchez-Rodríguez, E., Moreno, D.A., Ferreres, F., Rubio-Wilhelmi, M.d.M., Ruiz, J.M., 2011. Differential responses of five cherry tomato varieties to water stress: changes on phenolic metabolites and related enzymes. Phytochemistry 72, 723-729.

Sasaki, H., Ichimura, K., Okada, K., Oda, M., 1998. Freezing tolerance and soluble sugar contents affected by water stress during cold-acclimation and deacclimation in cabbage seedlings. Sci. Hortic. 76, 161-169.

Scalabrin, E., Radaelli, M., Rizzato, G., Bogani, P., Buiatti, M., Gambaro, A., Capodaglio, G., 2015. Metabolomic analysis of wild and transgenic *Nicotiana langsdorffii* plants exposed to abiotic stresses: unraveling metabolic responses. Anal. Bioanal. Chem. 1-12.

Schachtman, D.P., Goodger, J.Q.D., 2008. Chemical root to shoot signaling under drought. Trends Plant Sci. 13, 281-287.

Schenke, D., Bottcher, C., Scheel, D., 2011. Crosstalk between abiotic ultraviolet-B stress and biotic (flg22) stress signalling in Arabidopsis prevents flavonol accumulation in favor of pathogen defence compound production, Plant. Cell Environ. 34, 1849-1864.

Schmuelling, T., Fladung, M., Grossmann, K., Schell, J., 1993. Hormonal content and sensitivity of transgenic tobacco and potato plants expressing single rol genes of Agrobacterium rhizogenes T-DNA. Plant J. 3, 371-382.

Shah, A.R., Khan, T.M., Sadaqat, H.A., Chatha, A.A., 2011. Alterations in leaf pigments in cotton (Gossypium hirsutum) genotypes subjected to drought stress conditions. Int. J. Agric. Biol. 13, 902-908.

Shkryl, Y.N., Veremeichik, G.N., Bulgakov, V.P., Tchernoded, G.K., Mischenko, N.P., Fedoreyev, S.A., Zhuravlev, Y.N., 2008. Individual and combined effects of the rolA, B, and C genes on anthraquinone production in Rubia cordifolia transformed calli. Biotechnol. Bioeng. 100, 118-125.

Suzuki, N., Suzuki, S., Koussevitzky, R.O.N., Mittler, G.A.D., Miller, N., 2012. Suzuki, ROS and redox signalling in the response of plants to abiotic stress. Plant Cell Environ. 35, 259-270.

Tejavathi, D., 2010. Effect of PEG induced osmotic stress on proline, protein and relative water content in in vitro plants of Macrotyloma uniflorum (Lam.) Verdc. Acta Hortic. 865, 87.

Tripathi, P., Rabara, R., Rushton, P., 2014. A systems biology perspective on the role of WRKY transcription factors in drought responses in plants. Planta 239, 255-266.

Urano, K., Kurihara, Y., Seki, M., Shinozaki, K., 2010. 'Omics' analyses of regulatory networks in plant abiotic stress responses. Curr. Opin. Plant Biol. 13, 132-138.

van der Weele, C.M., Spollen, W.G., Sharp, R.E., Baskin, T.I., 2000. Growth of Arabidopsis thaliana seedlings under water deficit studied by control of water potential in nutrient-agar media. J. Exp. Bot. 51, 1555-1562.

Wahid, A., Gelani, S., Ashraf, M., Foolad, M., 2007. Heat tolerance in plants: an overview. Environ. Exp. Bot. 61, 199-223.

Yildiz-Aktas, L., Dagnon, S., Gurel, A., Gesheva, E., Edreva, A., 2009. Drought tolerance in cotton: involvement of non-enzymatic ROS-scavenging compounds. J. Agron. Crop Sci. 195, 247-253.

Yokotani, N., Ichikawa, T., Kondou, Y., Iwabuchi, M., Matsui, M., Hirochika, H., Oda, K., 2013. Role of the rice transcription factor JAmyb in abiotic stress response. J. Plant Res. 126, 131-139.

Yuan, J.S., Galbraith, D.W., Dai, S.Y., Griffin, P., Stewart Jr., C.N., 2008. Plant systems biology comes of age. Trends Plant Sci. 13, 165-171.

Manuscript: "Polyphenol and sugar contents of wild type and genetically modified *Nicotiana langsdorffii* in response to water and heat stress" by C. Ancillotti et al.

SUPPLEMENTARY MATERIAL

S.1 Molecular analysis of transformed N. langsdorffii plants

S.1.1. Transgene copy number analysis using real-time quantitative PCR

The analysis of the copy number of transgenes was performed using the real-time PCR technique according to the TaqMan® chemistry. Primers pairs and fluorogenic probes were designed on *gr* gene (accession number M14053) and *rolC* gene (accession number X03433.1) using qPCR Primer & Probe Design service of Eurofins MWG Operon (Germany) (http://www.eurofinsdna.com/home.html). *gr*-Probe and *rolC*-probe were modified with fluorescein (6-FAM) on their 5' ends and TAMRA Quencher on their 3' ends. Real-time PCR assays were carried out in triplicate in the 7300 Real-Time PCR System (Applied Biosystems, Life Technology, Milan, Italy) with a final volume of 25 µL. The PCR reaction mixture contained 12.5 µL TaqMan® Universal PCR Master Mix 2X (Applied Biosystems), 300 ng each primer, 5 µM probes and 5 ng genomic DNA. PCR reactions were run with the following conditions: 2 min at 50°C, 10 min at 95°C and 40 cycles of 15 s at 95°C and 1 min at 60°C. A standard curve-based quantification method was applied for calculating PCR efficiency and interpolating unknown sample quantities. Standard reference curve was performed in triplicate in 25 µL PCR reaction containing 5 ng genomic DNA from *Nicotiana* wild type plants spiked with 1, 5, 10, 15, 20

copies of pTI18 vector, containing the rat *gr* gene, or pUC19 plasmid, containing the *A. rhizogenes rolC* gene, respectively. To determine the plasmid copy number, we calculated the weight of each DNA plasmid single copy as follows: [plasmid length (bp) x103 x660]/6.02 x1023 = g plasmid vector. Since the weight of haploid *N. langsdorffii* genomic DNA is 4.25 pg (NCBI), the total number of genome copies contained in 5 ng is 1176. In order to have 1 copy of vector per *Nicotiana* haploid genome 1176 copies of the plasmid vector were added to 5 ng genomic DNA. Primers for real time amplification on gr gene were GR-RTfw: 5'-GAAGGAAAAACTGCCCAGCAT-3' (forward) and *GR*-RTrev: 5'-TTTTCGAGCTTCAAGGTTCATT-3' (reverse), and the sequence of the internal probe was 5'-CCGCTATCGAAAATGTCTTCAGGC-3'. Primers for real time amplification on *rolC* gene were rolCArhiFW: 5'-TTCGGTTACGCGGATCCTAT-3' (forward) and *rolC*ArhiRev: 5'-CACGCCCAGGGAAAGAAAAT-3' (reverse), and the sequence of the internal probe was 5'-CGGAGCGCCTACTTCGCTGCA-3'. Data were analysed with 7300 system SDS software, 1.2.3 version (Applied Biosystems) and Microsoft Excel (Microsoft, Redmont, WA, USA).

Results showed that the copy number of the integrated *gr* gene per haploid *Nicotiana* genome, varied from 1 copy in the transgenic lines indicated as *GR*2, *GR*4, *GR*6, *GR*7 and *GR*9, to 2 copies present in *GR*1, *GR*3, *GR*5 and *GR*10 or 3 copies in *GR*8 plant (Fig. S1-A). In the GR7-primary transgenic plant, transgene is present as a single hemizygous copy. This finding was confirmed in different individuals of the selfed T3 progeny (data not shown).

The *rolC* transgene was found to be present as one single copy in the transgenic lines *rolC*8, *rolC*16 and *rolC*211 selected lines, whereas 3 copies were detected in rolC11 (Fig. S1-B).

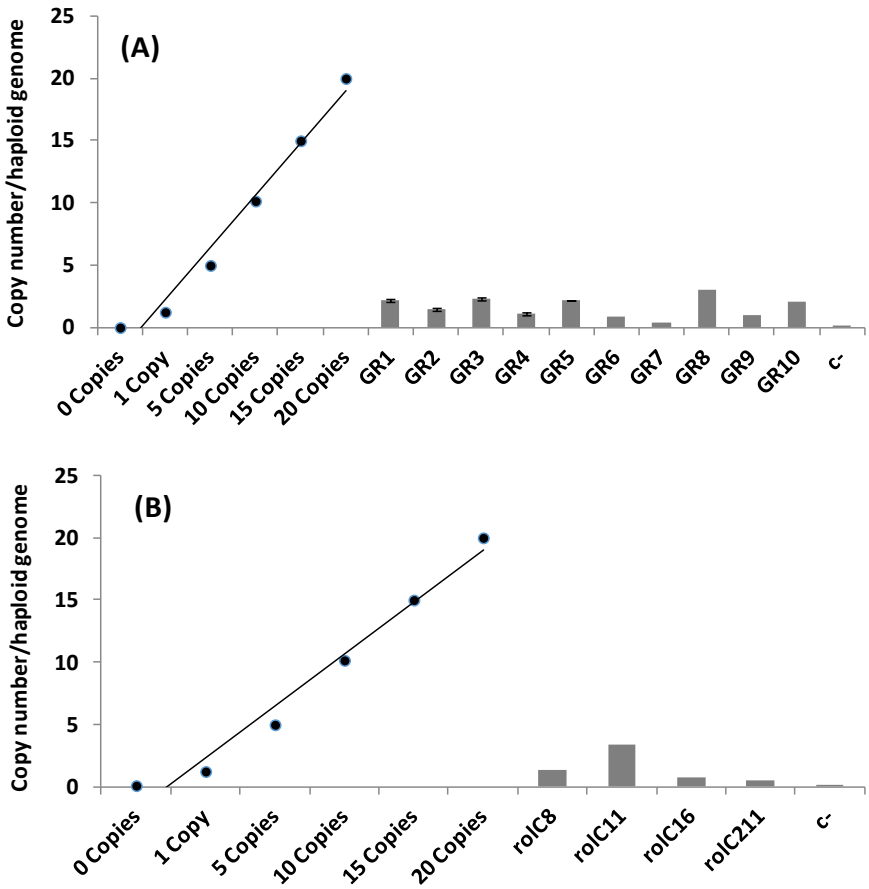

Figure S1. Mean results (n=5) obtained by real-time PCR on the copy number of *gr* (A) and *rolC* (B) transgenes integrated in ten and four independent transgenic primary T_0 lines, respectively. Standard reference curves for assessing *gr* (R^2=0.9742) and *rolC* (R^2=0.9728) copy number were performed in PCR reaction. Genomic DNA from wild type *N. langsdorffii* was spiked with 0, 1, 5, 10, 15, 20 copies of pTI18 vector, integrating the rat *gr* gene or pUC19 plasmid, integrating the *A. rhizogenes rolC* gene. WT: *N. langsdorffii* wild type; *GR*1-*GR*10: independent *GR* transgenic primary plants; *rolC*8, *rolC*11, *rolC*16 and *rolC*211: independent *rolC* transgenic primary plants. c- is the negative control of the PCR. Error bars represent the standard deviation.

S.1.2. RNA extraction

Leaves from axenic transgenic and wild type *Nicotiana* plantlets were harvested and immediately frozen in liquid nitrogen prior RNA isolation. 100-500 mg of fresh tissue were then homogenized with a pestle and mortar and total RNA was extracted following instructions of the Macherey-Nagel ‘‘Nucleospin RNA Plant’’ kit. RNA obtained was treated with 0.1 U/µL DNase I (Roche Diagnostics, Milan, Italy) overnight at 37°C. Total RNA was then precipitated with 2.5 M LiCl at -20°C for 2 h, washed twice in 70% ethanol and resuspended in sterile distilled water. RNA was then spectrophotometrically quantified at 260 nm and stored at -80°C until further use. To check for DNA contamination 1 µg total RNA was used as template in a PCR amplification reaction.

S.1.3. Real time RT-PCR

1 µg of total RNA from transgenic and untransformed *Nicotiana* leaves was reverse transcribed according to specifications of the First Strand cDNA Synthesis kit for RT-PCR (AMV) (Roche Diagnostics, Milan, Italy). Real-time RT-PCR for the quantitative expression analysis of *gr* and *rolC* genes was performed with an ABI Prism 7700 System using the TaqMan® technology (Applied Biosystems). PCR reactions were performed in five replicates in a 25 µL volume using 300 ng each forward and reverse primers, 5 µM of the TaqMan fluorogenic probe, 12.5 µL of TaqMan® Universal PCR Master Mix 2X and 5 µL of cDNA samples. Transcript levels of *gr* or *rolC* transgenes in the RNA samples were normalized with transcript levels of the *gr* or *rolC* coding sequence, PCR amplified and subcloned in the pBluescript II SK vector (Stratagene). For each TaqMan assay a reference calibration curve was prepared containing 0.1, 0.01, 0.001, 0.0001, 0.00001 and 0.0000001 ng of the retrotranscribed Bluescript plasmid. Retrotranscription of the plasmid was performed with the

Maxiscript kit from Ambion. Primers and probes used for the amplification of *gr* and *rolC* cDNAs were those used for the analysis of the copy number of the genes. Reactions were performed in MicroAmp 96-well plates (Applied Biosystems). Samples were subjected to one cycle of 2 min at 50°C, one cycle of 10 min at 95°C, and 50 cycles at 95°C for 15 sec, followed by anneal extension at 60°C for 1 min.

As regards the *gr* transcription profiles, amounts of *gr*-mRNA/µg RNA ranged from 0.081 to 0,49 pg/µg RNA in *GR*5 and *GR*9 transgenic lines, respectively (Fig. S2-A).

The transgenic lines *rolC*8, *rolC*16 and *rolC*211expressed 0.01, 0.014 and 0.0025 pg rolC-mRNA/µgRNA, respectively; rolC11, which integrated three copies, showed the lowest level of expression (0.0018 pg rolC-mRNA/µgRNA) (Fig. S2-B).

S.1.4. Reverse-transcription PCR

Reverse transcription PCR (RT-PCR) was performed on different individuals of the T1 selfed progeny to confirm the expression of these two transgenes. RT-PCR was performed with the "Transcriptor One-Step RT-PCR" Kit (Roche Diagnostics, Milan, Italy) following the manufacturer's instructions. Control amplifications lacking the reverse transcriptase enzyme were always included to confirm the absence of contaminating DNA.

GR primers used for retro-transcription reactions were DBDtop: 5'-CAGATGTAAGCTCTCTCCAT-3' (forward) and HDBbottom: 5'-GGAACTGAGGAGAGAAGCAG-3' (reverse). rolC expression was evaluated with the following specific RolC primers: 5'-ATGGCTGAAGACGACCTGTGT-3' (forward) and 5'-TCATCGAGAGTCACATCATGC-3' (reverse).

The amplification of an expected 822 bp fragment from GR cDNA samples (Fig. S3) and an expected 300 bp rolC cDNA samples (Fig. S4) is shown for all transgenic lines. No signal was obtained with cDNA from not transformed *N. langsdorffii* plants.

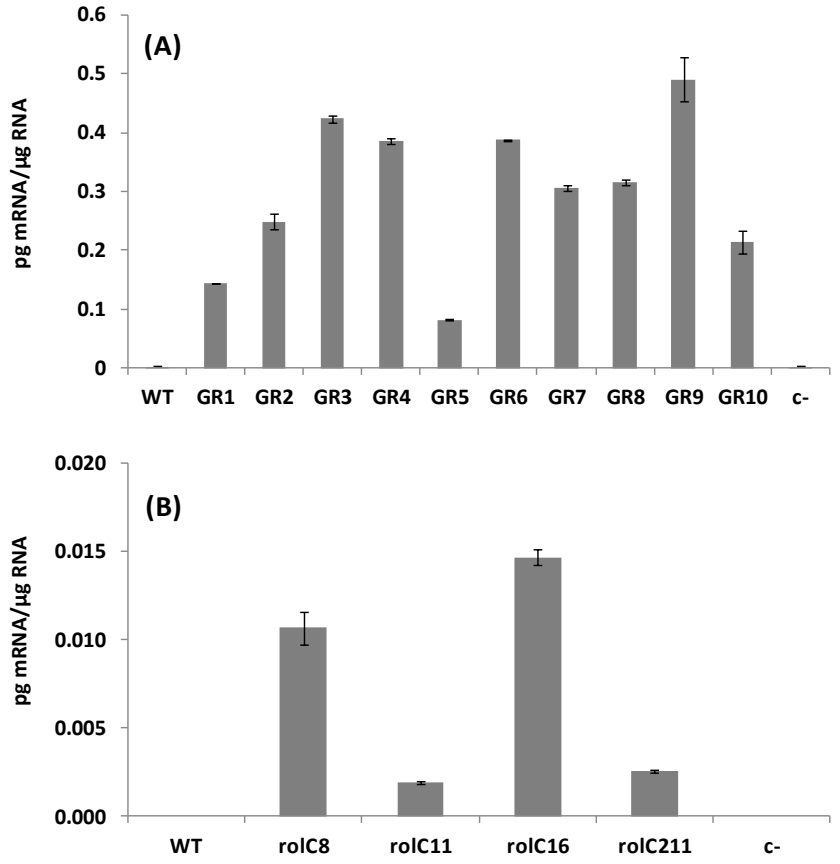

Figure S2. Mean results (n=5) obtained by real-time PCR on expression levels of *gr* (A) and *rolC* (B) transgenes integrated in ten and four independent transgenic primary T_0 lines, respectively. WT: *N. langsdorffii* wild type; *GR*1-*GR*10: independent *GR* transgenic primary plants; *rolC*8, *rolC*11, *rolC*16 and *rolC*211: independent *rolC* transgenic primary plants. c- is the negative control of the PCR. Error bars represent the standard deviation.

Figure S3. RT-PCR analysis of *gr* gene in transgenic *Nicotiana langsdorffii* GR T_1 plants (GR1-GR10) obtained from the corresponding primary transformants. WT: untransformed controls; c-: amplification control without DNA; c+: amplification from DNA of pTI18 plasmid (822 bp) used as positive control; M: Molecular weight marker (GeneRuler 100 bp Plus DNA Ladder, Fermentas, Thermo Scientific).

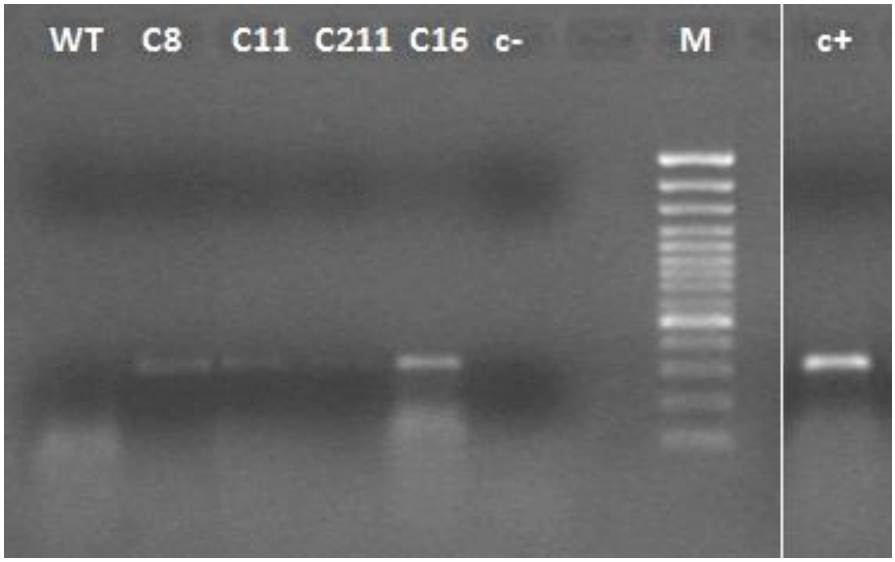

Figure S4. RT-PCR analysis of *rol*C gene in transgenic *Nicotiana langsdorffii* *rol*CT_1 plants (C8, C11, C211, C16) obtained from the corresponding primary transformants. NLWT: untransformed controls; c-: amplification control without DNA; c+: amplification from DNA of pUC19::*rol*C plasmid (300 bp) used as positive control; M: Molecular weight marker (GeneRuler 100 bp Plus DNA Ladder, Fermentas, Thermo Scientific).

S2. Electrolyte leakage

Electrolyte leakage percentage was calculated according the equation S1

$$\text{Electrolyte leakage} = \frac{Lt}{Lc} \cdot 100 \qquad \text{(S1)}$$

where Lt and Lc are the ionic releases measured at a given temperature and after freezing of plant tissue, respectively. More in detail, the release of ions from 10 leaf discs in 5 mL of 1 M sucrose solution was measured in triplicate using a Pabisch (Milan, Italy) FE 280 Top µS 5650 conductivity meter after 30 min of incubation at a given temperature. Leaf discs were then frozen at -80°C and afterward equilibrated at 25°C before measuring conductivity. The electrolyte leakage determined at 25, 35, 40, 44, 45, 46, 48 and 50°C (see Fig. S5) clearly evidenced the occurrence of a stress

condition for the test temperature of 50°C that was therefore selected for the heat stress induction using an exposure time of two h.

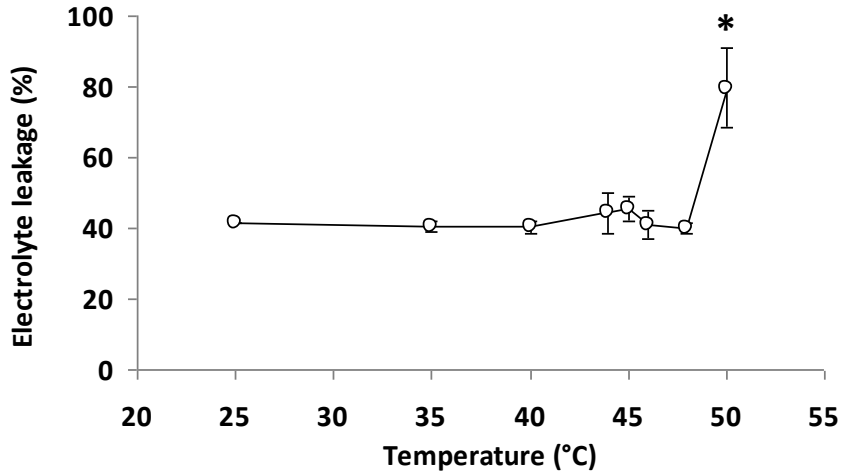

Figure S5. Response of WT *Nicotiana langsdorffii* plants to the heat stress induction, expressed as electrolyte leakage percentage at different temperatures. Datum labelled with the star (*) is statistically significant different from the others ($P<0.01$), according to the Dunnet T3 nonparametric test.

S3. Water content calculation

Water content percent (WC%) of underground and aboveground tissues of each individual plant was calculated according to the equation S2

$$WC\ (\%) = 100 \cdot \frac{(FW - DW)}{FW} \qquad (S2)$$

where FW and DW are the fresh and the dry weights, respectively.

S4. Analytical methods

5.1 S4.1. Sample extraction

About 200 mg of freeze dried shoots and roots of each plant sample were homogenised in an ice bath under magnetic stirring with 15 mL of a

methanol/water solution 80/20 (v/v) containing 10 mM NaF to inactivate polyphenol oxidase; the mixture was centrifuged at 1500×g for 10 min and the supernatant recovered. The procedure was replicated three times and the three fractions were combined and evaporated under vacuum to remove the organic solvent. The aqueous residue of the extract was split in two aliquots and acidified up to pH=2.5±0.1 with formic acid or hydrochloric acid for phenolic or carbohydrate analysis, respectively. These solutions were stored at -20 °C until analysis. The extraction method described above was the result of a recovery evaluation procedure in which four sequential extractions on three aliquots of the same plant sample were carried out separately for root and shoot using the above-mentioned extraction mixture. Total polyphenols, target phenolics, RSA and sugars were determined by the methods following described. The results showed that in the fourth extract of either root or shoot samples total polyphenols accounted in any case for less than 5.5% of the whole recovery, whereas all the target phenolics and sugars were below detection limit (bdl); according to these findings, three sequential extractions were chosen for the recovery of the target compounds. The resulting extract was used for the analysis of total polyphenols, selected phenolics, RSA and sugars. Five aliquots of each plant sample were routinely analyzed in this study.

S4.2. Analysis of total polyphenols

Appropriate extract-aliquots (0.2-0.8 mL) are mixed with 200 µL of F-C reagent; after 3 min 400 µL of a supersaturated sodium carbonate solution are added and the obtained mixture is made up to 10 mL with Milli-Q water. After dark incubation for 1 h the absorbance is read at 740 nm.

S4.3. Analysis of phenolic compounds

The analysis was carried out on the extract after elimination of the organic solvent by rotating evaporation and filtration at 0.2 μm. A Prominence UFLC system (Shimadzu, Kyoto, Japan) consisting of two solvent delivery pumps LC-20ADXR, an auto-injector SIL-20A HT, a column thermostat CTO/20A and a system controller CBM-20A coupled with a 3200QTrap™ mass detector (AB Sciex, Ontario, Canada) by a Turbo V™ interface equipped with a heated nebuliser and a turbo ion spray (TIS) probes, was used for the determination of the selected phenolic compounds in the extract.

Chromatographic separation was performed on a 2.6 μm Phenomenex (Torrance, CA, USA) Kinetex XB-C18 column, 100 × 4.6 mm i.d., operating at 40 °C with a flow rate of 0.8 mL/min.

The following solvents were used: solvent A (water/acetic acid 99.5/0.5 *v/v*); solvent B (acetonitrile/methanol/acetic acid 69.75/29.75/0.5 *v/v/v*). Gradient elution was carried out at 40°C as follows: 0-1 min, isocratic 3% B; 1-21 min, linear gradient 3-40% B; 21-23 min, linear gradient 40-100% B; 23-28 min, isocratic 100% B; 28-30 min, linear gradient 100-3% B. The flow rate was 0.8 mL/min and the injection volume 10 μl. Table 1S shows the optimized values of the m/z ratios of precursor and product ions and the compound dependent parameters.

MS-MS analyses were carried out in negative ion mode, keeping a full width at half maximum of about 0.7 amu and a dwell time of at least 100 msec for each monitored transition, using the optimized conditions reported in Table S1. All the HPLC and mass spectrometer functions, including the acquisition and processing of chromatograms, were controlled by the Analyst software version 1.52 (AB Sciex). The instrumental quantification limits (LOQs, S/N=10) were: 120 pg injected for cryptochlorogenic acid and caffeic acid, 90 pg injected for chlorogenic acid, 80 pg injected for

esculetin, 25 pg injected for ferulic acid, 15 pg injected for p-coumaric acid, neochlorogenic acid and scopoletin. Linearity of the calibration curves was investigated within the concentration ranges included between LOQs and 0.5-25 ng injected, depending on the compound investigated and achieving in all cases determination coefficients higher than 0.995.

Matrix effect (ME) was investigated by spiking two representative shoot and root extracts with target analytes and comparing the response factors of each individual phenolic compound in the extracts with those found in solvent. ME was found to be included approximately in the range of 71-118% (100% means absence of matrix effect), depending on the compound considered.

The recovery was evaluated by spiking the plant material with 100 μL of a 100 mg L^{-1} solution of 1,5-dicaffeoylquinic, which was found to be absent in the samples. According to this procedure, mean recovery percentages were 81% and 94% in shoot and root, respectively.

S4.4. RSA

Five appropriate volumes of each aqueous alcoholic extract were added to a proper volume of a DPPH solution to give five samples to be analysed, each one with a DPPH concentration of 0.1 mM. For each one of the five samples, a blank was performed by replacing the extract volume with ultra pure water. The decrease in absorbance at 517 nm was monitored after 10 min, and then every 10 min up until 60 min, every 30 min after 60, and up until 240 min when the reaction reached a plateau. For each extract volume tested, the reaction kinetics was plotted.

The percentage of DPPH neutralized at the steady state (%DPPH) was determined by using the equation S3:

$$\%DPPH = 100 \times \frac{\left(A_0^E - A_{ss}^E\right) - \left(A_0^B - A_{ss}^B\right)}{A_0^E} \quad (S3)$$

where are the absorbances of the extract (E) and the blank (B) at time zero (0) and at the steady state (ss).

The DPPH inhibition percentages obtained were plotted as a function of the corresponding amount of root/shoot in the five samples analysed and the best equation fitting the experimental points was calculated by the least square method. IC50 was defined as the concentration of the sample (mg of root/shoot, DW) in 1 mL of reaction mixture, necessary to decrease the initial DPPH concentration (which was kept constant in all the experiments) by 50%; therefore, higher IC50 values correspond to lower radical scavenging activities.

The radical scavenging activity of plant samples (RSAsample) can be derived from IC50 values (µg DW/µmol DPPH solution) determined on plant extracts (IC50,sample) by using the equation S4, allowing for obtaining a parameter that increases with the rise in antiradical activity and that is expressed as µg DPPH inhibited by one µg of DW plant sample.

$$RSA_{sample} = \frac{MW_{DPPH}}{IC_{50,\ sample}} \quad (S4)$$

S4.5. Analysis of soluble sugars

After elimination of the organic solvent by rotating evaporation, 0.5 mL of the aqueous extract were loaded on the top of a Supelclean LC-18 SPE Tubes (Supelco, Bellefonte, PO, USA) and eluted with 2.0 mL of ultrapure water acidified at pH 2.5 with hydrochloric acid. The cartridge was preconditioned with 10 mL of methanol and 10 mL of ultrapure water acidified at pH 2.5 with hydrochloric acid.

Chromatographic separation was performed on a Shimadzu HPLC system consisting of two pumps LC-10ADVP, an autoinjector SIL-10AD VP and

an evaporative light scattering detector Sedex 75 (Sedere Inc., Alfortville, France). The separation of sucrose, glucose and fructose was achieved on a Supelcogel Ca column (300×7.8 mm of internal diameter; particle size 9 μm, Supelco) equipped with a guard column (Supelguard Ca). The mobile phase was ultrapure water and the separation was carried out with an isocratic elution at a constant flow rate of 0.4 mL min^{-1} at 80 °C for 25 min. The injection volume was 10 μL. Identification of the above-mentioned sugars was confirmed by elution on a Asahipak NH_2P-50 4E column (250×4.6 mm of internal diameter; particle size 5 μm) (Showa Denko K.K., Kanagawa, Japan) equipped with a Asahipak NH2P-50G 4A guard column (Showa Denko K.K.), eluting at 30 °C by the isocratic mode with CH_3CN/H_2O 75/25 (v/v) at a flow rate of 1.0 mL min^{-1} for 25 min. Conditions set for the detection were in both cases the following: evaporation temperature 42 °C, pressure of the nebulizer gas=2.4 bar, and a gain value=10.

The instrumental quantification limits (LOQs) were considered as the minimum concentration giving rise to a signal to noise ratio (S/N) equal to10. LOQs at S/N=10 were the following: 150 ng injected for sucrose and 300 ng injected for fructose and glucose. The linearity of the calibration curves was investigated within the concentration ranges included between LOQs and 10 μg injected, achieving in all cases determination coefficients higher than 0.996.

ME was investigated as previously described for phenolic compounds, evidencing a very limited influence of the matrix on the recovery (ME=92-106%, depending on the sugar considered).

The recovery was evaluated by spiking the plant material with 90 μL of a 50 g L^{-1} solution of raffinose, which was found to be absent in the samples. According to this procedure, mean recovery percentages were 101% and 97% in shoot and root, respectively.

Table S1 - Optimized MS parameters for the investigated phenolic compounds. Letters A and B after each compound name refer to the quantifier and qualifier transitions respectively. (DP) declustering potential; (CEP) collision cell entrance potential; (CE) collision energy; (CXP) collision cell exit potential.

Compound	Precursor ion (m/z)	Product ion (m/z)	DP (V)	CEP (V)	CE (eV)	CXP (V)
Chlorogenic acid-A	353.0	191.1	-30	-25	-6	-28
Chlorogenic acid-B	353.0	85.0	-30	-25	-6	-58
Neochlorogenic acid-A	353.0	191.1	-40	-25	-6.5	-32
Neochlorogenic acid-B	353.0	135.1	-40	-25	-6.5	-44
Cryptochlorogenic acid-A	353.0	173.1	-35	-25	-4	-22
Cryptochlorogenic acid-B	353.0	179.2	-35	-25	-4	-28
Caffeic acid-A	178.9	135.2	-30	-8	-8	-22
Caffeic acid-B	178.9	134.0	-30	-18	-8	-32
p-Coumaric acid-A	163.0	119.0	-30	-18	-2.5	-20
p-Coumaric acid-B	163.0	92.9	-30	-18	-2.5	-44
Ferulic acid-A	193.0	134.1	-35	-19	-6	-24
Ferulic acid-B	193.0	177.9	-35	-19	-6	-22
Scopoletin-A	190.9	176.0	-30	-19	-6	-22
Scopoletin-B	190.9	104.0	-30	-19	-6	-32
Esculetin-A	176.9	133.1	-40	-18	-8	-26
Esculetin-B	176.9	105.0	-40	-18	-8	-26

Chapter 3

Polyphenolic profiles and antioxidant and antiradical activity of Italian berries from *Vaccinium myrtillus* L. and *Vaccinium uliginosum* L. subsp. *gaultherioides* (Bigelow) S.B. Young

Claudia Ancillotti
Lorenzo Ciofi
Daniele Pucci
Eva Sagona
Edgardo Giordani
Stefano Biricolti
Massimo Gori
William Antonio Petrucci
Fabio Giardi
Riccardo Bartoletti
Ugo Chiuminatto
Serena Orlandini
Stefano Mosti
Massimo Del Bubba

Food Chemistry 204 (2016) 176–184

Abstract

Total soluble polyphenols (TSP), total monomeric anthocyanins (TMA), radical scavenging activity (RSA), ferric reducing antioxidant power (FRAP), and a number of anthocyanins, phenolic acids, coumarins, flavanols, dihydrochalcones and flavonols were investigated in Tuscan bilberry (i.e. *Vaccinium myrtillus*) and "false bilberry" (i.e. *Vaccinium uliginosum* subsp. *gaultherioides* Bigelow). *V. myrtillus* berries showed much higher TSP, TMA, RSA and FRAP values than *V. uliginosum* subsp. *gaultherioides* fruits. Moreover, very different profiles of individual phenolics were observed in the two species, being *V. myrtillus* mainly characterized by delphinidin and cyanidin glycosides, together with chlorogenic acid, and *V. uliginosum* subsp. *gaultherioides* dominated by malvidin derivatives and flavonols. Strong differences between the two species regarded also metabolites investigated herein for the first time, such as scopoletin, which was approximately two magnitude orders higher in *V. uliginosum* subsp. *gaultherioides* than in *V. myrtillus* berries. Very different abundances were also highlighted for cryptochlorogenic acid and quercetin-3-rhamnoside that were about ten-fold higher in bilberry than in "false bilberry". When the anthocyanin composition pattern of Tuscan "false bilberry" was compared to those elsewhere reported for *V. uliginosum* fruits harvested in different world areas, some important differences were observed.

Keywords: *Vaccinium myrtillus*, *Vaccinium uliginosum* subsp. *gaultherioides*, anthocyanins, flavonols, flavanols, phenolic acids, DPPH radical scavenging activity, FRAP antioxidant activity.

1. Introduction

Vaccinium myrtillus is a spontaneous plant species native to mountain areas of Northern and Central Europe, widely diffused also in Italian Alps and Apennines. The fruit of this species (commonly identified as bilberry) has a large commercial importance, due to its consume, mainly in processed products, as well as for the preparation of dietary supplements. The interest in this berry species is due to its high content of phenolic compounds, which are plant secondary metabolites, well-known for their health-protecting attributes, as anti-inflammatory (Kim et al., 2014), anti-hypertensive (Rodrigo, Gil, Miranda Merchak, & Kalantzidis, 2012), anti-microbial (Daglia, 2012) and anti-cancer agents (Paller et al., 2013; Wang & Stoner, 2008).

Many researches aiming at the characterization of phenolic compounds in *V. myrtillus* berries from different European countries (e.g. Finland, Slovenia, Serbia, Sweden and Italy) have been published in recent years (Aakerstrom, Jaakola, & Bång, 2010; Jovancevic et al., 2011; Lätti, Riihinen, & Kainulainen, 2008; Moze et al., 2011). However, only two papers focused on polyphenols in spontaneous bilberry grown in Italy, analysing a quite limited group of phenolic secondary metabolites (i.e. some anthocyanins, phenolic acids and quercetins) were recently issued (Giovanelli & Buratti, 2009; Prencipe et al., 2014).

According to these studies, the most abundant class of polyphenols in *V. myrtillus* berries are anthocyanins. More in detail, the *V. myrtillus* berry profile is characterised by glucosides, galactosides and arabinosides of delphinidin, cyanidin, petunidin, peonidin and malvidin (Lätti et al., 2008). Flavanols (i.e. catechin, epicatechin), phenolic acids (e.g. gallic, caffeic, p-coumaric, ferulic and chlorogenic acids) and flavonols (i.e. quercetin, myricetin, rutin) have also been determined in fruits of *V. myrtillus*, even though at much lower concentrations (Moze et al., 2011). Significant

differences in the relative abundance of these secondary metabolites have been however observed in berries harvested in different areas, due to the diverse environmental conditions and/or genotypes evaluated (Aakerstrom et al., 2010; Jovancevic et al., 2011).

The composition of phenolic compounds of *V. myrtillus* berries has been found different from the one of other *Vaccinium* species (Giovanelli & Buratti, 2009; Prencipe et al., 2014), indicating the potential use of phenolic profile for the chemotaxonomic discrimination of *V. myrtillus* fruits from other cultivated and wild species (Mochioka, Yamaguchi, Horiuchi, Matsui, & Kurooka, 1995; Siracusa, Patane, Avola, & Ruberto, 2012).

In recent years, a decrease in the presence of *V. myrtillus* plants has been observed in many mountain zones of Italian Northern Apennines, together with the abnormal diffusion of another *Vaccinium* species, the latter being locally named ‘‘false bilberry”, owing to their similar phenotype. More in detail, plants of the two species have been observed to closely coexist in the same growing area, making difficult the selective harvest of bilberry, with possible consequences in the production chain of fresh and processed fruits. In this regard, it should be stressed that, according to local oral history, ‘‘false bilberry”, which is consumed as fresh fruit, exhibits worse sensorial properties (i.e. taste and odour) than bilberry.

Thus, the contamination of the commercial chain of *V. myrtillus* berries by the ‘‘false bilberry”, may represent a very important problem, especially in Italian zones, such as Tuscan-Emilian Apennines, where bilberry is an important resource for local economy. It is also worth of noting that the high concentration of phenolic compounds in the *V. myrtillus* berry promoted this fruit as a ‘‘functional food”, widely used as the main ingredient of supplements of bioactive compounds in human diet (Beccaro & Beccaro., 2006), besides to be particularly appreciated by consumers, either as fresh or processed product.

According to botanical literature information, ‘‘false bilberry” plants growing above the timberline in the Italian Northern Apennines, belong to the *Vaccinium uliginosum* L. subsp. *Gaultherioides* (Bigelow) S.B. Young (Jansen, den Nijs, & Paiva, 2000), which is common in mountain and high arctic areas, whereas *V. uliginosum* L. subsp. *uliginosum* (‘‘bog bilberry” or ‘‘bog whortleberry”) as well as *V. uliginosum* L. subsp. *pubescens* (Wormsk. ex Hornem.) Young, are lowland plants occurring within bogs in Western and Northern Europe (Jansen et al., 2000). The attribution of the subspecies or the species status to *Vaccinium uliginosum* L. subsp. *gaultherioides* (Bigelow) S.B. Young is a matter of debate and some authors have reported it as true plant species (Di Pietro, Copiz, & Catonica, 2007; Gennai, Foggi, Viciani, Carbognani, & Tomaselli, 2014). The species attribution of V. gaultherioides has been recently reported also on the basis of DNA barcoding (Combik & Mirek, 2015).

According to the common scientific search engines (i.e. SciFinder, Scopus and Google Scholar), only few papers concerning polyphenols in *V. uliginosum* berries have been published; in these studies the identification and quantification of selected anthocyanins and/or other phenolic compounds were reported in fruits collected in various areas of Finland (Häkkinen, Kärenlampi, Heinonen, Mykkänen, & Törrönen, 1999; Häkkinen & Törrönen, 2000; Määttä-Riihinen, Kamal-Eldin, Mattila, González-Paramás, & Törrönen, 2004), in north western United States (Taruscio, Barney, & Exon, 2004), in a north-eastern region of China (Li, Wang, Guo, & Wang, 2011) and in a central area of the Japanese islands (Masuoka et al., 2007), without reporting information regarding the subspecies investigated. However, as a matter of fact, no information regarding polyphenolic composition of *V. uliginosum* subsp. *gaultherioides* berries grown in Italy have been reported in the scientific literature until now.

Based on the aforementioned considerations, the aim of this study was to obtain, for the first time, information regarding the polyphenolic fraction, as well as the antioxidant and antiradical activity of *V. uliginosum* subsp. *gaultherioides* berries, in comparison with the ones of *V. myrtillus*, both originating from central Italian Apennines (Tuscany). To achieve this goal, the determination of total soluble polyphenols (TSP), total monomeric anthocyanins (TMA), selected individual anthocyanins, flavanols, flavonols and phenolic acids, together with ferric reducing antioxidant power (FRAP) and radical scavenging activity (RSA) based on the 2,2-diphenyl-1-picrylhydrazil (DPPH) radical model, was performed in *V. uliginosum* subsp. *gaultherioides* and *V. myrtillus* berries collected in various mountain sites of Tuscan Apennines to better represent a species average of the whole investigated area.

2. Materials and methods

2.1. Reagent and standards

Polyphenol standards were supplied as follows: cyanidin-3-galactoside (CYA-3-GAL), cyanidin-3-glucoside (CYA-3-GLU), cyanidin-3-arabinoside (CYA-3-ARA), delphinidin-3-glucoside (DEL-3-GLU), delphinidin-3-galactoside (DEL-3-GAL), pelargonidin-3-glucoside (PEL-3-GLU), malvidin-3-glucoside (MAL-3-GLU) and malvidin-3-galactoside (MAL-3-GAL) by Extrasynthese (Genay, France); peonidin-3-glucoside (PEO-3-GLU), peonidin-3-galactoside (PEO-3-GAL), peonidin-3-arabinoside (PEO-3-ARA) and petunidin-3-glucoside (PET-3-GLU) by Polyphenols Laboratories AS (Sandnes, Norway); gallic acid (GAC), caffeic acid (CAF), p-coumaric acid (COU), sinapic acid (SIN), ferulic acid (FER), salicylic acid (SAL), chlorogenic acid (CHL), neochlorogenic acid (NEO), cryptochlorogenic acid (CRY), esculetin (ESC), scopoletin (SCO),

(+)-catechin (CAT), epicatechin (EPI), luteolin (LUT), myricetin (MYR), phloretin (PHL), phloridzin (PHZ), quercetin (QUE), quercetin-3-rhamnoside (QUE-3-RHA), quercetin-3-glucoside (QUE-3-GLU), quercetin-3-galactoside (QUE-3-GAL) and querectin-3-rutinoside (QUE-3-RUT) by Sigma–Aldrich (St. Louis, MO, USA). LC–MS grade methanol and water were obtained from J.T. Baker (Deventer, the Netherlands). HPLC-grade methanol was purchased from Sigma–Aldrich (St. Louis, MO, USA). Ultrapure water was taken from a Milli-Q system supplied by Millipore (Billerica, MA). Nylon membranes (porosity 0.2 μm) for the filtration of the bilberry extracts before HPLC analysis were obtained from VWR^{TM} International (Radnor, PA).

Reagents were supplied as follows: formic acid, sodium fluoride, Folin–Ciocalteu (F–C) reagent and sodium carbonate by Merck (Darmstadt, Germany); 6-hydroxy-2,5,7,8-tetramethylchroman-2-carboxylic acid (Trolox), 2,4,6-tripyridyl-s-triazine (TPTZ) and DPPH radical by Sigma–Aldrich (St. Louis, USA); acetic acid and hydrochloric acid (36–37%) by J. T. Baker (Center Valley, PA, USA); iron (III) chloride hexahydrate by Panreac (Barcelona, Spain); potassium chloride and sodium acetate trihydrate by Carlo Erba (Milan, Italy).

2.2. Plant material

V. myrtillus and *V. uliginosum* subsp. *gaultherioides* plants were identified in the field according to their phenotypic characteristics (Pignatti, 1997). In order to confirm the attribution of *V. uliginosum* plants included in the present study to the ‘‘gaultherioides” subspecies, we also conducted a parallel molecular analysis using the matK chloroplast genomic region, which is considered as the most universal barcoding standard locus, in order to assess the genetic origin of the material used for the chemical analyses (Combik & Mirek, 2015). A couple of primers were designed on the

consensus sequence after aligning the sequences of *V. uliginosum* and *V. gaultherioides*, available in the gene bank (JN966729.1, AF419717.1, JN966056.1, AF421107.1, KF163393.1, KF163394.1, KF163395.1, KF163392.1). Leaf DNA extracts from 10 plants providing berries for the chemical analyses from the different investigated areas, have been used as template for PCR amplification. The obtained fragments (about 880 bp) have been purified and sequenced. Sequence chromatograms were edited and assembled using the open access MultAlin software (Corpet, 1988). The set of DNA sequence variations at specific nucleotide sites detected in the investigated sequences perfectly matched with the haplotype which have been previously identified as that of the *V. gaultherioides* species by Combik and Mirek (2015). However, since the attribution of the species or the subspecies status to the ‘‘gaultherioides” berries herein analysed is not a purpose of this study, we preferred to indicate the investigated fruits as *V. uliginosum* L. subsp. *gaultherioides* or, shortly, as ‘‘false bilberry”.

Fully ripe *V. myrtillus* and *V. uliginosum* L. subsp. *gaultherioides* berries were harvested in August 2014 in eighteen microzones belonging to three main areas of Tuscan Apennines (see Table S1 in the ‘‘Supplementary material” section). The fruits of each species were frozen in liquid nitrogen within one hour from the collection and transported to the laboratory where they were freeze-dried, until constant weight and finally grinded in order to obtain a representative sample of each investigated species in the growth area of Tuscan Apennines. The samples were finally stored at -20 °C until analyses were performed.

2.3. Samples analysis (see ‘‘Supplementary material” for full details)

2.3.1. Sample extraction

Freeze-dried berry aliquots (500 mg dry weight, d.w.) were extracted twice with a methanol/water solution 8/2 (v/v) in ice bath under magnetic stirring. The extraction method, described in detail in the ‘‘Supplementary material”, was the result of a recovery evaluation procedure in which three sequential extractions on three independent aliquots of the same berry sample were carried out and F-C TSP and TMA were determined in each extract, by the methods following described. The results showed that the third extraction in comparison with the first two steps, provided a recovery in the ranges of 5.2–6.4% and 3.4–4.9%, for TSP and TMA, respectively; accordingly, two sequential extractions were chosen.

For each *Vaccinium* species, five independent freeze-dried berry samples were extracted and analysed for the following parameters: TSP, TMA, DPPH-RSA, FRAP, selected anthocyanins, phenolic acids, flavanols and flavonols.

2.3.2. Total soluble polyphenols

Total soluble polyphenols (TSP) were spectrophotometrically determined at k = 740 nm on the berry extract, according to the F-C method using (+)-catechin as a reference standard (Doumett et al., 2011).

2.3.3. Total monomeric anthocyanins

Total monomeric anthocyanins (TMA) were determined with the pH differential method (Lee, 2005) using CYA-3-GLU as reference standard, with few modifications (see Supplementary material for details).

2.3.4. Radical scavenging activity

RSA was spectrophotometrically determined by monitoring the absorbance decrease (k = 517 nm) of 0.1 mM DPPH solutions containing different amount of berry extract (see ‘‘Supplementary material” for details). Results were expressed as µg DPPH inhibited by one µg of d.w. berry sample.

2.3.5. Antioxidant activity

The antioxidant activity of berry extract was tested by the FRAP assay, developed by Benzie and Strain (Benzie & Strain, 1996), with some modifications (see ‘‘Supplementary material” for details). Results were expressed as mmol of Trolox equivalent (TE) per g of d.w berries

2.3.6. UHPLC–MS/MS analysis of phenolic compounds

The analysis of phenolic compounds was carried out on the extracts after removal of organic solvent by vacuum evaporation, followed by acidification with formic acid up to pH = 2.0 ± 0.1 and filtration at 0.2 µm with nylon membranes.

UHPLC–MS/MS analysis was performed on an Acquity BEH C18 column (150 x 2.1 mm i.d.; particle size 1.7 µm) equipped with a guard column containing the same stationary phase (Waters, Milford, MA, USA), using a Shimadzu (Kyoto, Japan) chromatographic system consisting of a low pressure gradient quaternary pump Nexera X2 LC-30AD, a CTO/20AC thermostatted column compartment, a SIL-30AC autosampler, a DGU-20A 5R degassing unit and a CBM-20A module controller. The UHPLC system was coupled with a 3200 QTrap™ mass spectrometer (ABSciex, Ontario, Canada) by a Turbo V™ interface equipped with an electrospray probe. Chromatograms were elaborated by the 1.5.2. release of the software Analyst (AB Sciex).

Unknown compound recognition was performed according to a previously reported identification protocol consisting of a triggered multiple mass experiments method, which is briefly described in the ‘‘Supplementary Material” section (Del Bubba et al., 2012).

The optimised chromatographic conditions and mass spectrometer parameters used for quantitative determinations were described in details in the ‘‘Supplementary Material”.

The method for the analysis of individual polyphenols was evaluated for the following figures of merit: (i) instrumental limits of quantifications (LOQs); (ii) apparent recoveries, as estimated by PEL-3-GLU, SIN and LUT; (iii) source-dependent matrix effects (ME) (see ‘‘Supplementary material” for details).

LOQs were included in the range of 10–500 pg injected, corresponding to 1–50 μg/L (injection volume: 10 μL) and were in any case suitable to the quantification of target analytes in the real samples. In fact, in the worst case, which was represented by SCO in *V. myrtillus* extracts, a chromatographic area about three times higher than the one corresponding to its LOQ was observed.

For anthocyanins, which were detected under positive ionisation, ME was found to be mostly suppressive and quite similar for the two species. In most cases ME values well-below 20% were observed; galactoside and glucoside derivatives of MAL and above all CYA represented significant exceptions, being their ME respectively included in the ranges of 23–28% and 28–39% (see Fig. 1A).

For phenolic compounds detected under negative ionisation (Fig. 1B), ME was generally higher in berry extracts from *V. myrtillus* than *V. uliginosum* subsp. *gaultherioides*, with the only significant exception of MYR, which showed a signal enhancement of about 50% in the fruit extracts of the latter species. Enhancement effects, included between 25% and 39%, were observed in *V. myrtillus* berries for CAF, NEO and QUE glycosides (Fig.

1B). A suppressive ME, in the ranges of 25–54% and 36–41% for bilberry and ‘‘false bilberry” extracts, respectively, was conversely evidenced for COU, FER, ESC and SCO.

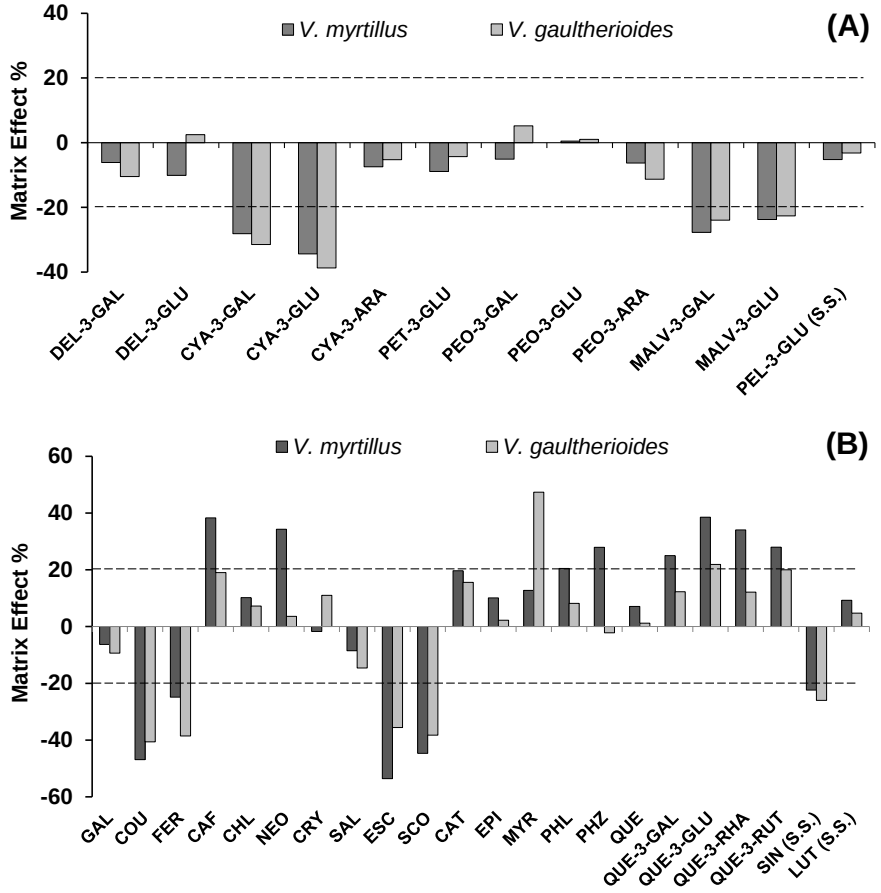

Figure 1. Matrix effect percentages obtained for target compounds detected in *V. myrtillus* and *V. uliginosum* subsp. *gaultherioides* under (A) positive ionisation or (B) negative ionisation, following the specifications reported in the paragraph S6 of the ‘‘Supplementary material”. For the meaning of the analyte abbreviations, see paragraph 2.1.

The mean values of apparent recovery, calculated by spiking freeze-dried berry samples with PEL-3-GLU, SIN and LUT resulted equal to 91%, 74% and 103%, respectively. The much lower value found for SIN, in respect to

LUT and PEL-3-GLU can be explained by its suppressive ME, which was included between 22% and 26%, depending on the species analysed (Fig. 1B).

3. Results and discussion

3.1. Total anthocyanins and phenolic compounds, antiradical and antioxidant activity

Fig. 2 illustrates the mean values and standard deviations found for TMA, TSP, DPPH-RSA and FRAP in five independent replicated analysis of representative samples of *V. myrtillus* and *V. uliginosum* subsp. *gaultherioides* collected in the Tuscan Apennines.

For all the investigated parameters, statistically significant differences were observed, being bilberries richer than ‘‘false bilberries” in both TSP (4768 vs. 3670 mg CAT/100 g d.w.) and TMA (3666 vs. 1519 mg CYA-3-GLU/100 g d.w.), and exhibiting correspondingly higher antiradical and antioxidant activities (0.179 vs. 0.143 μg DPPH inhibited/μg d.w. and 0.663 vs. 0.425 mmol TE/g d.w., respectively). Thus, from this point of view, V. myrtillus berries represent a superior functional food than *V. uliginosum* subsp. *gaultherioides* fruits. The two species differed also in terms of relative percentages of TMA in respect to TSP, being them the prevailing polyphenolic class in bilberry, but not in ‘‘false bilberry”.

As previously mentioned in the ‘‘Introduction”, no data have been elsewhere published regarding *V. uliginosum* subsp. *gaultherioides* berries grown in Italy. However, it is interesting to compare our data with those elsewhere obtained in berries from *V. uliginosum* species, which is considered the closest to the *V. uliginosum* subsp. *gaultherioides* one (Combik & Mirek, 2015).

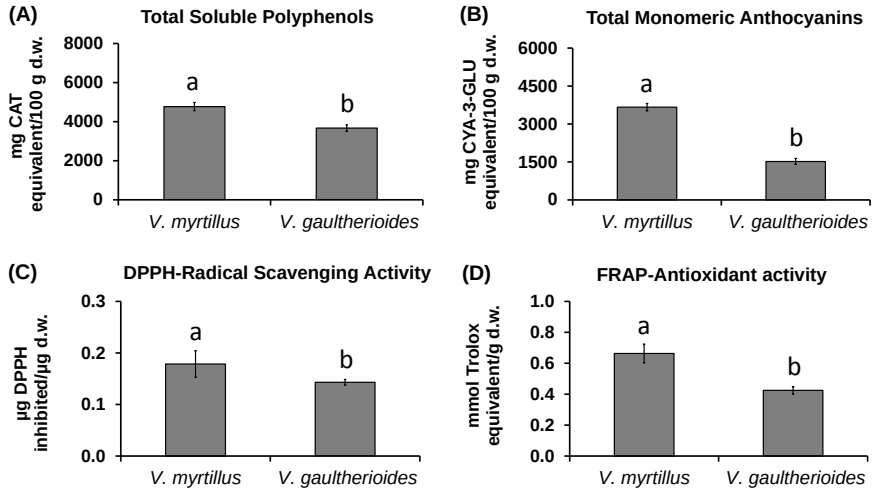

Figure 2. Mean values and standard deviations (n = 5) of: (A) total soluble polyphenols expressed as mg catechin (CAT) equivalent/100 g d.w.; (B) total monomeric anthocyanins expressed as mg cyanidin-3-glucoside (CYA-3-GLU) equivalent/100 g d.w.; (C) radical scavenging activity expressed as lg DPPH inhibited/lg d.w. and (D) ferric reducing/antioxidant power (FRAP) expressed as mmol Trolox equivalents/g d.w. in *V. myrtillus* and *V. uliginosum* subsp. *gaultherioides* berries. Rectangular bars labelled with different letters indicate values statistically different ($P \leq 0.002$), according to the T test.

For example, TMA were determined in Chinese *V. uliginosum* berries, evidencing a much lower anthocyanin content compared to Tuscan ‘‘false bilberry” (901 vs. 1519 mg CYA-3-GLU/100g d.w.) (Li et al., 2011). Concentrations herein determined in *V. uliginosum* subsp. *gaultherioides* for TMA (1519 mg CYA-3-GLU/100g d.w., corresponding to 228 mg CYA-3-GLU/100g f.w.) and TSP (3670 mg CAT/100g d.w., corresponding to 550 mg CAT/100g f.w. and equivalent to 322 mg GAC/100g f.w.) were also much higher than those reported by Taruscio and co-workers in *V. uliginosum* berries collected in United States (124 mg CYA-3-GLU/100g f.w. and 161 mg GAC/100g f.w. for TMA and TSP, respectively) (Taruscio et al., 2004).

The results obtained in our study for *V. myrtillus* berries can be compared with those reported in literature for bilberries grown in Italy and other

European areas. Data obtained from Italian bilberries are few and referred to fruits harvested in Modena Apennines (Emilia-Romagna Region) (Giovanelli & Buratti, 2009) and North Western Alps (Piedmont Region) (Beccaro & Beccaro, 2006; Bounous, Beccaro, Mellano, & Botta, 2009), whereas no information are available in the scientific literature for Tuscan bilberries. In these studies, TSP ranged approximately from 470 to 600 mg GAC/100 g fresh weight (f.w.) and were therefore similar or higher than those determined in Tuscan bilberry (4768 mg CAT/100 g d. w., corresponding to 715 mg CAT/100 g f.w. and equivalent to 420 mg GAC/100 g f.w.). Conversely, for TMA, much higher concentrations were determined in Tuscan bilberry (3666 mg CYA-3-GLU/100 g d.w., corresponding to approximately 550 mg/100 g f. w.), compared to the fruits collected in Emilia-Romagna (330–344 mg CYA-3-GLU/100 g f.w.) (Giovanelli & Buratti, 2009) and Piedmont (327 mg CYA-3-GLU/100 g f.w.) (Beccaro & Beccaro, 2006).

Our results were included in the very wide range of concentrations measured for TSP (44–584 mg GAC/100 g f.w.) and TMA (144–1095 mg CYA-3-GLU/100 f.w.) on bilberries picked up in other European countries, such as Norway (Uleberg et al., 2012), Serbia (Miletic, Popovic, Mitrovic, Kandic, & Leposavic, 2014) and Montenegro (Jovancevic et al., 2011). Based on literature information, such a great variability can be attributed to different growing habitats and production years (Aakerstrom et al., 2010; Jovancevic et al., 2011; Uleberg et al., 2012); moreover, differences in the extraction procedure are often present in the aforementioned studies, possibly affecting final results. Data concerning the determination of FRAP and/or DPPH-RSA on bilberry extracts were occasionally reported together with TSP and TMA concentrations. More in detail, FRAP was found higher in Tuscan bilberries (0.663 mmol TE/g d.w., corresponding to about 99 µmol TE/g f.w.) than in those harvested in other Italian areas (33–55 lmol TE/g f.w.), as well as in Norway (9.6–10.8 µmol TE/g f.w.) (Uleberg et al.,

2012). Interestingly, in all these studies TSP concentrations were found higher than those determined for Tuscan berries, whereas for TMA an opposite trend was evidenced. These findings suggest the important role of anthocyanins for explaining antioxidant activity, compared to other phenolic classes. In this regard, it should be noted that a strong correlation between the FRAP values and the anthocyanin concentrations ($R2 > 0.92$; $P < 0.001$) was observed in 11 commercial powdered bilberry extracts from various countries of origin (Chu, Cheung, Lau, & Benzie, 2011). DPPH-RSA values present in literature were limited to two papers and were included in an extremely wide range, from 3.07 (Miletic et al., 2014) to 10,900 µmol TE/g f.w. (Giovanelli & Buratti, 2009), being the former much closer to the data herein obtained (0.179 µg DPPH inhibited/lg d.w. corresponding to 34 µmol TE/g f.w.).

3.2. Individual anthocyanins

Typical MRM reconstructed UHPLC–MS/MS chromatograms of target anthocyanins determined in *V. myrtillus* and *V. uliginosum* subsp. *gaultherioides* berry extracts under positive ionisation are shown in Fig. 3A and B, respectively. In agreement with findings elsewhere observed under chromatographic conditions similar to those herein adopted (Moze et al., 2011; Müller, Schantz, & Richling, 2012), the elution order of anthocyanins glycosylated with a same sugar was: DEL < CYA < PET < PEO < MAL; moreover, for a same aglycone, galactosides eluted firstly, followed by glucosides and arabinosides. As shown in Fig. 3A and B, isobaric compounds characterised by the same transitions (i.e. galactoside and glucoside derivatives of the same aglycone) were baseline resolved, thus allowing their accurate quantification.

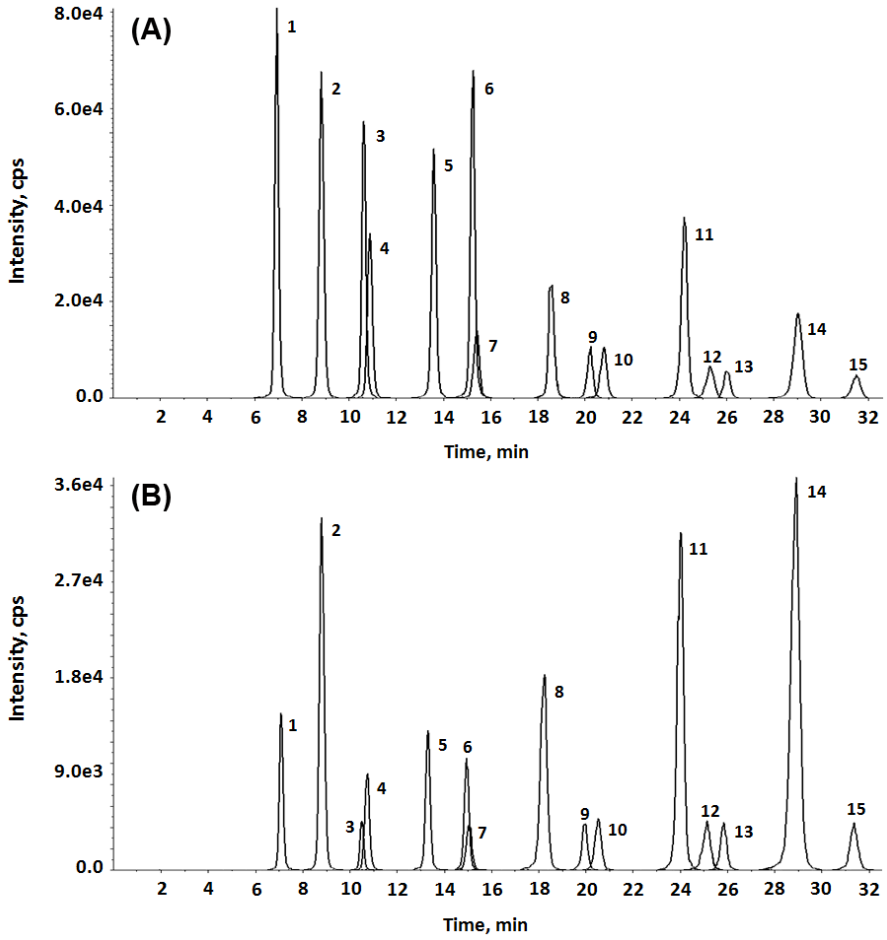

Figure 3. Typical MRM reconstructed UHPLC–MS/MS chromatograms of *V. myrtillus* (A) and *V. uliginosum* subsp. *gaultherioides* (B) berry extracts, illustrating the anthocyanidin glycosides quantified in the two berries. (1) Delphinidin-3-galactoside; (2) delphinidin-3-glucoside; (3) cyanidin-3-galactoside; (4) delphinidin-3-arabinoside; (5) cyanidin-3-glucoside; (6) cyanidin-3-arabinoside; (7) petunidin-3-galactoside; (8) petunidin-3-glucoside; (9) peonidin-3-galactoside; (10) petunidin-3-arabinoside; (11) peonidin-3-glucoside; (12) malvidin-3-galactoside; (13) peonidin-3-arabinoside; (14) malvidin-3-glucoside; (15) malvidin-3-arabinoside.

In both species, all the fifteen investigated anthocyanins showed an s/n ratio well-higher than 10 (see paragraph S6 of ‘‘Supplementary material” for further details) and were therefore quantified.

Mean concentrations and standard deviations of selected individual anthocyanins determined in the five independent replicated analysis of representative samples of *V. myrtillus* and *V. uliginosum* subsp. *gaultherioides* collected in the Tuscan Apennines are shown in Fig. 4.

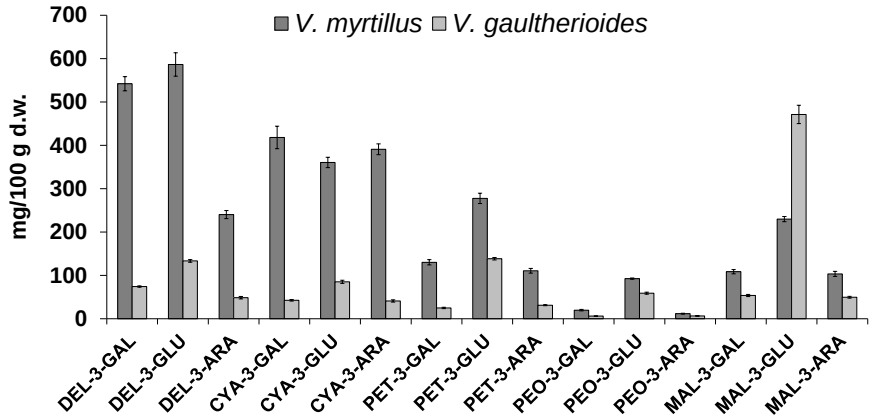

Figure 4. Mean values and standard deviations (n = 5), expressed on a dry weight basis, as mg/100 g, of selected anthocyanins in *V. myrtillus* and *V. uliginosum* subsp. *gaultherioides* berries. All the anthocyanin concentrations determined in *V. myrtillus* fruits are statistically different ($P < 0.001$) in respect to those found in *V. uliginosum* subsp. *gaultherioides* berries, according to the T test. Delphinidin-3-galactoside (DEL-3-GAL), delphinidin-3-glucoside (DEL-3-GLU), delphinidin-3-arabinoside (DEL-3-ARA), cyanidin-3-galactoside (CYA-3-GAL), cyanidin-3-glucoside (CYA-3-GLU), cyanidin-3-arabinoside (CYA-3-ARA), petunidin-3-galactoside (PET-3-GAL), petunidin-3-glucoside (PET-3-GLU), petunidin-3-arabinoside (PET-3-ARA), peonidin-3-galactoside (PEO-3-GAL), peonidin-3-glucoside (PEO-3-GLU), peonidin-3-arabinoside (PEO-3-ARA), malvidin-3-galactoside (MAL-3-GAL), malvidin-3-glucoside (MAL-3-GLU) and malvidin-3-arabinoside (MAL-3-ARA).

In bilberry the following concentration order was observed for the sets of anthocyanins characterised by a same aglycone: PEO << MAL < PET << CYA < DEL. More in detail, differences of only about 15% were found between MAL and PET glycosides, as well as between CYA and DEL

derivatives, which accounted together for more than 70% of target anthocyanins. The above-reported anthocyanin relative abundance was in accordance with literature data; in fact, the anthocyanin proportion found in this study was the same reported by Moze and co-workers in Slovenian bilberries (Moze et al., 2011). Moreover, as a general result found in various studies and typifying *V. myrtillus* berries irrespective of the geographical origin, DEL and CYA glycosides showed the highest occurrence, whereas PEO derivatives were the least present (Lätti et al., 2008; Prencipe et al., 2014; Primetta, Jaakola, Ayaz, Inceer, & Riihinen, 2013). As a sole exception to this latter finding, PEO-3-GAL concentration higher than those of CYA, PET and MAL glycosides was surprisingly reported by Giovanelli and colleagues (Giovanelli & Buratti, 2009).

As regard the relative content of sugar moieties of anthocyanins, a clear prevalence of glucoside derivatives was observed, in agreement with data from various European regions (Moze et al., 2011; Primetta et al., 2013), including Italy (Prencipe et al., 2014). Galactosides were about 50% higher than arabinosides; a similar result was previously observed in bilberries from Italian Northern Apennines (Prencipe et al., 2014), whereas for fruits harvested in other European countries these glycosides were found to be at similar concentrations, and occasionally arabinoside concentrations even higher than the galactoside ones (Moze et al., 2011; Primetta et al., 2013), thus suggesting a possible peculiar characteristic of bilberry from Tuscany.

The sum of the fifteen individual anthocyanins, expressed as CYA-3-GLU, was 3557 mg/100 g d.w., equivalent to 533 mg CYA-3-GLU/100 g f.w., that is much higher than the value found by Giovanelli and co-workers (Giovanelli & Buratti, 2009) and very similar to that reported by Prencipe and colleagues (Prencipe et al., 2014) in Italian berries (386 and 553 mg CYA-3- GLU/100 g f.w., respectively). The value found in this study was also included in the range of data reported in literature for bilberries harvested in other European countries (Lätti et al., 2008; Moze et al., 2011;

Primetta et al., 2013; Uleberg et al., 2012). Interestingly, the sum of the target anthocyanins herein determined accounted for 97% of TMAs. Hence, target individual anthocyanins seem to be highly representative of the whole anthocyanin fraction of *V. myrtillus* berries; this finding is in accordance with data elsewhere obtained on Italian bilberries (Giovanelli & Buratti, 2009).

The comparison between the two *Vaccinium* species highlighted a very different relative abundance of the 15 anthocyanins investigated, being all of them found at statistically different concentrations ($P < 0.001$). As a general finding, a prevalence of all target anthocyanins was observed in bilberry, with the only exception of MAL-3-GLU, the concentration of which in *V. uliginosum* subsp. *gaultherioides* fruits (471 mg/100 g d.w.) was more than double than the one found in *V. myrtillus* berries (230 mg/100 g d.w.). This very high value significantly contributed to make MAL derivatives by far the most abundant anthocyanins in ‘‘false bilberry”, accounting for about 50% of the total concentrations of the target anthocyanins. The other anthocyanins were in the following increasing order: PEO < CYA = PET < DEL; hence an aglycone content very different from the one observed in *V. myrtillus* was highlighted. The relative abundance of glycosides also differed in respect to that of *V. myrtillus*, since glucosides accounted for 70% of the total, whereas arabinosides and galactosides were found at very similar percentages (14% and 16%, respectively). The predominance of MAL derivatives found in *V. uliginosum* subsp. *gaultherioides* was a metabolomics trait common with *V. uliginosum* berries collected in various European and Asian regions (Wang et al., 2014; Latti, Jaakola, Riihinen, & Kainulainen, 2010; Masuoka et al., 2007; Määttä-Riihinen et al., 2004). However, it should also be mentioned that in Tuscan ‘‘false bilberry” CYA and PET glycosides were found at very similar concentrations, whereas as reported by other authors, in *V. uliginosum* fruits elsewhere collected, the former were twofold-threefold

lower than the latter, irrespective of the origin area. The relative anthocyanidin abundance found in *V. uliginosum* subsp. *gaultherioides* fruits was also very different from the one reported for *V. uliginosum* berries collected in United States, for which DEL glycosides surprisingly resulted the most abundant anthocyanidin class, followed by CYA; moreover, MAL derivatives were present at relatively low concentrations (Taruscio et al., 2004), thus suggesting for this berry sample a higher similarity with bilberry, rather than ‘‘false bilberry”.

3.3. Non-anthocyanidin phenolics

The non-anthocyanidin phenolic compounds investigated in this study are reported in Table 1. In this group we included some phenolic acids, flavanols and flavonols such as GAC, CHL, CAT, EPI, QUE and selected QUE-glycosides, already investigated in *V. myrtillus* (Miletic et al., 2014; Moze et al., 2011; Prencipe et al., 2014). Two dihydrochalcones (i.e. PHL and PHZ) and other phenolic acids and coumarins belonging to the shikimate pathway (i.e. CRY, SAL, ESC and SCO), never investigated before in *V. myrtillus*, were also comprised in the group of target analytes. These latter compounds were included in the study because the shikimate pathway has been previously demonstrated to be involved in plant response to genetic and epigenetic factors (Ancillotti et al., 2015).

Typical MRM reconstructed UHPLC–MS/MS chromatograms of selected phenolic compounds determined under negative ionisation in *V. myrtillus* and *V. uliginosum* subsp. *gaultherioides* berry extracts, are shown in Fig. 5A and B, respectively. As illustrated by these figures, isobaric compounds characterised by the same transition (i.e. CHL/NEO and QUE-3-GLU/QUE-3-GAL) were baseline resolved, thus allowing their accurate quantification.

Table 1 - Mean values and standard deviations (n = 5), expressed on a dry weight basis, as mg/kg, of selected phenolic acids, coumarins, flavanols, dihydrochalcones and flavonols in *V. myrtillus* and *V. uliginosum* subsp. *gaultherioides* berries. For each compound, different letters indicate statistically different concentrations ($P < 0.001$) in the two investigated species, according to the T test.

Analyte	***V. myrtillus***	***V. gaultherioides***
Gallic acid	33.3 ± 1.5 (a)	20.3 ± 0.8 (b)
p-Coumaric acid	1.20 ± 0.05 (a)	1.11 ± 0.06 (a)
Ferulic acid	0.44 ± 0.01 (a)	2.09 ± 0.07 (b)
Caffeic acid	3.1 ± 0.2 (a)	4.9 ± 0.3 (b)
Chlorogenic acid	1320 ± 35 (a)	66 ± 3 (b)
Neochlorogenic acid	0.70 ± 0.08 (a)	2.86 ± 0.09 (b)
Cryptochlorogenic acid	1.45 ± 0.05 (a)	0.11 ± 0.01 (b)
Salicylic acid	0.46 ± 0.02 (a)	0.80 ± 0.03 (b)
Esculetin	2.8 ± 0.2 (a)	0.72 ± 0.05 (b)
Scopoletin	0.046 ± 0.002 (a)	4.1 ± 0.2 (b)
Catechin	13.9 ± 0.9 (a)	4.4 ± 0.2 (b)
Epicatechin	255 ± 16 (a)	256 ± 15 (a)
Phloretin	n.d.	n.d.
Phloridzin	3.2 ± 0.1 (a)	2.5 ± 0.1 (b)
Myricetin	36.9 ± 1.3 (a)	24.1 ± 1.2 (b)
Quercetin	2.2 ± 0.1 (a)	9.0 ± 0.3 (b)
Quercetin-3-galactoside	786 ± 38 (a)	2355 ± 68 (b)
Quercetin-3-glucoside	32.5 ± 1.4 (a)	33.6 ± 1.2 (a)
Quercetin-3-rhamnoside	22.6 ± 1.0 (a)	2.4 ± 0.2 (b)
Quercetin-3-rutinoside	n.d.	n.d.

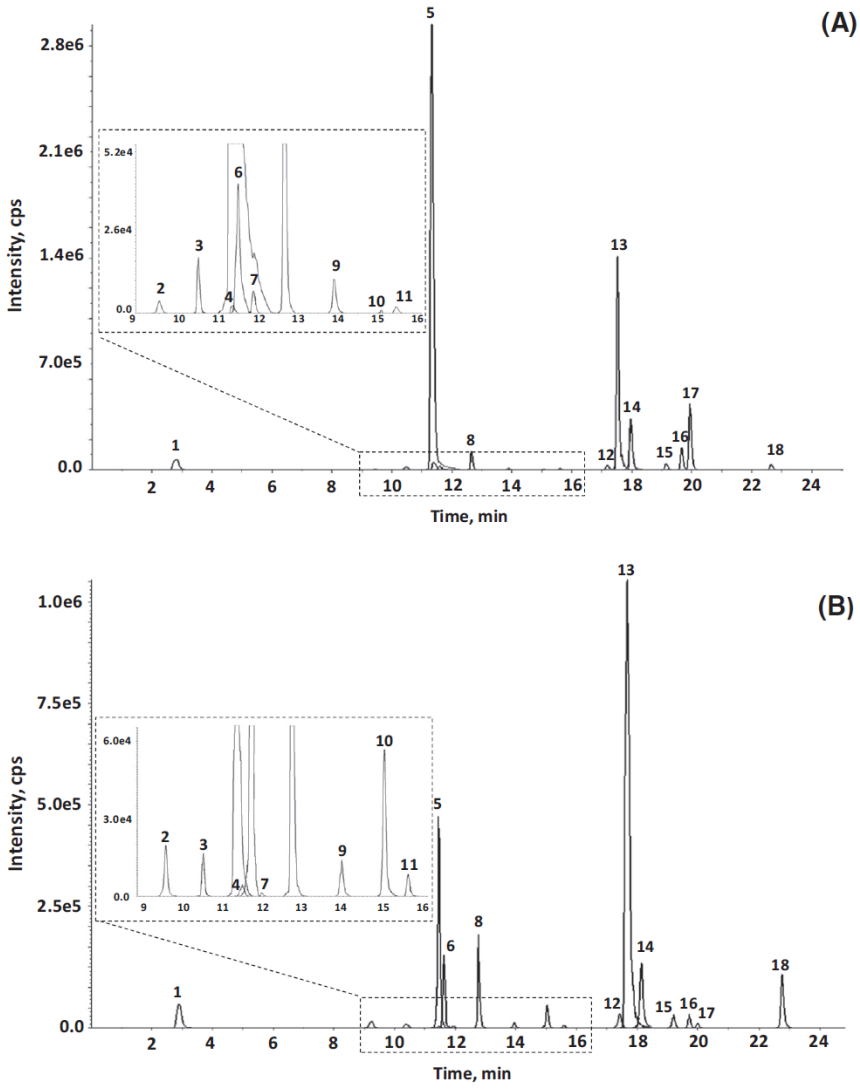

Figure 5. Typical MRM reconstructed UHPLC–MS/MS chromatograms of V. myrtillus (A) and V. uliginosum subsp. gaultherioides (B) berry extracts illustrating the phenolic compounds quantified in the two berries. (1) Gallic acid; (2) neochlorogenic acid; (3) catechin; (4) esculetin; (5) chlorogenic acid; (6) caffeic acid; (7) cryptochlorogenic acid; (8) epicatechin; (9) p-coumaric acid; (10) scopoletin; (11) ferulic acid; (12) salicylic acid; (13) quercetin-3-galactoside; (14) quercetin-3-glucoside; (15) myricetin; (16) phloridzin; (17) quercetin-3-rhamnoside; (18) quercetin. Note that phloretin and quercetin-3-rutinose were found to be lower than their limits of detection in both the berry extracts.

Target phenolics were found to be present in both species at quantifiable concentrations, with the only exceptions of PHL and QUE-3-RUT (Table 1). Among the investigated non-anthocyanidin phenolic compounds, CHL, QUE-3-GAL and EPI were by far the most abundant analytes found in *V. myrtillus*, being their concentrations equal to 1320, 786 and 255 mg/kg d.w., respectively. The other investigated phenolics were determined at much lower concentrations, ranging from tens of µg/kg to tens of mg/kg, on a d.w. basis.

The comparison with literature of concentrations herein found in *V. myrtillus* berries for non-anthocyanidin phenolic compounds is complicated by the absence of an already-published homogeneous dataset in terms of target analytes, but also regarding to the extraction procedure, since the presence of a hydrolysis step can alter the native composition of phenolics.

One of the most complete study, carried out with an extraction procedure similar to the one adopted by us, was reported by Moze and co-workers. In this study a number of phenolic acids, flavanols and flavonols were investigated in bilberry, highlighting the prevalence of CHL and concentrations of CHL, CAT and EPI quite similar to the ones herein determined (Moze et al., 2011).

As previously mentioned for anthocyanins, also for the investigated phenolic acids, flavanols, dihydrochalcones and flavonols, different composition patterns were found in *V. myrtillus* and *V. uliginosum* subsp. *gaultherioides* berries. In fact, most non-anthocyanidin target analytes were found at statistically different concentrations in the two berry species. COU, EPI and QUE-3-GLU represented exceptions to this behaviour, since they showed very similar concentration values in bilberry and ‘‘false bilberry”; moreover, PHL and QUE-3-RUT were not detected in both *Vaccinium* species. Major differences between the two species regarded SCO, which was approximately two magnitude orders higher in *V. uliginosum* subsp. *gaultherioides*, and CHL which was found to be twenty-fold higher in *V.*

myrtillus. Very different abundances were also highlighted for CRY and QUE-3-RHA that were about ten-fold higher in bilberry than in ‘‘false bilberry”. It is however remarkable that the prevalence of QUE-3-RHA in bilberry is a finding in contrast to the general trend of QUE and its derivatives that were more abundant in *V. uliginosum* subsp. *gaultherioides*, above all owing to the very high concentration of QUE-3-GAL.

A qualitative evaluation of the flavonol fraction of the two *Vaccinium* species was also performed, by using the triggered multiple experiment protocol described in the S6 section of ‘‘Supplementary Material”. According to this protocol, myricetin, laricitrin, kaempferol, isorhamnetin and syringetin hexosides, pentosides and glucuronides, as well as QUE glucuronide and pentosides, were tentatively identified both in *V. myrtillus* and *V. uliginosum* subsp. *gaultherioides*, highlighting very different relative abundances in the two species and a general flavonol predominance in ‘‘false bilberry”.

4. Conclusions

This study provided the first information on TSP, TMA, DPPH-RSA, FRAP, as well as concentrations of a wide number of anthocyanins, phenolic acids, coumarins, flavanols, dihydrochalcones and flavonols in Tuscan bilberry (i.e. *V. myrtillus*), confirming its role as ‘‘functional food” for dietary supplement of antioxidant compounds. In this regard, it should be stressed that the group of target analytes comprised some coumarins and chlorogenic acid isomers, never investigated before in *V. myrtillus* berries. These compounds belonged to the shikimate pathway that has been recently investigated by our team as a phenolic biosynthesis path very sensitive to genetic modifications in model plants (Ancillotti et al., 2015). Interestingly, the contents of SCO and chlorogenic acids were actually among the most affected non-anthocyanidin compounds by the ‘‘species effect”.

Moreover, this research was the first one investigating the above-mentioned parameters in Tuscan ‘‘false bilberry” (i.e. *V. uliginosum* subsp. *gaultherioides*) that closely coexists with bilberry in the same growing areas of Tuscan Apennines, thus complicating the selective harvest of bilberry. In this regard, it should be underlined an interesting metabolic profile complementarity with bilberry, both for anthocyanin and non-anthocyanin phenolic compounds, for the production, for instance, of more balanced functional foods. Furthermore, such metabolic complementarity could make feasible the chemotaxonomic discrimination of *V. myrtillus* and *V. uliginosum* subsp. *gaultherioides* species, with the purpose of discovering possible contaminations of the bilberry commercial chain by ‘‘false bilberry”. However, it should be also noted that the different quali-quantitative polyphenolic composition of the two berries can be considered as a natural bio-diverse source of dietary phenolics from the Tuscan Apennines.

When the anthocyanin composition pattern of Tuscan ‘‘false bilberry” was compared to those elsewhere reported for bog bilberry harvested in different world areas, some important differences were observed, thus supporting the recent report of Combik and Mirek that considered *V. gaultherioides* as a true plant species, different from *V. uliginosum* (Combik & Mirek, 2015).

Further studies need in order to investigate more in depth the polyphenolic composition of *V. uliginosum* subsp. *gaultherioides*, as well as that of *V. myrtillus*, for which new secondary phenolic metabolites have been highlighted in this study.

5. Contribution

Claudia Ancillotti performed all the described analytical methods including the analyses of total soluble polyphenols, total monomeric anthocyanins,

antiradical/antioxidant activity and LC-MS/MS determination of selected anthocyanins and polyphenols.

Acknowledgements

This research was funded by Regione Toscana and the private companies ‘‘Il Baggiolo S.r.l.”, Danti Giampiero & C. S.n.c.”, ‘‘Azienda Agricola Il Sottobosco” and ‘‘Farmaceutica MEV S.r.l.”, within the ‘‘PRAF Misura 1.2. e)” grant.

References

Aakerstrom, A., Jaakola, L., & Bång, U. (2010). Effects of Latitude-Related Factors and Geographical Origin on Anthocyanidin Concentrations in Fruits ofVaccinium myrtillusL. (Bilberries). Journal of agricultural and food chemistry, 58(22), 11939-11945.

Ancillotti, C., Bogani, P., Biricolti, S., Calistri, E., Checchini, L., Ciofi, L., Gonnelli, C., & Del Bubba, M. (2015). Changes in polyphenol and sugar concentrations in wild type and genetically modified Nicotiana langsdorffii Weinmann in response to water and heat stress. Plant Physiology and Biochemistry, 97, 52-61.

Beccaro, G., & Beccaro. (2006). Phenolic and anthocyanin content and antioxidant activity in fruits of bilberry (Vaccinium myrtillus L.) and of highbush blueberry (Vaccinium corymbosum L.) cultivars in North Western Italy. Acta horticulturae, 715(Proceedings of the 8th International Symposium on Vaccinium Culture, 2004), 553.

Benzie, I. F. F., & Strain, J. J. (1996). The Ferric Reducing Ability of Plasma (FRAP) as a Measure of "Antioxidant Power": The FRAP Assay. Analytical Biochemistry, 239(1), 70-76.

Bounous, G., Beccaro, G., Mellano, M., & Botta, R. (2009). Nutritional value and antioxidant activity of minor fruits grown in Piemonte (Italy). Acta horticulturae, 818, 249-252.

Chu, W.-K., Cheung, S. C. M., Lau, R. A. W., & Benzie, I. F. F. (2011). Bilberry (Vaccinium myrtillus L.). In I. F. F. Benzie & W.-G. S. (Eds.), Herbal Medicine: Biomolecular and Clinical Aspects 2 ed.). Boca Raton (FL): CRC Press.

Combik, M., & Mirek, Z. (2015). Estimating the effectiveness of species identification by sequencing of two chloroplast DNA loci (matK and rbcL) in selected groups of Polish flora. DNA Barcodes, 3(1).

Corpet, F. (1988). Multiple sequence alignment with hierarchical clustering. Nucleic acids research, 16(22), 10881-10890.

Daglia, M. (2012). Polyphenols as antimicrobial agents. Current opinion in biotechnology, 23(2), 174-181.

Del Bubba, M., Checchini, L., Chiuminatto, U., Doumett, S., Fibbi, D., & Giordani, E. (2012). Liquid chromatographic/electrospray ionization tandem mass spectrometric study of polyphenolic composition of four cultivars of Fragaria vesca L. berries and their comparative evaluation. Journal of Mass Spectrometry, 47(9), 1207-1220.

Di Pietro, R., Copiz, R., & Catonica, C. (2007). Sulla presenza di Vaccinium gaultherioides Bigelow in Italia centrale. Biogeographia, 28, 275-285.

Doumett, S., Fibbi, D., Cincinelli, A., Giordani, E., Nin, S., & Del Bubba, M. (2011). Comparison of nutritional and nutraceutical properties in cultivated fruits of Fragaria vesca L. produced in Italy. Food research international, 44(5), 1209-1216.

Gennai, M., Foggi, B., Viciani, D., Carbognani, M., & Tomaselli, M. (2014). The Nardus-rich communities in the northern Apennines (N-Italy): a phytosociological, ecological and phytogeographical study. Phytocoenologia, 44(1-2), 55-85.

Giovanelli, G., & Buratti, S. (2009). Comparison of polyphenolic composition and antioxidant activity of wild Italian blueberries and some cultivated varieties. Food Chemistry, 112(4), 903-908.

Häkkinen, S. H., Kärenlampi, S. O., Heinonen, I. M., Mykkänen, H. M., & Törrönen, A. R. (1999). Content of the flavonols quercetin, myricetin, and kaempferol in 25 edible berries. Journal of agricultural and food chemistry, 47(6), 2274-2279.

Häkkinen, S. H., & Törrönen, A. R. (2000). Content of flavonols and selected phenolic acids in strawberries and Vaccinium species: influence of cultivar, cultivation site and technique. Food research international, 33(6), 517-524.

Jansen, J., den Nijs, H. C., & Paiva, J. A. (2000). Some notes on Vaccinium uliginosum L. subsp. gaultherioides (Bigelow) Young, a new species to the flora of Portugal. Portugaliae Acta Biologica, 19(1), 177-186.

Jovancevic, M., Balijagic, J., Menkovic, N., Savikin, K., Zdunic, G., Jankovic, T., & Dekic-Ivankovic, M. (2011). Analysis of phenolic compounds in wild populations of bilberry (Vaccinium myrtillus L.) from Montenegro. J. Med. Plants Res., 5(6), 910-914.

Kim, J., Lee, K., Lee, H., Watson, R. R., Preedy, V. R., & Zibadi, S. (2014). Polyphenols Suppress and Modulate Inflammation. Polyphenols in Human Health and Disease, 1, 393-408.

Lätti, A., Riihinen, K., & Kainulainen, P. (2008). Analysis of Anthocyanin Variation in Wild Populations of Bilberry (Vaccinium myrtillus L.) in Finland. Journal of agricultural and food chemistry, 56(1), 190-196.

Latti, A. K., Jaakola, L., Riihinen, K. R., & Kainulainen, P. S. (2010). Anthocyanin and flavonol variation in bog bilberries (Vaccinium

uliginosum L.) in Finland. Journal of agricultural and food chemistry, 58(1), 427-433.

Lee, J. (2005). Determination of total monomeric anthocyanin pigment content of fruit juices, beverages, natural colorants, and wines by the pH differential method: Collaborative study. Journal of AOAC International, 88(5), 1269.

Li, R., Wang, P., Guo, Q.-q., & Wang, Z.-y. (2011). Anthocyanin composition and content of the Vaccinium uliginosum berry. Food Chemistry, 125(1), 116-120.

Määttä-Riihinen, K. R., Kamal-Eldin, A., Mattila, P. H., González-Paramás, A. M., & Törrönen, A. R. (2004). Distribution and contents of phenolic compounds in eighteen Scandinavian berry species. Journal of agricultural and food chemistry, 52(14), 4477-4486.

Masuoka, C., Yokoi, K., Komatsu, H., Kinjo, J., Nohara, T., & Ono, M. (2007). Two novel antioxidant ortho-benzoyloxyphenyl acetic acid derivatives from the fruit of Vaccinium uliginosum. Food science and technology research, 13(3), 215-220.

Miletic, N., Popovic, B., Mitrovic, O., Kandic, M., & Leposavic, A. (2014). Phenolic compounds and antioxidant capacity of dried and candied fruits commonly consumed in Serbia. Czech J. Food Sci., 32(4), 360-368.

Mochioka, R., Yamaguchi, M., Horiuchi, S., Matsui, H., & Kurooka, H. (1995). Chemotaxonomic Classification of Native Wild Japanese Grapes by Anthocyanins in Berry Skin. 64(3), 463-470.

Moze, S., Polak, T., Koron, D., Vanzo, A., Poklar Ulrih, N., & Abram, V. (2011). Phenolics in Slovenian Bilberries (Vaccinium myrtillus L.) and Blueberries (Vaccinium corymbosum L.). Journal of agricultural and food chemistry, 59(13), 6998-7004.

Müller, D., Schantz, M., & Richling, E. (2012). High performance liquid chromatography analysis of anthocyanins in bilberries (Vaccinium

myrtillus L.), blueberries (Vaccinium corymbosum L.), and corresponding juices. Journal of food science, 77(4), C340-C345.

Paller, C. J., Paller, X., Ye, P. J., Wozniak, B. K., Gillespie, P. R., Sieber, R. H., Greengold, B. R., Stockton, B. L., Hertzman, M. D., Efros, R. P., Roper, H. R., Liker, M. A., & Carducci. (2013). A randomized phase II study of pomegranate extract for men with rising PSA following initial therapy for localized prostate cancer. Prostate Cancer and Prostatic Diseases, 16(1), 50-55.

Pignatti, S. (1997). Dicotyledones dalle Oxalidaceae alle Campanulaceae. In Flora d'Italia, vol. 2 (pp. 264). Bologna: Edagricole.

Prencipe, F. P., Bruni, R., Guerrini, A., Rossi, D., Benvenuti, S., & Pellati, F. (2014). Metabolite profiling of polyphenols in Vaccinium berries and determination of their chemopreventive properties. Journal of Pharmaceutical and Biomedical Analysis, 89(0), 257-267.

Primetta, A., Jaakola, L., Ayaz, F., Inceer, H., & Riihinen, K. (2013). Anthocyanin fingerprinting for authenticity studies of bilberry (Vaccinium myrtillus L.). Food control, 30(2), 662-667.

Rodrigo, R., Gil, D., Miranda Merchak, A., & Kalantzidis, G. (2012). Antihypertensive Role of Polyphenols. Advances in Clinical Chemistry, 58, 225-254.

Siracusa, L., Patane, C., Avola, G., & Ruberto, G. (2012). Polyphenols as Chemotaxonomic Markers in Italian "Long-Storage" Tomato Genotypes. J. Agric. Food Chem., 60(1), 309-314.

Taruscio, T. G., Barney, D. L., & Exon, J. (2004). Content and profile of flavanoid and phenolic acid compounds in conjunction with the antioxidant capacity for a variety of northwest Vaccinium berries. Journal of agricultural and food chemistry, 52(10), 3169-3176.

Uleberg, E., Rohloff, J., Jaakola, L., Trôst, K., Junttila, O., Häggman, H., & Martinussen, I. (2012). Effects of temperature and photoperiod on yield and chemical composition of northern and southern clones of

bilberry (Vaccinium myrtillus L.). Journal of agricultural and food chemistry, 60(42), 10406-10414.

Wang, L.-J., Su, S., Wu, J., Du, H., Li, S.-S., Huo, J.-W., Zhang, Y., & Wang, L.-S. (2014). Variation of anthocyanins and flavonols in Vaccinium uliginosum berry in Lesser Khingan Mountains and its antioxidant activity. Food Chemistry, 160, 357-364.

Wang, L.-S., & Stoner, G. (2008). Anthocyanins and their role in cancer prevention. Cancer letters, 269(2), 281-290.

Manuscript: "Polyphenolic profiles and antioxidant and antiradical activity of Italian berries from *Vaccinium myrtillus* L. and *Vaccinium uliginosum* L. subsp. *gaultherioides* (Bigelow) S.B. Young" by C. Ancillotti et al.

SUPPLEMENTARY MATERIAL

S1. Sampling

Fully ripe *V. myrtillus* and *V. uliginosum* subsp. *gaultherioides* berries were harvested in August 2014 in eighteen microzones belonging to three main areas of Tuscan Apennines, characterized by different environmental conditions, such as altitude and/or cardinal direction and traditionally involved in the harvest of spontaneous bilberry (Table S1). For each sampling zone and species, berries were hand-picked from 5-7 bushes.

Table S1 - Collection zones of *Vaccinium myrtillus* and *Vaccinium uliginosum* subsp. *gaultherioides* berries.

Location name	Coordinates	Cardinal direction	Altitude (m, asl)
Monte Gomito	44°07'36.7"N 10°38'36.2"E	SW	1824
Monte Gomito	44°07'36.1"N 10°38'34.4"E	SW	1826
Monte Gomito	44°07'35.8"N 10°38'33.9"E	SW	1847
Monte Gomito	44°07'34.7"N 10°38'35.5"E	SW	1806
Monte Gomito	44°07'34.4"N 10°38'34.9"E	SW	1820
Monte Gomito	44°07'38.8"N 10°38'50.8"E	NNE	1850
Monte Gomito	44°07'38.5"N 10°38'51.5"E	NNE	1852
Monte Gomito	44°07'40.2"N 10°38'54.1"E	NNE	1831
Monte Gomito	44°07'39.8"N 10°38'59.6"E	NNE	1821
Monte Gomito	44°07'40.9"N 10°39'00.8"E	NNE	1814
Lago Nero	44°06'54.9"N 10°38'14.5"E	NNE	1725
Lago Nero	44°06'52.6"N 10°38'13.5"E	NNE	1705
Lago Nero	44°06'52.7"N 10°38'09.4"E	ENE	1750
Libro Aperto	44°09'26.0"N 10°41'39.2"E	WSW	1597
Libro Aperto	44°09'24.7"N 10°41'39.9"E	WSW	1609
Libro Aperto	44°09'27.4"N 10°41'37.7"E	WSW	1590
Libro Aperto	44°09'27.6"N 10°41'33.2"E	WSW	1569
Libro Aperto	44°09'26.5"N 10°41'30.2"E	WSW	1537

S2. Sample extraction

About 500 mg aliquots of dry weight (d.w.) material were homogenized in an ice bath under magnetic stirring with 15 mL of a methanol/water solution 8/2 (v/v) containing 10 mM NaF to inactivate polyphenol oxidase; the mixture was centrifuged at 1800xg for 5 min and the supernatant recovered. This procedure was repeated twice and the extracts combined.

The following parameters were determined on each *Vaccinium myrtillus* and *Vaccinium uliginosum* subsp. *gaultherioides* berry extract: Total soluble polyphenols (TSP), total monomeric anthocyanins (TMA), radical scavenging activity (RSA), ferric reducing/antioxidant power (FRAP), selected anthocyanins, phenolic acids, coumarins, flavanols, dihydrochalcones and flavonols.

S3. Analysis of total soluble polyphenols

TSP were spectrophotometrically determined as following described: 100-200 µL of the extract (depending on the polyphenol concentration in the extract) were mixed with 200 µL of Folin-Ciocalteau reagent. After 3 min, 400 µL of an aqueous solution saturated with sodium carbonate were added and the mixture obtained was made up to 10 mL with ultra pure water. The solution was dark incubated for 1 h; afterwards the absorbance was measured at 740 nm and polyphenol concentration calculated on the basis of a catechin calibration curve; accordingly, the results were expressed as milligrams of catechin/100 g of d.w. berries.

S4. Analysis of total monomeric anthocyanins

Aliquots of 100-200 µL of berry extract were diluted in buffer solutions at pH=1 and pH=4.5, so as to obtain a final volume of 10 mL. The absorbance

(Abs) of both solutions were measured at 520 and 700 nm and the quantity "ΔAbs" was calculated according to equation 1.

$$\Delta Abs=\left(Abs_{pH=1}^{520\ nm}-Abs_{pH=1}^{700\ nm}\right)-\left(Abs_{pH=4.5}^{520\ nm}-Abs_{pH=4.5}^{700\ nm}\right)$$

Similarly, "ΔAbs" values were also calculated for different concentrations of CYA-3-GLU reference standard and plotted as a function of corresponding CYA-3-GLU concentrations. The best equation fitting the experimental points was calculated by the least square method, thus obtaining a linear calibration curve.
TSA in the extracts were finally calculated using this calibration curve.

S5. DPPH radical scavenging activity assay

RSA was spectrophotometrically measured, using the free radical DPPH, according to the following procedure. Five different amounts of each extract (10-50 µL) were added to 5 mL of a 0.1 mM DPPH solution. For each extract, a blank was performed by replacing the extract volume with ultra pure water. The decrease in absorbance at 517 nm was monitored after 10 min, and then every 10 min up until 60 min, every 30 min after 60, and up until 240 min when the reaction reached a plateau. For each concentration tested, the reaction kinetics was plotted. The percentage of DPPH neutralized at the steady state (%DPPH) was determined by using the equation 2:

$$\%DPPH = 100 \times \frac{\left(Abs_{0}^{E} - Abs_{ss}^{E}\right) - \left(Abs_{0}^{B} - Abs_{ss}^{B}\right)}{Abs_{0}^{E}}$$

where are the absorbances of the extract (E) and the blank (B) at time zero (0) and at the steady state (ss).

The DPPH inhibition percentages obtained were plotted as a function of the corresponding amount of berry (d.w.) in the five samples analyzed and the best equation fitting the experimental points was calculated by the least square method. IC50 was defined as the concentration of the sample (mg of fruit, d.w.) in 1 mL of reaction mixture, necessary to decrease the initial DPPH concentration (which was kept constant in all the experiments) by 50%; therefore, higher IC50 values correspond to lower RSA values.

The RSA of samples (RSAsample) can be derived from IC50 values (µg d.w./µmol DPPH solution) determined on plant extracts (IC50sample) by using the equation 3, allowing for obtaining a parameter that increases with the rise in antiradical activity and that is expressed as µg DPPH inhibited by one µg of d.w. berry sample.

$$RSA_{sample} = \frac{MW_{DPPH}}{IC50_{sample}}$$

S6. FRAP antioxidant activity assay

FRAP reagent was prepared with 10 volumes of 300 mM acetate buffer (pH = 3.6), 1 volume of 10 mM 2,4,6-tripyridyl-s-triazine in 40 mM HCl and 1 volume of 20 mM FeCl3. Aliquots of 100 µL of a properly diluted extract (so as to obtain an absorbance value included in the calibration line) were added to 5 mL of FRAP reagent pre-warmed at 37°C. After three hours of incubation in the dark, absorbance was read at 593 nm. Results are expressed as mmol of 6-hydroxy-2,5,7,8-tetramethylchroman-2-carboxylic acid (Trolox) equivalents (TE) per g of d.w berries.

S7. HPLC-MS/MS analysis of polyphenols

The following polyphenolic compounds were investigated: cyanidin-3-galactoside (CYA-3-GAL), cyanidin-3-glucoside (CYA-3-GLU), cyanidin-3-arabinoside (CYA-3-ARA), delphinidin-3-glucoside (DEL-3-GLU), delphinidin-3-galactoside (DEL-3-GAL), pelargonidin-3-glucoside (PEL-3-GLU), malvidin-3-glucoside (MAL-3-GLU), malvidin-3-galactoside (MAL-3-GAL), peonidin-3-glucoside (PEO-3-GLU), peonidin-3-galactoside (PEO-3-GAL), peonidin-3-arabinoside (PEO-3-ARA), petunidin-3-glucoside (PET-3-GLU), gallic acid (GAL), caffeic acid (CAF), p-coumaric acid (COU), sinapic acid (SIN), ferulic acid (FER), salicylic acid (SAL), chlorogenic acid (CHL), neochlorogenic acid (NEO), cryptochlorogenic acid (CRY), esculetin (ESC), scopoletin (SCO), (+)-catechin (CAT), epicatechin (EPI), luteolin (LUT), myricetin (MYR), phloretin (PHL), phloridzin (PHZ), quercetin (QUE), quercetin-3-rhamnoside (QUE-3-RHA), quercetin-3-glucoside (QUE-3-GLU), quercetin-3-galactoside (QUE-3-GAL) and querectin-3-rutinoside (QUE-3-RUT).

The chromatographic separation was performed on a Waters Acquity BEH C18 column (15 cm × 2.1 cm i.d.; particle size 1.7 μm) equipped with a guard column containing the same stationary phase. Chromatographic analysis of anthocyanins was performed at 50°C with water/formic acid 95:5 v/v (eluent A) and methanol/formic acid 95:5 v/v (eluent B) according to the following gradient: 0.1-33 min linear gradient 7-17% B, 33-38 min isocratic 95% B.

Chromatographic analysis of phenolic acids, coumarins, flavanols, dihydrochalcones and flavonols was performed at 50°C, by eluting with water/formic acid 99.9:0.1 v/v (eluent A) and methanol/formic acid 99.9:0.1 v/v (eluent B) according to the following gradient:0-3 min isocratic 2% B,

3-4 min linear gradient 2-15% B, 4-27 min linear gradient 15-60% B, 27-29 min linear gradient 60-95% B, 29-33 min isocratic 95% B.

The flow rate was 0.3 mL/min and the injection volume was 10 μL for both chromatographic analyses.

Unknown compound identification was carried out using a comprehensive general screening workflow, consisting of triggered multiple mass experiments driven by the Information Dependent Acquisition (IDA) software (Sciex). After a survey scan acquisition (from 150 to 1000 Da), an enhanced resolution experiment is instantly triggered to confirm the charge state and isotope pattern of ions that satisfy the entering conditions in the IDA loop. Once the ions of interest have been identified, a dependent enhanced product ion scan is performed on the masses identified. The IDA loop is repeated for the entire duration of the LC analysis.

Target compound MS/MS analysis was carried out using the Multiple Reaction Monitoring mode by ESI both in negative (for phenolic acids, coumarins, flavanols, dihydrochalcones and flavonols) and positive mode (for anthocyanins). For each investigated compound, the most intense transition was used for quantification and the second most intense for confirming identification. Compound dependent parameters were optimized by direct infusion of properly diluted target analyte standard solutions (Tables S2 and S3).

Table S2 - Optimized MS parameters for the investigated anthocyanins. Letters A and B after each compound name refer to the quantifier and qualifier transitions respectively. (DP) declustering potential; (EP) entrance potential; (CEP) collision cell entrance potential; (CE) collision energy; (CXP) collision cell exit potential.

Compound	Precursor Ion (m/z)	Product Ion (m/z)	DP (V)	EP (V)	CEP (V)	CE (V)	CXP (V)
DEL-3-GLU-A	465.3	303.1	50	4	20	40	3
DEL-3-GLU-B	465.3	229.2	50	4	20	70	2
DEL-3-GAL-A	465.3	303.1	55	5	20	40	3
DEL-3-GAL-B	465.3	229.2	55	5	20	75	1
CYA-3-GAL-A	449.3	287.2	50	5	15	35	3
CYA-3-GAL-B	449.3	137.2	50	5	15	80	2

Table S2 (continued)

Compound	Precursor Ion (m/z)	Product Ion (m/z)	DP (V)	EP (V)	CEP (V)	CE (V)	CXP (V)
CYA-3-GLU-A	449.3	287.1	45	6	20	35	3
CYA-3-GLU-B	449.3	137.2	45	6	20	80	1
CYA-3-ARA-A	419.3	287.1	50	5	20	35	3
CYA-3-ARA-B	419.3	137.2	50	5	20	75	2
PET-3-GLU-A	479.3	317.3	50	5	20	35	3
PET-3-GLU-B	479.3	302.3	50	5	20	60	3
PEO-3-GAL-A	463.3	301.2	45	7	15	35	3
PEO-3-GAL-B	463.3	286.1	45	7	15	55	2
PEO-3-GLU-A	463.3	301.2	45	7	15	35	3
PEO-3-GLU-B	463.3	286.1	45	7	15	55	2
PEO-3-ARA-A	433.3	301.2	45	7	15	35	3
PEO-3-ARA-B	433.3	286.1	45	7	15	55	2
MAL-3-GAL-A	493.3	331.2	55	4	20	35	3
MAL-3-GAL-B	493.3	315.1	55	4	20	65	2
MAL-3-GLU-A	493.3	331.2	50	4	20	35	3
MAL-3-GLU-B	493.3	315.1	50	4	20	65	2
PEL-3-GLU-A	433.3	271.2	50	4	15	35	2
PEL-3-GLU-B	433.3	121.0	50	4	15	80	1

Table S3 - Optimized MS parameters for the investigated polyphenols. Letters A and B after each compound name refer to the quantifier and qualifier transitions respectively. (DP) declustering potential; (EP) entrance potential; (CEP) collision cell entrance potential; (CE) collision energy; (CXP) collision cell exit potential.

Compound	Precursor Ion (m/z)	Product Ion (m/z)	DP (V)	EP (V)	CEP (V)	CE (V)	CXP (V)
GAL-A	169.1	125.2	-45	-8	-15	-23	-1
GAL-B	169.1	79.0	-45	-8	-15	-32	-1
COU-A	163.0	119.0	-30	-2.5	-18	-20	0
COU-B	163.0	92.9	-30	-2.5	-18	-44	0
CAF-A	178.9	135.2	-30	-8	-8	-22	0
CAF-B	178.9	134.0	-30	-8	-18	-32	-2
FER-A	193.0	134.1	-40	-6	-19	-24	0
FER-B	193.0	177.9	-40	-6	-19	-22	0
CHL-A	353.0	191.1	-30	-6	-25	-28	-2
CHL-B	353.0	85.0	-30	-6	-25	-58	0
NEO-A	353.0	191.1	-40	-6.5	-25	-32	0
NEO-B	353.0	135.1	-40	-6.5	-25	-44	0
CRY-A	353.0	173.1	-35	-4	-25	-22	0
CRY-B	353.0	179.2	-35	-4	-25	-28	0
SAL-A	137.2	93.1	-40	-8	-10	-25	-1
SAL-B	137.2	65.1	-40	-8	-10	-40	-1
ESC-A	176.9	133.1	-40	-8	-18	-26	0
ESC-B	176.9	105.0	-40	-8	-18	-26	0
SCO-A	190.9	176.0	-30	-6	-19	-22	0
SCO-B	190.9	104.0	-30	-6	-19	-32	0
CAT-A	289.2	109.1	-50	-7	-20	-37	-1
CAT-B	289.2	122.9	-50	-7	-20	-40	-1
EPI-A	289.2	109.1	-50	-6	-20	-37	-1
EPI-B	289.2	122.9	-50	-6	-20	-40	-1

Table S3 (continued)

Compound	Precursor Ion (m/z)	Product Ion (m/z)	DP (V)	EP (V)	CEP (V)	CE (V)	CXP (V)
EPI-A	289.2	109.1	-50	-6	-20	-37	-1
EPI-B	289.2	122.9	-50	-6	-20	-40	-1
QUE-A	301.2	151.1	-45	-9	-20	-32	-1
QUE-B	301.2	120.8	-45	-9	-20	-35	-1
QUE-3-GLU-A	463.4	300.2	-50	-8	-20	-37	-2
QUE-3-GLU-B	463.4	270.8	-50	-8	-20	-55	-2
QUE-3-GAL-A	463.4	300.2	-50	-7	-20	-35	-2
QUE-3-GAL-B	463.4	271.1	-50	-7	-20	-58	-2
QUE-3-RHA-A	447.3	300.1	-60	-8	-20	-35	-1
QUE-3-RHA-B	447.3	271.2	-60	-8	-20	-53	-1
QUE-3-RUT-A	609.5	300.3	-65	-8	-20	-50	-2
QUE-3-RUT-B	609.5	271.0	-65	-8	-20	-75	-2
PHL-A	273.1	167.2	-35	-10	-20	-25	-1
PHL-B	273.1	123.2	-35	-10	-20	-32	-1
PHZ-A	435.4	273.0	-40	-4	-15	-25	-1
PHZ-B	435.4	167.0	-40	-4	-15	-40	-1
MYR-A	317.2	137.3	-40	-7	-20	-37	-1
MYR-B	317.2	137.3	-40	-7	-20	-37	-1
SIN-A	223.0	121.0	-40	-8	-15	-40	-1
SIN-B	223.0	207.9	-40	-8	-15	-23	-1
LUT-A	285.2	133.0	-50	-8	-20	-48	-2
LUT-B	285.2	150.9	-50	-8	-20	-38	-2

Source dependent parameters were optimized in flow injection analysis at optimal LC flow and mobile phase composition. For negative ion determination optimal source dependent parameters were as follows: Curtain Gas 30, CAD Gas Medium, Temperature 600°C, Gas 1 50, Gas 2 65, Interface Heater ON and IonSpray Voltage -4500 V. For positive ion determination optimal source dependent parameters were as follows: Curtain Gas 30, CAD Gas Medium, Temperature 600°C, Gas 1 40, Gas 2 65, Interface Heater ON and IonSpray Voltage 5500 V.

The instrumental quantification limits (LOQs) were experimentally determined by successive injections of standard solutions at increasing dilutions, monitoring the signal to noise ratio (s/n). Accordingly, LOQs (s/n=10) were the following. 10 pg injected for SCO, PHL and PHZ; 30 pg injected for NEO, CHL CRY, COU, FER, QUE-3-GAL, QUE-3-GLU, QUE and QUE-3-RUT; 50 pg injected for SAL, LUT, ESC and QUE-3-RHA; 100 injected pg for SIN, GAL, CAF, PEO-3-GLU, PEO-3-GAL,

CAT and EPI; 150 pg injected for CYA-3-ARA and PEO-3-ARA; 200 pg injected for DEL-3-GLU, DEL-3-GAL, CYA-3-GAL, CYA-3-GLU and PET-3-GLU; 300 pg injected for MAL-3-GAL, MAL-3-GLU and PEL-3-GLU and 500 pg injected for MYR.

The apparent recovery was evaluated by spiking the freeze-dried berry powder of *V. myrtillus* and *V. uliginosum* subsp. *gaultherioides* with 100 µL of a 50 mg/L solution of PEL-3-GLU, SIN and LUT, which were found to be absent in the investigated samples and therefore used as surrogate standards. For each surrogate standard, the recovery values were calculated by subtracting the ME from the apparent recovery.

Matrix effect (ME) was investigated by spiking the *V. myrtillus* and *V. uliginosum* subsp. *gaultherioides* extracts with three different concentrations of target analytes (i.e. 100, 200 and 300 µg/L) and analysing them by HPLC, together with the non-spiked ones. For each compound and specie, chromatographic areas found in spiked extracts were subtracted from that of the non-spiked one and the resulting differences were plotted as a function of spiked concentrations. The best line fitting the experimental points (with intercept equal to zero) was calculated by the least square method and its slope (s_{matrix}) was compared with the one of the corresponding calibration line in water ($s_{solvent}$). ME values were finally calculated according to the equation 4.

$$ME(\%) = \left(\frac{s_{matrix}}{s_{solvent}} \cdot 100\right) - 100$$

Chapter 4

Liquid chromatographic/electrospray ionization quadrupole/time of flight tandem mass spectrometric study of polyphenolic composition of different *Vaccinium* berry species and their comparative evaluation

Claudia Ancillotti
Lorenzo Ciofi
Daniele Rossini
Ugo Chiuminatto
Jianru Stahl-Zeng
Serena Orlandini
Sandra Furlanetto
Massimo Del Bubba

Analytical and Bioanalytical Chemistry 409 (2017) 1347–1368

Abstract

Ultra-high-performance liquid chromatography coupled with high resolution quadrupole-time of-flight mass spectrometry with both negative and positive ionization was used for comprehensively investigating phenolic and polyphenolic compounds in berries from three spontaneous or cultivated *Vaccinium* species (i.e. *V. myrtillus*, *V. uliginosum* subsp. *gaultherioides* and *V. corymbo*sum). More than 200 analytes, among phenolic and polyphenolic compounds belonging to the classes of anthocyanins, monomeric and oligomeric flavonols, flavanols, dihydrochalcones, phenolic acids, together with other polyphenolic compounds of mixed structural characteristics, were identified. Some of the polyphenols herein investigated, such as anthocyanidin glucuronides and malvidin-feruloyl-hexosides in *V. myrtillus*, or anthocyanindin aldopentosides and coumaroyl-hexosides in *V. uliginosum* subsp. *gaultherioides* and a large number of proanthocyanidins with high molecular weight in all species, were described for the first time. Principal component analysis applied on original LC-TOF data, acquired in survey scan mode, successfully discriminated the three *Vaccinium* species investigated, on the basis of their polyphenolic composition, underlying one more time the fundamental role of mass spectrometry for food characterization.

Keywords: Polyphenols, flavonoids, *Vaccinium* species, liquid chromatography, high-resolution mass spectrometry, principal component analysis.

1 Introduction

The consumption of berries (e.g. blackberry, bilberry, blueberry, and cranberry) is considered an important contribution to healthy diets, owing to the various classes of phenolic compounds contained in large quantities in these fruits (1). In fact, the class of phenolic compounds comprises a very high and increasing number of bioactive compounds (2), which are suggested to provide important health-protecting attributes such as anti-inflammatory, anti-hypertensive, anti-microbial and anti-cancer properties (3).

Among the different berry species, *Vaccinium myrtillus* is the wild bilberry native to mountain areas of Northern and Central Europe, widely diffused also in Italian Alps and Apennines. In these zones the increasing presence of a different spontaneous *Vaccinium* species, recently identified through genetic analyses as the *V. uliginosum* subsp. *gaultherioides* (locally named "false bilberry"), has been recently observed (4). The cultivation and commercialization of *V. corymbosum* berries (i.e. the blueberry) is also widespread in the same area.

V. myrtillus is one of the richest fruit in polyphenols, with particular regard to anthocyanins (5) and is therefore considered a "functional food" (6). Accordingly, *V. myrtillus* berries are largely consumed both as fresh fruits and processed products, such as juices and dietary supplements.

Many researches focusing on the determination of selected anthocyanins were carried out on bilberries from different European areas (7-11). Interestingly, the composition of the most abundant anthocyanins (i.e. glucosides, galactosides and arabinosides of cyanidin, delphinidin, petunidin, peonidin and malvidin) of *V. myrtillus* berries has been found different from the ones of blueberry (7), suggesting the potential use of polyphenolic profiles for the discrimination of transformed products from these fruit species. This aspect is very important since *V. myrtillus* is

supposed to be a food with a higher nutraceutical value than *V. corymbosum* (6).

Furthermore, the feasibility of using the anthocyanin profile as a species fingerprint, becomes noteworthy for discerning *V. myrtillus* from *V. uliginosum* L. subsp. *gaultherioides*. In fact, the phenotype of this latter berry is very similar to the *V. myrtillus* one and the two fruits might be confused by the harvesters involved in the production chain of transformed bilberry. Italian *V. uliginosum* L. subsp. *gaultherioides* fruits were recently analysed for the first time by our team, evidencing a lower content of total soluble polyphenols and total monomeric anthocyanins, as well as smaller antioxidant and antiradical activities, compared to *V. myrtillus* ones (4). Hence, from this point of view, a lower nutraceutical value of "false bilberry", compared to bilberry, can be assumed. Concentrations of individual anthocyanins found in "false bilberry" were in most cases lower than those of bilberry, as well. Moreover, the relative abundance of the predominant anthocyanins of *V. uliginosum* L. subsp. *gaultherioides* berries was found very different from that of *V. myrtillus* fruits (4) and, interestingly, rather similar to the profile of *V. corymbosum*, being for instance both "false bilberry" and blueberry characterized by the predominance of malvidin derivatives (4, 7).

The analysis of further classes of polyphenols, such as flavonols, flavanols and phenolic acids, which might be also important for discriminating one *Vaccinium* species from another, has been performed only occasionally in *V. myrtillus* (12, 13) and *V. corymbosum* berries (14). Data concerning some phenolic compounds have been recently reported also for *V. uliginosum* L. subsp. *gaultherioides* berries (4).

Nevertheless, in the current literature, there is a lack of in-depth studies dealing with the simultaneous investigation of the different polyphenolic classes in *V. myrtillus*, *V. corymbosum* and *V. uliginosum* L. subsp. *gaultherioides* berries.

In order to carry out such a kind of studies, complex analytical approaches, involving non-target metabolomic investigations, are required. These investigations are commonly performed using liquid chromatography (LC) coupled with mass spectrometry (MS) (15, 16), employing in some cases also ultraviolet detection (17, 18) and occasionally nuclear magnetic resonance, as well (19). Actually, LC-MS is one of the most powerful analytical technique for polyphenol analysis. In fact, atmospheric pressure ionization sources provide a soft ionization of target analytes, which is particularly recommended for structure elucidation of polar, non-volatile and thermally labile compounds, such as flavonoids. Moreover, the use of tandem mass spectrometry (MS/MS) enables to obtain important structurally-related information through the fragmentation of parent molecules. In this context, the adoption of high-resolution mass spectrometry (e.g. time-of-flight based instruments), allows for obtaining accurate mass read-out, thus facilitating the assignment of an elemental formula to the parent molecule and/or to the fragments and its fragmentation characteristics (20).

Based on the above-reported considerations, this study aimed at comprehensively investigating the polyphenolic profiles of *V. myrtillus*, *V. corymbosum* and *V. uliginosum* L. subsp. *gaultherioides* berries through a non-target LC-MS/MS approach, using a quadrupole/time of flight mass spectrometry (Q/TOF).

2 Materials and methods

2.1 Reagent and standards

Polyphenol standards were supplied as follows: cyanidin-3-galactoside, cyanidin-3-glucoside, cyanidin-3-arabinoside, delphinidin-3-glucoside, delphinidin-3-galactoside, malvidin-3-glucoside and malvidin-3-galactoside

by Extrasynthese (Genay, France); peonidin-3-glucoside, peonidin-3-galactoside, peonidin-3-arabinoside and petunidin-3-glucoside by Polyphenols Laboratories AS (Sandnes, Norway); (+)-catechin, epicatechin, procyanidin B1, procyanidin B2, procyanidin A2, quercetin-3-galactoside, quercetin-3-glucoside, querectin-3-rutinoside, quercetin-3-rhamnoside, quercetin-3-glucuronide, quercetin, myricetin, keampferol-7-neohesperidoside, gallic acid, caffeic acid, p-coumaric acid, ferulic acid, chlorogenic acid, neochlorogenic acid, cryptochlorogenic acid, 1,5-dicaffeoylquinic acid, esculetin, scopoletin and phloridzin by Sigma-Aldrich (St. Louis, MO, USA).

LC-MS grade methanol and water were obtained from J.T. Baker (Deventer, the Netherlands). HPLC grade methanol and formic acid eluent additive for LC-MS were purchased from Sigma-Aldrich (St. Louis, MO, USA). Sodium fluoride was obtained by Merck (Darmstadt, Germany). Ultrapure water was taken from a Milli-Q system supplied by Millipore (Billerica, MA, USA). Nylon membranes (porosity 0.2 µm) for the filtration of the bilberry extracts before HPLC analysis were obtained from VWR™ International (Radnor, PA, USA).

2.2 Fruits sampling and post-harvest treatment

V. myrtillus and *V. uliginosum* L. subsp. *gaultherioides* samples analysed in the present study, consisted of blends of berries collected in fifteen different zones of Tuscan Apennines in August 2014 (see Table S1 of the Electronic Supplementary Material). Hence, representative samples of the two wild berry species were obtained for the whole investigated area. In these samples the variations in polyphenolic composition within the species, due to different genotypes and/or environmental conditions (such as altitude and solar exposure of collection areas) should be therefore minimized.

In order to confirm the attribution to *V. uliginosum* subsp. *gaultherioides* of the "false bilberry" plants included in the present study, a genetic analysis was carried out following the specifications reported by Ancillotti and co-workers (4)

The *V. corymbosum* sample was a mixture of berries of the genotypes "Duke", "Berkely" and "Bluecrop", cultivated in a site included in the area of Tuscan Apennines selected for the harvest of wild species. These cultivars were chosen on the basis of their wide diffusion in the Italian market (21).

After the sampling, all berries were immediately frozen in liquid nitrogen, freeze-dried and finally grinded in order to obtain a homogeneous powder. All samples were stored at −20 °C until analyses were performed.

2.3 Sample Extraction

Three representative aliquots from each berry sample were extracted according to a procedure previously developed for *Fragaria vesca* berries (22) and successively verified for bilberry and "false bilberry" (4). Briefly, about 500 mg dry weight (d.w.) berry aliquots were homogenized in an ice bath under magnetic stirring with 15 mL of a methanol/water solution 8/2 (v/v), containing NaF 10 mM to inactivate polyphenol oxidase; the mixture was centrifuged at 1800xg for 5 min and the supernatant recovered. This procedure was repeated three times and the resulting extracts were combined. The organic solvent was removed by vacuum evaporation, acidified with formic acid up to pH = 2.0±0.1 (volume of formic acid 170-190 µL) and filtrated at 0.2 µm with nylon membranes, before LC-MS/MS analysis. A final extract volume of approximately 9.2 mL was therefore obtained.

2.4 LC-TOF and LC-Q/TOF analysis

LC analysis was performed on an Agilent Infinity 1290 system equipped with an Acquity BEH C18 column (15 cm × 2.1 cm i.d., particle size 1.7 μm) and a guard column containing the same stationary phase (Waters, Milford, MA, USA). Column temperature was set at 50°C. Water/formic acid 95:5 *v/v* (eluent A) and methanol/formic acid 95:5 *v/v* (eluent B) were used for the analyte elution, according to the following gradient:0-2 min isocratic 2% B, 2-30 min linear gradient 2-30% B, 30-35 min linear gradient 30-95% B, 35-37 min isocratic 95% B. The flow rate was 450 μL/min and the injection volume was 2 μL.

The LC system was coupled with a SCIEX (Framingham, MA, USA) TripleTOF® 5600 hybrid Q/TOF mass analyzer by the DuoSpray™ Source for MS and MS/MS analysis and the following source parameters were kept constant during the whole acquisition: heater temperature 400 ºC; Curtain Gas™ 25; nebulizing gas 45; heating gas 45; spray voltage +5300 V and -4500 V for positive and negative polarity, respectively.

Each sample was analyzed, both under positive and negative ionization, using two different mass acquisition methods for each ionization mode. The first one consisted of a high resolution TOF MS survey scan (from 100 to 2000 Da, cycle time 250 ms). The second acquisition method was a TOF survey scan experiment from 100 to 2000 Da (accumulation time 250 ms), followed by the selection of the top 10 candidate ions collected within each cycle, by the Information Dependent Acquisition (IDA) software. Q/TOF MS/MS spectra of the ions selected in each cycle were then acquired from 100 to 2000 Da, each one with an accumulation time of 75 ms, using a collision energy of 35 eV and a collision energy spread of ±15 eV (whole cycle time 1050 msec). In order to enhance the general quality of MS/MS spectra of peaks with low signal intensity, Q/TOF MS/MS analysis was also

performed using narrower mass ranges, typically from 100 to 1250 Da (accumulation time of 50 msec and whole cycle time 800 ms).
Automated calibration was performed using an external calibrant delivery system (CDS) which infuses proper calibration solution prior to sample introduction.

2.5 Data Processing and metabolite identification

The high number of information deriving from the 5600 TripleTOF® analysis of investigated samples, both in negative and positive ionization, needs to be processed with specific software. PeakView® 2.2 and MasterView® 1.1 software were used for the compound identification based on the TOF accurate mass and isotope pattern determinations, as well as on the Q/TOF fragmentation spectra of parent ions.
The following identification criteria were adopted in this study.

- TOF accuracy of the pseudo-molecular ion: < 5 ppm;
- Isotope ratio difference compared to the theoretical isotope profile: < 20%;
- Purity score of the MS/MS spectra compared to the one of available standards: ≥ 80%.

In this manuscript we used the words “identification/identified”, sometimes stressed by the words “undoubted/undoubtedly”, “unequivocal/unequivocally” when an authentic reference standard was available. Conversely, the terms “putative/putatively” or “tentative/tentatively” were used in the sentence when the reference standard was not available.
Then, in order to compare the polyphenolic compositions of the three investigated species and to highlight the polyphenols that mainly contributed to their differentiation, Principal Component Analysis (PCA) of molecular or quasi-molecular ions of identified and putatively assigned

compounds was performed using MarkerView 1.2.1 software. This approach was carried out separately for negative and positive ionization modes. Quality control (QC) of PCA was performed, using a QC sample, consisting of a mixture of equal aliquots of each berry extract. QC evaluation was carried out by verifying if PCA object scores obtained by replicated injections of the QC sample were close to the origin of PCA coordinates.

3 Results and discussion

3.1 Compound identification by LC-ESI-TOF and LC-ESI-Q/TOF analysis

The polyphenols found in berries of the investigated *Vaccinium* species were identified according to their chromatographic behaviour, their TOF MS and Q/TOF MS/MS spectra, also in comparison with standard reference compounds, when available. Both positive and negative ionization modes were used for compound attribution.

Molecules that were unequivocally or putatively identified belonged to the compound classes of anthocyanins, flavonols, flavanols and phenolic acids; other polyphenolic compounds belonging to miscellaneous classes (e.g. coumarins and dihydrochalcones) were also tentatively recognized.

Compound identification within each class is detailed below and summarised in Tables 1-4, which show retention time (Rt, min), mass (Da) found by the TOF survey scan experiment and main MS/MS fragments (Da) obtained by the Q/TOF experiment, proposed formula and corresponding exact mass (Da), mass accuracy (Δ, ppm), and putative identification of the peaks considered. Peaks reported in these tables were also shown in Fig. S1-S4 of the Electronic Supplementary Material.

3.1.1 Anthocyanins

Anthocyanins are characterized by a positive charge at pH<3 and therefore are typically determined in form of molecular ion $[M]^+$ (23); accordingly, these polyphenols were identified under positive ionization (Table 1). Moreover, their attribution was also confirmed under negative ionization, by monitoring the quasi-molecular ion $[M-2H]^-$, according to the mass spectrometric behaviour observed for these polyphenols by Sun and colleagues (24). However, for this latter ionization mode, a less complete profile of the anthocyanin fraction was obtained, owing to its generally lower sensitivity that prevented in several cases the signal detection (data not shown).

It should also be remarked that when the anthocyanin has molecular weight one Da higher than that of a flavonol (i.e. delphinidin vs. quercetin, cyanidin vs. kaempferol and petunidin vs. isorhamnetin derivatives of a same sugar), the $[M]^+$ or the $[M-2H]^-$ ions of the former and the $[M+H]^+$ or the $[M-H]^-$ ions of the latter are isobars, thus making relevant for their discrimination the chromatographic behaviour.

As widely reported elsewhere (15, 18, 25), also in this study MS/MS fragmentation of anthocyanins produced only the loss of the sugar units (e.g. 162 Da for a hexose and 132 Da for a pentose) and the corresponding detection of the aglycone fragment (i.e. 287.06 Da for cyanidin, 303.05 Da for delphinidin, 317.07 Da for petunidin, 301.07 Da for peonidin and 331.08 Da for malvidin) (Table 1).

Using the IDA TOF-Q/TOF workflow and, when possible, by comparing the retention time and mass spectra of unknowns with those of authentic standards, the undoubted or at least the tentative identification of 64 anthocyanins was achieved. TOF MS $[M]^+$ molecular ions matched the proposed formulae with very high mass accuracy, being Δ absolute values

Table 1. Retention times (Rt, min), $[M]^+$ molecular ions (TOF MS, Da), mass fragments (Q/TOF MS/MS, Da), proposed formula, corresponding exact mass (Da) and accuracy (Δ, ppm) of peaks tentatively identified as anthocyanins in *V. myrtillus* (M), *V. uliginosum* L. subsp. *gaultherioides* (G) and *V. corymbosum* (C) under positive ionization. Symbols "+" and "–", mean detected and not detected.

Peak	Rt	TOF MS	Q/TOF MS/MS	Proposed formula	Exact mass	Δ	M	G	C	Tentative identification
1	9.7	627.1565	465.1078; 303.0485	$C_{27}H_{31}O_{17}$	627.1556	1.4	+	–	–	Delphinidin-dihexoside (I) [a]
2	10.2	611.1677	449.1052; 287.0551	$C_{27}H_{31}O_{16}$	611.1607	0.9	+	–	–	Cyanidin-dihexoside (I) [a]
3	10.5	627.1549	465.1078; 303.0485	$C_{27}H_{31}O_{17}$	627.1556	-1.0	+	–	–	Delphinidin-dihexoside (II) [a]
4	11.0	611.1609	449.1118; 287.0559	$C_{27}H_{31}O_{16}$	611.1607	0.3	+	–	–	Cyanidin-dihexoside (II) [a]
5	11.4	627.1551	465.1007; 303.0502	$C_{27}H_{31}O_{17}$	627.1556	-0.8	+	–	–	Delphinidin-dihexoside (III) [a]
6	12.6	465.1031	303.0501	$C_{21}H_{21}O_{12}$	465.1027	0.8	+	+	+	Delphinidin-3-*O*-galactoside [b]
7	13.0	479.0818	303.0495	$C_{21}H_{19}O_{13}$	479.0820	-0.1	+	–	–	Delphinidin-glucuronide
8	13.2	597.1447	303.0499	$C_{26}H_{29}O_{16}$	597.1450	-0.6	+	–	–	Delphinidin-aldopentose-hexoside (I) [c]
9	13.8	465.1032	303.0510	$C_{21}H_{21}O_{12}$	465.1027	0.9	+	+	+	Delphinidin-3-*O*-glucoside [b]
10	14.0	597.1447	303.0502	$C_{26}H_{29}O_{16}$	597.1450	-0.6	+	–	–	Delphinidin-aldopentose-hexoside (II) [c]
11	14.8	435.0926	303.0505	$C_{20}H_{19}O_{11}$	435.0922	0.9	+	+	+	Delphinidin-3-*O*-arabinoside
12	14.8	449.1081	287.0554	$C_{21}H_{21}O_{11}$	449.1078	0.7	+	+	+	Cyanidin-3-*O*-galactoside [b]
13	15.4	611.1598	287.0551	$C_{27}H_{31}O_{16}$	611.1607	-1.5	+	–	–	Cyanidin-dihexoside (III) [c]
14	15.7	581.1502	287.0551	$C_{26}H_{29}O_{15}$	581.1501	0.3	+	–	–	Cyanidin-aldopentose-hexoside (I) [c]
15	15.8	463.0867	287.0543	$C_{21}H_{19}O_{12}$	463.0871	-0.9	+	–	–	Cyanidin-glucuronide
16	16.3	449.1080	287.0555	$C_{21}H_{21}O_{11}$	449.1078	0.3	+	+	+	Cyanidin-3-*O*-glucoside [b]
17	16.9	479.1188	317.0659	$C_{22}H_{23}O_{12}$	479.1184	0.8	+	+	+	Petunidin-3-*O*-galactoside
18	17.0	419.0976	287.0558	$C_{20}H_{19}O_{10}$	419.0978	0.9	+	+	+	Cyanidin-3-*O*-arabinoside [b]
19	17.2	581.1503	287.0555	$C_{26}H_{29}O_{15}$	581.1501	0.3	+	–	–	Cyanidin-aldopentose-hexoside (II) [c]
20	17.6	493.0973	317.0652	$C_{22}H_{21}O_{13}$	493.0977	-0.8	+	–	–	Petunidin-glucuronide
21	17.9	611.1603	317.0650	$C_{27}H_{31}O_{16}$	611.1607	-0.6	+	–	–	Petunidin-aldopentose-hexoside [c]
22	18.1	479.1188	317.0657	$C_{22}H_{23}O_{12}$	479.1184	0.9	+	+	+	Petunidin-3-*O*-glucoside [b]
23	18.6	551.1392	287.0546	$C_{25}H_{27}O_{14}$	551.1395	-0.5	+	–	–	Cyanidin-aldodipentoside [c]
24	18.7	435.0932	303.0492	$C_{20}H_{19}O_{11}$	435.0922	2.2	+	+	+	Delphinidin-3-*O*-xyloside
25	18.9	463.1235	301.0713	$C_{22}H_{23}O_{11}$	463.1235	0.1	+	+	+	Peonidin-3-*O*-galactoside [b]
26	19.0	449.1081	317.0660	$C_{21}H_{21}O_{11}$	449.1078	0.5	+	+	+	Petunidin-3-*O*-arabinoside

Table 1 (continued)

Peak	Rt	TOF MS	Q/TOF MS/MS	Proposed formula	Exact mass	Δ	M	G	C	Tentative identification
27	19.6	595.1652	301.0715	$C_{27}H_{31}O_{15}$	595.1657	-0.9	+	–	–	Peonidin-aldopentose-hexoside (I) [c]
28	20.2	463.1238	301.0714	$C_{22}H_{23}O_{11}$	463.1235	0.7	+	+	+	Peonidin-3-*O*-glucoside [b]
29	20.3	493.1342	331.0816	$C_{23}H_{25}O_{12}$	493.1340	0.4	+	+	+	Malvidin-3-*O*-galactoside [b]
30	20.5	419.0971	287.0552	$C_{20}H_{19}O_{10}$	419.0973	-0.4	+	+	+	Cyanidin-aldopentoside
31	20.8	595.1661	301.0708	$C_{27}H_{31}O_{15}$	595.1657	0.6	+	–	–	Peonidin-aldopentose-hexoside (II) [c]
32	21.0	433.1131	301.0711	$C_{21}H_{21}O_{10}$	433.1129	0.5	+	+	+	Peonidin-3-*O*-arabinoside [b]
33	21.1	507.1137	303.0502	$C_{23}H_{23}O_{13}$	507.1133	0.7	–	–	+	Delphinidin-acetyl-hexoside (I)
34	21.3	493.1345	331.0818	$C_{23}H_{25}O_{12}$	493.1340	0.8	+	+	+	Malvidin-3-*O*-glucoside [b]
35	21.4	419.0976	287.0540	$C_{20}H_{19}O_{10}$	419.0973	0.7	+	+	+	Cyanidin-3-*O*-xyloside
36	22.3	463.1237	331.0822	$C_{22}H_{23}O_{11}$	463.1235	0.4	+	+	+	Malvidin-3-*O*-arabinoside
37	23.1	449.1086	317.0659	$C_{21}H_{21}O_{11}$	449.1078	1.8	+	+	+	Petunidin-3-*O*-xyloside
38	23.2	639.1924	331.0807	$C_{29}H_{35}O_{16}$	639.1919	0.7	–	–	+	Malvidin-deoxyhexose-hexoside
39	23.5	535.1076	287.0556	$C_{24}H_{23}O_{14}$	535.1082	-1.1	–	–	+	Cyanidin-malonyl-hexoside
40	23.7	491.1186	287.0550	$C_{23}H_{23}O_{12}$	491.1184	0.4	+	–	+	Cyanidin-acetyl-hexoside (I)
41	24.5	507.1136	303.0405	$C_{23}H_{23}O_{13}$	507.1133	0.6	–	–	+	Delphinidin-acetyl-hexoside (II)
42	25.2	579.1339	331.0819	$C_{26}H_{27}O_{15}$	579.1344	-0.9	–	–	+	Malvidin-malonyl-hexoside (I)
43	25.4	521.1290	317.0645	$C_{24}H_{25}O_{13}$	521.1290	0.1	+	–	+	Petunidin-acetyl-hexoside (I)
44	25.4	433.1138	301.0714	$C_{21}H_{21}O_{10}$	433.1129	2.1	+	+	+	Peonidin-3-*O*-xyloside
45	26.2	463.1240	331.0820	$C_{22}H_{23}O_{11}$	463.1235	1.2	+	+	+	Malvidin-3-*O*-xyloside
46	27.2	505.1343	301.0703	$C_{24}H_{25}O_{12}$	505.1340	0.5	+	–	+	Peonidin-acetyl-hexoside (I)
47	27.2	491.1189	287.0552	$C_{23}H_{23}O_{12}$	491.1184	1.0	+	–	+	Cyanidin-acetyl-hexoside (II)
48	27.5	579.1349	331.0825	$C_{26}H_{27}O_{15}$	579.1344	0.9	–	–	+	Malvidin-malonyl-hexoside (II)
49	27.9	535.1455	331.0813	$C_{25}H_{27}O_{13}$	535.1446	1.7	+	–	+	Malvidin-acetyl-hexoside (I)
50	28.2	521.1293	317.0662	$C_{24}H_{25}O_{13}$	521.1290	0.7	+	–	+	Petunidin-acetyl-hexoside (II)
51	29.3	611.1401	303.0503	$C_{30}H_{27}O_{14}$	611.1395	1.0	+	–	–	Delphinidin-coumaroyl-hexoside (I)
52	30.5	505.1345	301.0702	$C_{24}H_{25}O_{12}$	505.1340	0.8	+	–	+	Peonidin-acetyl-hexoside (II)
53	30.7	535.1456	331.0814	$C_{25}H_{27}O_{13}$	535.1446	1.9	+	–	+	Malvidin-acetyl-hexoside (II)
54	31.3	595.1451	287.0549	$C_{30}H_{27}O_{13}$	595.1446	0.8	+	+	–	Cyanidin-coumaroyl-hexoside (I)
55	31.5	611.1395	303.0496	$C_{30}H_{27}O_{14}$	611.1395	0.0	+	–	–	Delphinidin-coumaroyl-hexoside (II)
56	31.7	625.1551	317.0652	$C_{31}H_{29}O_{14}$	625.1552	-0.1	+	–	+	Petunidin-coumaroyl-hexoside (I)

Table 1 (continued)

Peak	Rt	TOF MS	Q/TOF MS/MS	Proposed formula	Exact mass	Δ	M	G	C	Tentative identification
57	32.1	595.1457	287.0556	$C_{30}H_{27}O_{13}$	595.1446	1.9	+	+	–	Cyanidin-coumaroyl-hexoside (II)
58	32.1	609.1609	301.0712	$C_{31}H_{29}O_{13}$	609.1603	1.1	+	–	–	Peonidin-coumaroyl-hexoside (I)
59	32.2	625.1557	317.0656	$C_{31}H_{29}O_{14}$	625.1552	0.8	+	–	+	Petunidin-coumaroyl-hexoside (II)
60	32.2	639.1717	331.0811	$C_{32}H_{31}O_{14}$	639.1708	1.4	+	–	+	Malvidin-coumaroyl-hexoside (I)
61	32.3	669.1821	331.0812	$C_{33}H_{33}O_{15}$	669.1814	1.0	+	–	–	Malvidin-feruloyl-hexoside (I)
62	32.4	609.1611	301.0712	$C_{31}H_{29}O_{13}$	609.1603	1.3	+	–	–	Peonidin-coumaroyl-hexoside (II)
63	32.4	639.1719	331.0824	$C_{32}H_{31}O_{14}$	639.1708	1.8	+	+	+	Malvidin-coumaroyl-hexoside (II)
64	32.5	669.1819	331.0810	$C_{33}H_{33}O_{15}$	669.1814	0.8	+	–	–	Malvidin-feruloyl-hexoside (II)

[a] Hexoses separately linked to the aglycone; [b] confirmed by spiking the extracts with authentic standards; [c] hexoses linked as disaccharides

≤1 ppm in about 80% of the cases, and included in the range of 1.1-2.2 ppm for the remaining compounds (Table 1). Among the 64 anthocyanins identified, the presence of the 3-O-glucoside derivatives of delphinidin, cyanidin, petunidin, peonidin and malvidin (peaks 9, 16, 22, 28 and 34), 3-O-galactoside derivatives of delphinidin, cyanidin, peonidin and malvidin (peaks 6, 12, 25 and 29), and 3-O-arabinoside derivatives of cyanidin and peonidin (peaks 18 and 32) was confirmed by spiking the extracts with authentic reference standards (Table 1). Peaks 11, 17, 26 and 36 were putatively annotated to delphinidin-3-O-arabinoside, petunidin-3-O-galactoside, petunidin-3-O-arabinoside, and malvidin-3-O-arabinoside on the basis of their (i) TOF MS accuracy, isotope ratio difference and MS/MS data (Y_0 cleavage of the sugar and formation of the aglycone ion), as well as (ii) relative chromatographic retention, the latter being in agreement with the retention observed by various authors under reversed-phase conditions for different glycosides with the same aglycone (i.e. increasing retention in the order galactoside<glucoside<arabinoside) and for different anthocyanins glycosylated with the same sugar (i.e. increasing retention in the order delphinidin<cyanidin<petunidin<peonidin<malvidin) (4, 7, 23). The 15 anthocyanins reported above were detected in all the investigated species and resulted in all cases among the most abundant anthocyanidin derivatives (signal intensities approximately included in between $1 \cdot 10^5$ and $1 \cdot 10^6$ counts), as widely reported elsewhere (4, 7, 8, 26).

Among the first eluting analytes (peaks 1-5, Rt = 9.7-11.4 min), which were detected only in the *V. myrtillus* berry extracts and with very low signal intensity (i.e. 1000-1800 counts), peaks 1, 3 and 5 exhibited an $[M]^+$ ion at 627.15 Da and a fragmentation pattern with ions at m/z 465.10 (loss of 162 Da, hexose residue) and m/z 303.05 (further loss of a hexose unit), the latter corresponding to the delphinidin aglycone. Similarly, peaks 2 and 4 ($[M]^+$ ion at m/z 611.16), gave rise to two independent losses of 162 Da, producing the fragments at m/z 449.11 (i.e. cyanidin monoglycoside) and

m/z 287.06 (i.e. cyanidin). In order to correctly interpret these findings, it should be noted that the ESI-MS/MS fragmentation of anthocyanin derivatives with two sugars linked to different hydroxyls of the aglycone, actually produces the aglycone monoglycoside as a consequence of the Y_0 cleavage of one sugar (27). Conversely, in the case of disaccharide derivatives of anthocyanins, only the molecular ion and the aglycone fragment have been reported (28). On the basis of the aforementioned considerations, peaks 1-5 can be putatively ascribed to dihexoside derivatives of delphinidin and cyanidin, the two hexoses being separately linked to the aglycone. Remarkably, only one anthocyanidin derivative with two hexose units linked in different aglycone positions (i.e. cyanidin) was elsewhere reported (25).

Peak 13 (Rt = 15.4 min, signal intensity 1200 counts) showed a $[M]^+$ at m/z 611.16 and only one fragment at m/z 287.05. Accordingly, it was tentatively assigned to a cyanidin hexose-hexose disaccharide. In this regard, it should be noted that such an attribution is in agreement with the reversed-phase chromatographic behaviour of anthocyanidins diglycosides, since, for example, 3,5-diglycoside derivatives have been reported to elute before the corresponding 3-diglycosides (23, 29). Interestingly, the occurrence of cyanidin disaccharides was not previously reported in bilberry.

Peaks 7, 15 and 20, which had moderate intensity (i.e. 4000-11000 counts) were peculiar of the *V. myrtillus* extract. These peaks were ascribed to glucuronide derivatives of delphinidin, cyanidin and petunidin, respectively. In fact, peaks 7, 15 and 20 were characterized by the loss in common of 176 Da, consistent with glucopyranuronic acid, and the consequent formation of fragments at m/z 303.05, m/z 287.05 and m/z 317.07, respectively attributable to delphinidin, cyanidin and petunidin. Relative chromatographic retention of these peaks in respect to the corresponding glucoside derivatives was also in accordance with their putative identification as glucuronide derivatives (30, 31). It should be underlined

that this study is the first one reporting the identification of delphinidin, cyanidin and petunidin glucuronides in *V. myrtillus* fruits.

Peaks 8, 10, 14, 19, 21, 27 and 31, which were detected only in the *V. myrtillus* extract, exhibited the communal loss of 294 Da, attributable to an aldopentose-hexose residue, and MS/MS resulting fragments at m/z 303.05 (delphinidin), m/z 287.05 (cyanidin), m/z 317.07 (petunidin) and m/z 301.07 (peonidin). In this regard, it is notable that the chromatographic retention order of the aforementioned peaks was in agreement with the proposed aglycone attribution. It should also be noted that peaks 8 (i.e. delphinidin disaccharide), 14 (i.e. cyanidin disaccharide), 21 (i.e. petunidin disaccharide) and 27 (peonidin disaccharide) eluted between galactoside and glucoside derivatives of the corresponding aglycone, thus suggesting their putative identification as sambubioside derivatives (23). This hypothesis is in agreement with the findings of Du and co-workers, who reported the occurrence of delphinidin-3-sambubioside and cyanidin-3-sambubioside in bilberry (32).

Peak 23 showed a neutral loss of 264 Da, corresponding to an aldopentose disaccharide, and the resulting formation of a fragment at m/z 287.05 (i.e. cyanidin). This peak was found only in *V. myrtillus* extract, in agreement with the results previously reported by Latti and co-workers (25).

Peaks 24, 30, 35, 37, 44 and 45 were detected in berries from all the investigated *Vaccinium* species (Table 1) and can be ascribed to aldopentoside derivatives of delphinidin (peak 24), cyanidin (peaks 30 and 35), petunidin (peak 37), peonidin (peak 44) and malvidin (peak 45), based on the neutral loss of 132 Da (i.e. aldopentose) and the formation of the corresponding aglycone fragment. These peaks occurred in the three investigated berry species with very different intensities, being those determined in *V. uliginosum* subsp. *gaultherioides* characterized by much higher signals than the others. It should also be underlined that peak 30 differentiate itself from the others, owing to a much lower signal intensity.

It is remarkable that this study is the first one putatively identifying anthocyanidin aldopentosides in blueberry and aldopentose derivatives of delphinidin, cyanidin and peonidin in bilberry, whereas the occurrence of petunidin and malvidin xylosides were previously reported in this latter species (25, 33). Aldopentose derivatives were elsewhere detected in *V. uliginosum* berries and identified as xylosides of the five anthocyanidin mentioned above (34). Accordingly, for delphinidin, petunidin, peonidin and malvidin aldopentose herein detected, the attribution to xyloside derivatives can be proposed. This putative attribution is also confirmed by the earlier elution of arabinosides compared to the compounds tentatively identified as xylosides (23), being in our study the difference in retention included in the range 3.9-4.4 min. Moreover, considering peaks 30 and 35, retention time was found to be 3.5 and 4.4 min higher than cyanidin arabinoside (peak 18, Table 1), respectively. Accordingly, peak 35 (Rt = 21.4 min) should be putatively ascribed to cyanidin-3-O-xyloside, whereas peak 30 (Rt = 20.5 min) must be attributed to another cyanidin-aldopentoside, such as cyanidin-7-O-arabinoside, which is characterized by a lesser retention under reversed-phase chromatographic conditions and was found in other fruits (29).

Peak 38, which was detected only in blueberry, at quite low intensity (about 3000 counts) showed a MS/MS spectra characterized by the fragment at m/z 331.08, thus indicating a malvidin derivative. The neutral loss from the $[M]^+$ ion was 308 Da, which is consistent with a deoxyhexose-hexoside unit, as well as with a coumaroyl-hexoside fragment. However, the $[M]^+$ ion of peak 38 matched the exact mass of a malvidin deoxyhexose-hexoside with much higher accuracy (Δ = 0.7 ppm) than a malvidin coumaroyl-hexoside (Δ = 34 ppm). Furthermore, peak 38 eluted between the arabinoside and xyloside malvidin derivatives, as elsewhere reported for malvidin-3-O-rutinoside (23), the occurrence of which was previously highlighted in *V. corymbosum* berries, by Ramirez and co-workers (18).

Peaks 33, 40, 41, 43, 46, 47, 49, 50, 52 and 53 were characterized by the neutral loss of 204 Da (consistent with an acetyl-hexose unit) and formation of the aglycone fragment, thus suggesting their attribution to acetyl-hexosides of delphinidin (peaks 33 and 41), cyanidin (peaks 40 and 47), petunidin (peaks 43 and 50), peonidin (peaks 46 and 52) and malvidin (peaks 49 and 53). Interestingly, these acylated anthocyanins showed much higher intensities in blueberry ($1.0 \cdot 10^4$–$1.4 \cdot 10^5$ counts) than in bilberry ($4.0 \cdot 10^3$–$1.0 \cdot 10^4$ counts) (29), whereas they were never detected in false bilberry (Table 1), thus representing a potential group of markers for the differentiation of these fruit species.

Peaks 39, 42 and 48 were also characteristic of blueberry, being them absent in bilberries and "false bilberries". The MS/MS spectra evidenced the presence of cyanidin and malvidin aglycone fragments as a consequence of the communal loss of 248 Da, which can be ascribed to a malonyl-hexose group. These peaks were therefore tentatively assigned to cyanidin-malonyl-hexoside (peak 39) and malvidin-malonyl-hexosides (peaks 42 and 48), in partial agreement with results obtained by Wu and Prior (29), which reported the occurrence of malonyl-glucoside derivatives of delphinidin, cyanidin and malvidin in blueberry.

Peaks 51, 54-60, 62 and 63 fragmented with a neutral loss of 308 Da and the resulting formation of ions at m/z 303.05 (i.e. delphinidin, peaks 51 and 55), m/z 287.05 (i.e. cyanidin, peaks 54 and 57), m/z 317.07 (i.e. petunidin, peaks 56 and 59), m/z 301.07 (i.e. peonidin, peaks 58 and 62), m/z 331.08 (i.e. malvidin peaks 60 and 63). The signal intensities of these compounds were much higher in *V. myrtillus* berries (approximately from $1 \cdot 10^4$ to $1 \cdot 10^5$ counts) in respect to *V. uliginosum* L. subsp. *gaultherioides* and *V. corymbosum* ones. Based on the $[M]^+$ TOF accurate mass values determined for these analytes, the putative attribution to coumaroyl-hexoside anthocyanidin derivatives can be proposed ($\Delta \leq 1.9$ ppm), in agreement with

findings obtained under very similar chromatographic conditions by Zoratti and colleagues in *V. myrtillus* fruits collected in Alps of Northern Italy (35). Finally, peaks 61 ($8.6 \cdot 10^3$ counts) and 64 ($1.7 \cdot 10^5$ counts), which were peculiar of *V. myrtillus* fruits, exhibited a single neutral loss of 338 Da (i.e. feruloyl-hexoside) with formation of the fragment at m/z 331.08 (i.e. malvidin). Accordingly, these peaks were tentatively identified as malvidin-feruloyl-hexosides. It is remarkable that these compounds, previously found in others fruits (e.g. grape) (36), were herein identified in bilberry for the first time.

3.1.2 Flavonols

According to literature, the detection of flavonols by ESI-MS techniques can be achieved with high sensitivity under negative ionization mode (37). Hence, in this study flavonols were identified via negative polarity, by monitoring the quasi-molecular $[M-H]^-$ ion and its fragments (Table 2). Furthermore, peak assignment was confirmed under positive ionization, by monitoring the quasi-molecular $[M+H]^+$ ion, which allowed to pinpoint all the analytes found by negative mode, even though with lower signal intensity.

Using the IDA TOF-Q/TOF workflow and comparisons among retention times and mass spectra of unknown and authentic standards, the unequivocal or at least tentative identification of 55 flavonols was achieved. As illustrated in Table 2, among the identified flavonols, we found 36 glycosides (peaks 66-71, 74-79, 82, 86-88, 91-94, 96-97, 99-101, 103-104, 107-110, 112-114, 116 and 117), 6 glucuronides (peaks 65, 73, 83, 90, 106 and 111), 9 acyl derivatives (peaks 72, 80, 84, 85, 89, 95, 98, 102 and 105) and 4 aglycones (peaks 81, 115, 118 and 119). TOF MS $[M-H]^-$ quasi-molecular ions matched the proposed formulae with very high mass

Table 2. Retention times (Rt, min), $[M-H]^-$ quasi-molecular ions (TOF MS, Da), main mass fragments (Q/TOF MS/MS, Da), proposed formula, corresponding exact mass (Da) and accuracy (Δ, ppm) of peaks tentatively identified as flavonols in *V. myrtillus* (M), *V. uliginosum* L. subsp. *gaultherioides* (G) and *V. corymbosum* (C) under negative ionization. Mass fragments in bold character refer to the most intense signals. Symbols "+" and "–", mean detected and not detected.

Peak	Rt	TOF MS	Q/TOF MS/MS	Proposed formula	Exact mass	Δ	M	G	C	Tentative identification
65	19.6	493.0617	**317.0297**; 178.9989; 151.0036	$C_{21}H_{18}O_{14}$	493.0624	-1.3	+	+	+	Myricetin-glucuronide
66	19.9	479.0826	317.0299; **316.0225**; 271.0229	$C_{21}H_{20}O_{13}$	479.0831	-1.1	+	+	+	Myricetin-3-*O*-galactoside
67	20.6	479.0830	317.0299; **316.0216**; 271.0236	$C_{21}H_{20}O_{13}$	479.0831	-0.1	+	+	+	Myricetin-3-*O*-glucoside
68	20.9	449.0713	317.0288; **316.0207**; 271.0236	$C_{20}H_{18}O_{12}$	449.0725	-2.8	+	+	–	Myricetin-3-*O*-aldopentoside (I)
69	22.5	449.0714	317.0281; **316.0212**; 271.0230	$C_{20}H_{18}O_{12}$	449.0725	-2.6	–	+	+	Myricetin-3-*O*-aldopentoside (II)
70	22.9	449.0715	317.0240; **316.0211**; 271.0251	$C_{20}H_{18}O_{12}$	449.0725	-2.4	+	+	+	Myricetin-3-*O*-aldopentoside (III)
71	24.1	463.0876	301.0346; **300.0271**; 271.0248	$C_{21}H_{20}O_{12}$	463.0882	-1.4	+	+	+	Quercetin-3-*O*-galactoside [a]
72	24.2	521.0926	317.0278; **316.0216**; 271.0246	$C_{23}H_{22}O_{14}$	521.0937	-2.1	–	–	+	Myricetin-acetyl-hexoside (I)
73	24.4	477.0661	**301.0352**; 178.9979; 151.0028	$C_{21}H_{18}O_{13}$	477.0675	-2.8	+	+	+	Quercetin-glucuronide [a]
74	24.6	609.1452	301.0335; **300.0262**; 271.0235	$C_{27}H_{30}O_{16}$	609.1461	-1.5	+	–	+	Quercetin-3-*O*-deoxyhexose-hexoside
75	25.0	463.0879	301.0346; **300.0267**; 271.0248	$C_{21}H_{20}O_{12}$	463.0882	-0.7	+	+	+	Quercetin-3-*O*-glucoside [a]
76	25.6	609.1454	301.0335; **300.0255**	$C_{27}H_{30}O_{16}$	609.1461	-1.2	–	–	+	Quercetin-3-*O*-rutinoside [a]
77	25.7	433.0762	301.0341; **300.2630**; 271.0230	$C_{20}H_{18}O_{11}$	433.0776	-3.3	+	+	+	Quercetin-3-*O*-aldopentoside (I)
78	26.1	493.0983	331.0450; **330.0369**; 315.1320	$C_{22}H_{22}O_{13}$	493.0988	-1.0	+	+	+	Laricitrin-3-*O*-galactoside
79	26.4	433.0768	301.0341; **300.0267**; 271.0237	$C_{20}H_{18}O_{11}$	433.0776	-1.9	+	+	+	Quercetin-3-*O*-aldopentoside (II)
80	26.4	521.0941	317.0271; **316.0202**; 271.0225	$C_{23}H_{22}O_{14}$	521.0937	0.7	–	–	+	Myricetin-acetyl-hexoside (II)
81	26.5	317.0294	178.9983; 165.0192; **151.0031**; 137.0237	$C_{15}H_{10}O_8$	317.0303	-2.8	+	+	+	Myricetin[a]
82	26.6	493.0989	331.0461; **330.0383**; 315.0151	$C_{22}H_{22}O_{13}$	493.0988	0.3	+	+	+	Laricitrin-3-*O*-glucoside
83	26.7	507.0777	**331.0445**; 316.0210; 178.9978	$C_{22}H_{20}O_{14}$	507.0780	-0.7	+	+	+	Laricitrin-glucuronide
84	26.7	549.0876	505.0983; 463.0870; 301.0333; **300.0263**	$C_{24}H_{22}O_{15}$	549.0886	-1.8	–	–	+	Quercetin-malonyl-hexoside (I)
85	27.0	549.0877	505.0997; 463.0892; 301.0350; **300.0271**	$C_{24}H_{22}O_{15}$	549.0886	-1.6	–	–	+	Quercetin-malonyl-hexoside (II)
86	27.2	447.0912	285.0395; **284.0308**; 255.0280; 227.0335	$C_{21}H_{20}O_{11}$	447.0933	-3.2	+	+	+	Kaempferol-3-*O*-galactoside
87	27.5	433.0768	301.0343; **300.0270**; 271.0236	$C_{20}H_{18}O_{11}$	433.0776	-2.0	–	+	+	Quercetin-3-*O*-aldopentoside (III)
88	28.0	463.0862	331.0456; **330.0361**; 315.0149	$C_{21}H_{20}O_{12}$	463.0882	-4.4	+	+	+	Laricitrin-3-*O*- xyloside

Table 2 (continued)

Peak	Rt	TOF MS	Q/TOF MS/MS	Proposed formula	Exact mass	Δ	M	G	C	Tentative identification
89	28.2	505.0972	301.0338; **300.0273**; 271.0237	$C_{23}H_{22}O_{13}$	505.0988	-3.0	–	–	+	Quercetin-acetyl-hexoside (I)
90	28.4	461.0721	**285.0390**; 257.0438; 229.0491	$C_{21}H_{18}O_{12}$	461.0725	-0.9	+	+	+	Kaempferol-glucuronide
91	28.5	463.0869	331.0431; **330.0378**; 315.0140	$C_{21}H_{20}O_{12}$	463.0882	-2.9	+	+	+	Laricitrin-3-*O*-aldopentoside (I)
92	28.8	447.0923	301.0350; **300.0271**; 271.0238	$C_{21}H_{20}O_{11}$	447.0933	-2.1	+	–	+	Quercetin-3-*O*-rhamnoside [a]
93	28.9	447.0923	285.0397; **284.0325**; 255.0293; 227.0348	$C_{21}H_{20}O_{11}$	447.0933	-2.1	–	+	–	Kaempferol-3-*O*-glucoside
94	29.3	417.0823	**284.0316**; 255.0291; 227.0343	$C_{20}H_{18}O_{10}$	417.0827	-0.9	+	+	+	Kaempferol-3-*O*-aldopentoside
95	29.3	505.0979	301.0352; **300.0272**; 271.0237	$C_{23}H_{22}O_{13}$	505.0988	-1.6	–	–	+	Quercetin-acetyl-hexoside (II)
96	29.5	593.1504	**285.0398**; 284.0326	$C_{27}H_{30}O_{15}$	593.1512	-1.3	–	–	+	Kaempferol-7-*O*-neohesperidoside [a]
97	29.6	477.1032	**314.0419**; 271.0232; 243.0290	$C_{22}H_{22}O_{12}$	477.1038	-1.4	+	+	+	Isorhamnetin-3-*O*-galactoside
98	29.7	505.0977	301.0337; **300.0268**; 255.0293	$C_{23}H_{22}O_{13}$	505.0988	-2.1	–	–	+	Quercetin-acetyl-hexoside (III)
99	30.0	463.0870	**330.0355**; 331.0455; 315.0133	$C_{21}H_{20}O_{12}$	463.0882	-2.5	–	+	+	Laricitrin-3-*O*-aldopentoside (II)
100	30.0	579.1350	301.0351; **300.0262**; 271.0235	$C_{26}H_{28}O_{15}$	579.1355	-0.9	+	–	–	Quercetin-3-*O*-deoxyhexose-pentoside
101	30.2	623.1613	315.0496; **314.0405**; 299.0174	$C_{28}H_{32}O_{16}$	623.1618	-0.8	–	–	+	Isorhamnetin-3-*O*-deoxyhexose-hexoside
102	30.2	505.0983	301.0335; **300.0255**; 271.0226	$C_{23}H_{22}O_{13}$	505.0988	-0.9	–	–	+	Quercetin-acetyl-hexoside (IV)
103	30.4	477.1029	**314.0426**; 271.0258; 243.0299	$C_{22}H_{22}O_{12}$	477.1038	-2.0	+	+	–	Isorhamnetin-3-*O*-glucoside
104	30.4	477.1029	**331.0438**; 330.0362; 315.0135	$C_{22}H_{22}O_{12}$	477.1038	-2.0	–	–	+	Laricitrin-3-*O*-rhamnoside
105	30.6	535.1078	**330.0362**; 315.097	$C_{24}H_{24}O_{14}$	535.1093	-2.9	–	–	+	Laricitrin-acetyl-hexoside
106	30.7	491.0833	**315.0509**; 300.0255; 271.0239	$C_{22}H_{20}O_{13}$	491.0831	0.4	+	+	+	Isorhamnetin-glucuronide
107	30.8	507.1141	345.0616; **344.0530**; 301.0353	$C_{23}H_{24}O_{13}$	507.1144	-0.7	+	+	+	Syringetin-3-*O*-galactoside
108	30.9	623.1611	**315.0492**; 314.0419; 299.0203	$C_{28}H_{32}O_{16}$	623.1618	-1.0	–	–	+	Isorhamnetin-7-*O*-deoxyhexose-hexoside
109	31.3	507.1147	345.0609; **344.0533**; 301.0343	$C_{23}H_{24}O_{13}$	507.1144	0.6	+	+	+	Syringetin-3-*O*-glucoside
110	31.4	417.0814	285.0405; **284.0323**; 255.0299	$C_{20}H_{18}O_{10}$	417.0827	-3.1	–	–	+	Kaempferol-3-*O*-aldopentoside
111	31.5	521.0932	**345.0600**; 330.0363; 315.0129	$C_{23}H_{22}O_{14}$	521.0937	1.9	+	+	+	Syringetin-glucuronide
112	31.6	447.0931	**314.0426**; 271.0238; 243.0289	$C_{21}H_{20}O_{11}$	447.0933	-0.3	+	+	+	Isorhamnetin-3-*O*-aldopentoside (I)
113	31.8	447.0919	**314.0413**; 299.0251	$C_{21}H_{20}O_{11}$	447.0933	-3.2	+	+	+	Isorhamnetin-3-*O*-aldopentoside (II)
114	32.0	477.1025	**344.0544**; 301.0341; 273.0390	$C_{22}H_{22}O_{12}$	477.1038	-2.8	+	+	+	Syringetin-3-*O*-aldopentoside (I)
115	32.1	301.0347	178.9980; **151.0033**; 149.0219; 121.0282	$C_{15}H_{10}O_7$	301.0354	-2.4	+	+	+	Quercetin [a]
116	32.2	447.0920	**314.0411**; 271.0218; 243.0283	$C_{21}H_{20}O_{11}$	447.0933	-2.8	–	+	+	Isorhamnetin-3-*O*-aldopentoside (III)
117	32.2	477.1026	**344.0537**; 301.0354; 273.0382	$C_{22}H_{22}O_{12}$	477.1038	-2.5	+	+	+	Syringetin-3-*O*-aldopentoside (II)
118	32.6	331.0458	**316.0196**; 178.9976; 151.0062	$C_{16}H_{12}O_8$	331.0459	-0.4	+	+	+	Laricitrin
119	33.3	315.0504	**300.0269**; 271.0227; 151.0026	$C_{16}H_{12}O_7$	315.0510	-1.9	+	+	+	Isorhamnetin

[a] confirmed by spiking the extracts with authentic standards

accuracy, being Δ absolute values ≤ 2.5 ppm for 75% of identified analytes, and included in the range of 2.6-4.4 ppm in the remaining cases (Table 2).

In agreement with literature findings (38), Q/TOF MS/MS spectrum of flavonol glycosides exhibited both the heterolytic and the homolytic cleavage of the glycosidic bond, producing the aglycone fragment ion $[Y_0]^-$ and the radical aglycone ion $[Y_0\text{-H}]^{-\bullet}$. Fig. S5A of the Electronic Supplementary Material illustrates as an example the MS/MS spectrum of quercetin-3-O-glucoside (peak 75), in which the ions deriving from heterolytic (m/z = 301.03) and homolytic (m/z = 300.03) fission of the glycosidic bond are shown. Neutral losses of 18 Da (H_2O), 28 Da (CO) and 30 Da (CH_2O), individual or combined one with the other, have been also observed starting from the $[Y_0]^-$ ion (Fig. S5A), in agreement with characteristic MS/MS behaviour of flavonols elsewhere reported (37, 39). Moreover, the loss of 15 Da ($-CH_3$) from the aglycone was occasionally observed and putatively attributed to methoxylated flavonols (e.g. peaks 78, tentatively identified as laricitrin-3-O-galactoside, see Fig. S5B of the Electronic Supplementary Material). Further typical ions, at m/z = 151.00 and m/z = 179.00, originating from different retro-cyclization cleavages of the "C" ring and commonly identified as $^{1,3}A^-$ (retro-Diels-Alder) and $^{1,2}A^-$ fragments (40, 41), were observed, even though with low signal intensity (Fig. S5A-B).

A different relative abundance of the aglycone fragment $[Y_0]^-$ and the aglycone radical $[Y_0\text{-H}]^{-\bullet}$ ions, resulting from heterolytic and homolytic cleavage of the glycosidic bond, has been elsewhere demonstrated for kaempferol glycosides and suggested also for other flavonol glycosides, on the basis of the linkage position, as well as of the length of the saccharide chain (38). More in detail, if the sugar is a monosaccharide, the cleavage of the 3-O position of the aglycone gives rise preferentially to the $[Y_0\text{-H}]^{-\bullet}$ than the $[Y_0]^-$, as observed for example in peaks 66-71 (Table 2). Conversely, in this study, the preferential heterolytic cleavage of the

monosaccharide glycosidic bond was never observed, thus excluding the presence of 7-O-glycoside derivatives of flavonols in the investigated *Vaccinium* species. Based on the aforementioned considerations, peaks 66, 67, 78, 82, 86, 93, 97, 103, 107 and 109 can be ascribed to 3-O-monohexoside flavonol derivatives. More in detail, considering the whole mass dataset, as well as the relative peak elution order, 3-O-galactoside and 3-O-glucoside derivatives of myricetin (peaks 66 and 67), laricitrin (peaks 78 and 82), kaempferol (peaks 86 and 93), isorhamnetin (peaks 97 and 103) and syringetin (peaks 107 and 109) can be putatively identified, whereas peaks 71 and 75 were unequivocally identified as quercetin-3-O-galactoside and quercetin-3-O-glucoside, due to the availability of the authentic reference standards (Table 2). These flavonols were found to be present in all the investigated *Vaccinium* species, with the only exception of the glucoside derivative of kaempferol in bilberry and blueberry, and of the glucoside derivative of isorhamnetin in blueberry. It should also be underlined that flavonol glucosides and especially galactosides occurred with much higher signal intensity in *V. uliginosum* L. subsp. *gaultherioides* berries, suggesting that these analytes could be a typical metabolomic trait of "false bilberry".

Peaks 68-70, 77, 79, 87, 88, 91, 94, 99, 110, 112-114, 116 and 117 showed the neutral loss of 132 Da, indicating the presence of the aldopentoside residue and were attributed to 3-O-aldopentoside derivatives of the aforementioned aglycones, on the basis of exact mass data of pseudomolecular ions and aglycone fragments. Interestingly, for the most abundant aldopentoside derivatives, a net predominance was observed in "false bilberry", whereas the others generally had higher signal intensities in blueberry.

Peaks 92 and 104 were characterized by the neutral loss of 146 Da (i.e. deoxyhexose unit). The identity of the former peak, which was found in both bilberry and blueberry, was unequivocally attributed to quercetin-3-O-

rhamnoside, using the reference standard. Peak 104, which was found only in blueberry, was identified as a laricitrin-deoxyhexoside and putatively attributed to larictrin-3-O-rhamnoside.

Data herein obtained for quercetin-3-O-rutinoside (peak 76, Fig. S6A of the Electronic Supplementary Material) and kaempferol-7-O-neohesperidoside (peak 96, Fig. S6B of the Electronic Supplementary Material), which were available as reference standards, suggested, also for flavonol disaccharides, the higher abundance of homolytic or heterolytic cleavages, as diagnostic of the 3-O- or 7-O- substitution, respectively. However, according to Lu and co-workers (38), a long saccharide chain substituted at the 3-O position, could hinder the occurrence of the $[Y_0\text{-H}]^{-\bullet}$ ion, resulting in product ion MS/MS spectra similar to those of flavonol-7-O-glycosides. Accordingly, even though the differentiation of 3-O and 7-O-disaccharides of flavonols is commonly performed on this basis (42, 43), their attribution was considered herein as putative. Following this approach, some 3-O-disaccharide (peaks 74, 76, 100 and 101) and 7-O-disaccharide (peaks 96 and 108) derivatives of various flavonols were detected (Table 2).

The tentative identification of glucuronide derivatives of myricetin (peak 65), quercetin (peak 73, see Fig. S7 of the Electronic Supplementary Material), laricitrin (peak 83), kaempferol (peak 90), isorhamnetin (peak 106) and syringetin (peak 111) was associated to the neutral loss of 176 Da (i.e. glucopyranuronic acid) and formation of the $[Y_0]^-$ ion, consequent to the heterolytic cleavage of the glucuronic bond, whereas the homolytic fragmentation was absent. This mass behaviour was probably due to the lower electrophilic nature of glucuronic acid compared to glucose. Interestingly, the above-mentioned glucuronides showed comparable signal intensities in bilberry and “false bilberry”, whereas a much lower occurrence was highlighted in blueberry.

Peaks 72, 80, 89, 95, 98, 102 and 105, which were found exclusively in blueberry, were putatively identified as acetyl-hexosides of myricetin,

quercetin and laricitrin. Peaks 84 and 85 were also exclusively present in blueberry, and tentatively ascribed to malonyl-hexosides of quercetin (Table 2). These attributions were proposed on the basis of neutral losses of 205/204 Da (homolytic/heterolytic cleavage of the acetyl-hexose unit) or 249/248 Da (homolytic/heterolytic cleavage of the malonyl-hexose group), respectively (Table 2).

Four aglycones were also detected in all the investigated *Vaccinium* species (peaks 81, 115, 118 and 119). These molecules fragmented according to retrocyclization ($^{1,2}A^-$ and $^{1,2}B^-$) and retro-Diels-Alder cleavages ($^{1,3}A^-$ and $^{1,3}B^-$) of the "C" ring, and were identified as myricetin, quercetin, laricitrin and isorhamnetin. Different signal intensities were observed for the four aglycones, being myricetin the predominant aglycone in bilberry and quercetin the compound more abundant in "false bilberry" and blueberry.

3.1.3 Flavanols

Flavanol ESI-MS detection can be achieved both via positive and negative ionization (44). Accordingly, in this study, the two ionization modes were evaluated for flavanol identification. The results highlighted a slightly better sensitivity using the negative polarity, notwithstanding the high percentage of formic acid used in the eluents that lowered the ionization efficiency under negative potential. The IDA TOF-Q/TOF workflow applied to berry samples and also to some authentic standards allowed for certainly or putatively identifying 54 flavanols with a very good agreement between TOF MS quasi-molecular ions and proposed formulae (Δ absolute values $\leq$ 4.2 ppm). The identification data obtained with the negative ionization are reported in Table 3.

Peaks 121 and 135 were respectively assigned to gallocatechin (GC) and epigallocatechin (EGC), which are stereoisomers not distinguishable by mass spectrometry, but well-discriminated by reversed-phase LC.

Table 3. Retention times (Rt, min), quasi-molecular ions (TOF MS, Da), main mass fragments (Q/TOF MS/MS, Da), proposed formula, corresponding exact mass (Da) and accuracy (Δ, ppm) of peaks tentatively identified as flavanols in *V.myrtillus* (M), *V. uliginosum* L. subsp. *gaultherioides* (G) and *V. corymbosum* (C) under negative ionization. Mass fragments in bold character refer to the most intense signals. Symbols "+" and "–", mean detected and not detected.

Peak	Rt	TOF MS	Q/TOF MS/MS	Proposed formula	Exact mass	Δ	M	G	C	Tentative Identification
120	3.6	609.1247 [a]	441.0775; **423.0701**; 305.0639 177.0200; 125.0250	$C_{30}H_{26}O_{14}$	609.1250	-0.4	+	+	–	B-type (E)GC-(E)GC (I)
121	4.2	305.0661 [a]	219.0667; 167.0345; 165.0182; 139.0391; 137.0245; **125.0239**	$C_{15}H_{14}O_7$	305.0667	-1.7	+	+	+	Gallocatechin
122	4.7	609.1237 [a]	441.0814; **423.0709**; 305.0645; 177.0187; 125.0226	$C_{30}H_{26}O_{14}$	609.1250	-2.2	+	–	+	B-type (E)GC-(E)GC (II)
123	5.8	1167.2377 [a]	981.1887; **863.1795**; 711.1422; 573.1045; 411.0698	$C_{60}H_{48}O_{25}$	1167.2412	-3.0	+	+	–	A/B-type (E)C-(E)C-(E)C-(E)GC
124	6.5	1151.2463 [a]	**863.1837**; 711.1409; 573.1057; 411.0717	$C_{60}H_{48}O_{24}$	1151.2422	-3.6	+	+	–	A/B-type (E)C-(E)C-(E)C-(E)C (I)
125	6.7	911.1676 [a]	**743.1238**; 483.0904; **427.0650**; 423.0672; **305.0637**; 301.0308	$C_{45}H_{36}O_{21}$	911.1646	-3.3	+	–	–	A/B-type (E)GC-(E)GC-(E)GC
126	6.8	451.1229 [a]	**289.0719**; 245.0780; 123.0460	$C_{21}H_{24}O_{11}$	451.1246	-3.7	+	+	+	Catechin-hexoside
127	7.0	1153.2619 [a]	1027.2401; 863.1865; 577.1324; **575.1191**; 287.0543	$C_{60}H_{50}O_{24}$	1153.2588	-2.7	–	–	+	B-type (E)C-(E)C-(E)C-(E)C (I)
128	7.1	913.1833 [a]	609.1281; 541.0794; **423.0702**; 305.0641	$C_{45}H_{38}O_{21}$	913.1802	-3.4	+	+	–	B-type (E)GC-(E)GC-(E)GC
129	7.5	881.1900 [a]	713.1523; **695.1375**; 591.1141; 577.1326; 451.1031; 303.0479	$C_{45}H_{38}O_{19}$	881.1935	-3.9	–	–	+	B-type (E)C-(E)C-(E)GC (I)
130	7.7	584.1232 [b]	577.1389; **289.0701**; 287.0542	$C_{60}H_{50}O_{25}$	584.1248	-2.8	–	–	+	B-type (E)C-(E)C-(E)C-(E)GC (I)
131	7.8	727.1469 [b]	591.1163; **289.0704**; 125.0236	$C_{75}H_{60}O_{31}$	727.1486	-2.5	+	+	–	A/B-type (E)C-(E)C-(E)C-(E)C-(E)GC
132	8.0	895.1704 [a]	**727.1298**; 467.0960; **427.0654**; 289.0691; 177.0183	$C_{45}H_{36}O_{20}$	895.1727	-2.6	+	–	–	A/B-type (E)C-(E)GC-(E)GC (I)
133	8.5	577.1335 [a]	425.0869; **407.0766**; **289.0711**	$C_{30}H_{26}O_{12}$	577.1351	-2.9	+	+	+	Procyanidin B1 [c]
134	8.7	895.1705 [a]	725.1105; **467.0955**; 427.0676; 305.0661; 125.0238	$C_{45}H_{36}O_{20}$	895.1727	-2.5	+	–	–	A/B-type (E)C-(E)GC-(E)GC (II)
135	8.9	305.0663 [a]	219.0653; 167.0340; 165.0192; 139.0391; 137.0240; **125.0241**	$C_{15}H_{14}O_7$	305.0667	-1.2	+	+	+	Epigallocatechin

Table 3 (continued)

Peak	Rt	TOF MS	Q/TOF MS/MS	Proposed formula	Exact mass	Δ	M	G	C	Tentative Identification
136	9.0	289.0711 [a]	**245.0811**; 205.0501; **203.0712**; 125.0238; **123.0451**; 109.0294	$C_{15}H_{14}O_6$	289.0718	-2.2	+	+	+	(+)-Catechin [c]
137	9.2	719.1489 [b]	575.1182; 451.1036; 411.0698; **289.0701**; **287.0550**; **125.0243**	$C_{75}H_{60}O_{30}$	719.1512	-3.2	+	+	–	A/B-type (E)C-(E)C-(E)C-(E)C-(E)C (I)
138	9.3	1153.2571 [a]	865.2038; **575.1184**; 287.0549	$C_{60}H_{50}O_{24}$	1153.2619	-4.2	–	–	+	B-type (E)C-(E)C-(E)C-(E)C (II)
139	9.3	897.1852 [a]	711.1469; **593.1353;** 543.0920; **407.0776**; 303.0499; 177.0249	$C_{45}H_{38}O_{20}$	897.1884	-3.5	+	+	–	B-type (E)GC-(E)C-(E)GC (I)
140	9.5	865.1957 [a]	695.1393; **577.1343**; 407.0755; **287.0546**	$C_{45}H_{38}O_{18}$	865.1985	-3.3	+	+	+	B-type (E)C-(E)C-(E)C (I)
141	9.8	577.1336 [a]	425.0869; **407.0760**; **289.0713**	$C_{30}H_{26}O_{12}$	577.1351	-2.7	+	+	+	B-type procyanidin (I)
142	10.0	879.1757 [a]	**727.1312**; 451.1026; **427.0655**; 289.0713	$C_{45}H_{36}O_{19}$	879.1778	-2.4	+	+	–	A/B-type (E)GC-(E)C-(E)C
143	10.2	720.1573 [b]	407.0819; **289.0701**; 287.0554;	$C_{75}H_{62}O_{30}$	720.1590	-2.4	–	–	+	B-type (E)C-(E)C-(E)C-(E)C-(E)C (I)
144	10.3	865.1965 [a]	**577.1344**; **575.1179**; **287.0544**	$C_{45}H_{38}O_{18}$	865.1985	-2.3	–	–	+	B-type (E)C-(E)C-(E)C (II)
145	10.4	451.1237 [a]	**289.0707**; 245.0802; 125.0247	$C_{21}H_{24}O_{11}$	451.1246	-2.0	+	+	+	Epicatechin-hexoside
146	10.7	720.1579 [b]	577.1352; 407.0765; **289.0701**; 287.0572; 125.0229	$C_{75}H_{62}O_{30}$	720.1590	-1.5	–	–	+	B-type (E)C-(E)C-(E)C-(E)C-(E)C (II)
147	10.8	576.1258 [b]	**449.0874**; **289.0698**; 287.0563; **125.0259**	$C_{60}H_{50}O_{24}$	576.1273	-2.6	–	–	+	B-type (E)C-(E)C-(E)C-(E)C (III)
148	10.9	865.1962 [a]	**577.1353**; **575.1171**; 425.0870; **407.0752**; 287.0542	$C_{45}H_{38}O_{18}$	865.1985	-2.7	+	+	+	B-type (E)C-(E)C-(E)C (III)
149	11.0	897.1864 [a]	**711.1323**; 593.1368; 591.1121; 423.0715	$C_{45}H_{38}O_{20}$	897.1884	-2.2	+	+	–	B-type (E)GC-(E)C-(E)GC (II)
150	11.5	720.1568 [b]	575.1249; 405.0628; **289.0702**; 243.0290; 125.0244	$C_{75}H_{62}O_{30}$	720.1590	-3.1	–	–	+	B-type (E)C-(E)C-(E)C-(E)C-(E)C (III)
151	11.7	576.1260 [b]	425.0828; **289.0603**; **287.0545**; 245.0436; **125.0229**	$C_{60}H_{50}O_{24}$	576.1273	-2.3	+	+	+	B-type (E)C-(E)C-(E)C-(E)C (IV)
152	11.8	879.1755 [a]	**727.1377**; 709.1207; 467.0984; **411.0685**; **305.0644**	$C_{45}H_{36}O_{19}$	879.1778	-2.6	+	+	–	A/B-type (E)C-(E)C-(E)GC
153	12.2	577.1346 [a]	425.0870; **407.0762**; **289.0704**	$C_{30}H_{26}O_{12}$	577.1351	-1.0	+	+	+	Procyanidin B2 [c]
154	12.6	576.1259 [b]	425.0895; 407.0774; **289.0717**; 287.0543; **125.0230**	$C_{60}H_{50}O_{24}$	576.1273	-2.5	+	+	+	B-type (E)C-(E)C-(E)C-(E)C (V)
155	13.3	576.1661 [b]	407.0732; **289.0706**; 287.0542; 151.0376; **125.0241**	$C_{60}H_{50}O_{24}$	576.1273	-2.1	+	+	+	B-type (E)C-(E)C-(E)C-(E)C (VI)

Table 3 (continued)

Peak	Rt	TOF MS	Q/TOF MS/MS	Proposed formula	Exact mass	Δ	M	G	C	Tentative Identification
156	13.9	863.1816 [a]	711.1353; 693.1265; 573.1040; 451.1048; **411.0716**; 289.0707	$C_{45}H_{36}O_{18}$	863.1829	-1.5	+	+	–	A/B-type (E)C-(E)C-(E)C (I)
157	14.0	865.1959 [a]	**713.1508**; 695.1377; **577.1352**; 575.1213; 407.0788; 287.0582	$C_{45}H_{38}O_{18}$	865.1985	-3.1	–	–	+	B-type (E)C-(E)C-(E)C (IV)
158	14.1	720.1570 [b]	289.0710; **125.0235**	$C_{75}H_{62}O_{30}$	720.1590	-3.5	–	–	+	B-type (E)C-(E)C-(E)C-(E)C-(E)C (IV)
159	14.2	289.0718 [a]	**245.0818**; 205.0499; **203.0705**; 125.0233; **123.0448**; 109.0299	$C_{15}H_{14}O_6$	289.0718	0.1	+	+	+	(-)-Epicatechin [c]
160	14.3	881.1909 [a]	713.1545; **695.1432**; 591.1146; 577.1374; 425.0868; 303.0491	$C_{45}H_{38}O_{19}$	881.1935	-2.9	+	+	+	B-type (E)C-(E)C-(E)GC (II)
161	14.5	720.1581 [b]	575.1223; **289.0701**; 125.0249	$C_{75}H_{62}O_{30}$	720.1590	-1.3	+	+	+	B-type (E)C-(E)C-(E)C-(E)C-(E)C (V)
162	15.4	1169.2538 [a]	865.2056; 739.1659; 591.1202; 423.0709; 287.0549	$C_{60}H_{50}O_{25}$	1169.2568	-2.6	+	+	+	B-type (E)C-(E)C-(E)C-(E)GC (II)
163	15.5	575. 1189 [b]	411.0730; 407.0722; **289.0697**; 151.0389; **125.0235**	$C_{60}H_{48}O_{24}$	575.1195	-1.0	+	+	–	A/B-type (E)C-(E)C-(E)C-(E)C (II)
164	15.5	865.1962 [a]	695.1408; **577.1339**; 575.1191; 407.0752; 289.0686; **287.0538**	$C_{45}H_{38}O_{18}$	865.1985	-2.7	+	+	+	B-type (E)C-(E)C-(E)C (V)
165	16.2	576.1255 [b]	**407.0756**; **289.0713**; 287.0556; **125.0247**	$C_{60}H_{50}O_{24}$	576.1273	-3.2	+	+	+	B-type (E)C-(E)C-(E)C-(E)C (VII)
166	16.5	720.1578 [b]	289.0707; 125.0238	$C_{75}H_{62}O_{30}$	720.1590	-1.6	+	+	+	B-type (E)C-(E)C-(E)C-(E)C-(E)C (VI)
167	16.7	720.1583 [b]	289.0712; 125.0244	$C_{75}H_{62}O_{30}$	720.1590	-0.9	+	+	+	B-type (E)C-(E)C-(E)C-(E)C-(E)C (VII)
168	17.8	863.1826 [a]	711.1386; 693.1277; **575.1197**	$C_{45}H_{36}O_{18}$	863.1829	-0.3	–	+	–	A/B-type (E)C-(E)C-(E)C (II)
169	18.1	719.1500 [b]	411.0728; **289.0684**; 287.0578	$C_{75}H_{60}O_{30}$	719.1512	-1.6	+	+	–	A/B-type (E)C-(E)C-(E)C-(E)C-(E)C (II)
170	21.0	575.1191 [a]	**449.0856**; 423.0718; **289.0706**; **285.0383**	$C_{30}H_{24}O_{12}$	575.1195	-0.7	+	+	–	Procyanidin A2 [c]
171	22.0	863.1812 [a]	711.1381; 693.1276; **575.1184**	$C_{45}H_{36}O_{18}$	863.1829	-2.0	–	+	–	A/B-type (E)C-(E)C-(E)C (III)
172	22.7	577.1343 [a]	425.0873; **407.0759**; **289.0704**	$C_{30}H_{26}O_{12}$	577.1351	-1.4	+	+	+	B-type procyanidin (II)
173	27.0	576.1267 [b]	407.0749; 287.0517; 151.0388; **125.0233**	$C_{60}H_{50}O_{24}$	576.1273	-1.0	+	+	+	B-type (E)C-(E)C-(E)C-(E)C (VIII)

E(C) = (epi)catechin, (E)GC = (epi)gallocatechin, [a] mono-charged quasi-molecular ion $[M-H]^-$; [b] double-charged quasi-molecular ion $[M-2H]^{2-}/2$;
[c] confirmed by spiking the extracts with authentic standards.

These peaks showed $[M-H]^-$ quasi-molecular ion at m/z 305.07 and the same MS/MS spectra (see Fig. S8-A of the Electronic Supplementary Material) with main fragments at m/z 261.04 (loss of 44 Da, CH_2=CHOH), m/z 221.05 (cleavage of the "A" ring), m/z 219.03 (consecutive losses of 44 Da and 42 Da) and m/z 125, the last being by far the most intense ion of the MS/MS spectrum. The high intensity of this ion can be explained on the basis of its dual origin that is from the fission of the heterocyclic ring or the cleavage of the "B" ring, both characterized by the loss of 180 Da (see fragmentation paths 4 and 8 of the Scheme S1 of the Electronic Supplementary Material). Moreover, in accordance to findings previously reported for catechin (C) and (EC) (45, 46), fragments at m/z 139.04 (probably attributable to the cleavage of the "A" and "C" rings) and m/z 137.03 (loss of 168 Da, retro Diels-Alder reaction) were observed. GC and EGC, herein found in all the investigated *Vaccinium* species, were previously reported only in *V. myrtillus* fruits (44). When MS/MS spectra of peaks 121 and 135 (Fig. S8-A) were compared to the ones of peaks 136 and 159 (Fig. S8-B), delta mass of 16 Da were observed in most cases. Spiking procedure of the authentic standards unequivocally confirmed the identification of the latter peaks as C and EC (see also Scheme S1 for the detailed fragmentation paths). The predominance of catechin in *V. corymbosum* fruits and of epicatechin in *V. myrtillus* and *V. uliginosum* L. subsp. *gaultherioides* berries has been observed, in agreement with findings already reported in literature (4, 7).

MS/MS spectra of peaks 126 and 145, revealed the loss of 162 Da (hexose unit) with formation of the ion at m/z 289.07, which is attributable to both C or EC, due to their stereoisomeric nature (following the possible presence of the C or the EC unit is indicated as (E)C). Moreover, the aforementioned typical fragments of (E)C were observed, thus indicating the presence of (E)C-hexosides, never reported in *Vaccinium* species, but previously identified in other berries (15).

Peaks 133 and 153 exhibited the typical fragmentation of B-type (E)C-(E)C dimers, consisting in the retro Diels-Alder fission of the "C" ring (m/z 425.09) and successive loss of water (m/z 407.08), as well as the cleavage of the B-type linkage with formation of the (E)C monomer (m/z 289.07). These peaks were undoubtedly attributed to Procyanidin B1 and Procyanidin B2, respectively, on the basis of identity confirmation with authentic standards. Peaks 141 and 172 showed the same MS/MS spectrum and were therefore putatively ascribed to B-type procyanidin isomers, in which the C4→C6 interflavanoid bond, instead of the C4→C8 one, is present between the two (E)C units.

The comparison between MS/MS spectra of B-type procyanidins and peaks 120 and 122, highlighted m/z values 16 Da higher in most detected fragments of the latter peaks (i.e. m/z 441.08, 423.07 and 305.06, see Fig. 1), Accordingly, peaks 120 and 122 were tentatively identified as B-type (E)GC-(E)GC dimers (Table 3). It is remarkable that for these peaks the fragment at m/z 177.02 has been also observed, in contrast to MS/MS findings of (E)C dimers, in which this ion was absent. It should also be noted that the fragment at m/z 177.02 was absent in (E)GC (see Fig. S8-A), thus suggesting that it derives from the m/z 303.05 ion, as proposed in the Scheme 1.

Peak 170 showed the typical fragmentation of A-type procyanidins (e.g. cleavage of the "C" ring, fission of the heterogeneous C2→O interflavanyl linkage and rearrangement with formation of the ion at m/z 449.09) was unequivocally identified as procyanidin A2, based on its authentic standard.

A number of proanthocyanidin trimers, tetramers and pentamers, characterized by B-type and both A and B-types (following A/B) interflavanyl linkages were identified (Table 3) on the basis of the typical mass fragmentation mechanisms of this polyphenol class: retro-Diels Alder (RDA), quinone methide formation (QM) and heterocyclic ring fissions (HRF) (47).

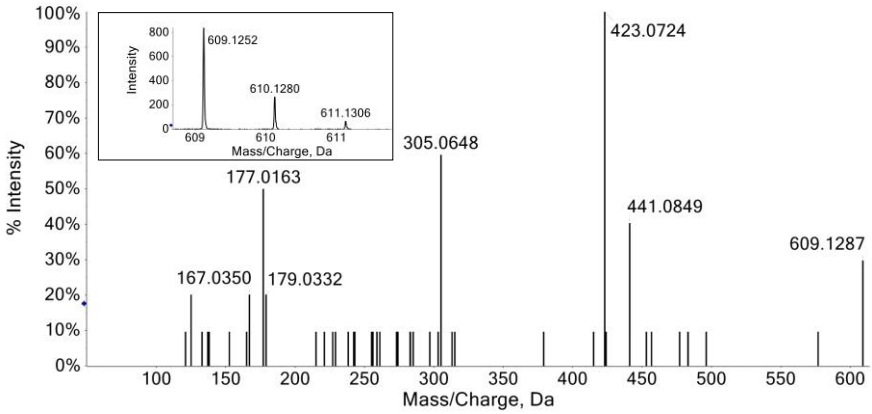

Figure 1. Q/TOF MS/MS spectrum of peak 122, identified as B-type dimer of (epi)gallocatechin.

Most of these proanthocyanidins were trimers (peaks 140, 144, 148, 157 and 164), tetramers (peaks 127, 138, 147, 151, 154, 155, 165 and 173) and pentamers (peaks 143, 146, 150, 158, 161, 166 and 167) consisting of only B-linked (E)C units. More in detail, the MS/MS spectrum of B-type procyanidin trimers was characterized by ions deriving from RDA fission (m/z 713.15) and successive loss of water (m/z 695.14), as well as the typical fragmentation pattern of B-type procyanidin dimers (i.e. m/z 425.09 and 407.08) previously discussed. Moreover, the presence of monomer (m/z 289.07 and 287.06) and dimer (E)C units (m/z 577.13 and 575.12) deriving from QM reaction confirmed the identity of B-type procyanidin trimers. B-type procyanidin tetramers were detected both as mono-charged (m/z 1153.26) and double-charged (m/z 576.13) quasi-molecular ions and produced fragments related to trimeric (m/z = 865.20 and 863.19), dimeric (m/z = 577.13 and 575.12) and monomeric (m/z = 289.07 and 287.07) units, up to the characteristic MS/MS spectra of (E)C. Similarly, B-type procyanidin pentamers showed the typical fragmentations of the lower molecular weight B-type procyanidin oligomers.

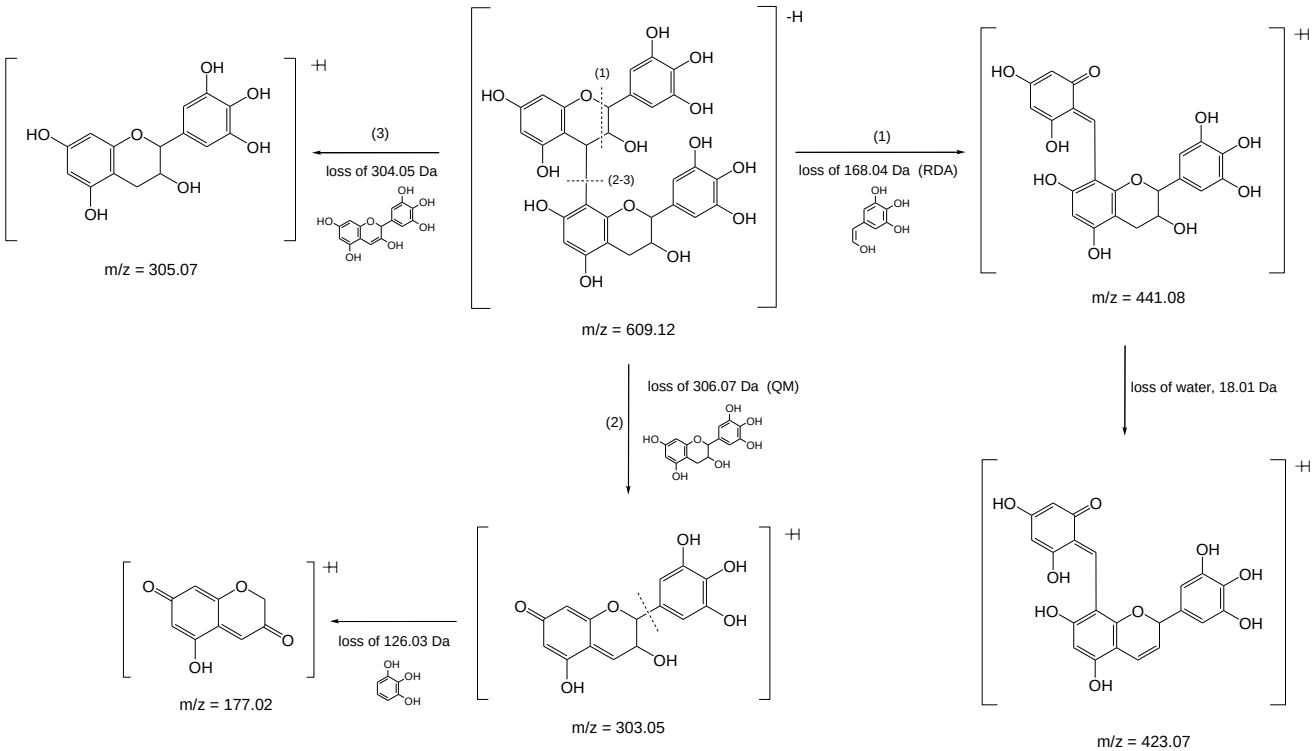

Scheme 1. Hypothesized structure and fragmentation scheme for peaks 120 and 122 ($[M-H]^-$ = 609.12), putatively attributed to an (epi)gallocatechin dimer. RDA = retro Diels-Alder; QM = quinone methide formation

A/B-linked proanthocyanidin trimers (peaks 156, 168 and 171), tetramers (peaks 124 and 163) and pentamers (peaks 137 and 169) formed only of (E)C units were also putatively identified. For these compounds the RDA reaction affecting the B-type linked (E)C caused the ion at m/z 711.14 and, after the loss of water, the ion at m/z = 693.13. The QM reaction produced the fragments at m/z 573.10 and 289.07, whereas the ions at 451.10 and 411.07 derived from HRF reactions. Similarly, A/B type procyanidin tetramers and pentamers were identified on the basis of their MS/MS fragments consisting of the above-mentioned typical product ions of A/B type procyanidin trimer (m/z = 863.18) and dimer (m/z = 575.12).

Interestingly, two compounds exclusively formed by (E)GC units (i.e. peak 125, A/B-type trimer and peak 128, B-type trimer) were herein identified for the first time in *V. myrtillus* and *V. uliginosum* L. subsp. *gaultherioides* fruits. Peak 125 was identified as A/B type prodelphinidin trimer on the basis of the characteristic fragments deriving from RDA (m/z = 743.13) and HRF (m/z 483.09 and 427.07) reactions, whereas the MS/MS spectrum of peak 128 exhibited the product ions corresponding to the formation of dimer (m/z 609.13) and monomer (m/z 305.07) ions. In addition, the ion at m/z 541.08, deriving from the cleavage of the "B" rings of the trimer, was observed.

Four B-type proanthocyanidin trimers (peaks 129, 139, 149 and 160) and two tetramers (peaks 130 and 162) formed by both (E)C and (E)GC monomers were also identified (Table 3), but no information about the relative position of the different units could be obtained by MS/MS spectra.

Finally, six proanthocyanidin oligomers were identified as trimers, tetramers and pentamers consisting of both (E)C and (E)GC units, linked with and A/B-type (peaks 123, 131, 132, 134, 142 and 152) bonds. Interestingly, in this case, fragmentation spectra highlighted in most cases diagnostic ions that indicated the relative position of a certain monomer and/or the type of linkage (A-type or B-type) between two monomers. For

instance, peaks 142 and 152 were identified as A/B type trimers constituted by two units of (E)C and one unit of (E)GC. For both peaks, the RDA reaction and the successive loss of water, producing the ions at m/z 727.13 and 709.12, were observed. Nevertheless, peak 142 was characterized by fragments at m/z 427.07 and 451.10, fully consistent with the occurrence in the molecule of (i) one terminal (E)GC linked to one (E)C by an A-type linkage and (ii) two (E)C units linked by a B-type interflavanyl bond, respectively. Moreover, a high-intensity fragment at m/z 289.07 was observed, in accordance with the presence of a B-type terminal (E)C (Fig. 2A). Analogously, the MS/MS spectrum of peak 152 showed fragments at m/z 411.07 and 467.10, which are in agreement with the presence of (i) one terminal (E)C linked to the other portion of the molecule by an A-type linkage and (ii) one (E)C and one (E)GC unit linked each other by a B-type bond. Moreover, it should be noted that an intense fragment at m/z 305.06, attributable to the (E)GC unit, was also observed (Fig. 2B). Accordingly, peaks 142 and 152 were putatively identified as A/B type (E)GC-(E)C-(E)C and A/B type (E)C-(E)C-(E)GC, respectively.

A similar consideration can be done for peaks 132 and 134, which were A/B type trimer constituted by one unit of (E)C and two units of (E)GC. In both these peaks the ion at m/z 427.07 indicated the presence of one terminal (E)GC unit linked with an A-type bond with the rest of the molecule, whereas the ion at m/z 467.10 was diagnostic for the occurrence of B-type linked (E)GC and (E)C. However, peak 132 was also characterized by the presence of an intense fragment at m/z 289.07, differently from peak 142 that showed a high-intensity ion at m/z 305.07. Therefore, peaks 132 and 134 were putatively identified as A/B type (E)GC-(E)GC-(E)C and A/B type (E)GC-(E)C-(E)GC, respectively (see Fig. 3A-B).

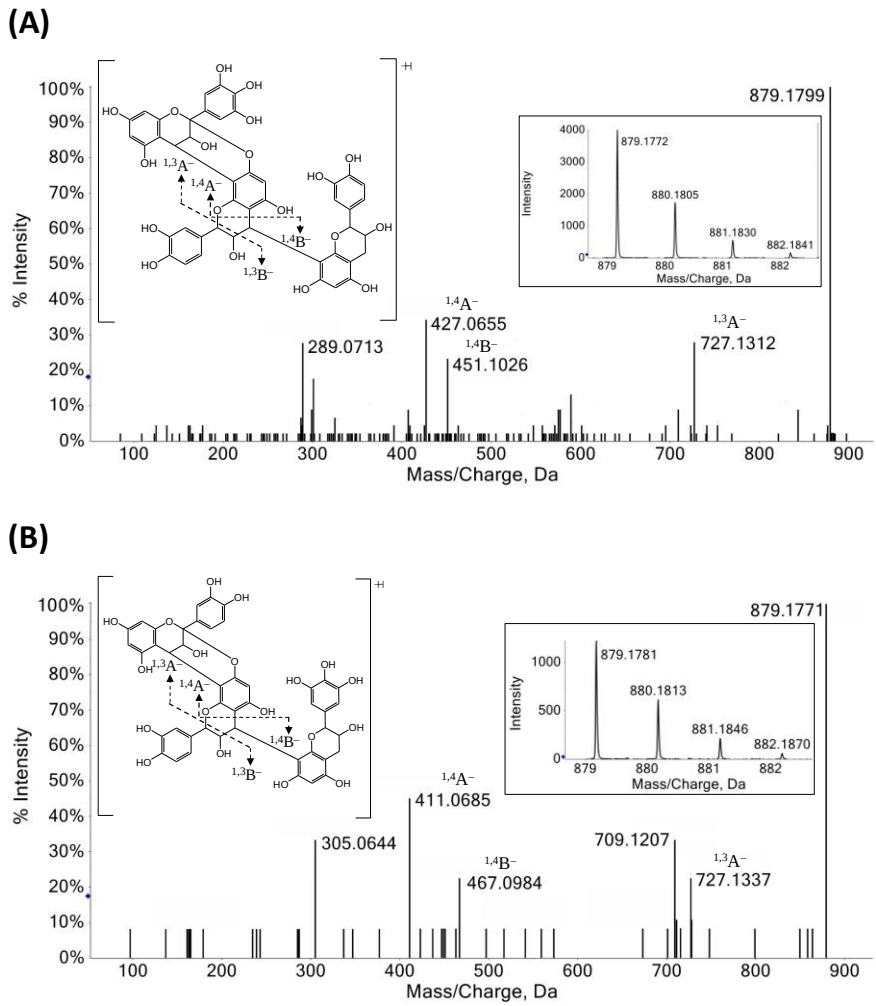

Figure 2. Q/TOF MS/MS spectrum of peaks: (A) 142 and (B) 152, identified as A/B-type (E)GC-(E)C-(E)C and A/B-type (E)C-(E)C-(E)GC, respectively. (E)C = (epi)catechin; (E)GC = (epi)gallocatechin. Note that ion $^{1,3}B^-$ is not evidenced in the mass spectra.

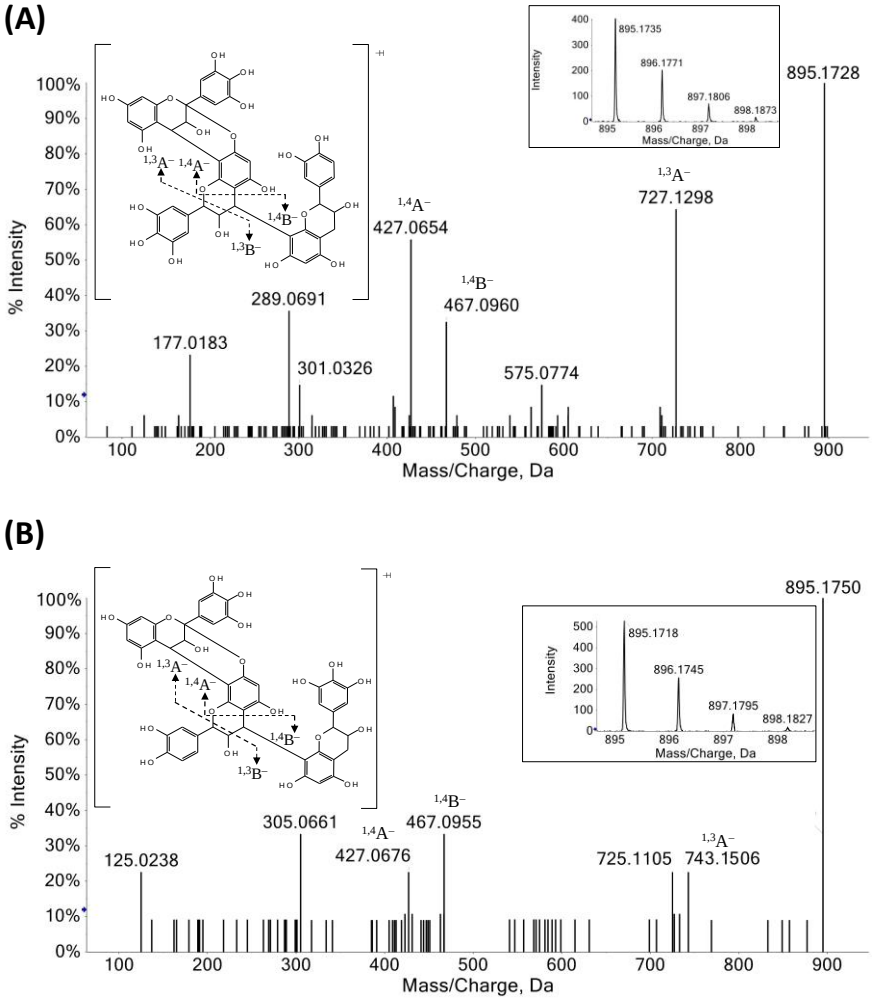

Figure 3. Q/TOF MS/MS spectrum of peaks: (A) **132** and (B) **134**, identified as A/B-type (E)GC-(E)GC-(E)C and A/B-type (E)GC-(E)C-(E)GC, respectively. (E)C = (epi)catechin; (E)GC = (epi)gallocatechin. Note that ion $^{1,3}B^-$ is not evidenced in the mass spectra.

Peak 123 was identified as an A/B-type tetramer formed by three units of (E)C and one unit of (E)GC. This peak fragmented originating the ion at m/z 863.18, which is consistent with the formation of an (epi)catechin trimer with one A-type and one B-type linkage, together with other characteristic ions (i.e. m/z 711.14, 573.10 and 411.07), deriving from the catechin trimer fragmentation. Accordingly, in peak 123 the (E)GC unit should be terminal and linked through a B-type interflavanyl linkage.

Finally, peak 131, which was formed by four units of (E)C and one unit of (E)GC, two of them linked by an A-type interflavanyl bond, showed, among other, a quite intense fragment at m/z 591.12. This ion is compatible with the presence of an A-type bond between the (E)GC and one (E)C units.

3.1.4 Other compounds

Using the IDA TOF-Q/TOF workflow under negative ionization, 29 further phenolic compounds belonging to various classes, were putatively or unequivocally identified in berry samples (Table 4). Also in these cases, a very good agreement between TOF MS quasi-molecular ions and proposed formulae was obtained (Δ absolute values $\leq$3.8 ppm).

Peak 199 was found to be in common to the three species and unequivocally identified as phloridzin after comparison with the corresponding authentic standard. The use of the reference standard allowed for certainly identifiying also peak 190 as scopoletin, which was detected only in "false bilberry".

Peak 174, which was present at quite similar intensities in all berry species, was unambiguously identified as gallic acid, due to the availability of the authentic reference standard.

Several phenolic acids belonging to the class of the hydroxycinnamic acids (peaks 175-178, 180, 182, 185, 186, 192, 193, 197 and 198) were also putatively or unequivocally identified, depending on the availability of the authentic standards. These compounds were generally found at higher

intensity in *V. corymbosum* and in some cases (peaks 176, 177, 193, 197 and 198) detected exclusively in this berry species.

Peak 179 exhibited a quasi-molecular ion at m/z 353.08, which fragmented giving rise to a neutral loss of 162 Da and ions attributable to caffeic acid.

This peak was therefore putatively attributed to a caffeic acid hexoside. Analogously, peaks 181 and 183 were tentatively identified as coumaric acid and ferulic acid hexosides.

Peaks 188, 194 and 202 showed pseudo-molecular ions at m/z 335.08, 367.10 and 445.11, respectively, and shared the typical fragments of caffeic acid (Table 4), thus suggesting their putative attribution as caffeic acid derivatives.

For peaks 201 and 202 the same quasi-molecular ion at m/z 411.17 was found. The fragmentation gave rise to a neutral loss corresponded to a malonyl hexoside (248 Da) with formation of a fragment consistent with coumaric acid $[M-H]^-$ ion (m/z 163.04), as well as various fragments typical of coumaric acid, thus suggesting the putative identification of both peaks as coumaric acid-malonyl-hexosides.

Fragmentations of the quasi-molecular $[M-H]^-$ ions of peaks 195 and 196 (m/z 535.15) were in full agreement with data reported by Hokkanen et al. (44) for coumaroyl iridoids. These peaks, previously identified in *V. myrtillus* fruits (48), were much more intense in bilberry than in "false bilberry", whereas were absent in blueberry.

Peaks 184, 187, 189 and 191 were putatively identified as cinchonain II isomers, in agreement with the fragmentation scheme reported by Hokkanen and co-workers (44); all these compounds have been found in *V. corymbosum* berries, whereas only the last isomer was detected in *V. myrtillus* fruits. The presence of cinchonain isomers was previously highlighted in other plants (49), as well as in leaves of various *Vaccinium* plant species (44, 50), but never observed before in berries.

Table 4. Retention times (Rt, min), $[M-H]^-$ quasi-molecular ions (TOF MS, Da), main mass fragments (Q/TOF MS/MS, Da), proposed formula, corresponding exact mass (Da) and accuracy (Δ, ppm) of peaks tentatively identified as other phenolic compounds in *V.myrtillus* (M), *V. uliginosum* L. subsp. *gaultherioides* (G) and *V. corymbosum* (C) under negative ionization. Mass fragments in bold character refer to the most intense signals. Symbols "+" and "–", mean detected and not detected.

Peak	Rt	TOF MS	Q/TOF MS/MS	Proposed formula	Exact mass	Δ	M	G	C	Tentative identification
174	2.0	169.0146	**125.0240**; 124.0244; 79.0189	$C_7H_6O_5$	169.0142	2.0	+	+	+	Gallic acid [a]
175	6.8	353.0866	**191.0554**; 179.0345; 135.0446	$C_{16}H_{18}O_9$	353.0878	-3.4	+	+	+	Neochlorogenic acid [a]
176	9.2	337.0918	191.0562; **163.0390**; 119.0499	$C_{16}H_{18}O_8$	337.0929	-3.2	–	–	+	Coumaroylquinic acid (I)
177	9.4	337.0916	**191.0554**; **163.0387**; 119.0505	$C_{16}H_{18}O_8$	337.0929	-3.7	–	–	+	Coumaroylquinic acid (II)
178	10.0	179.0351	**135.0444**; 134.0368	$C_9H_8O_4$	179.0350	0.6	+	+	+	Caffeic acid [a]
179	10.6	341.0872	**179.0342**; **135.0446**; 134.0358	$C_{15}H_{18}O_9$	341.0878	-1.7	+	+	+	Caffeic acid-hexoside
180	11.0	353.0869	**191.0566**	$C_{16}H_{18}O_9$	353.0878	-2.6	+	+	+	Chlorogenic acid [a]
181	12.3	325.0920	**163.0395**; **119.0504**	$C_{15}H_{18}O_8$	325.0929	-2.6	+	+	+	Coumaric acid-hexoside
182	12.4	353.0868	**191.0552**; 179.0348; **173.0451**; 135.0448	$C_{16}H_{18}O_9$	353.0878	-2.8	+	+	+	Cryptochlorogenic acid [a]
183	13.7	355.1031	193.0507; **175.0398**; **160.0163**; 132.0210	$C_{16}H_{20}O_9$	355.1035	-1.0	+	+	+	Ferulic acid-hexoside
184	13.9	739.1657	**587.1205**; 339.0494; 289.0707; 177.0190	$C_{39}H_{32}O_{15}$	739.1668	-1.5	–	–	+	Cinchonain IIx (I)
185	14.7	337.0918	**191.0547**; 163.0384	$C_{16}H_{18}O_8$	337.0929	-3.3	+	–	+	Coumaroylquinic acid (III)
186	15.4	353.0873	**191.0568**	$C_{16}H_{18}O_9$	353.0878	-1.4	+	–	+	Caffeoylquinic acid
187	16.0	739.1658	587.1192; 449.0864; 339.0498; **289.0704**	$C_{39}H_{32}O_{15}$	739.1668	-1.5	–	–	+	Cinchonain IIx (II)
188	16.2	335.0767	**179.0343**; 161.0207; **135.0446**; 134.0372	$C_{16}H_{16}O_8$	335.0772	-1.6	+	+	+	Caffeic acid derivative
189	16.9	739.1641	**587.1170;** 339.0510; **289.0704**	$C_{39}H_{32}O_{15}$	739.1668	-3.8	+	–	+	Cinchonain IIx (III)

Table 4 (continued)

Peak	Rt	TOF MS	Q/TOF MS/MS	Proposed formula	Exact mass	Δ	M	G	C	Tentative identification
190	17.4	191.0349	**176.0109**; **104.0277**	$C_{10}H_8O_4$	191.0350	-0.5	–	+	–	Scopoletin[a]
191	17.5	739.1667	**587.1195**; 449.0871; 339.0484; **289.0688**; **177.0174**	$C_{39}H_{32}O_{15}$	739.1668	-0.2	+	–	+	Cinchonain IIx (IV)
192	17.6	367.1025	193.0494; **191.0555**; 173.0452; 134.0373	$C_{17}H_{20}O_9$	367.1035	-2.6	+	+	+	Feruloylquinic acid
193	17.9	193.0504	**134.0367**; 133.0302	$C_{10}H_{10}O_4$	193.0506	-1.3	–	–	+	Ferulic acid[a]
194	21.2	367.1026	**179.0342**; 161.0256 **135.0446**; 134.0357	$C_{17}H_{20}O_9$	367.1035	0.8	+	+	+	Caffeic acid derivative
195	24.4	535.1454	371.0980; 329.1038; 191.0346; **163.0398**; **147.0450**; 119.0501	$C_{25}H_{28}O_{13}$	535.1457	-0.5	+	+	–	Coumaroyl iridoid (I)
196	25.7	535.1453	371.0987; 329.1025; 191.0337; **163.0396**; **147.0443**; 119.0500	$C_{25}H_{28}O_{13}$	535.1457	-0.7	+	+	–	Coumaroyl iridoid (II)
197	26.2	515.1184	**353.0867**; **191.0555**; **179.0345**; 173.0452; 135.0450	$C_{25}H_{24}O_{12}$	515.1195	-2.2	–	–	+	Dicaffeoylquinic acid
198	26.8	515.1179	**353.0872**; **191.0550**; 179.0347; 135.0445	$C_{25}H_{24}O_{12}$	515.1195	-3.0	–	–	+	1,5-Dicaffeoylquinic acid[a]
199	28.0	435.1291	**273.0751**; 167.0322	$C_{21}H_{24}O_{10}$	435.1297	-1.3	+	+	+	Phloridzin[a]
200	32.1	411.1659	163.0402; **145.0290**; 119.0481	$C_{20}H_{28}O_9$	411.1661	1.5	+	+	–	Coumaric acid-malonyl-hexoside (I)
201	32.5	411.1659	**163.0398**; **145.0292**; 119.0498	$C_{20}H_{28}O_9$	411.1661	-0.3	+	+	–	Coumaric acid-malonyl-hexoside (II)
202	32.6	445.1143	**179.0346**; **135.0441**; 134.0367	$C_{22}H_{22}O_{10}$	445.1040	0.6	+	+	+	Caffeic acid derivative

[a] confirmed by spiking the extracts with authentic standards

3.2 Comparison of polyphenolic compositions by PCA

The polyphenolic compositions of the three investigated berry species, as reported in Tables 1-4 and discussed in the previous paragraphs, appear very complex. Therefore, PCAs were separately performed on the LC-ESI-TOF-MS data acquired in positive and negative ionization in order to highlight which of the identified polyphenols are the most representative for describing the composition of the three *Vaccinium* species under investigation.

As regards positive ionization, two PCs had eigenvalues higher than 1 and were therefore considered as significant for describing the variance of the original TOF data. These two latent variables explained together 98.6% of the original variance (Fig. 4A). PC1, which accounted for 66.5% of the original variance, was positively and strongly correlated with coumaroyl-hexosides (e.g. peaks 51, 57, 58 and 63) and glucuronides (e.g. peaks 7 and 15), as well as with malvidin-feruloyl-hexosides (peaks 61 and 64) and various anthocyanidin glycosides, such as dihexosides (e.g. peaks 3, 5 and 13) and aldopentose-hexosides (e.g. peaks 21 and 27).

An opposite behaviour (i.e. strong and negative correlation with PC1) was observed for malonyl (e.g. peak 39) and acetyl (e.g. peaks 49, 50 and 52) derivatives of anthocyanidins, as well as for various malvidin glycosides (e.g. peaks 29 and 36). Conversely, these last metabolites showed high and positive loadings on PC2 (explained variance equal to 32.1%), which was on the other hand negatively correlated with the five xyloside derivatives herein identified (i.e. peaks 24, 35, 37, 44 and 45). A very high and negative loading on PC2 was also observed for malvidin-3-O-glucoside (peak 34).

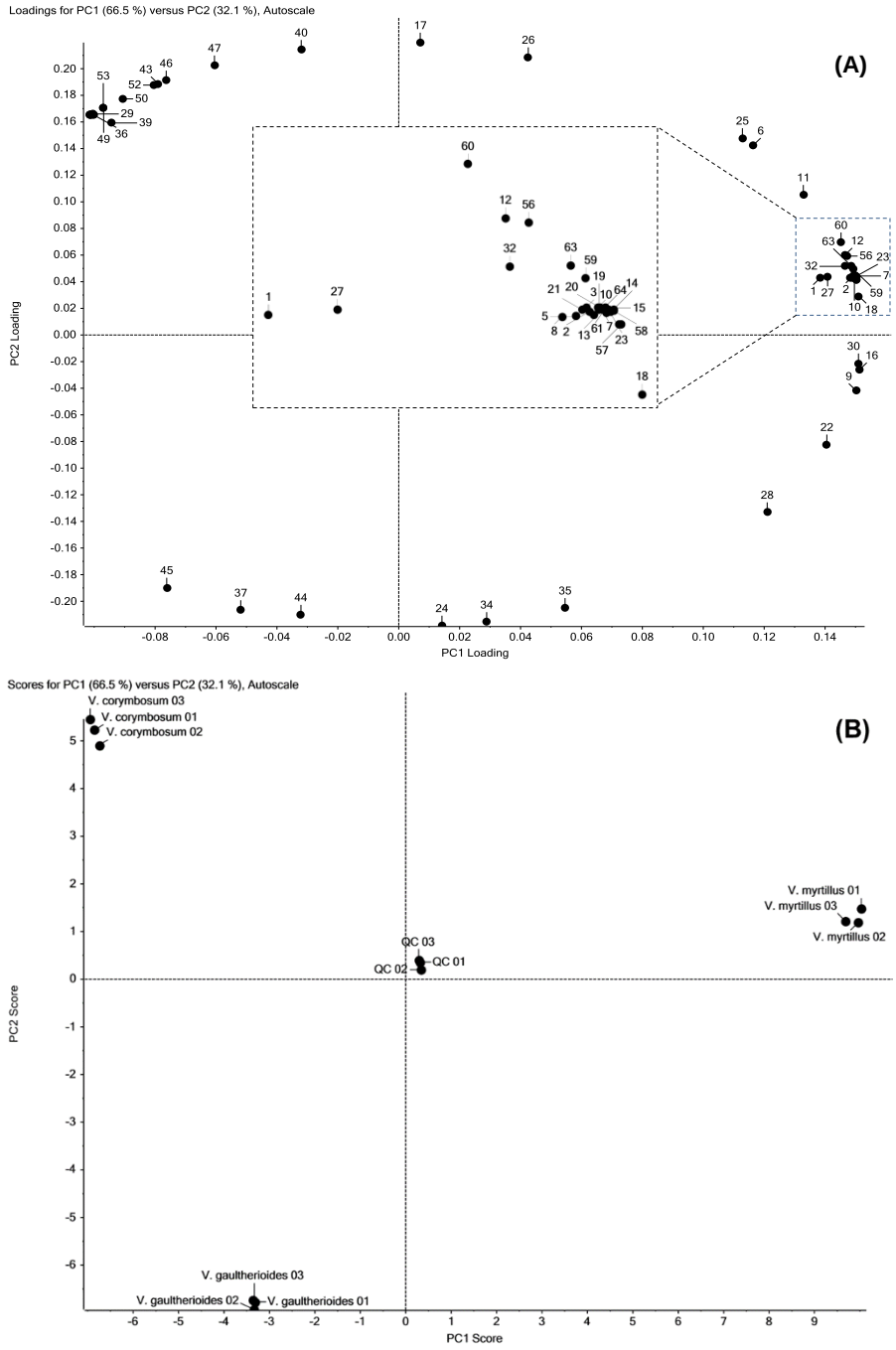

Figure 4. Loading (A) and score (B) plots of PC1 versus PC2 (PCA of original LC-ESI-TOF-MS data acquired in positive ionization). Numbers shown in the loading plot refer to the peak numbers reported in Table 1.

Fig. 4B illustrated how the three analyzed samples of each species, and the quality control samples (obtained by mixing equal amounts of each extracted sample) were located in the PC1 vs PC2 Cartesian plane. It is remarkable that different samples of each species were very close one to the other, generating three well-separated clusters in the PC space. Accordingly, the repeatability of the whole analytical process, as well as the robustness of the chemometric approach was demonstrated. It should also be noted that the quality controls were very close to the origin of the PC coordinates, confirming the accuracy and precision of PCA. The clusterization of the three *Vaccinium* species clearly highlighted their very different whole anthocyanin compositions. More in detail, an important role in the discrimination of *V. myrtillus* samples, which showed very high and positive scores on PC1 and small and positive scores on PC2, was clearly played by the aforementioned coumaroyl-hexosides and glucuronides. Conversely, acetyl and malonyl derivatives were the major responsible for the separation of *V. corymbosum* fruits. Finally, *V. uliginosum* subsp. *gaultherioides* berries, even though generally poorer in the number of identified anthocyanins, as well as in their signal intensity, were interestingly characterized by xyloside derivatives of petunidin (peak 37), peonidin (peak 44) and malvidin (peak 45).

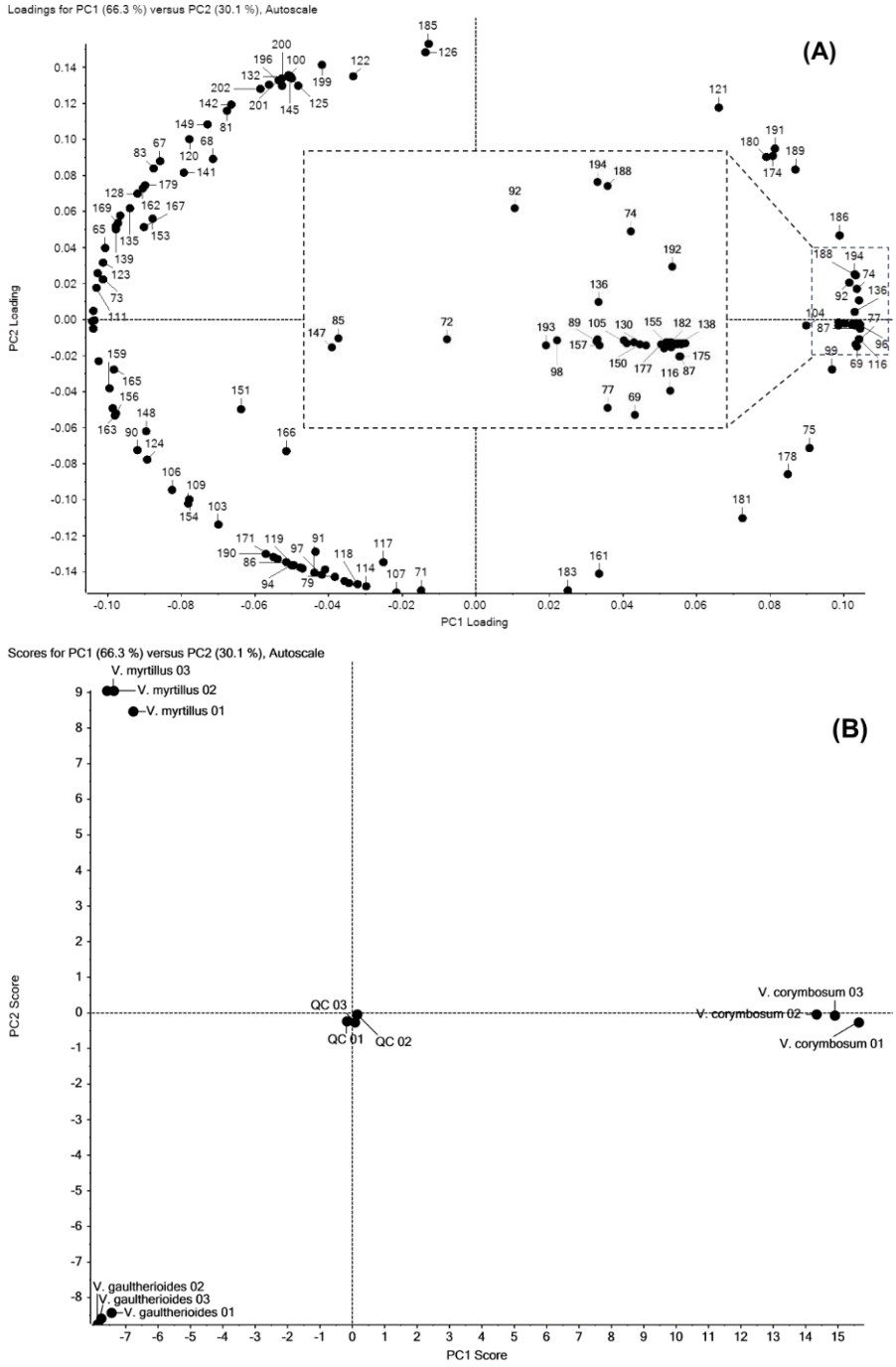

Figure 5. Loading (A) and score (B) plots of PC1 versus PC2 (PCA of original LC-ESI-TOF-MS data acquired in negative ionization). Numbers shown in the loading plot refer to the peak numbers reported in Tables 2-4.

PCA was also applied to the TOF data acquired in negative mode, highlighting two factors with eigenvalues higher than 1, which accounted for a total explained variance of 96.4% (66.3% and 30.1% for PC1 and PC2, respectively). The variable separation on the two PCs was in this case not as good as that obtained for compounds detected under positive ionization, probably also due to the much higher number of analytes detected in negative polarity. In fact, many metabolites were distributed in a very wide range of negative PC1 values, with both positive and negative loadings on PC2. However, some analytes showed very high and positive loadings on PC1 and a very narrow range of PC2 values, thus forming a cluster (see Fig. 5A and the zoomed area). This cluster contained all the identified flavonol acetyl-hexosides (e.g. peaks 89 and 105), some flavonol aldopentosides (e.g. peaks 69, 77 and 87) and a number of B-type proanthocyanidins eluting at relatively low retention times, whereas no A/B-type derivatives were found in this group. Furthermore, some hydroxycinnamic acids, such as neochlorogenic (peak 175), cryptochlorogenic (peak 182) and coumaroylquinic (peak 177) belonged to the cluster. Cinchonains exhibited high loadings on PC1 and low loadings on PC2, as well. Conversely, very high and negative values on the former latent variable were observed for all flavonol glucuronides (e.g. peaks 65, 73, 83, 90, 106 and 111).

The score plot (Fig. 5B) highlighted a very good accuracy and precision of PCA also for data obtained under negative ionization, with quality control samples well centred on the origin of the PC coordinates and evident separations among *V. corymbosum* (high scores on PC1 and close to zero on PC2), *V. myrtillus* (high and negative scores on PC1 and very high and positive on PC2) and *V. uliginosum* subsp. *gaultherioides* (negative scores on both PC1 and PC2) berries. Thus, LC-ESI-MS/MS in negative ionization gave useful and complementary information with respect to the positive mode for the discrimination of the investigated species.

4 Conclusions

LC-ESI-TOF and LC-ESI-Q/TOF analysis, performed both in positive and negative mode allowed for obtaining a comprehensive picture of the polyphenolic composition of *V. myrtillus*, *V. corymbosum* and *V. uliginosum* subsp. *gaultherioides* berries.

More in detail, 58 of the 64 anthocyanins identified in this study were present in *V. myrtillus*, 39 in *V. corymbosum* and 24 in *V. uliginosum* L. subsp. *gaultherioides*. As regards this last species, it is remarkable that aldopentosides and coumaroyl-hexosides have been detected herein for the first time. It should also be underlined that this study is the first one reporting the occurrence in *V. myrtillus* berries of anthocyanidin glucuronides and malvidin-feruloyl-hexosides, which represented an intense and characteristic metabolomic trait of this *Vaccinium* species, together with the already reported aldopentose-hexosides and cyanidin-aldodipentoside (Table S2). This study also indicated the exclusive presence of acetyl- and malonyl-hexosides in *V. corymbosum* berries (Table S2), compared to the other two investigated *Vaccinium* species.

Flavonols resulted generally more abundant in *V. corymbosum*. In fact, 51 of the 55 flavonols identified herein, were found to be present in blueberries, whereas only 37 in "false bilberry" and 35 in bilberry. Remarkably, in previous works, the flavonol derivatives discussed above, were only partially detected in *V. myrtillus* (12, 13, 44) and *V. corymbosum* (24, 51, 52) berries, whereas very few data were elsewhere reported for *V. uliginosum* L. subsp. *gaultherioides* (4). Hence, this work represents also for flavonol glycosides a more comprehensive study of such metabolites in the investigated *Vaccinium* species.

A similar number of flavanols were identified in the three species (i.e. 41, 39 and 35 compounds in bilberry, "false bilberry" and blueberry, respectively) and some of them, including trimers, tetramers and pentamers,

were found to be present in all species. However, some species-specific metabolites were found. For instance, flavanols containing A-type interflavanyl linkages were never observed in *V. corymbosum* (Table S2). Moreover, some B-type trimers (peaks 129, 144 and 157), tetramers (peaks 127, 130, 138 and 147) and pentamers (peaks 143, 146, 150 and 158) were exclusively found in blueberry (see Table 3). Interestingly, these compounds eluted at earlier retention times, compared to the metabolites common to the three species, thus suggesting a greater presence of catechin and gallocatechin, rather than the corresponding epimers, in *V. corymbosum* berries. It should be underlined that, for the first time, this research provides in-depth data on flavanols in *V. uliginosum* subsp. *gaultherioides* and *V. corymbosum* berries. Furthermore, even though data regarding flavanols in *V. myrtillus* fruits have been already reported in literature (13, 44), this study provides a much more detailed description of the flavanol composition in these berries, identifying for the first time a large number of proanthocyanidins with high molecular weight.

All the aforementioned LC-MS data were well-integrated using the PCA approach, which demonstrated to be suitable for a clear discrimination of the investigated berry species both in positive and negative ionization modes.

The comprehensive investigation herein illustrated, which evidenced phenolic metabolites exclusively detected in one species or characterized by extremely different intensities in the three berries, can be useful for future developments of methods aiming at evaluating the quality of *Vaccinium* berry transformation products and to avoid frauds. These products, in fact, are not only fruit juices or jams that are not subjected to any particular regulation concerning their phenolic content, but also supplements or actual drugs, which must conversely respect what is written in the label, both in terms of plant material used for its preparation and amount of active ingredients contained in the product.

5 Contribution

Claudia Ancillotti performed the LC-ESI-Q/TOF analysis of different *Vaccinium* berry species carrying out the untargeted metabolomics study. Then, she performed the data processing and analysis together with the identification of the reported polyphenols.

Acknowledgements

This research was funded by Regione Toscana and the private companies "Il Baggiolo S.r.l.", Danti Giampiero & C. S.n.c.", "Azienda Agricola Il Sottobosco" and "Farmaceutica MEV S.r.l.", within the "PRAF Misura 1.2. e)" grant.

References

1. Paredes-López O, Cervantes-Ceja M, Vigna-Pérez M, Hernández-Pérez T. Berries: Improving Human Health and Healthy Aging, and Promoting Quality Life-A Review. Plant Foods Hum Nutr. 2010;65(3):299-308.
2. Ignat I, Volf I, Popa VI. A critical review of methods for characterisation of polyphenolic compounds in fruits and vegetables. Food Chemistry. 2011;126(4):1821-35.
3. Daglia M. Polyphenols as antimicrobial agents. Curr Opin Biotech. 2012;23(2):174-81.
4. Ancillotti C, Ciofi L, Pucci D, Sagona E, Giordani E, Biricolti S, et al. Polyphenolic profiles and antioxidant and antiradical activity of Italian berries from *Vaccinium myrtillus* L. and *Vaccinium uliginosum* L. subsp. *gaultherioides* (Bigelow) S.B. Young. Food Chem. 2016;204:176-84.

5. Määttä-Riihinen KR, Kamal-Eldin A, Mattila PH, González-Paramás AM, Törrönen AR. Distribution and contents of phenolic compounds in eighteen Scandinavian berry species. J Agric Food Chem. 2004;52(14):4477-86.

6. Beccaro G, Mellano MG, Botta R, Chiabrando V, Bounous G, editors. Phenolic And Anthocyanin Content And Antioxidant Activity In Fruits Of Bilberry (*Vaccinium Myrtillus* L.) And Of Highbush Blueberry (*V. Corymbosum* L.) Cultivars In North Western Italy2006: International Society for Horticultural Science (ISHS), Leuven, Belgium.

7. Može Š, Polak T, Gašperlin L, Koron D, Vanzo A, Poklar Ulrih N, et al. Phenolics in Slovenian Bilberries (*Vaccinium myrtillus* L.) and Blueberries (*Vaccinium corymbosum* L.). J Agric Food Chem. 2011;59(13):6998-7004.

8. Lätti AK, Riihinen KR, Kainulainen PS. Analysis of Anthocyanin Variation in Wild Populations of Bilberry (*Vaccinium myrtillus* L.) in Finland. J Agric Food Chem. 2008;56(1):190-6.

9. Jovančević M, Balijagić J, Menković N, Šavikin K, Zdunić G, Janković T, et al. Analysis of phenolic compounds in wild populations of bilberry (*Vaccinium myrtillus* L.) from Montenegro. J. Med. Plants Res. 2011;5(6):910-4.

10. Giovanelli G, Buratti S. Comparison of polyphenolic composition and antioxidant activity of wild Italian blueberries and some cultivated varieties. Food Chem. 2009;112(4):903-8.

11. Åkerström A, Jaakola L, Bång U, Jäderlund A. Effects of Latitude-Related Factors and Geographical Origin on Anthocyanidin Concentrations in Fruits of *Vaccinium myrtillus* L. (Bilberries). J Agric Food Chem. 2010;58(22):11939-45.

12. Laaksonen O, Sandell M, Kallio H. Chemical factors contributing to orosensory profiles of bilberry (*Vaccinium myrtillus*) fractions. Eur Food Res Technol. 2010;231(2):271-85.

13. Mikulic-Petkovsek M, Schmitzer V, Slatnar A, Stampar F, Veberic R. A comparison of fruit quality parameters of wild bilberry (*Vaccinium myrtillus* L.) growing at different locations. J Sci Food Agric. 2015;95(4):776-85.

14. Gavrilova V, Kajdžanoska M, Gjamovski V, Stefova M. Separation, Characterization and Quantification of Phenolic Compounds in Blueberries and Red and Black Currants by HPLC−DAD−ESI-MSn. J Agric Food Chem. 2011;59(8):4009-18.

15. Del Bubba M, Checchini L, Chiuminatto U, Doumett S, Fibbi D, Giordani E. Liquid chromatographic/electrospray ionization tandem mass spectrometric study of polyphenolic composition of four cultivars of *Fragaria vesca* L. berries and their comparative evaluation. J Mass Spectrom. 2012;47(9):1207-20.

16. Sun J, Liu X, Yang T, Slovin J, Chen P. Profiling polyphenols of two diploid strawberry (*Fragaria vesca*) inbred lines using UHPLC-HRMS n. Food Chem. 2014;146:289-98.

17. Ieri F, Martini S, Innocenti M, Mulinacci N. Phenolic Distribution in Liquid Preparations of *Vaccinium myrtillus* L. and *Vaccinium vitis idaea* L. Phytochem Anal. 2013;24(5):467-75.

18. Ramirez JE, Zambrano R, Sepúlveda B, Kennelly EJ, Simirgiotis MJ. Anthocyanins and antioxidant capacities of six Chilean berries by HPLC–HR-ESI-ToF-MS. Food Chem. 2015;176:106-14.

19. Liu P, Lindstedt A, Markkinen N, Sinkkonen J, Suomela J-P, Yang B. Characterization of Metabolite Profiles of Leaves of Bilberry (*Vaccinium myrtillus* L.) and Lingonberry (*Vaccinium vitis-idaea* L.). J Agric Food Chem. 2014;62(49):12015-26.

20. van der Hooft JJ, Vervoort J, Bino RJ, Beekwilder J, de Vos RC. Polyphenol identification based on systematic and robust high-resolution accurate mass spectrometry fragmentation. Anal Chem. 2010;83(1):409-16.

21. Beccaro GL, Giongo L, De Salvador FR, Ughini V, Folini L, Draicchio P, et al. Scegliere le cultivar di lampone, mirtillo e rovo per il 2011. L'Informatore Agrario. 2011;20:58-61 (In Italian).

22. Doumett S, Fibbi D, Cincinelli A, Giordani E, Nin S, Del Bubba M. Comparison of nutritional and nutraceutical properties in cultivated fruits of Fragaria vesca L. produced in Italy. Food Res Int. 2011;44(5):1209-16.

23. Barnes JS, Nguyen HP, Shen S, Schug KA. General method for extraction of blueberry anthocyanins and identification using high performance liquid chromatography–electrospray ionization-ion trap-time of flight-mass spectrometry. J Chromatogr A. 2009;1216(23):4728-35.

24. Sun J, Lin Lz, Chen P. Study of the mass spectrometric behaviors of anthocyanins in negative ionization mode and its applications for characterization of anthocyanins and non- anthocyanin polyphenols. Rapid Communications in Mass Spectrometry. 2012;26(9):1123-33.

25. Lätti AK, Riihinen KR, Jaakola L. Phenolic compounds in berries and flowers of a natural hybrid between bilberry and lingonberry (Vaccinium × intermedium Ruthe). Phytochemistry. 2011;72(8):810-5.

26. Veberic R, Slatnar A, Bizjak J, Stampar F, Mikulic-Petkovsek M. Anthocyanin composition of different wild and cultivated berry species. LWT-Food Sci Technol. 2015;60(1):509-17.

27. Oliveira M, Esperanca P, Ferreira A. Characterisation of anthocyanidins by electrospray ionisation and collision- induced dissociation tandem mass spectrometry. Rapid Commun Mass Spectrom. 2001;15(17):1525-32.

28. Giusti MM, Rodríguez-Saona LE, Griffin D, Wrolstad RE. Electrospray and tandem mass spectroscopy as tools for anthocyanin characterization. J Agric Food Chem. 1999;47(11):4657-64.

29. Wu X, Prior RL. Systematic identification and characterization of anthocyanins by HPLC-ESI-MS/MS in common foods in the United States:

fruits and berries. Journal of agricultural and food chemistry. 2005;53(7):2589-99.

30. Felgines C, Talavera S, Texier O, Gil-Itsquierdo A, Lamaison JL, Remesy C. Blachberry anthocyanins are mainly recovered from urine as methylated and glucuronidated conjugates in humans. J Agric Food Chem. 2005;53(20):7721-27.

31. Ferrars R, Czank C, Zhang Q, Botting N, Kroon P, Cassidy A, Kay CD. The pharmacokinetics of anthocyanins and their metabolites in humans. Brit J Pharmacol. 2014;171(13):3268-82.

31. Du Q, Jerz G, Winterhalter P. Isolation of two anthocyanin sambubiosides from bilberry (*Vaccinium myrtillus*) by high-speed counter-current chromatography. J Chromatogr A. 2004;1045(1):59-63.

32. Paes J, Dotta R, Barbero GF, Martínez J. Extraction of phenolic compounds and anthocyanins from blueberry (*Vaccinium myrtillus* L.) residues using supercritical CO2 and pressurized liquids. J Supercrit Fluids. 2014;95:8-16.

33. Lätti AK, Jaakola L, Riihinen KR, Kainulainen PS. Anthocyanin and flavonol variation in bog bilberries (*Vaccinium uliginosum* L.) in Finland. J Agric Food Chem. 2010;58(1):427-33.

34. Zoratti L, Jaakola L, Häggman H, Giongo L. Anthocyanin Profile in Berries of Wild and Cultivated *Vaccinium* spp. along Altitudinal Gradients in the Alps. J Agric Food Chem. 2015;63(39):8641-50.

35. He J-J, Liu Y-X, Pan Q-H, Cui X-Y, Duan C-Q. Different anthocyanin profiles of the skin and the pulp of Yan73 (Muscat Hamburg× Alicante Bouschet) grape berries. Molecules. 2010;15(3):1141-53.

36. Cuyckens F, Claeys M. Mass spectrometry in the structural analysis of flavonoids. J Mass Spectrom. 2004;39(1):1-15.

37. Lu L, Song FR, Tsao R, Jin YR, Liu ZQ, Liu SY. Studies on the homolytic and heterolytic cleavage of kaempferol and kaempferide

glycosides using electrospray ionization tandem mass spectrometry. Rapid Commun Mass Spectrom. 2010;24(1):169-72.

38. Justesen U. Collision- induced fragmentation of deprotonated methoxylated flavonoids, obtained by electrospray ionization mass spectrometry. J Mass Spectrom. 2001;36(2):169-78.

39. Domon B, Costello CE. A systematic nomenclature for carbohydrate fragmentations in FAB-MS/MS spectra of glycoconjugates. Glycoconjugate J. 1988;5(4):397-409.

40. Ma Y, Li Q, Van den Heuvel H, Claeys M. Characterization of flavone and flavonol aglycones by collision- induced dissociation tandem mass spectrometry. Rapid Commun Mass Spectrom. 1997;11(12):1357-64.

41. Cuyckens F, Claeys M. Determination of the glycosylation site in flavonoid mono- O- glycosides by collision- induced dissociation of electrospray- generated deprotonated and sodiated molecules. J Mass Spectrom. 2005;40(3):364-72.

42. Petsalo A, Jalonen J, Tolonen A. Identification of flavonoids of Rhodiola rosea by liquid chromatography-tandem mass spectrometry. J Chromatogr A. 2006;1112(1):224-31.

43. Hokkanen J, Mattila S, Jaakola L, Pirttilä AM, Tolonen A. Identification of phenolic compounds from lingonberry (*Vaccinium vitis-idaea* L.), bilberry (Vaccinium myrtillus L.) and hybrid bilberry (Vaccinium x intermedium Ruthe L.) leaves. J Agric Food Chem. 2009;57(20):9437-47.

44. Gómez-Romero M, Zurek G, Schneider B, Baessmann C, Segura-Carretero A, Fernández-Gutiérrez A. Automated identification of phenolics in plant-derived foods by using library search approach. Food Chem. 2011;124(1):379-86.

45. Simirgiotis MJ, Theoduloz C, Caligari PD, Schmeda-Hirschmann G. Comparison of phenolic composition and antioxidant properties of two native Chilean and one domestic strawberry genotypes. Food Chem. 2009;113(2):377-85.

46. Teixeira N, Azevedo J, Mateus N, de Freitas V. Proanthocyanidin screening by LC–ESI-MS of Portuguese red wines made with teinturier grapes. Food Chem. 2016;190:300-7.

47. Jensen HD, Krogfelt KA, Cornett C, Hansen SH, Christensen SB. Hydrophilic carboxylic acids and iridoid glycosides in the juice of American and European cranberries (*Vaccinium macrocarpon* and V. oxycoccos), lingonberries (V. vitis-idaea), and blueberries (*V. myrtillus*). J Agric Food Chem. 2002;50(23):6871-4.

48. Nonaka G, Nishioka I. Tannins and related compounds. VII. Phenylpropanoid-substituted epicatechins, cinchonains from Cinchona succirubra. Chem Pharm Bull. 1982;30:4268-76.

49. Matsuo Y, Fujita Y, Ohnishi S, Tanaka T, Hirabaru H, Kai T, et al. Chemical constituents of the leaves of rabbiteye blueberry (*Vaccinium ashei*) and characterisation of polymeric proanthocyanidins containing phenylpropanoid units and A-type linkages. Food Chem. 2010;121(4):1073-9.

50. Cho MJ, Howard LR, Prior RL, Clark JR. Flavonoid glycosides and antioxidant capacity of various blackberry, blueberry and red grape genotypes determined by high- performance liquid chromatography/mass spectrometry. J Sci Food Agric. 2004;84(13):1771-82.

51. Vrhovsek U, Masuero D, Palmieri L, Mattivi F. Identification and quantification of flavonol glycosides in cultivated blueberry cultivars. J Food Compos Anal. 2012;25(1):9-16.

Manuscript: "Liquid chromatographic/electrospray ionization quadrupole/time of flight tandem mass spectrometric study of polyphenolic composition of different *Vaccinium* berry species and their comparative evaluation" by C. Ancillotti et al.

Electronic Supplementary Materials

Table S1. Collection zones of *Vaccinium myrtillus* and *Vaccinium uliginosum* subsp. *gaultherioides* berries.

Location name	Coordinates	Cardinal direction	Altitude (m, asl)
Monte Gomito	44°07'36.7"N 10°38'36.2"E	SW	1824
Monte Gomito	44°07'36.1"N 10°38'34.4"E	SW	1826
Monte Gomito	44°07'35.8"N 10°38'33.9"E	SW	1847
Monte Gomito	44°07'34.7"N 10°38'35.5"E	SW	1806
Monte Gomito	44°07'34.4"N 10°38'34.9"E	SW	1820
Monte Gomito	44°07'38.8"N 10°38'50.8"E	NNE	1850
Monte Gomito	44°07'38.5"N 10°38'51.5"E	NNE	1852
Monte Gomito	44°07'40.2"N 10°38'54.1"E	NNE	1831
Monte Gomito	44°07'39.8"N 10°38'59.6"E	NNE	1821
Monte Gomito	44°07'40.9"N 10°39'00.8"E	NNE	1814
Lago Nero	44°06'54.9"N 10°38'14.5"E	NNE	1725
Lago Nero	44°06'52.6"N 10°38'13.5"E	NNE	1705
Lago Nero	44°06'52.7"N 10°38'09.4"E	ENE	1750
Libro Aperto	44°09'26.0"N 10°41'39.2"E	WSW	1597
Libro Aperto	44°09'24.7"N 10°41'39.9"E	WSW	1609
Libro Aperto	44°09'27.4"N 10°41'37.7"E	WSW	1590
Libro Aperto	44°09'27.6"N 10°41'33.2"E	WSW	1569
Libro Aperto	44°09'26.5"N 10°41'30.2"E	WSW	1537

Table S2. List of phenolic compounds detected exclusively in one *Vaccinium* berry species. Note that only the compounds with a signal intensity of the quasi-molecular ion ≥ 5000 cps were reported.

Species	Anthocyanins	Flavonols	Flavanols	Other phenolic compounds
V. myrtillus	Delphinidin-glucuronide Delphinidin-aldopentose-hexoside (II) Cyanidin-aldopentose-hexoside (I) Cyanidin-aldopentose-hexoside (II) Cyanidin-glucuronide Petunidin-glucuronide Petunidin-aldopentose-hexoside Peonidin-aldopentose-hexoside (II) Delphinidin-coumaroyl-hexoside (I) Delphinidin-coumaroyl-hexoside (II) Peonidin-coumaroyl-hexoside (I) Peonidin-coumaroyl-hexoside (II) Malvidin-feruloyl-hexoside (I) Malvidin-feruloyl-hexoside (II)	Quercetin-3-*O*-deoxyhexose-pentoside	A/B-type(E)GC-(E)GC-(E)GC A/B-type (E)C-(E)GC-(E)GC (I) A/B-type (E)C-(E)GC-(E)GC (II)	
V. gaultherioides		Kaempferol-3-*O*-glucoside	A/B-type (E)C-(E)C-(E)C (II) A/B-type (E)C-(E)C-(E)C (III)	Scopoletin
V. corymbosum	Delphinidin-acetyl-hexoside (I) Delphinidin-acetyl-hexoside (II) Malvidin-malonyl-hexoside (I) Malvidin-malonyl-hexoside (II)	Quercetin-3-*O*-rutinoside Quercetin-malonyl-hexoside (I) Quercetin-malonyl-hexoside (II) Quercetin-acetyl-hexoside (I) Quercetin-acetyl-hexoside (II) Quercetin-acetyl-hexoside (IV) Kaempferol-7-*O*-neohesperidoside Isorhamnetin-3-*O*-deoxyhexose-hexoside Laricitrin-3-O-rhamnoside Isorhamnetin-7-*O*-deoxyhexose-hexoside Kaempferol-3-*O*-aldopentoside	B-type (E)C-(E)C-(E)GC (I) B-type (E)C-(E)C-(E)C (II) B-type (E)C-(E)C-(E)C (IV) B-type (E)C-(E)C-(E)C-(E)C (I) B-type (E)C-(E)C-(E)C-(E)C (II) B-type (E)C-(E)C-(E)C-(E)C (III) B-type (E)C-(E)C-(E)C-(E)C-(E)C (I) B-type (E)C-(E)C-(E)C-(E)C-(E)C (II) B-type (E)C-(E)C-(E)C-(E)C-(E)C (III) B-type (E)C-(E)C-(E)C-(E)C-(E)C (IV)	Coumaroylquinic acid (I) Coumaroylquinic acid (II) Cinchonain IIx (II) Dicaffeoylquinic acid

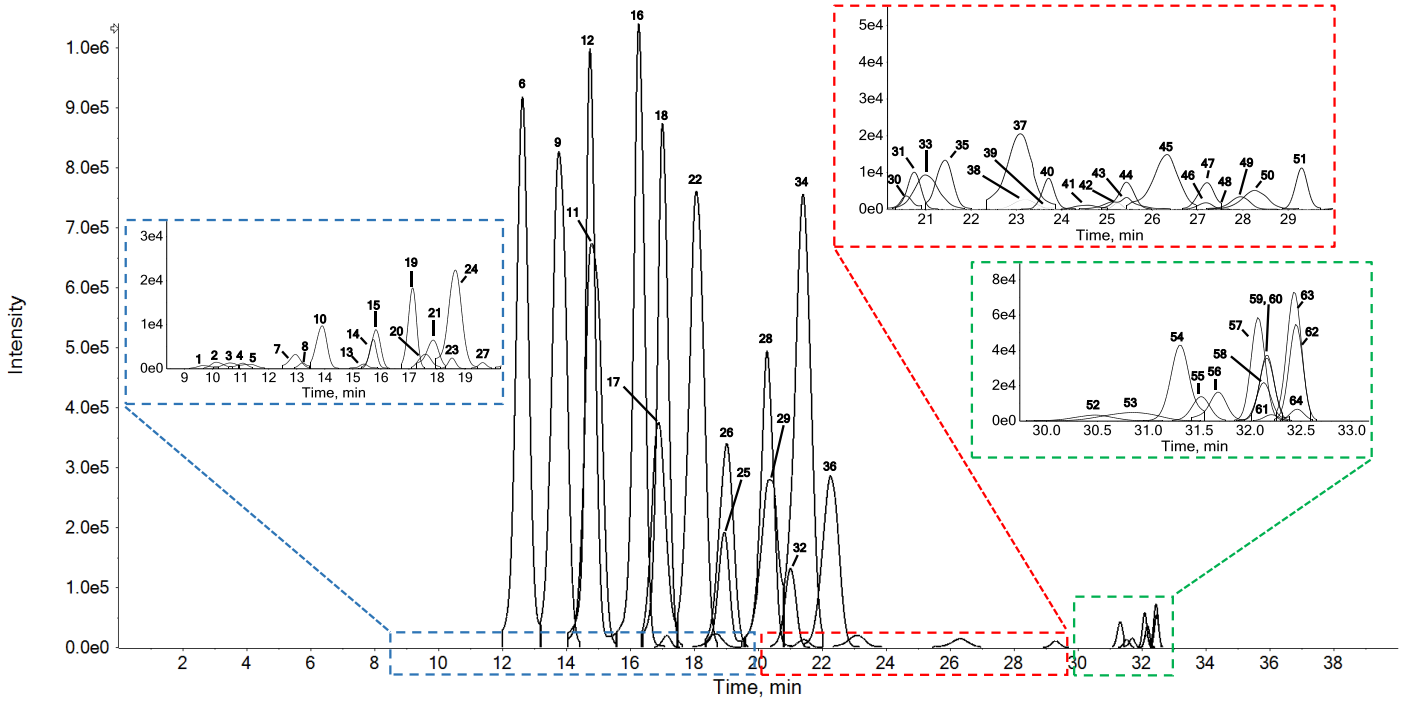

Figure S1. Reconstructed LC-MS chromatogram of the identified anthocyanins. Peak numbers refer to compounds reported in Table 1.

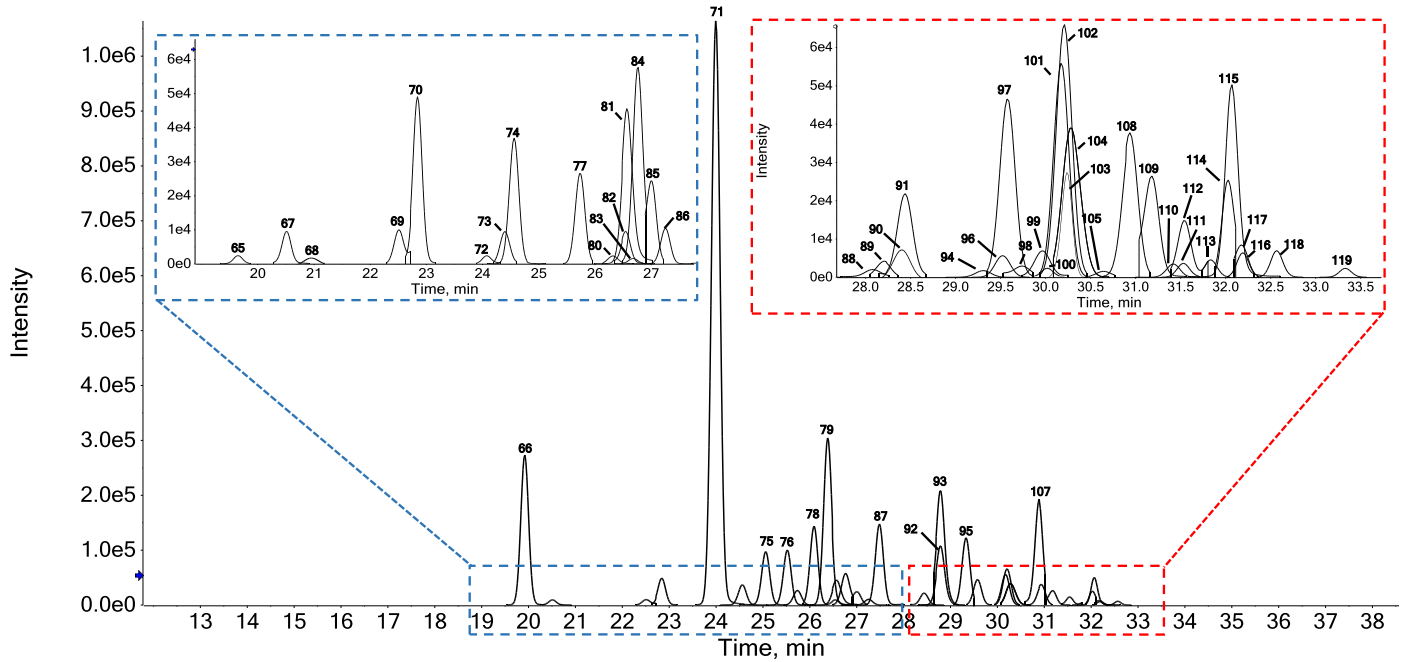

Figure S2. Reconstructed LC-MS chromatogram of the identified flavonols. Peak numbers refer to compounds reported in Table 2.

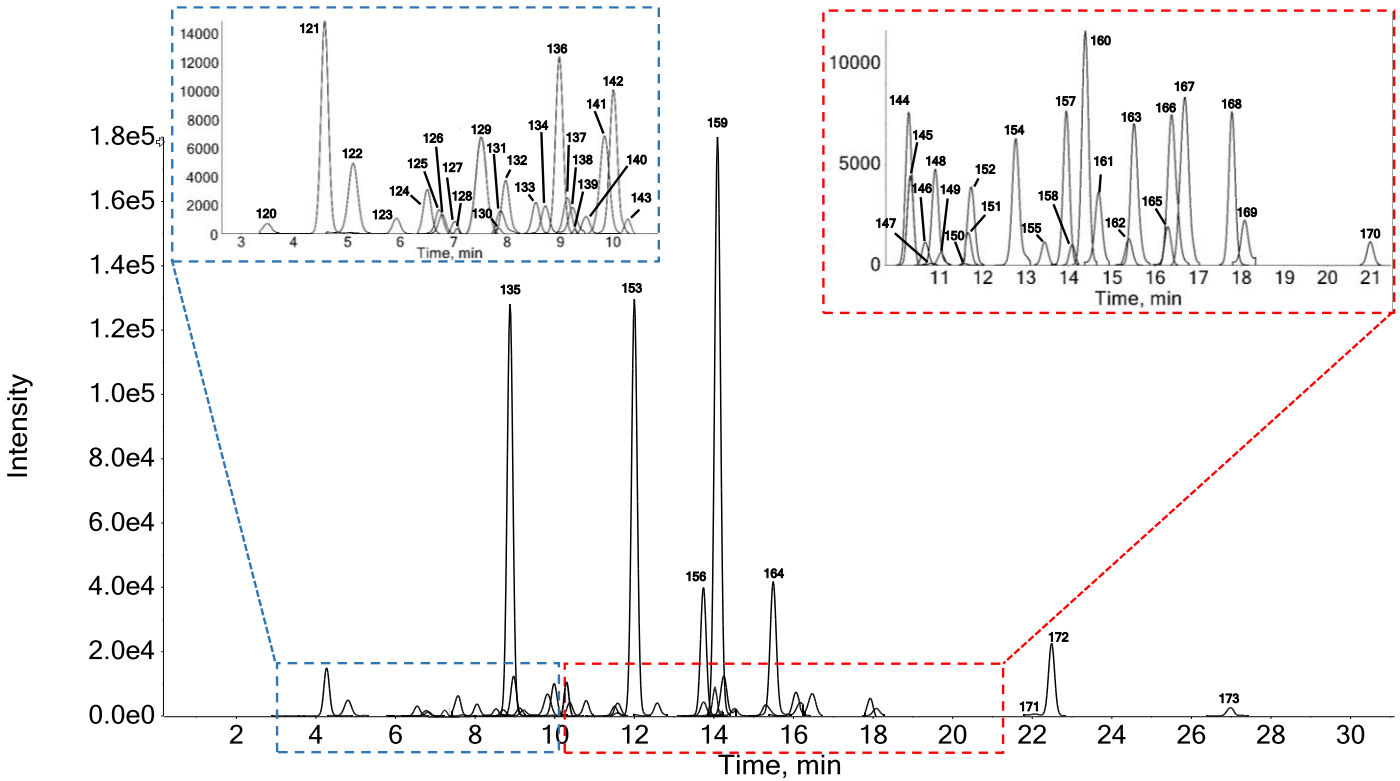

Figure S3. Reconstructed LC-MS chromatogram of the identified flavanols. Peak numbers refer to compounds reported in Table 3.

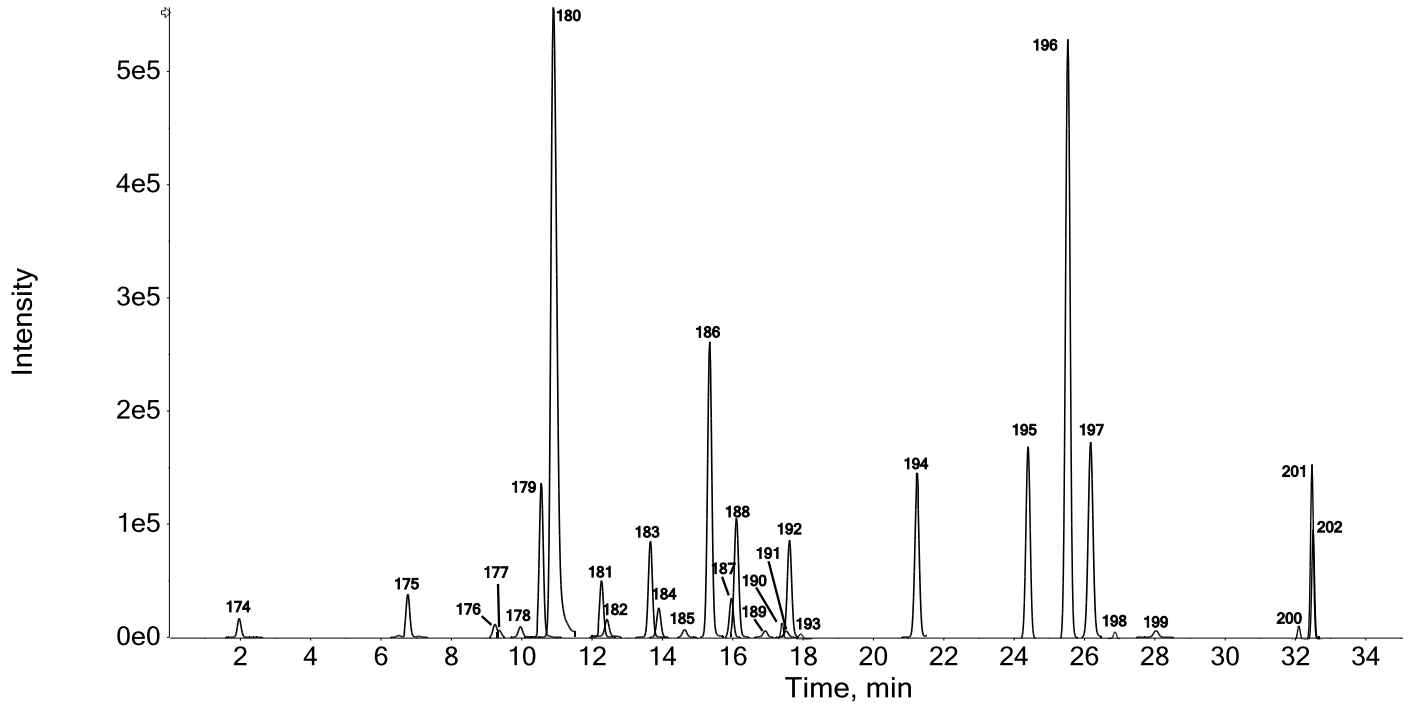

Figure S4. Reconstructed LC-MS chromatogram of the identified other phenolic compounds. Peak numbers refer to compounds reported in Table 4.

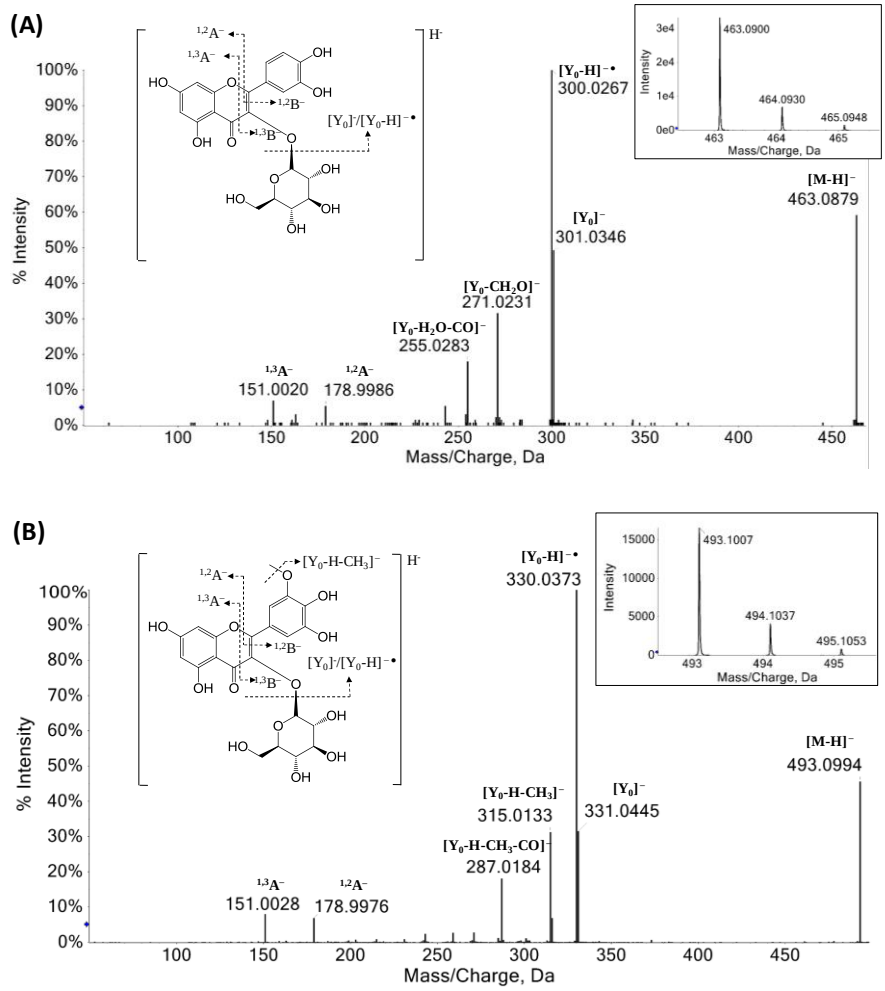

Figure S5. Q/TOF MS/MS spectrum of: (A) peak **75**, unequivocally identified as quercetin-3-glucoside and (B) peak **78**, putatively identified as laricitrin-3-galactoside.

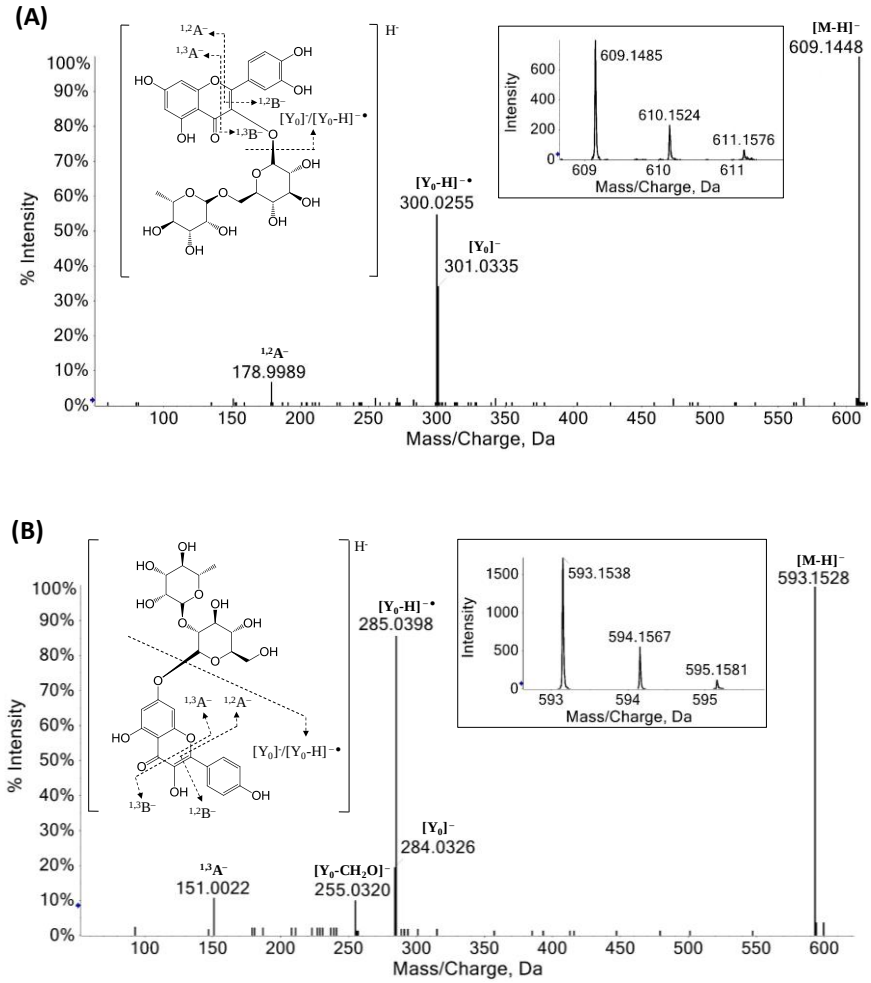

Figure S6. Q/TOF MS/MS spectrum of: (A) peak **76**, unequivocally identified as quercetin-3-rutinoside and (B) peak **96**, unequivocally identified as kaempferol-7-neohesperidoside.

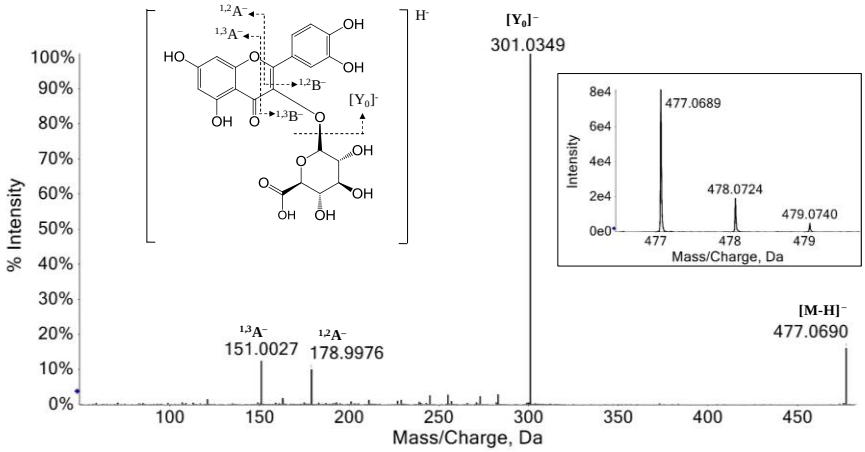

Figure S7. Q/TOF MS/MS spectrum of peak **73**, unequivocally identified as quercetin-3-glucuronide.

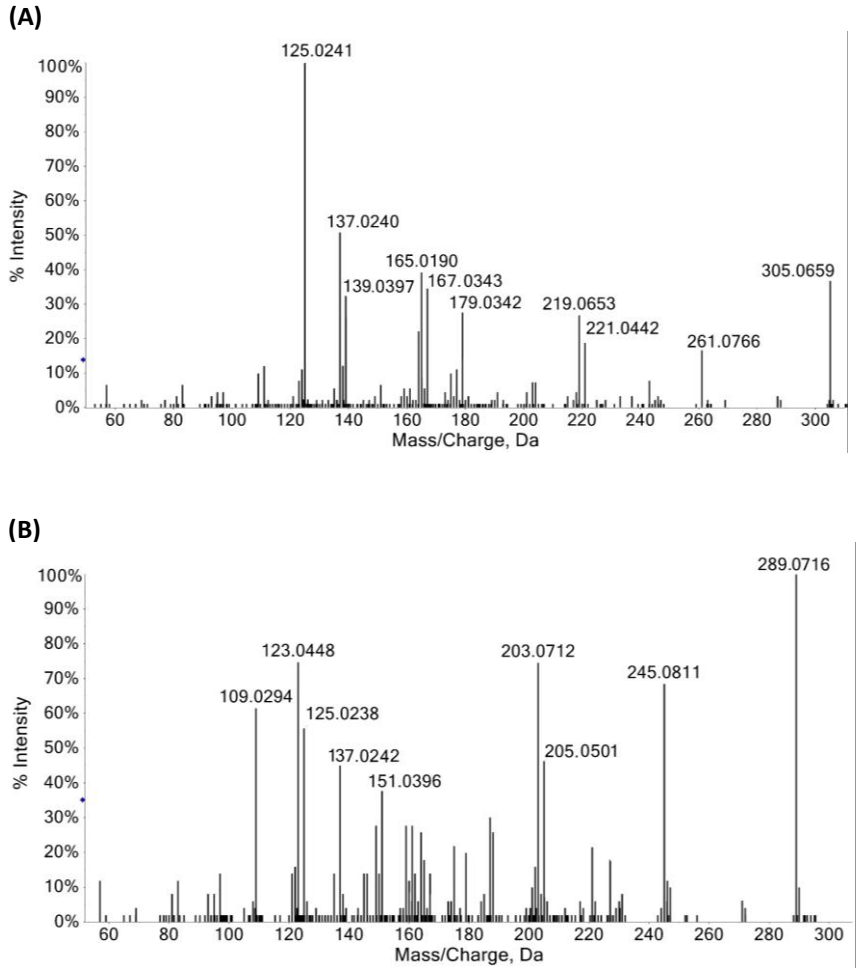

Figure S8. Q/TOF MS/MS spectrum of: (A) peak **135**, putatively identified as epigallocatechin and (B) peak **136**, unequivocally identified as (+)-catechin.

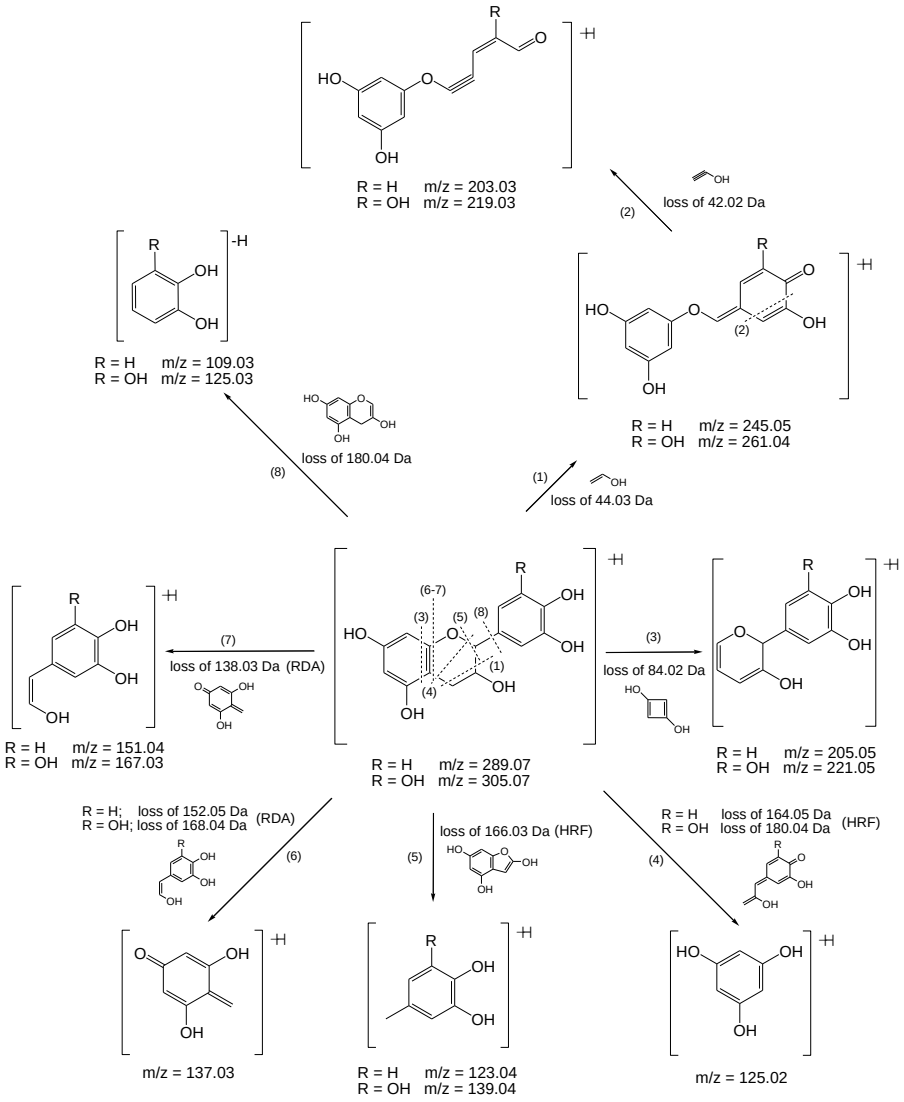

Scheme S1 – Hypothesized structure and fragmentation scheme for peaks **121** ([M-H]$^-$ = 305.07, putatively attributed to gallocatechin), **135** ([M-H]$^-$ = 305.07, putatively attributed to epigallocatechin), **136** ([M-H]$^-$ = 289.07, catechin) and **159** ([M-H]$^-$ = 289.07, epicatechin). HRF = heterocyclic ring fission; RDA = retro Diels-Alder.

Chapter 5

Untargeted metabolomics study for the comparative evaluation of plasma and urinary phenolic metabolites after acute ingestion of *Vaccinium myrtillus* and *Vaccinium corymbosum* berries.

Claudia Ancillotti
Marynka Ulaszewska
Fulvio Mattivi
Lorenzo Ciofi
Daniele Rossini
Lapo Renai
Leonardo Checchini
Riccardo Bartoletti
Marco Carini
Edgardo Giordani
Massimo Del Bubba

Submitted to Analytical Chemistry

1. Introduction

Nowadays, a great attention is turned to nutrition because a lot of epidemiological studies have suggested diet habits as key factors in the prevention of several pathologies (1-3). In particular, some researches highlighted the relation between fruit consumption and the decreased risk of developing cardiovascular diseases (1) and different kinds of neoplasm, such as lung carcinoma (2), as well as gastric and colon cancer (4, 5). The health benefits of fruits were often attributed to their high content of antioxidant compounds, such as polyphenols, able to neutralize the reactive oxygen species (ROS) and, consequently, reduce the oxidative stress related to the most common degenerative and chronic diseases (6, 7).

Among fruits, small berries (e.g. strawberry, blueberry and raspberry) represent an abundant source of phenolic compounds in human diet (8). In detail, the fruits belonging to the *Vaccinium* genus, above all *V. myrtillus* berries, have been suggested as functional foods and used for supplement preparation (9).

Interestingly, *in vitro* studies have shown anti-proliferative and apoptotic effects against different cancer cell lines (e.g. breast and colon cancer cells) of small berry extracts containing high concentrations of polyphenols (10-13). Moreover, some clinical trials investigating the effectiveness of polyphenol-based functional foods in patients affected by different kind of cancer have shown promising results (14). More in detail, as regards small berry supplements, the chemopreventive properties of an anthocyanin-rich *V. myrtillus* extract has been suggested in a pilot study with patients affected by colon cancer (15).

Nevertheless, in spite of the healthy properties suggested for small berries, the absorption, distribution, metabolism and elimination (ADME) of the most abundant *Vaccinium* fruits polyphenols, i.e. anthocyanins, is currently poorly understood (16). Studies aiming at a better understanding of the

metabolism of anthocyanins in human body were carried out by the investigation of their fate in biological fluids (e.g. serum and urine) after the administration of small berries as fresh fruits (17), freeze-dried fruits (18, 19), juices (20, 21), dried extract (22, 23) or standardized extracts (24, 25) to rats or humans. In these studies, biofluids were analysed using liquid chromatographic/diode-array (LC-DAD) or liquid chromatographic/tandem mass spectrometric (LC-MS/MS) methods, adopting in almost all cases a targeted approach. Targeted analytes were the anthocyanins originally present in small berries and their predicted metabolites, the latter being mainly glucuronide, methylated and sulphate conjugates, selected on the basis of the well-known reactions occurring during the phase II metabolism for the xenobiotic molecule elimination (20, 24, 26). Based on this approach, a low bioavailability of anthocyanins was evidenced, since detected metabolites accounted for 1-2% of the ingested dose (22, 27). Accordingly, some authors claimed that such a low concentration cannot result in a biological activity, suggesting that other metabolites, not yet identified, could be responsible for the healthy properties evidenced by clinical trials (16, 28).

For this reason, some recent literature studies focused on the analysis of phenolic acids (i.e. benzoic, phenylacetic and hydrocinnamic acids), which have been suggested by *in vitro* studies as the gut microflora metabolites of anthocyanins (28). In detail, benzoic acids were found in rat biological fluids after *V. angustifolium* administration (29), whereas phenylacetic, hydroxycinnamic and benzoic acids were reported in human urine after *V. myrtillus* assumption (30). However, also in these studies, a targeted LC-MS/MS approach was adopted, thus strongly limiting the number and type of potentially identified metabolites. As regards *Vaccinium* berry metabolism, only two untargeted metabolomics approach were applied to the investigation of serum and urinary polyphenolic metabolites of *V. angustifolium* berries in human biofluids (31, 32).

The much higher number of targeted studies is also due to the very high analytical complexity of untargeted metabolomics analysis of biofluids, that gives rise to tens of thousands signals and requires a long elaboration of acquired data (33). Moreover, because of this complexity, the untargeted metabolomics analysis of biofluids was often performed with a high-resolution mass spectrometer (HRMS) able to provide the exact mass of the detected ion, thus drastically reducing the number of possible elemental formula ascribable to the parent molecule.

In addition, the low concentrations (i.e. pmol/mL-nmol/mL) of serum metabolites have brought to the preferred use of the targeted methods, more sensitive than the untargeted ones. In fact, the use of the former analytical approach allows the quantification of known and predicted polyphenol conjugates even when they are present at low concentrations, but it does not permit the identification of new metabolites potentially responsible of biological activities.

Furthermore, it is important to underline that almost all literature researches focused on anthocyanins metabolites after *Vaccinium* berries administration but these fruits contain significant concentrations of a number of polyphenols belonging to other classes. In this regard, the polyphenolic compositions of *V. myrtillus* (bilberry) and *V. corymbosum* (blueberry) fruits were recently investigated using an untargeted metabolomics approach by our research group. Among the identified phenolic compounds, many anthocyanins, flavonols, flavanol oligomers and phenolic acids showed a high "species-specificity" and discriminated the different investigated *Vaccinium* species (34). A such in-depth knowledge of polyphenolic composition of investigated berries is essential for the identification of polyphenol metabolites in human biofluids.

For these reasons, the aim of this research was the application of a LC-HRMS/MS method for the untargeted metabolomics analysis of serum and urine polyphenolic metabolites in healthy volunteers after the administration

of *V. myrtillus* and *V. corymbosum* berry supplements, attempting the identification of new specific metabolites of the two species. The choice of these *Vaccinium* species was related to their wide consumption as functional foods as well as their aforementioned different polyphenolic composition.

2. Materials and Methods

2.1. Reagents and standards

Methanol and acetonitrile LC-MS Ultra CHROMASOLV™ and formic acid were purchased from Sigma Aldrich (St. Louis, MO, USA). The ultrapure water was obtained by purifying demineralized water in a Milli-Q system from Millipore (Bedford, MA, USA). The internal standard trans-cinnamic-d5 acid (CIN-d5) was purchased from CDN ISOTOPES Inc. (Pointe-Claire, Quebec, Canada). The surrogate standards L-Triptophan-2',4',5',6',7'-d5 (TRI-d5) and N-Benzoyl-d5-glycine (Hippuric acid-d5, HIP-d5) were obtained from Sigma Aldrich and CDN ISOTOPES Inc., respectively. Commercial standard of vanillic acid, ferulic acid and abscisic acid used for the comparison during metabolite identification were purchased by Sigma Aldrich.

2.2. Subjects and study design

The study aimed to investigate the metabolic food-kinetics of bilberry and blueberry fruits in healthy voluntary subjects. The study followed the guidelines set by the Helsinki Declaration (http://www.fda.gov/ohrms/dockets/dockets/06d0331/06D-0331-EC20-Attach-1.pdf) and all subjects provided written informed consent prior to the study.

The supplements used in the study were obtained by cryo-milling of *V. myrtillus* and *V. corymbosum* freeze-dried berries resulting in a very homogeneous powder. The bilberry-based supplement was characterized by total soluble polyphenol (TSP) and total monomeric anthocyanin (TMA) contents equal to 38.8 mg catechin equivalent/g dried fruits and 30.1 mg cyanidin-3-glucoside equivalent/g dried fruits, respectively. The blueberry-based supplement contained TSP and TMA concentrations equal to 9.4 mg catechin equivalent/g dried fruits and 6.2 mg cyanidin-3-glucoside equivalent/g dried fruits, respectively. Ethical approval for freeze-dried *V. myrtillus* and *V. corymbosum* powdered supplement administration was obtained for a phase I-II study (approval n. SPE 14.178 AOUC, 30th May 2016).

Twenty healthy voluntary subjects participated in the study (11 males and 9 females aged between 25 and 60 years). None of them presented concomitant food allergies or metabolic diseases.

All the subjects convened early in the morning after 10h of fasting and were randomly divided in two groups according to an electronic randomisation key. A single dose of 25 g of *V. myrtillus* supplement mixed with 500 mL of water was orally administered to the first group (VM group), whereas the same amount of *V. corymbosum* berry supplement mixed with 500 mL of water was orally administered to the second group (VC group).

Serum and urine of each volunteer were collected at baseline and different sampling times (30, 60, 120, 240 and 360 minutes) after the supplement assumption. After the collection, both plasma and urine samples were divided in aliquots of 500 µL, frozen at -80ºC and stored until the LC-MS analysis was performed.

2.3. Sample preparation

Before the LC-MS analysis, the urine and plasma aliquots were thawed and extracted according to the methods following reported. As regards urine samples, the filtration was performed using the Millipore 96-well plate (Waters, Milford, MA, USA). Briefly, for each sample 100 µL of urine were placed into the well and 100 µL of surrogate standards in methanol (25 µg/mL TRI-d5 and HIP-d5) were added. Then, a cap mat was applied on the well plate and the system was mixed for 5 minutes. After mixing, the well plate and the collection plate were placed on the positive pressure processor (Positive Pressure-96 Processor, Waters) and the filtration was performed setting the flow for 60 psi for 5 minutes. Then, 300 µL of internal standard (0.83 µg/mL CIN-d5) were added to each position of the collection plate and the system was mixed for 5 minutes. The resulting filtrated and diluted urine samples were transferred in labelled brown vials for LC-MS analysis. For testing the urine filtration procedure, a quality control (QC) sample consisting of a pool of the same volume of all urine samples was prepared. The same extraction protocol was performed on QC aliquots randomly placed in the well plate. The QC extracts together with the extraction blanks were injected before the LC-MS analysis of individual samples.

As regards serum samples, the precipitation of proteins and the removal of phospholipids were performed using the Ostro 96-well plate (Waters, Milford, MA, USA). In detail, for each sample, 100 µL of serum were placed into the well and 100 µL of surrogate standards in methanol (12.5 µg/mL TRI-d5 and HIP-d5) were added. Then, 300 µL of the first cold solvent (acetonitrile/formic acid 99:1 v/v) were added to each well, the system was covered and the well plate/collection plate were firstly mixed for 5 minutes and then placed on the positive pressure processor for the filtration (60 psi for 10 minutes). This procedure was repeated after the addition of 400 µL of the second cold solvent (acetonitrile/water 3:1 v/v

with the 1% of formic acid). The resulting solutions were dried under nitrogen flow and re-diluted in 250 µL of the internal standard solution (0.42 µg/mL CIN-d5). The resulting serum extracts were transferred in labelled brown vials for LC-MS analysis. For testing the serum extraction procedure, a quality control (QC) sample was prepared, by mixing same volumes of all serum samples. The same extraction protocol was performed on these quality control samples randomly placed in the well plate. The QC extracts together with the extraction blanks were injected before the samples LC-MS analysis.

2.4. LC-MS and LC-MS/MS analysis

LC analysis was performed on a Dionex Ultimate 3000 HPLC system equipped with a Kinetex C18 column (150 mm x 2.1 mm I.D., particle size 2.6 µm) and a guard column containing the same stationary phase (Phenomenex, Torrance, CA, USA). Column temperature was set at 40°C. Water (eluent A) and acetonitrile (eluent B), both with 0.1 % formic acid, were used as mobile phases according to the following gradient: 0-1 min isocratic 5% B, 1-7 min linear gradient 5-45% B, 7-8.5 min linear gradient 45-80% B, 8.5-10.5 min isocratic 80% B. The flow rate was 350 µL/min and the injection volume was 5 µL.

The LC system was coupled with a hybrid linear ion trap Fourier Transform (LTQ FT) Orbitrap high-resolution mass spectrometer (Thermo Fisher, Bremen, Germany) by an electrospray ionization (ESI) probe for MS and MS/MS analysis both in positive and negative ionization. The ESI conditions in positive (and negative) mode were: spray voltage 5.0 kV (-3.5 kV), heated capillary temperature 320ºC, capillary voltage 35 V (-35 V) and tube lens 110 V (-110 V). In the LTQ component of the instrument, nitrogen was used as both the sheath gas (35 U) and auxiliary gas (5 U), and helium was used as the damping gas.

Each sample was analysed both under positive and negative ionization using a LC-MS method in order to obtain the full-scan accurate mass spectra (mass range from 100 to 1000 Da) at a mass resolution of 30,000 FWHM (m/z 400) in centroid mode.

Then, based on the data dependent acquisition (DDA) mode, the LC-MS/MS analysis of each sample was performed in order to achieve the mass fragmentation spectra, essential for the identification of the ions of interest. In this method during the chromatographic run, both full scan and MS/MS spectra of the 3 most intense ions of each full scan were acquired. The resolving power for MS2 scans was 7500. Product ions were generated in the LTQ trap at collision energy 35 eV using an isolation width of 2 Da.

All measurements were done using the automatic gain control of the LTQ to adjust the number of ions entering the trap. Mass calibration was performed with every sequence run just prior to starting the batch by using flow injection of the manufacturer's calibration standards mixture allowing for mass accuracies lower than 5 ppm in external calibration mode.

For both urine (or serum) LC-MS and LC-MS/MS analysis, a QC sample consisting of a pool of all urine (or serum) samples, together with a solvent solution (methanol/water 1:1) were injected every 10 samples for the evaluation of the performance of the analytical system in terms of retention times, mass accuracy, signal drift, and carry over phenomena (35). For the injection order, samples were randomized within each injection batch.

2.5. Data processing and mining

All raw data were manually inspected using the Qual browser module of Xcalibur version 2.0.7 (Thermo Fisher Scientific, Les Ulis, France). The LC-MS raw files were converted to mzXML with the MSConvert utility included in ProteoWizard (36). Then, the mzXML files were processed with the software XCMS*plus* (The Scripps Research Institute, La Jolla, CA) that

allow for obtaining data processing (feature detection and retention time alignment) and data analysis through statistics tools (37). Firstly, feature detection step aimed to the identification of all signals caused by true ions and avoid detection of false positives. During this processing, the maximum mass accuracy was set equal to 5 ppm, the minimum signal to noise ratio was fixed equal to three and only peaks with an intensity greater than 10000 cps for at least three consecutive scan were considered as features. Then, retention time alignment is needed for correcting retention time differences among runs and combining data from different samples. After this step, the maximum retention time deviation across samples to consider two peaks in two different samples as the same compound, was set equal to 2 seconds.

After data processing, in order to highlight the polyphenol metabolites of the investigated berries in human biofluids, data analysis was performed. Both for serum and urine samples, the statistic comparisons between groups (see Table S1 for full details on the groups) were performed using one-way analysis of variance (ANOVA) and Fisher test, at the 95% confidence level ($p \leq 0.05$). Briefly, the group labelled with "VM" included samples (serum or urine) of volunteers assuming *V. myrtillus* berries, whereas the group labelled with "VC" contained samples (serum or urine) of subjects assuming *V. corymbosum* fruits. In addition, different groups were identified, depending on the diverse sampling time (e.g. "0min" means baseline sampling, whereas "60min" means sampling performed 60 minutes after assumption), in order to evidence features with statistically different intensities in urine and serum before and after berry assumption.

2.6. Compound identification

The identification of features of interest, evidenced by data analysis previously described, was performed according to the following identification criteria. The detected mass of the pseudo-molecular ion must

differ from the exact mass of proposed formula in a maximum value of 5 ppm (mass accuracy ≤ 5 ppm) and the isotope ratio difference compared to the theoretical isotope profile must be below 20%. Then, the structural elucidation of ions of interest was performed through the evaluation of fragment ions present in MS/MS spectra obtained with DDA mass method.
According to metabolomics guidelines, four levels of identification were distinguished (38). Nevertheless, the absence of commercial standards of glucuronide and sulphate conjugated made impossible the identification with level I (comparison with an authentic standard). For this reason, almost all the features analysed corresponded to putatively annotated compounds (level II) namely without chemical reference standards, based upon physicochemical properties and/or spectral similarity with spectral libraries.

3. Results and Discussion

3.1. Assessment of data quality

The QC injected each ten samples during every LC-MS and LC-MS/MS batches assessed the quality of metabolomics data excluding mass calibration problems and retention times drift. Indeed, the mass accuracy and the retention time variations of surrogate and internal standards were found below 5 ppm and 2 seconds, respectively. Moreover, the variation of integrated area of the surrogate standards (added before the extraction) and internal standard (added before the analysis) in all the QC samples resulted lower than 20% confirming the repeatability of the extraction and excluding the possibility of signal drift and carry over phenomena during the LC-MS and LC-MS/MS analysis.

3.2. Data mining

The data processing resulted in a large number of ions in both serum and urinary samples. More in detail, tens of thousands features were found in serum and urine samples acquired in positive and negative ionization modes. The data analysis allowed to reduce ions of interest (tens of hundreds) comparing the different sampling time groups of each treatment and highlighting features that showed intensity statistically different ($p < 0.05$) between groups characterized by different sampling times (e.g. VM 0min, VM 30min, VM 60min, VM 120min, VM 240min, VM 360min). Nevertheless, the time profile intensities of ions were further processed in order to highlight only features showing an increasing trend in respect to baseline. Finally, the resulting feature list has been reviewed in order to manually excluded false positive data, such as in-source fragmentation and other solvent/metal adducts of the same ion.

3.3. Feature identification

The list of features resulting from the data processing and analysis was reported in **Table 1** which shows retention time (Rt, min), mass to charge ratio (m/z) of parent ion found by the high-resolution full scan experiment, the main mass fragments obtained by LC-MS/MS experiment, the proposed formula and the corresponding exact mass, the mass accuracy (Δ, ppm) and the putative identification of peaks considered. Moreover, for each identified metabolite in serum and urine, **Table 2** reported the sampling times at which a statistically significant maximum intensity was observed, compared to the baseline ones.

Almost all the features reported in **Table 1** were detected in negative ionization mode as the pseudo-molecular ion $[M-H]^-$ and for most of these ions, this finding was in accordance with their putative annotation as phenolic acids.

Table 1. Retention time (Rt, min), experimental mass of the parent ion (Da), main mass fragments (MS/MS), proposed formula, corresponding exact mass (Da), and accuracy (Δ, ppm) of peaks tentatively identified in serum and/or urine samples after acute ingestion of *Vaccinium myrtillus* and *Vaccinium corymbosum* supplements.

Peak	Rt	Parent ion	MS/MS	Proposed Formula	Exact Mass	Δ	Identification
1	2.4	343.0663[a]	175.0243, 167.0346, **113.0243**	$C_{14}H_{16}O_{10}$	343.0671	-2.3	Hydroxy-methoxy benzoic acid glucuronide (I)
2	3.0	194.0455 [a]	**150.0561**	$C_9H_9NO_4$	194.0459	-2.1	Hydroxy-hippuric acid
3	3.3	277.0017 [a]	233.0121, **197.0452**	$C_9H_{10}O_8S$	277.0024	-2.6	Hydroxy-dimethoxy benzoic acid sulphate
4	3.3	373.0768 [a]	**197.0452**, 182.0212, 175.0247, 113.0243	$C_{15}H_{18}O_{11}$	373.0776	-2.1	Hydroxy-dimethoxy benzoic acid glucuronide (I)
5	3.4	188.9860 [a]	**109.0297**,79.9576	$C_6H_6O_5S$	188.9863	-1.6	Catechol sulphate
6	3.5	329.0873 [a]	167.0347, **123.0451**	$C_{14}H_{18}O_9$	329.0870	0.9	Hydroxy-methoxy benzoic acid glucoside
7	3.6	343.0663 [a]	175.0246, **167.0349**, 113.0245	$C_{14}H_{16}O_{10}$	343.0671	-2.3	Hydroxy-methoxy benzoic acid glucuronide (II)
8	3.7	399.0924 [a]	**223.0606**, 175.0241	$C_{17}H_{20}O_{11}$	399.0933	-2.2	Hydroxy-dimethoxy cinnamic acid glucuronide (I)
9	3.8	401.1081 [a]	**225.0768**, 207.0663, 163.0765	$C_{17}H_{22}O_{11}$	401.1089	-2.0	Hydroxy-(dihydroxyphenyl) valeric acid glucuronide (I)
10	3.9	373.0767 [a]	**197.0455**, 175.0249, 113.0246	$C_{15}H_{18}O_{11}$	373.0776	-2.4	Hydroxy-dimethoxy benzoic acid glucuronide (II)
11	3.9	224.0561 [a]	180.0661, 123.0452, **100.0040**	$C_{10}H_{11}NO_5$	224.0564	-1.3	Hydroxy-methoxy hippuric acid
12	4.0	303.0173 [a]	**223.0606**	$C_{11}H_{12}O_8S$	303.0180	-2.3	Hydroxy-dimethoxy cinnamic acid sulphate
13	4.0	401.1081 [a]	**225.0766**	$C_{17}H_{22}O_{11}$	401.1089	-2.0	Hydroxy-(dihydroxyphenyl) valeric acid glucuronide (II)
14	4.0	465.1029 [b]	**303.0501**	$C_{21}H_{21}O_{12}$	465.1028	0.2	Delphinidin-hexoside

Table 1 (continued)

Peak	Rt	Parent ion	MS/MS	Proposed Formula	Exact Mass	Δ	Identification
15	4.2	415.1234 [a]	**239.0923**, 175.0249	$C_{18}H_{24}O_{11}$	415.1246	-2.9	Hydroxy-(hydroxy-methoxyphenyl) valeric acid glucuronide
16	4.2	305.0328 [a]	**225.0764**, 207.0659, 163.0764, 123.0450	$C_{11}H_{14}O_8S$	305.0337	-2.9	Hydroxy-(dihydroxyphenyl) valeric acid sulphate
17	4.2	285.0609 [a]	175.0245, **113.0244**, 109.0245	$C_{12}H_{14}O_8$	285.0616	-2.4	Catechol glucuronide
18	4.2	369.0817 [a]	193.0501, 175.0243, **113.0243**	$C_{16}H_{18}O_{10}$	369.0827	-2.7	Hydroxy-methoxycinnamic acid glucuronide (I)
19	4.3	449.1080 [b]	**287.0544**	$C_{21}H_{21}O_{11}$	449.1078	0.5	Cyanidin-hexoside
20	4.3	287.0224 [a]	**207.0663**, 163.0767	$C_{11}H_{12}O_7S$	287.0231	-2.4	Hydroxy-(hydroxyphenyl) pentenoic acid sulphate (I)
21	4.4	353.0870 [a]	**191.0558**, 179.0350	$C_{16}H_{18}O_9$	353.0878	-2.3	Caffeoylquinic acid
22	4.5	317.0329 [a]	302.0095, **237.0764**, 222.0528	$C_{12}H_{14}O_8S$	317.0337	-2.5	Trimethoxy-cinnamic acid sulphate
23	4.6	399.0925 [a]	**223.0610**, 175.0247	$C_{17}H_{20}O_{11}$	399.0933	-2.0	Hydroxy-dimethoxy cinnamic acid glucuronide (II)
24	4.7	413.1079 [a]	**237.0763**	$C_{18}H_{22}O_{11}$	413.1089	-2.4	Trimethoxy-cinnamic acid glucuronide (I)
25	4.8	383.0977 [a]	**207.0658**, 175.0244, 113.0243	$C_{17}H_{20}O_{10}$	383.0984	-1.8	Hydroxy-(hydroxyphenyl) pentenoic acid glucuronide
26	4.8	369.0819 [a]	193.0502, 175.0246, **113.0244**	$C_{16}H_{18}O_{10}$	369.0827	-2.2	Hydroxy-methoxycinnamic acid glucuronide (II)
27	4.9	413.1080 [a]	**237.0765**, 222.0528, 175.0246, 113.0245	$C_{18}H_{22}O_{11}$	413.1089	-2.2	Trimethoxy-cinnamic acid glucuronide (II)
28	5.0	287.0224 [a]	**207.0659**	$C_{11}H_{12}O_7S$	287.0231	-2.4	Hydroxy-(hydroxyphenyl) pentenoic acid sulphate (II)
29	5.1	357.0819 [a]	**181.0502**	$C_{15}H_{18}O_{10}$	357.0827	-2.2	Dihydroxyphenyl-propionic acid glucuronide
30	5.3	455.1549 [a]	**279.1231**, 217.1229, 175.0244, 151.0762	$C_{21}H_{28}O_{11}$	455.1559	-2.2	Hydroxy-abscisic acid glucuronide

Table 1 (continued)

Peak	Rt	Parent ion	MS/MS	Proposed Formula	Exact Mass	Δ	Identification
31	5.4	367.1027 [a]	193.0500, **191.0557**, 173.0454	$C_{17}H_{20}O_9$	367.1035	-2.2	Feruloylquinic acid
32	5.9	439.1599 [a]	**263.1289**, 219.1387, 175.0245, 153.0919	$C_{21}H_{28}O_{10}$	439.1610	-2.5	Abscisic acid glucuronide
33	6.1	333.0607 [a]	183.0296, **165.0191**, 137.0243	$C_{16}H_{14}O_8$	333.0616	-2.7	Methyl-dihydromyricetin
34	6.4	279.1231 [a]	**217.1230**, 151.0763	$C_{15}H_{20}O_5$	279.1238	-2.5	Hydroxy-abscisic acid
35	6.5	245.0120 [a]	**165.0556**	$C_9H_{10}O_6S$	245.0125	-2.0	Hydroxyphenyl propionic acid sulphate
36	7.2	263.1283 [a]	219.1391, **153.0921**	$C_{15}H_{20}O_4$	263.1289	-2.3	Abscisic acid

[a] Quasi-molecular ion $[M-H]^-$

[b] Molecular ion $[M]^+$

The only two exceptions were represented by the two compounds putatively identified as delphinidin-hexoside (peak **14**) and cyanidin-hexoside (peak **19**). Indeed, these two ions were detected in positive ionization mode as molecular ion $[M]^+$ according to their chemical structure being characterized by a positive charge at pH < 3 (39). It should also be noted that the mass of detected molecular ions was in very good agreement with the exact mass of the proposed formula being the mass accuracies the highest among all the identified features (**Table 1**). The mass fragments found for peaks **14** and **19** corresponded to the cleavage of the sugar and formation of aglycones at m/z 303.0501 and 287.0544 for delphinidin and cyanidin, respectively. The loss of only the glycoside unit during the mass fragmentation, as well as the earlier elution of delphinidin-hexoside in respect to cyanidin-hexoside, were typically reported in literature for these compounds (34, 40, 41).

Interestingly, these compounds were native anthocyanins of both *V. myrtillus* and *V. corymbosum* berries but they were found with a statistically significant increasing trend only in urine of volunteers assuming *V. myrtillus* supplement (**Table 2**). This result was probably due to the much higher concentrations of delphinidin and cyanidin anthocyanins in bilberry compared to blueberry (41). It is important to underline that these two compounds were the only native anthocyanins found in the investigated biofluids in spite of more than sixty anthocyanidin glycosides found in *V. myrtillus* and *V. corymbosum* fruits (34). Moreover, a list of predicted anthocyanin metabolites (i.e. glucuronides, sulphate and methylated conjugates) were investigated both in serum and urine, but none of these compounds were found in our samples. On the contrary, many literature studies reported anthocyanin predicted metabolites, even if at very low concentrations, i.e. at maximum 1-2% of the ingested dose (19-22, 24, 42). Nevertheless, the difference between our results and these studies can be due to some variables of the study design, such as the form of anthocyanin

ingested dose (fruits, juice, supplement or enriched-extract) with or without a meal, the sampling time (twenty-four hours urine in respect to spot samples) and the duration of administration (long-term intake in respect to an acute dose). In addition, the use of targeted approach, even though unable to discover unknown metabolites, is characterized by higher sensitivity compared to the untargeted one, thus allowing for the detection of low concentrations of predicted anthocyanin conjugates.

Among the features listed in **Table 1**, a group of compounds were putatively identified as benzoic acids conjugates (peaks **1**, **3**, **4**, **6**, **7**, **10**). More in detail, peaks **1** and **7** were characterized by the quasi-molecular ion $[M-H]^-$ at m/z 343.0663 and showed the neutral loss of 176.0321 giving rise to the fragment at m/z 167.0349 (**Fig. 1A**). In addition, the glucuronate "fingerprint" ions found at m/z 175.0246 and 113.0245 (formed by the elimination of H_2O and CO_2 from the ion at m/z 175.0246) suggested that the pseudo-molecular ion was a glucuronide conjugated compound (43). It should also be noted that for peaks **1** and **7** the ion-source loss of glucuronate ensured the MS/MS spectrum of the non-conjugated ion at m/z 167.0349 (**Fig. 1B**) that showed fragments at m/z 152.0114 (loss of methyl radical), 123.0452 (loss of CO_2) and 108.0216 (consequent losses of CO_2 and methyl radical), in agreement with the fragmentation pattern of hydroxy-methoxy benzoic acid (**Scheme 1**) (44, 45). Furthermore, these ions exactly corresponded to the mass fragments obtained for the vanillic acid commercial standard. For these reasons peak **1** and **7** were putatively identified as hydroxy-methoxy benzoic acid glucuronides. This result was in agreement with the two isomers of vanillic acid glucuronide reported by Pimpão and co-workers in human urine of healthy volunteers after the assumption of a mixture of five small berries (46).

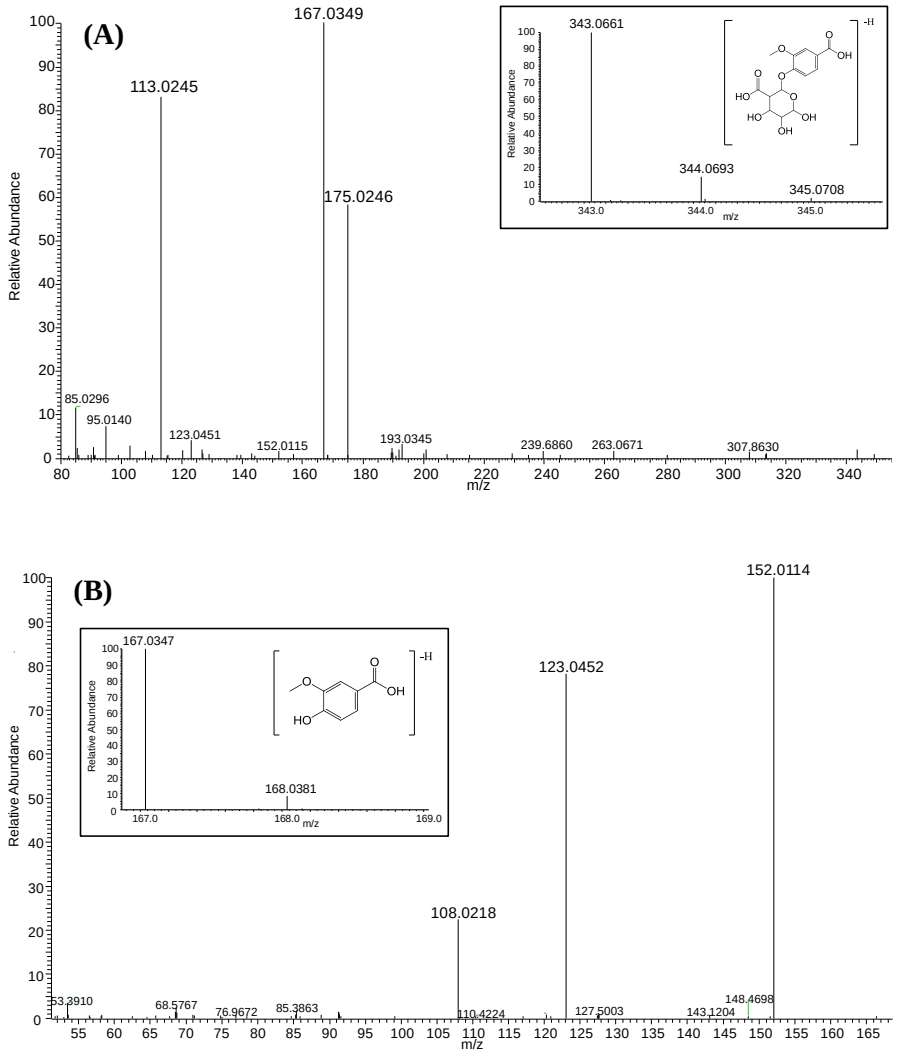

Figure 1. Isotopic profile and MS/MS spectrum of peak **7** (A) and its in-source fragment at m/z 167.0347 (B) identified as hydroxy-methoxy benzoic acid glucuronide and hydroxy-methoxy benzoic acid, respectively.

Analogously, peak **6** was ascribed to hydroxy-methoxy benzoic acid hexoside, being characterized by the neutral loss of 162.0526 and the same mass fragments (m/z 167.0347 and 123.0451) found for the previously described hydroxy-methoxy benzoic acid glucuronides (**Table 1**). Moreover, the retention times of peaks **6** and **7** suggested the earliest as the

hydroxy-methoxy benzoic acid glucoside typically eluted close to the corresponding glucuronide during a reversed-phase chromatographic analysis (34). To the best of our knowledge, hydroxy-methoxy benzoic acid glucoside was found in human urine after bilberry assumption in this study for the first time.

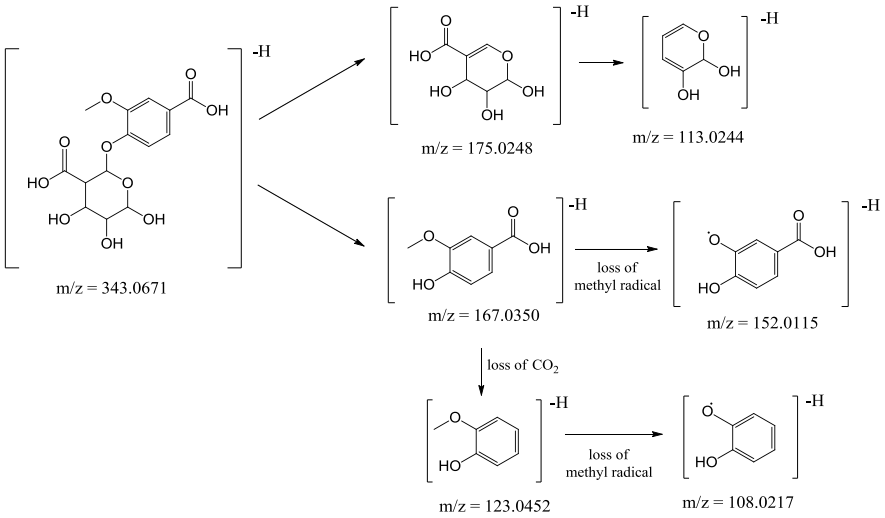

Scheme 1. Hypothesized structure and fragmentation scheme for peaks **1** and **7** ($[M-H]^-$ = 343.0663, attributed to two isomers of hydroxy-methoxy benzoic acid glucuronide).

Peak **3** exhibited the characteristic loss of 79.9565 Da observed for a sulphate conjugated compound (47), leading to the formation of the ion at m/z 197.0452 as the most intense fragment in MS/MS spectrum (**Table 1**). In addition, the ion at 233.0121 deriving from the loss of CO_2 from the pseudo-molecular ion confirmed the presence of carboxylic unit, thus suggesting for peak **3** the attribution to a sulphate conjugate of a carboxylic acid. A more accurate level of identification for peak **3** derived from the comparison with peaks **4** and **10** that resulted glucuronides of the ion at m/z 197.0455. Indeed, the fragmentation spectrum of peak **4** exhibited, in addition to the typical fragments of a glucuronide conjugate, an ion at m/z

182.0212 corresponding to the loss of methyl radical from the ion at m/z 197.0455. Since the mass transition 197 →182 was used in literature for the monitoring of syringic acid (29) we putatively identified peak **3** and peaks **4** and **10** as hydroxy-dimethoxy benzoic acid sulphate and hydroxy-dimethoxy benzoic acid glucuronides, respectively. These findings were in agreement with the presence of syringic acid, which was elsewhere reported in urine of volunteers, 2 hours after the assumption of wild blueberry (31).

Peaks **2** was putatively identified as hydroxy hippuric acid on the basis of the exact mass of the pseudo-molecular ion (m/z at 194.0455), as well as the loss of CO_2 and formation of the ion at m/z 150.0561, already suggested in literature for the identification of 2-hydroxyhippuric and 3-hydroxyhippuric acids as urinary metabolites of quercetin-rutinoside (48). Indeed, hydroxy hippuric acids were found in urine as metabolite of the ingestion of different foods, such as tomato juice, coffee (48, 49), as well as wild blueberry (31).

Based on similar consideration, peak **11** was ascribed to hydroxy-methoxy-hippuric acid because of the loss of CO_2 unit (ion at m/z 180.0661), as well as the presence of the fragments at m/z 123.0452 (corresponding to the methoxy-phenol unit) and at m/z 100.0040, this latter commonly reported for hydroxyhippuric acid identification (49).

Peaks **5** was putatively identified as catechol sulphate owing to the presence in the MS/MS spectrum of the typical accurate masses of a sulphate ion (m/z at 79.9576) and catechol (m/z at 109.0297). Similarly, peak **17** was ascribed to catechol glucuronide because of the aforementioned characteristic mass fragments of a glucuronide conjugated compound (i.e. m/z 175.0245 and 113.0244) and the presence of the exact mass of catechol in its MS/MS spectrum. According to our findings, catechol derivatives were reported in literature after berry and tea assumption (31, 46, 49).

Another group of putatively identified metabolites was represented by cinnamic acid derivatives (peaks **8**, **12**, **18**, **21**, **23** and **26**, see **Table 1**). In detail, peaks **8** and **23** were attributed to glucuronide conjugates of the ion at

m/z 223.0608 (**Fig. 2A**) that correspond to the exact mass of the pseudo-molecular ion $[M-H]^-$ of three different compounds: hydroxy-dimethoxy cinnamic acid, hydroxy-(dihydroxyphenyl) pentenoic acid and trihydroxy-phenyl valerolactone.

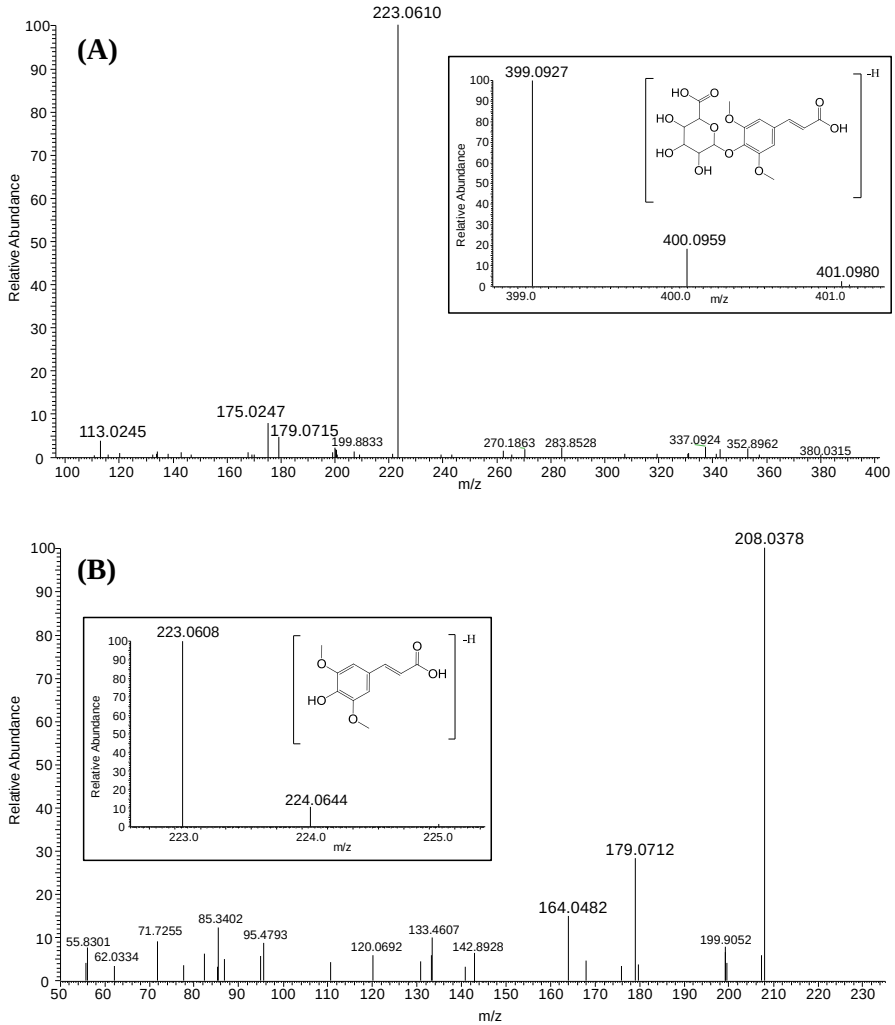

Figure 2. Isotopic profile and MS/MS spectrum of peak **23** (A) and its in-source fragment of m/z 223.0310 (B) identified as hydroxy-dimethoxy cinnamic acid glucuronide and hydroxy-dimethoxy cinnamic acid, respectively.

Each of these compound could be a metabolite of bilberry assumption because both cinnamic and valeric acid derivatives has been reported as

products of polyphenol metabolism (28, 50). Nevertheless, the in-source loss of glucuronate unit allowed for obtaining the fragmentation spectrum of non-conjugated compound at m/z 223.0610 that showed the ion deriving from the loss of methyl radical (m/z 208.0378) as the most abundant (**Fig. 2B**). In addition, the other ions at m/z 179.0716 and 164.0479 corresponded exactly to the fragments reported in literature for sinapic acid determination in vegetal matrices (51, 52). Moreover, hydroxy-dimethoxy cinnamic acid is the only compound providing the loss of a methyl radical unit among the proposed candidates (**Scheme 2**). For this reason, peaks **8** and **23** were ascribed to hydroxy-dimethoxy cinnamic acid glucuronides. Consequently, peak **12**, was putatively attributed to hydroxy-dimethoxy cinnamic acid sulphate being characterized by the fragment at m/z 223.0606 due to the loss of 79.9567 Da.

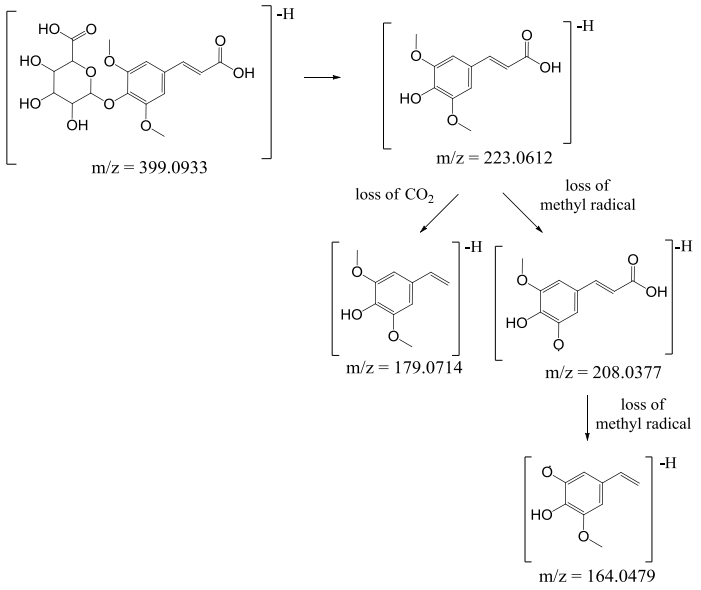

Scheme 2. Hypothesized structure and fragmentation scheme for peaks **8** and **23** ($[M-H]^-$ = 399.0925, attributed to two isomers of hydroxy-dimethoxy cinnamic acid glucuronide).

Peaks **18** and **26** were putatively attributed to two isomers of hydroxy-methoxy cinnamic acid glucuronide due to the typical fragments of a glucuronide conjugate (m/z 175.00243 and 113.0243), together with the exact mass of the ion at m/z 193.0501. Moreover, the further fragmentation of this last ion produced the individual losses of methyl radical (m/z 178.0272) and CO_2 (m/z 149.0610) as well as the consequent loss of methyl radical and CO_2 (m/z 134.0375), thus matching exactly the fragments of ferulic acid standard. Based on these findings peak **18** and **26** were ascribed to hydroxy-methoxy cinnamic acid glucuronides. These results were supported by literature findings that reported sinapic and ferulic acids in serum and urine after small berries assumption (31, 32, 46).

Among the other cinnamic acid derivatives, peak **21** was putatively identified as caffeoylquinic acid being its fragmentation spectrum characterized by the signal at m/z at 191.0558 and 179.0350 corresponding to the quasi-molecular ion of quinic and caffeic acid, respectively. Based on similar considerations, peak **31** was ascribed to feruloylquinic acid because of the characteristic fragment of quinic and ferulic acids (49).

Peaks **29** and **35** were putatively identified as phenylpropionic acid derivatives. Indeed, based on their exact mass, isotopic profile and mass fragments, peak **29** was ascribed to dihydroxy-phenyl propionic acid glucuronide, whereas peak **35** was putatively identified as hydroxy-phenyl propionic acid sulphate. The presence of phenylpropionic acids in serum and urine deriving from anthocyanin metabolism after berry assumption was in agreement with recent literature studies (30, 31).

Peaks **9** and **13** showed a pseudo-molecular ion $[M-H]^-$ at m/z 401.1081 corresponding to a mass 2 Da higher than peaks **8** and **23**. Similarly, peak **16** exhibited a quasi-molecular ion at m/z 305.0328 equal to a mass 2 Da greater than peak **12**. These findings could suggest the presence of glucuronide and sulphate conjugated of the hydroxy-dimethoxy hydrocinnamic acid according to the formation of the dihydro form of the

phenylpropionic acid during the polyphenol catabolism (28). Nevertheless, the mass fragmentation spectra of peaks **9**, **13** and **16** evidenced a different scenario because of the absence of the methyl radical losses (i.e. ions at m/z 210.0534 and 166.0635) observed for their corresponding cinnamic acid derivatives. Moreover, the mass fragmentation spectra of peak **16** (**Fig. 3**) highlighted a number of ions related to the consequent losses of sulphate (m/z at 225.0764), water (m/z 207.0659) and CO_2 (163.0764), as well as other ions (**Scheme 3**), corresponding exactly to fragments reported in literature for hydroxy-(dihydroxyphenyl) valeric acid conjugated (49). For this reason, the presence of two glucuronides (peak **9** and **13**) and one sulphate (peak **16**) of hydroxy-(dihydroxyphenyl) valeric acid in the investigated biological fluids was hypothesised. It is interesting to note that phenyl-valeric acid derivatives were reported in literature as metabolite of flavanols and proanthocyanidins (50, 53) thus evidencing that also metabolites deriving from polyphenols different from anthocyanins, can result as significant biomarker of bilberry assumption.

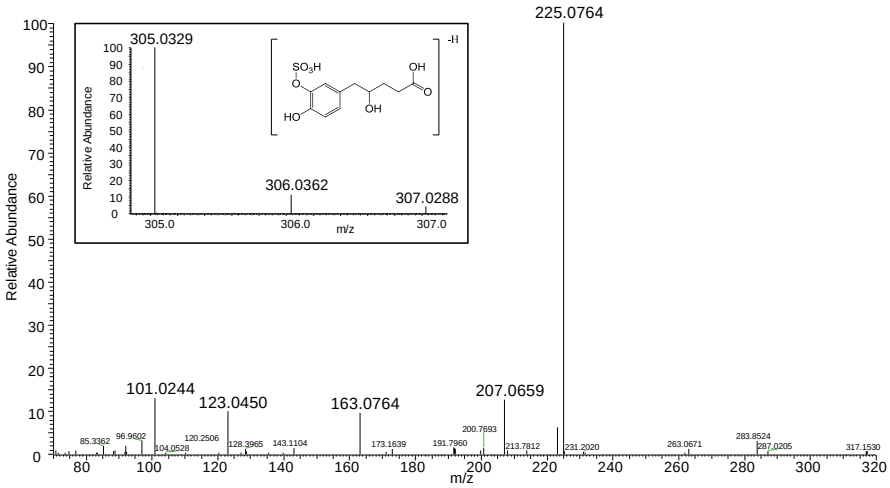

Figure 3. Isotopic profile and MS/MS spectrum of peak **16** attributed to hydroxy-(dihydroxyphenyl)-valeric acid sulphate.

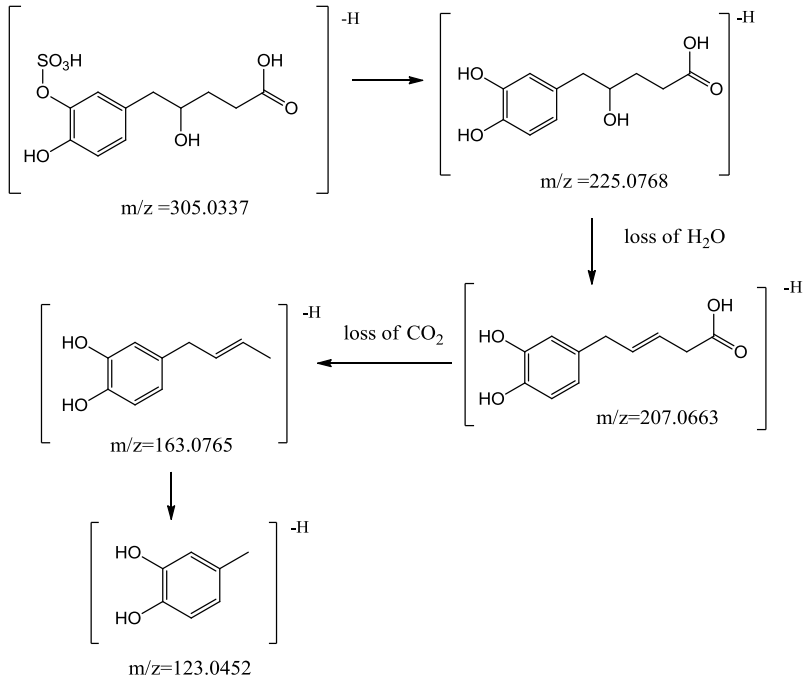

Scheme 3. Hypothesized structure and fragmentation scheme for peak **16** ($[M-H]^-$ = 305.0328) attributed to hydroxy-(dihydroxyphenyl)-valeric acid sulphate.

Peaks **20** and **28** showed the characteristic loss of a sulphate unit with the consequent formation of the ion at m/z 207.0663 (**Table 1**), which could be attributed to dihydroxyphenyl valerolactone, already reported in literature after the assumption of food rich in flavanols (49, 53). Nevertheless, in-source fragmentation of peaks **20** and **28** gave rise to the MS/MS spectrum of the non-conjugated compound at m/z 207.0663 (**Fig. 4A**) that showed different ions in respect to those obtained after the fragmentation of 3,4-dihydroxyphenyl valerolactone reference standard (**Fig. 4B**). The fragmentation pattern of the ion at m/z 207.0663 highlighted the loss of CO_2 (m/z 163.0767) and water (m/z 145.0660), thus matching well a hydroxy-(hydroxyphenyl) pentenoic acid (**Scheme 4**). Based on these consideration, peaks **20** and **28** were attributed to hydroxy-(hydroxyphenyl) pentenoic acid sulphates and peak **25** was ascribed to hydroxy-(hydroxyphenyl) pentenoic

acid glucuronide. To the best of our knowledge, these polyphenol metabolites were reported as markers of bilberry assumption in this research for the first time.

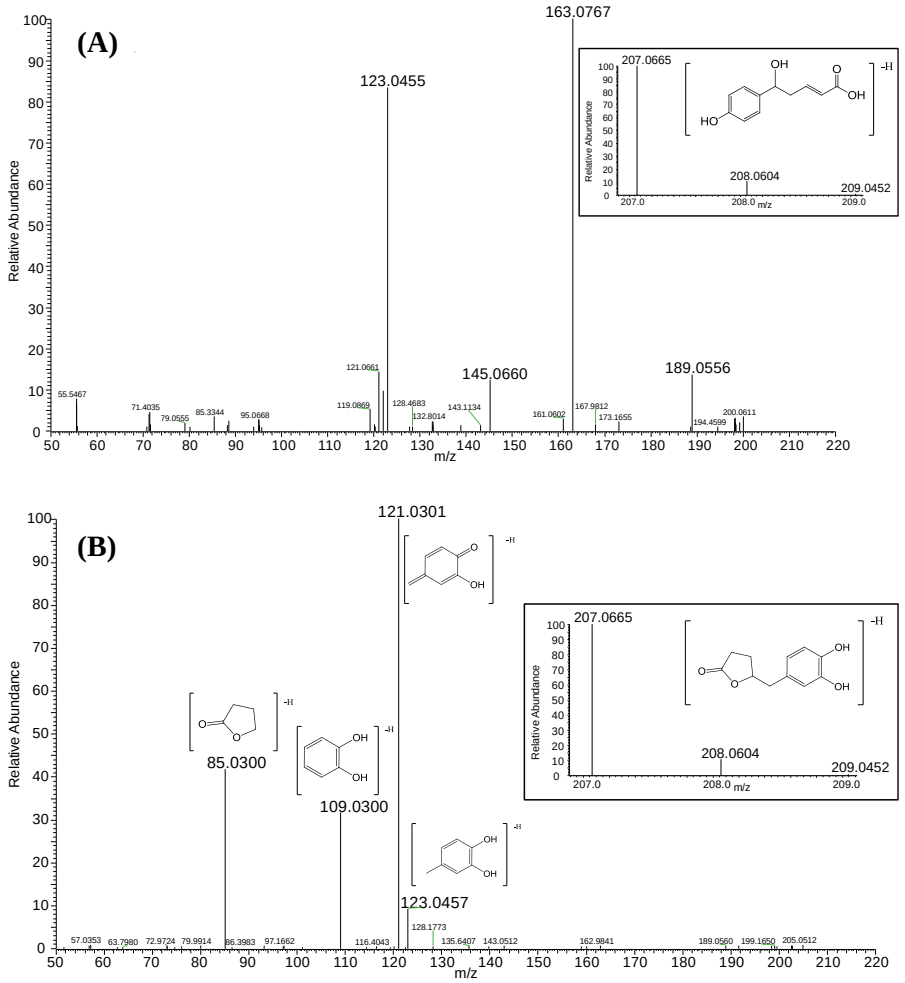

Figure 4. Isotopic profile and MS/MS spectrum of in-source fragment (m/z 207.0663) of peak **20** attributed to hydroxy-(hydroxyphenyl)-pentenoic acid sulphate (A); isotopic profile and fragmentation spectrum of 3,4-dihydroxyphenyl-valerolactone commercial standard (B).

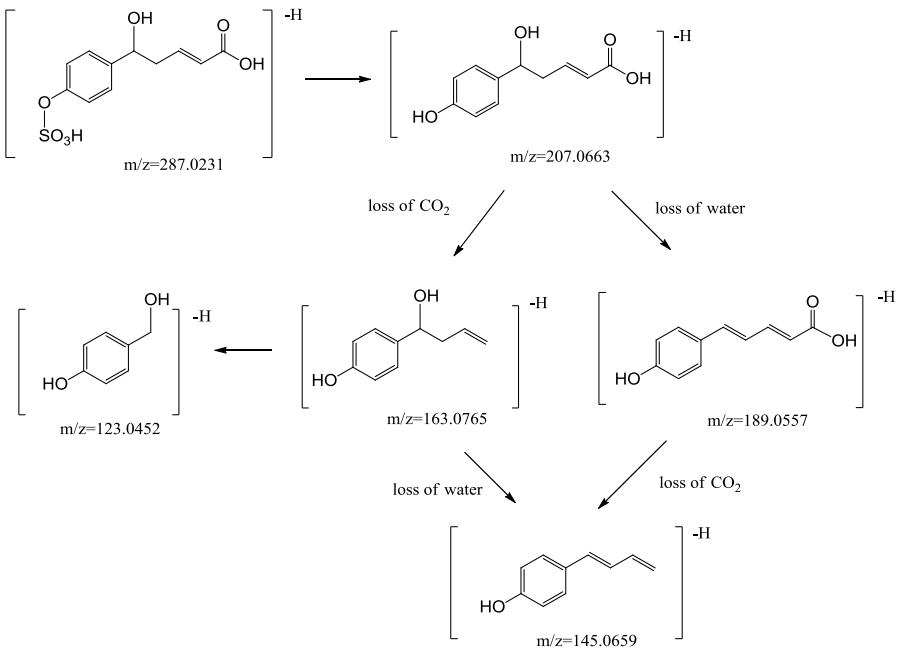

Scheme 4. Hypothesized structure and fragmentation scheme for peaks **20** and **28** ($[M-H]^-$ =287.0224) attributed to two isomers of hydroxy-(hydroxyphenyl)-pentenoic acid sulphate.

Peaks **15**, **22**, **24** and **27** could be ascribed both to cinnamic and phenyl-valeric acid derivatives, on the basis of their exact mass. More in detail, peak **15** could be identified either as trimethoxy hydroxycinnamic acid glucuronide or hydroxy-(hydroxy-methoxyphenyl) valeric acid glucuronide. Nevertheless, the absence of methyl radical loss in the MS/MS spectrum (**Fig. 5A**) suggested unlikely the identification as trimethoxy hydrocinnamic acid glucuronide because for this compound three methyl radical can be lost. In addition, the corresponding unsaturated compounds, i.e. peaks **24** and **27**, that could be attributed to trimethoxy cinnamic acid glucuronide or hydroxy-(hydroxy-methoxyphenyl)-pentenoic acid glucuronide, showed a different fragmentation pattern (**Fig. 5B**). Indeed, the presence of the ion at m/z 222.0528 in the MS/MS spectrum clearly evidenced the loss of a methyl radical. In addition, the further fragmentation of the non-conjugated

compound at m/z 237.0765 produced the only fragment at m/z 222.0533 (**Fig. 5C**) confirming the loss of a methyl radical as the most abundant fragment and trimethoxy cinnamic acid as the most likely identification of the precursor. Moreover, peak **22**, corresponding to the sulphate conjugated of the ion at m/z 237.0765, was also characterized by the fragment at m/z 302.0095, which is consistent with the loss of a methyl radical from the pseudo-molecular ion $[M-H]^-$ at m/z 317.0329 (**Fig 5D**). For these reasons, peak **15** was ascribed to hydroxy-(hydroxy-methoxyphenyl)-valeric acid glucuronide, peaks **24** and **27** were attributed to trimethoxy cinnamic acid glucuronides and peak **22** was putatively identified as trimethoxy cinnamic acid sulphate. To the best of our knowledge, none of these compounds were reported in literature as biomarkers of *Vaccinium* berry species assumption.

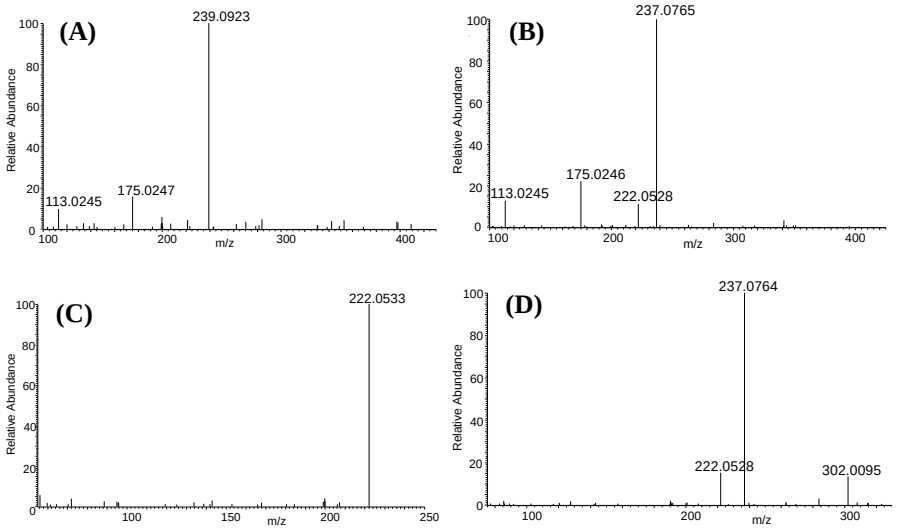

Figure 5. Fragmentation spectrum of peaks **15** (A), peak **27** (B), in-source fragment (m/z 237.0765) of peak **27** (C) and peak **22**.

Among features listed in **Table 1**, a group of compounds (peak **30**, **32**, **34** and **36**) were attributed to abscisic acid derivatives. More in detail, the exact mass of the pseudo-molecular ion $[M-H]^-$ (m/z 263.1283), the isotopic

profile and fragments (m/z 219.1391 and 153.00921) obtained for peak **36** exactly matched with those of abscisic acid standard. In addition, peak **32** showed the typical neutral loss of glucuronide conjugated compounds (m/z 176.031) together with the same fragmentation pattern of peak **36**. For these reasons, peaks **32** and **36** were identified as abscisic acid glucuronide and abscisic acid, respectively. Similarly, peak **30** and **34** were ascribed to hydroxyabscisic acid and hydroxyabscisic acid glucuronide, based on the ions found in their MS/MS spectra at m/z 217.1230 and 151.0763 already reported in literature for hydroxyabscisic acid fragmentation (54). It is interesting to note that abscisic acid is a plant hormone involved in the regulation of polyphenol biosynthesis (55) and abscisic acid glucuronide was recently reported for the first time as a marker of low-flavonoid diet (45).

Finally, peak **33** was putatively identified as methyl-dihydromyricetin on the basis of the exact mass and the isotopic profile of the quasi-molecular ion $[M-H]^-$ at m/z 333.0607, as well as the fragments deriving from the C ring fission at m/z 183.0299 and 165.0193. This is the only compound clearly deriving from flavonol metabolism even if literature researches often reported also glucuronide and sulphate conjugated as markers of flavonol rich-foods metabolism (56).

3.4. Kinetics trend of identified metabolites

The kinetic trend of putatively identified features, particularly the sampling time with the maximum intensity statistically different from the baseline one (**Table 2**), can highlight important information about the absorption and excretion of metabolites of interest.

Table 2. Sampling times exhibiting the maximum intensity of each metabolite detected in serum and/or urine after the assumption of *V. myrtillus* or *V. corymbosum* supplements. The maximum intensities are statistically different from the baseline ones according to one-way ANOVA and Fisher test ($p \leq 0.05$).

Metabolite	*V. myrtillus*		*V. corymbosum*	
	Serum	**Urine**	**Serum**	**Urine**
Delphinidin-hexoside	-	120 min	-	-
Cyanidin-hexoside	-	120 min	-	-
Hydroxy-methoxy benzoic acid glucuronide (I)	-	360 min	-	360 min
Hydroxy-methoxy benzoic acid glucuronide (II)	-	240 min	-	240 min
Hydroxy-methoxy benzoic acid glucoside	-	240 min	-	240 min
Hydroxy-dimethoxy benzoic acid sulphate	-	-	-	120 min
Hydroxy-dimethoxy benzoic acid glucuronide (I)	-	-	-	120 min
Hydroxy-dimethoxy benzoic acid glucuronide (II)	-	-	-	120 min
Hydroxy hippuric acid	120 min	240 min	-	-
Hydroxy-methoxy hippuric acid	-	240 min	-	240 min
Catechol sulphate	360 min	360 min	-	-
Cathecol glucuronide	360 min	360 min	-	-
Hydroxy-dimethoxy cinnamic acid glucuronide (I)	-	360 min	-	-
Hydroxy-dimethoxy cinnamic acid sulphate	-	360 min	-	-
Hydroxy-dimethoxy cinnamic acid glucuronide (II)	-	360 min	-	-
Hydroxy-methoxycinnamic acid glucuronide (I)	120 min	-	60 min	120 min
Hydroxy-methoxycinnamic acid glucuronide (II)	120 min	-	60 min	-
Caffeoylquinic acid	-	60 min	-	60 min
Feruloylquinic acid	-	60 min	-	60 min

Table 2 (continued)

Dihydroxyphenyl-propionic acid glucuronide	-	360 min	-	-
Hydroxyphenyl-propionic sulphate	120 min	-	-	-
Trimethoxy cinnamic acid sulphate	-	360 min	-	-
Trimethoxy cinnamic acid glucuronide (I)	-	360 min	-	-
Trimethoxy cinnamic acid glucuronide (II)	-	360 min	-	-
Hydroxy-(dihydroxyphenyl) valeric acid glucuronide (I)	-	360 min	-	-
Hydroxy-(dihydroxyphenyl) valeric acid sulphate	360 min	360 min	-	-
Hydroxy-(dihydroxyphenyl) valeric acid glucuronide (II)	-	360 min	-	-
Hydroxy-(hydroxyphenyl) pentenoic acid sulphate (I)	360 min	360 min		
Hydroxy-(hydroxyphenyl) pentenoic acid glucuronide	360 min	360 min	-	-
Hydroxy-(hydroxyphenyl) pentenoic acid sulphate (II)	360 min	360 min	-	-
Hydroxy-(hydroxy-methoxyphenyl) valeric acid glucuronide	-	360 min	-	-
Hydroxy-abscisic acid glucuronide	120 min	240 min	120 min	240 min
Abscisic acid glucuronide	120 min	120 min	60 min	120 min
Hydroxy-abscisic acid	-	120 min	-	120 min
Abscisic acid	-	120 min	30 min	30 min
Methyl-dihydromyricetin	-	120 min	-	120 min

For each class of investigated metabolites, the boxplot of the intensity distribution of the most representative compounds in each sampling times was reported in **Figures 6-10**. Each boxplot represents the interquartile range (75% of the intensity values are less than or equal to the top value of the box and 25% of the intensity values are less than or equal to the bottom value of the box), the upper and lower whiskers refer to the maximum and minimum data point, respectively, and the line within the box represents the median of the data.

The boxplot of intensity distribution of the two identified anthocyanins evidenced an intensity statistically higher in respect to baseline one in urines collected 120 minutes after *V. myrtillus* assumption (**Figure 6**). These results were in agreement with literature studies proposing a very rapid absorption of anthocyanins by gastric mucosa with the consequent plasma appearance within 15 minutes (23, 57) and urinary maximum excretion 2-3 hours after berry assumption (22, 24).

Among the compounds putatively identified as benzoic acid conjugated, the different trend observed for hydroxy-methoxy and hydroxy-dimethoxy benzoic acid derivatives suggested them belonging to different metabolic pathways (**Table 2**).

Benzoic acids were proposed as products of B-ring fragmentation of anthocyanidins and, in particular, protocatechuic and syringic acids seem to derive from cyanidin and malvidin, respectively (27, 28, 58). Moreover, the protocatechuic acid can be methylated to vanillic acid as confirmed by results reported by de Ferrars and co-workers evidencing the glucuronides and sulphates of protocathecuic and vanillic acids as the most important metabolites of cyanidin-3-glucoside (59).

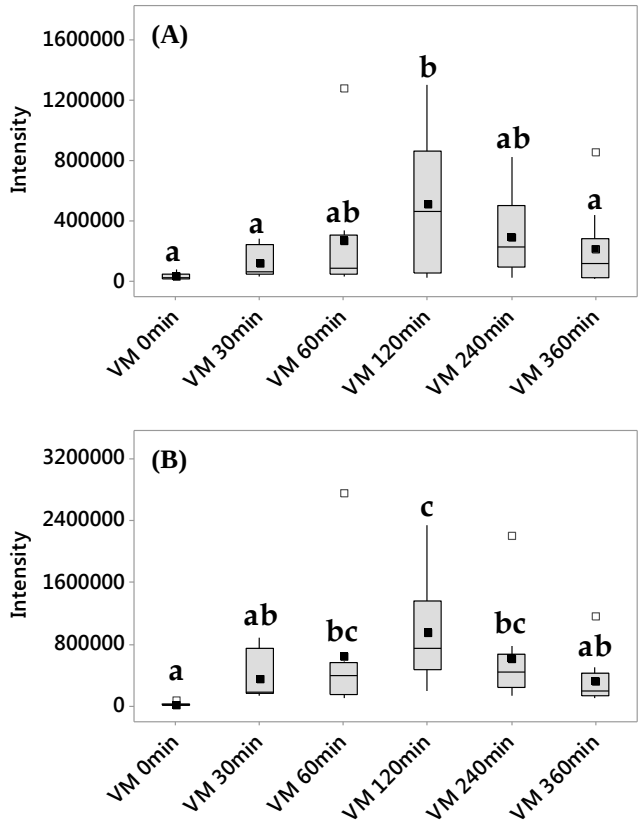

Figure 6. Box plot of intensities of metabolites putatively identified as delphinidin-hexoside (A) and cyanidin-hexoside (B) in urine of volunteers at baseline and after the assumption of *V. myrtillus* supplement. Means that do not share a letter are significantly different according to the Fisher test ($P < 0.05$).

However, in our study, the statistically significant variations of hydroxy-methoxy benzoic acid glucoside and glucuronides as a function of sampling time, with a maximum intensity at 240-360 minutes (**Fig. 7A and 7B**), were found in urine of volunteers who assumed both *V. myrtillus* and *V. corymbosum* supplements, although cyanidin glycosides were present at much higher concentration in bilberry, compared to blueberry (41).

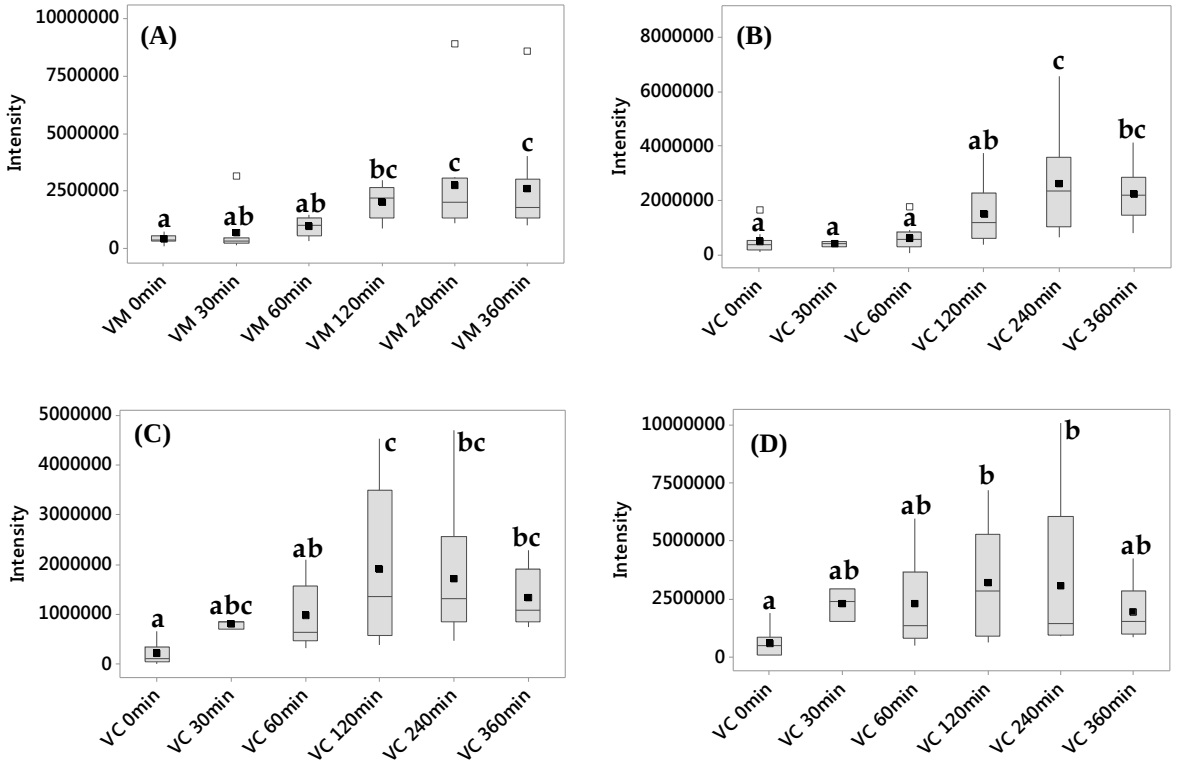

Figure 7. Box plot of intensities of metabolites putatively identified as: hydroxy-methoxy benzoic acid-glucoside in urine of volunteers at baseline and after the assumption of *V. myrtillus* (A) and *V. corymbosum* (B) supplement, hydroxy-dimethoxy benzoic acid glucuronide (C) and hydroxy-dimethoxy benzoic acid sulphate (D) in urine of volunteers at baseline and after the assumption of *V. corymbosum*. Means that do not share a letter are significantly different according to the Fisher test ($P < 0.05$).

This evidence can be due to the high content of phenolic acids (such as coumaroylquinic, caffeoylquinic and feruloylquinic acids) in *V. corymbosum* fruits (34) that can be hydrolysed to simpler unit (such as caffeic and ferulic acids) during the metabolism. Indeed, Nurmi and colleagues suggested vanillic acid formation from both anthocyanins and ferulic acid metabolisms (30). On the contrary, for putatively identified hydroxy-dimethoxy benzoic acid glucuronides and sulphate, the maximum intensities at 120 minutes were evidenced only in urines of volunteers after *V. corymbosum* assumption (**Fig 7C** and **7D**) and can be related to the much higher concentration of malvidin glycosides in blueberry in respect to bilberry (41).

The kinetic trend observed for hydroxy hippuric acid and its methylated derivative was in agreement with their origin from the metabolic pathway consisting in the cyanidin B-ring fragmentation and the further conjugation with a glycine unit (60).

The increasing trend observed for catechol glucuronide and sulphate in serum and urine was the same found by Pimpão and colleagues in human urine after the assumption of a mixture of small berries (46). The increase of catechol derivatives after 6 hours from the assumption, together with their chemical structure, suggested them as gut microflora metabolites.

For the putatively identified cinnamic acid derivatives, a bell shape with a maximum intensity at 60-120 minutes or an increasing trend at 360 minutes were differently observed for cinnamic acids with a different number of methylated groups (**Table 2**).

First of all, caffeoylquinic and feruloylquinic acids were found with a maximum intensity in urines collected after 60 minutes from the assumption of both bilberry and blueberry (**Fig 8A** and **Fig 8B**). The very rapid excretion in urine was in agreement with the maximum human plasma concentration of these compounds found at 0.7-0.8 hour after coffee intake (61). Similarly, the maximum intensity found for hydroxy-methoxy

cinnamic acid glucuronides in serum of volunteers treated with both *V. myrtillus* and *V. corymbosum* perfectly matched the data reported by Rodriguez-Mateos and co-workers that found a maximum plasma concentration of ferulic and isoferulic acids after 1 h from wild blueberry assumption (32). It is interesting to underline that volunteers who assumed blueberry showed twofold serum intensities of hydroxy-methoxy cinnamic acid glucuronides in respect to volunteers assuming bilberry. This finding might be correlated to the high concentration of caffeoylquinic and feruloylquinic acids found in blueberry that can be further hydrolysed to ferulic acid during metabolism (61).

The increasing trend of dihydroxy-phenylpropionic acid glucuronide in urine matched well with literature results reporting a very similar trend in human urine after small berry assumption (30, 46). Similarly, the serum maximum intensity found for hydroxyphenyl propionic acid sulphate at 120 minutes after bilberry intake (**Table 2**) was in agreement with a literature research reporting a slight increase of this metabolite two hours after the assumption of a mixture of *V. myrtillus* and *V. vitis-idea* (30). It is interesting to note that these phenyl propionic acids were proposed to derive from anthocyanins cleavage of C-ring, as well as the flavonol, flavanol and phenolic acids metabolism (28, 30).

The derivatives of hydroxy dimethoxy cinnamic acids and trimethoxy cinnamic acids showed an increasing trend with a maximum intensity in urines collected 360 minutes after the assumption of *V. myrtillus* (**Fig 8C** and **8D**), suggesting for these metabolites a colonic origin.

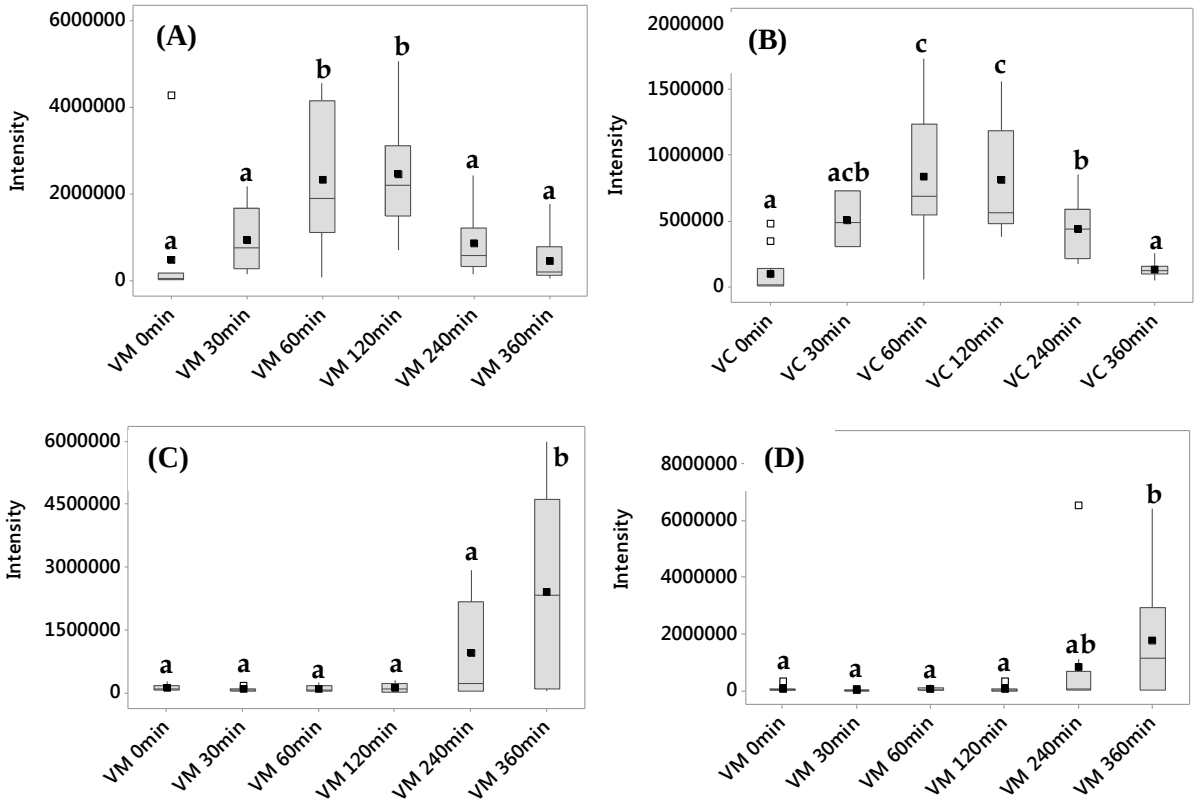

Figure 8. Box plot of intensities of metabolites putatively identified as: feruloylquinic acid in urine of volunteers at baseline and after the assumption of *V. myrtillus* (A) and *V. corymbosum* (B) supplement, hydroxy-dimethoxy cinnamic acid glucuronide (C) and trimethoxy cinnamic acid sulphate (D) in urine of volunteers at baseline and after the assumption of *V. myrtillus*. Means that do not share a letter are significantly different according to the Fisher test ($P < 0.05$).

Interestingly, this trend is the same found for hydroxy-(dihydroxyphenyl) valeric acid (**Fig 9A**) and hydroxy-(dihydroxyphenyl) pentenoic acid glucuronide and sulphate (**Fig 9B**) both in serum and urine after bilberry intake.

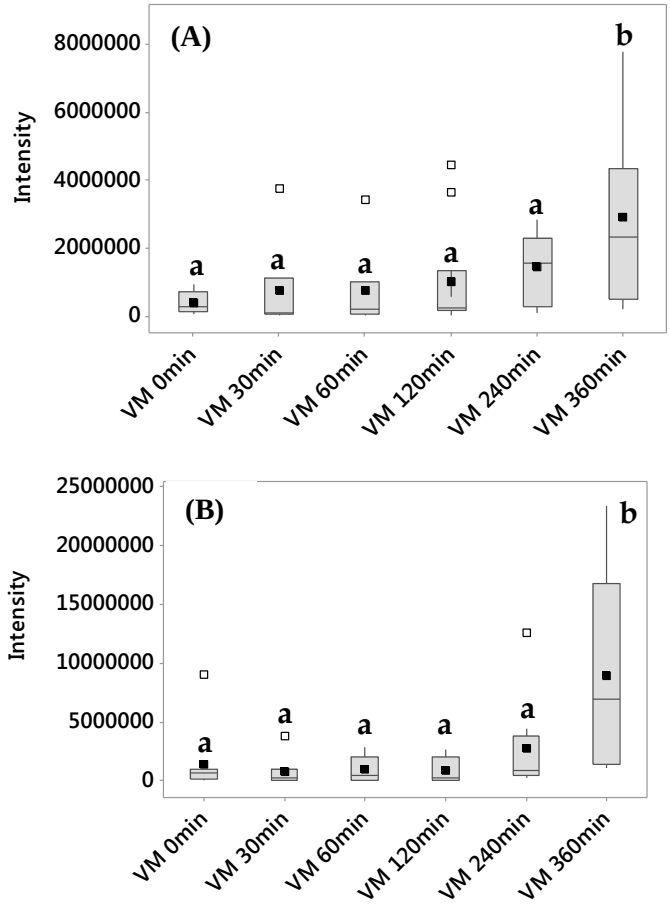

Figure 9. Box plot of intensities of metabolites putatively identified as: dihydroxyphenyl hydroxyvaleric acid glucuronide (A) and hydroxy-(hydroxyphenyl) pentenoic acid sulphate (B) in urine of volunteers at baseline and after the assumption of *V. myrtillus* (A) Means that do not share a letter are significantly different according to the Fisher test ($P < 0.05$).

All these polyphenols, with the only exception of sinapic acid derivatives, were never reported as markers of *V. myrtillus* assumption and found in

studies investigating the administration of single anthocyanins (27, 59) thus suggesting other polyphenol classes as native compounds. Indeed, dihydroxyphenyl valeric acid derivatives were reported as metabolites of flavanols and proanthocyanidins with an increasing trend many hours after incubation or oral assumption during *in vitro* or *ex vivo* studies, respectively (50, 53, 62, 63). For these reasons, hydroxy-(dihydroxyphenyl) valeric acids conjugated and the similar hydroxy-(dihydroxyphenyl) pentenoic acid derivatives were hypothesized biomarkers of *V. myrtillus* berry assumption deriving from flavanol and proanthocyanidin metabolism.

Moreover, trimethoxy cinnamic acid derivatives maybe originated from flavanol, flavonol and anthocyanins metabolism and then underwent to enterohepatic recycling with consequent methylation.

As regards abscisic acid, a very fast absorption seems to occur in volunteers that assumed *V. corymbosum* berry supplement that produced the metabolite appearance both in serum and urine after only 30 minutes from the consumption (**Table 2**). Interestingly, also abscisic acid glucuronide showed a serum maximum intensity early in volunteers treated with *V. corymbosum* in respect to those that assumed *V. myrtillus* maybe suggesting a different absorption rate as a function of other supplement constituents. Also hydroxy-abscisic acid showed a rapid metabolism and excretion in urine with a maximum at 120 minutes whereas its glucuronide provided a maximum intensity later (serum at 120 minutes and urine at 240 minutes, **Figure 10**) maybe due to the glucuronide conjugation step.

Similarly, also methyl-dihydromyricetin trend suggested a rapid absorption showing a maximum excretion in urine at 120 minutes after bilberry and blueberry intake (**Table 2**). In this case, the absorption rate could depend on the kind and concentration of the precursors, analogously to different maximum levels found in serum as a function of diverse ingested dose of quercetin (64).

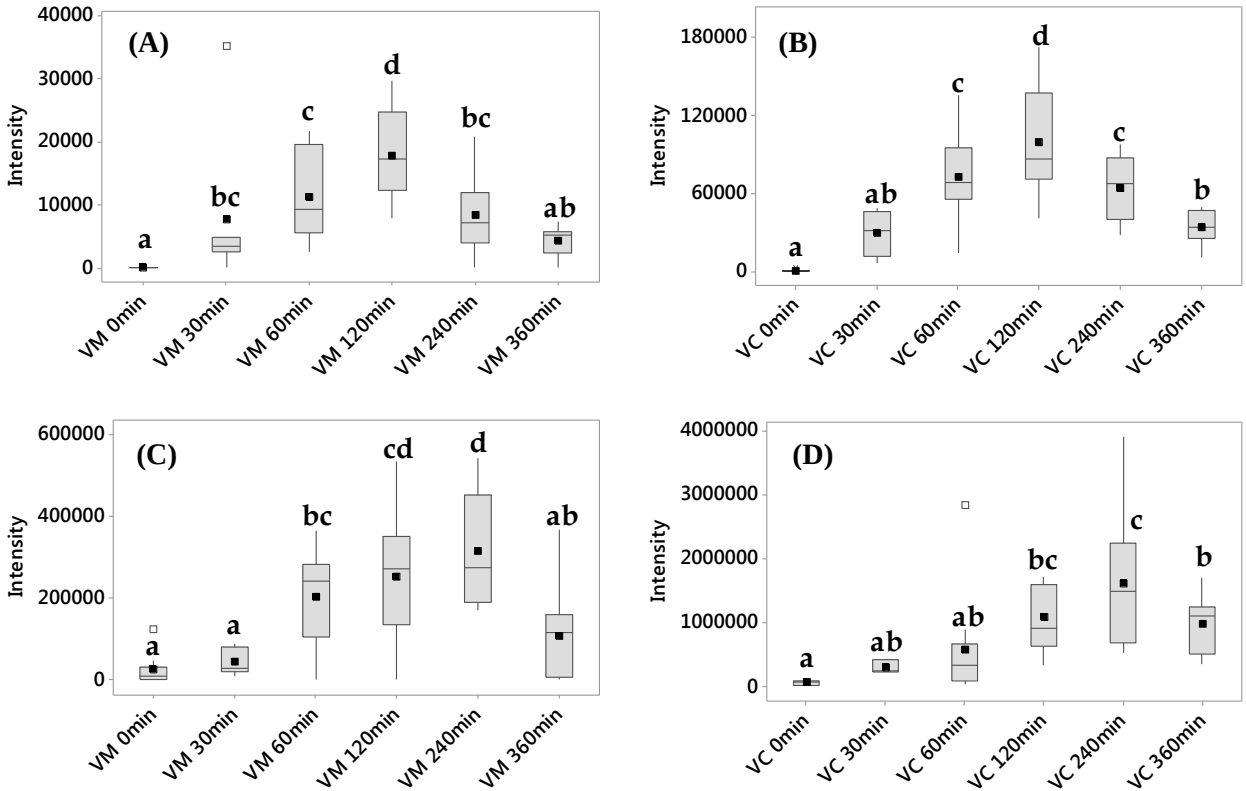

Figure 10. Box plot of intensities of metabolite putatively identified as hydroxy-abscisic acid glucuronide in serum (A-B) and urine (C-D) of volunteers at baseline and after the assumption of *V. myrtillus* (VM) and *V. corymbosum* (VC). Means that do not share a letter are significantly different according to the Fisher test ($P < 0.05$).

4. Conclusions

LC-HRMS and LC-HRMS/MS analysis, performed both in positive and negative modes, allowed to identify the most relevant serum and urinary polyphenol metabolites after the assumption of bilberry and blueberry supplements. In detail, compounds putatively attributed to conjugates of benzoic acids, hydroxyhippuric acids, cinnamic acids, phenylpropionic acids, phenylvaleric acids, phenylpentenoic acids and abscisic acid together with two anthocyanins, one flavonol metabolite and two catechol derivatives, were in-depth described.

Although *V. corymbosum* fruits were characterized by a lower concentration of anthocyanins and polyphenols in respect to *V. myrtillus* ones, some of the detected metabolites seem to be typical of blueberry polyphenol metabolism. In particular, the high abundance of phenolic acid (e.g. caffeoylquinic acids) and malvidin glycosides in *V. corymbosum* berries resulted in the preferential formation of hydroxy-dimethoxy benzoic and hydroxy-methoxycinnamic acid conjugated in serum or urine as a consequence of blueberry consumption.

On the contrary, metabolites ascribable to cyanidin-glycoside absorption, such as hydroxy-methoxy benzoic and hydroxyhippuric acid derivatives, together with native anthocyanin were found only as urinary biomarkers of *V. myrtillus* supplement assumption according to the high concentration of cyanidin and delphinidin glycosides reported for this berry species.

Interestingly, the application of the untargeted metabolomics approach allowed to identify compounds never reported as polyphenol metabolites after the ingestion of *V. myrtillus* fruits. In detail, some glucuronide and sulphate of hydroxy-(dihydroxyphenyl) valeric acid and hydroxyl-(hydroxyphenyl) pentenoic acid were evidenced with an increasing trend up to 6 hours after *V. myrtillus* supplement administration. These compounds

supposed to be flavanol monomer and oligomer metabolite could derive from the different proanthocyanidin profile of *V. myrtillus* in respect to *V. corymbosum* berries. Indeed, *V. corymbosum* berry was characterized only by B-type trimers, tetramers and pentamers whereas also A-type oligomers were found in *V. myrtillus* fruit.

In addition, the cinnamic acid conjugated characterized by a high methylation degree and observed for the first time as specific metabolites of bilberry assumption could derive from different polyphenol classes (anthocyanins, flavonol, flavanol and phenolic acids) after many conjugation steps according to their increasing trend 360 minutes after the assumption.

Interestingly, these new identified metabolites could be biologically active and might partially explain the healthy properties of *V. myrtillus* berries evidenced in clinical trials. For this reason, further studies focusing on the undoubted identification and accurate quantification of these compounds should be carried out together with *in vitro* studies in order to evaluate their potential efficiency against specific pathologies.

5. Contribution

Claudia Ancillotti performed the extraction of biofluids investigated in the metabolomics study as well as their LC-MS and LC-MS/MS analysis. Then, she performed the data processing and analysis using the dedicated software XCMS*plus*.

Acknowledgement

We thank volunteers for participating in the study. We also thank Nicola La Monica (Sciex, Framingham, MA, USA) for XCMS*plus* licence and Paul

Benton (Scripps Center for Metabolomics, The Scripps Research Institute) for the support in data elaboration.

Conflict of interest

The authors declare that they have no conflict of interest.

References

1. Bazzano LA, He J, Ogden LG, Loria CM, Vupputuri S, Myers L, et al. Fruit and vegetable intake and risk of cardiovascular disease in US adults: the first National Health and Nutrition Examination Survey Epidemiologic Follow-up Study. The American journal of clinical nutrition. 2002;76(1):93-9.

2. Gonzalez CA, Riboli E. Diet and cancer prevention: Contributions from the European Prospective Investigation into Cancer and Nutrition (EPIC) study. European Journal of Cancer. 2010;46(14):2555-62.

3. Hannan MT, Tucker KL, Dawson-Hughes B, Cupples LA, Felson DT, Kiel DP. Effect of dietary protein on bone loss in elderly men and women: the Framingham Osteoporosis Study. Journal of Bone and Mineral Research. 2000;15(12):2504-12.

4. Kobayashi M, Tsubono Y, Sasazuki S, Sasaki S, Tsugane S. Vegetables, fruit and risk of gastric cancer in Japan: A 10-year follow-up of the JPHC study Cohort I. International journal of cancer. 2002;102(1):39-44.

5. Vogtmann E, Xiang Y-B, Li H-L, Levitan EB, Yang G, Waterbor JW, et al. Fruit and vegetable intake and the risk of colorectal cancer: results from the Shanghai Men's Health Study. Cancer Causes & Control. 2013;24(11):1935-45.

6. Liu RH. Health-promoting components of fruits and vegetables in the diet. Advances in Nutrition: An International Review Journal. 2013;4(3):384S-92S.
7. Zhang H, Tsao R. Dietary polyphenols, oxidative stress and antioxidant and anti-inflammatory effects. Current Opinion in Food Science. 2016;8:33-42.
8. Manach C, Scalbert A, Morand C, Rémésy C, Jiménez L. Polyphenols: food sources and bioavailability. The American journal of clinical nutrition. 2004;79(5):727-47.
9. Patel S. Blueberry as functional food and dietary supplement: The natural way to ensure holistic health. Mediterranean Journal of Nutrition and Metabolism. 2014;7(2):133-43.
10. Aaby K, Grimmer S, Holtung L. Extraction of phenolic compounds from bilberry (Vaccinium myrtillus L.) press residue: Effects on phenolic composition and cell proliferation. LWT-Food Science and Technology. 2013;54(1):257-64.
11. Seeram NP, Adams LS, Hardy ML, Heber D. Total cranberry extract versus its phytochemical constituents: antiproliferative and synergistic effects against human tumor cell lines. Journal of agricultural and food chemistry. 2004;52(9):2512-7.
12. Yi W, Fischer J, Krewer G, Akoh CC. Phenolic compounds from blueberries can inhibit colon cancer cell proliferation and induce apoptosis. Journal of agricultural and food chemistry. 2005;53(18):7320-9.
13. Zhang Y, Seeram NP, Lee R, Feng L, Heber D. Isolation and identification of strawberry phenolics with antioxidant and human cancer cell antiproliferative properties. Journal of agricultural and food chemistry. 2008;56(3):670-5.
14. Thomasset SC, Berry DP, Garcea G, Marczylo T, Steward WP, Gescher AJ. Dietary polyphenolic phytochemicals—promising cancer

chemopreventive agents in humans? A review of their clinical properties. International Journal of Cancer. 2007;120(3):451-8.

15. Thomasset S, Berry DP, Cai H, West K, Marczylo TH, Marsden D, et al. Pilot study of oral anthocyanins for colorectal cancer chemoprevention. Cancer prevention research. 2009;2(7):625-33.

16. Lila MA, Burton-Freeman B, Grace M, Kalt W. Unraveling anthocyanin bioavailability for human health. Annual review of food science and technology. 2016;7:375-93.

17. Hollands W, Brett GM, Dainty JR, Teucher B, Kroon PA. Urinary excretion of strawberry anthocyanins is dose dependent for physiological oral doses of fresh fruit. Molecular nutrition & food research. 2008;52(10):1097-105.

18. Edirisinghe I, Banaszewski K, Cappozzo J, Sandhya K, Ellis CL, Tadapaneni R, et al. Strawberry anthocyanin and its association with postprandial inflammation and insulin. British journal of nutrition. 2011;106(6):913-22.

19. Mazza G, Kay CD, Cottrell T, Holub BJ. Absorption of anthocyanins from blueberries and serum antioxidant status in human subjects. Journal of agricultural and food chemistry. 2002;50(26):7731-7.

20. Kalt W, Liu Y, McDonald JE, Vinqvist-Tymchuk MR, Fillmore SA. Anthocyanin metabolites are abundant and persistent in human urine. Journal of agricultural and food chemistry. 2014;62(18):3926-34.

21. Kalt W, McDonald JE, Liu Y, Fillmore SA. Flavonoid Metabolites in Human Urine during Blueberry Anthocyanin Intake. Journal of Agricultural and Food Chemistry. 2017;65(8):1582-91.

22. McGhie TK, Ainge GD, Barnett LE, Cooney JM, Jensen DJ. Anthocyanin glycosides from berry fruit are absorbed and excreted unmetabolized by both humans and rats. Journal of Agricultural and Food Chemistry. 2003;51(16):4539-48.

23. Sakakibara H, Ogawa T, Koyanagi A, Kobayashi S, Goda T, Kumazawa S, et al. Distribution and excretion of bilberry anthocyanins in mice. Journal of agricultural and food chemistry. 2009;57(17):7681-6.

24. Cooke DN, Thomasset S, Boocock DJ, Schwarz M, Winterhalter P, Steward WP, et al. Development of analyses by high-performance liquid chromatography and liquid chromatography/tandem mass spectrometry of bilberry (Vaccinium myrtilus) anthocyanins in human plasma and urine. Journal of agricultural and food chemistry. 2006;54(19):7009-13.

25. Ichiyanagi T, Shida Y, Rahman MM, Hatano Y, Konishi T. Bioavailability and tissue distribution of anthocyanins in bilberry (Vaccinium myrtillus L.) extract in rats. Journal of agricultural and food chemistry. 2006;54(18):6578-87.

26. Felgines C, Talavera S, Texier O, Gil-Izquierdo A, Lamaison J-L, Remesy C. Blackberry anthocyanins are mainly recovered from urine as methylated and glucuronidated conjugates in humans. Journal of agricultural and food chemistry. 2005;53(20):7721-7.

27. Vitaglione P, Donnarumma G, Napolitano A, Galvano F, Gallo A, Scalfi L, et al. Protocatechuic acid is the major human metabolite of cyanidin-glucosides. The Journal of nutrition. 2007;137(9):2043-8.

28. Williamson G, Clifford MN. Colonic metabolites of berry polyphenols: the missing link to biological activity? British Journal of Nutrition. 2010;104(S3):S48-S66.

29. Bò CD, Ciappellano S, Klimis-Zacas D, Martini D, Gardana C, Riso P, et al. Anthocyanin absorption, metabolism, and distribution from a wild blueberry-enriched diet (Vaccinium angustifolium) Is affected by diet duration in the Sprague− Dawley rat. Journal of agricultural and food chemistry. 2009;58(4):2491-7.

30. Nurmi T, Mursu J, Heinonen M, Nurmi A, Hiltunen R, Voutilainen S. Metabolism of berry anthocyanins to phenolic acids in humans. Journal of agricultural and food chemistry. 2009;57(6):2274-81.

31. Feliciano RP, Istas G, Heiss C, Rodriguez-Mateos A. Plasma and urinary phenolic profiles after acute and repetitive intake of wild blueberry. Molecules. 2016;21(9):1120.

32. Rodriguez-Mateos A, Rendeiro C, Bergillos-Meca T, Tabatabaee S, George TW, Heiss C, et al. Intake and time dependence of blueberry flavonoid–induced improvements in vascular function: a randomized, controlled, double-blind, crossover intervention study with mechanistic insights into biological activity. The American journal of clinical nutrition. 2013;98(5):1179-91.

33. Katajamaa M, Orešič M. Data processing for mass spectrometry-based metabolomics. Journal of Chromatography A. 2007;1158(1):318-28.

34. Ancillotti C, Ciofi L, Rossini D, Chiuminatto U, Stahl-Zeng J, Orlandini S, et al. Liquid chromatographic/electrospray ionization quadrupole/time of flight tandem mass spectrometric study of polyphenolic composition of different Vaccinium berry species and their comparative evaluation. Analytical and bioanalytical chemistry. 2017;409(5):1347-68.

35. Dunn WB, Broadhurst D, Begley P, Zelena E, Francis-McIntyre S, Anderson N, et al. Procedures for large-scale metabolic profiling of serum and plasma using gas chromatography and liquid chromatography coupled to mass spectrometry. Nature protocols. 2011;6(7):1060.

36. Chambers MC, Maclean B, Burke R, Amodei D, Ruderman DL, Neumann S, et al. A cross-platform toolkit for mass spectrometry and proteomics. Nature biotechnology. 2012;30(10):918-20.

37. Gowda H, Ivanisevic J, Johnson CH, Kurczy ME, Benton HP, Rinehart D, et al. Interactive XCMS Online: simplifying advanced metabolomic data processing and subsequent statistical analyses. Analytical chemistry. 2014;86(14):6931-9.

38. Sumner LW, Amberg A, Barrett D, Beale MH, Beger R, Daykin CA, et al. Proposed minimum reporting standards for chemical analysis. Metabolomics. 2007;3(3):211-21.

39. Barnes JS, Nguyen HP, Shen S, Schug KA. General method for extraction of blueberry anthocyanins and identification using high performance liquid chromatography–electrospray ionization-ion trap-time of flight-mass spectrometry. Journal of Chromatography A. 2009;1216(23):4728-35.

40. Ancillotti C, Ciofi L, Pucci D, Sagona E, Giordani E, Biricolti S, et al. Polyphenolic profiles and antioxidant and antiradical activity of Italian berries from Vaccinium myrtillus L. and Vaccinium uliginosum L. subsp. gaultherioides (Bigelow) SB Young. Food chemistry. 2016;204:176-84.

41. Može Š, Polak T, Gašperlin L, Koron D, Vanzo A, Poklar Ulrih N, et al. Phenolics in Slovenian Bilberries (Vaccinium myrtillus L.) and Blueberries (Vaccinium corymbosum L.). Journal of Agricultural and Food Chemistry. 2011;59(13):6998-7004.

42. Wu X, Cao G, Prior RL. Absorption and metabolism of anthocyanins in elderly women after consumption of elderberry or blueberry. The Journal of nutrition. 2002;132(7):1865-71.

43. Gu J, Zhong D, Chen X. Analysis of O-glucuronide conjugates in urine by electrospray ion trap mass spectrometry. Fresenius' journal of analytical chemistry. 1999;365(6):553-8.

44. Grieman M, Greaves J, Saltzman E. A method for analysis of vanillic acid in polar ice cores. Climate of the Past. 2015;11(2):227.

45. Ulaszewska MM, Trost K, Stanstrup J, Tuohy KM, Franceschi P, Chong MF-F, et al. Urinary metabolomic profiling to identify biomarkers of a flavonoid-rich and flavonoid-poor fruits and vegetables diet in adults: the FLAVURS trial. Metabolomics. 2016;12(2):32.

46. Pimpão RC, Dew T, Figueira ME, McDougall GJ, Stewart D, Ferreira RB, et al. Urinary metabolite profiling identifies novel colonic metabolites and conjugates of phenolics in healthy volunteers. Molecular nutrition & food research. 2014;58(7):1414-25.

47. Cuparencu CS, Andersen M-BS, Gürdeniz G, Schou SS, Mortensen MW, Raben A, et al. Identification of urinary biomarkers after consumption of sea buckthorn and strawberry, by untargeted LC–MS metabolomics: a meal study in adult men. Metabolomics. 2016;12(2):31.

48. Jaganath IB, Jaganath IB, Mullen W, Edwards CA, Crozier A. The relative contribution of the small and large intestine to the absorption and metabolism of rutin in man. Free radical research. 2006;40(10):1035-46.

49. Edmands WM, Ferrari P, Rothwell JA, Rinaldi S, Slimani N, Barupal DK, et al. Polyphenol metabolome in human urine and its association with intake of polyphenol-rich foods across European countries. The American journal of clinical nutrition. 2015;102(4):905-13.

50. Ou K, Gu L. Absorption and metabolism of proanthocyanidins. Journal of Functional Foods. 2014;7:43-53.

51. Chandrasekara A, Shahidi F. Determination of antioxidant activity in free and hydrolyzed fractions of millet grains and characterization of their phenolic profiles by HPLC-DAD-ESI-MSn. Journal of Functional Foods. 2011;3(3):144-58.

52. Oszmiański J, Kolniak-Ostek J, Wojdyło A. Application of ultra-performance liquid chromatography-photodiode detector-quadrupole/time of flight-mass spectrometry (UPLC-PDA-Q/TOF-MS) method for the characterization of phenolic compounds of Lepidium sativum L. sprouts. European Food Research and Technology. 2013;236(4):699-706.

53. van der Hooft JJ, de Vos RC, Mihaleva V, Bino RJ, Ridder L, de Roo N, et al. Structural elucidation and quantification of phenolic conjugates present in human urine after tea intake. Analytical chemistry. 2012;84(16):7263-71.

54. Ordaz-Ortiz JJ, Foukaraki S, Terry LA. Assessing temporal flux of plant hormones in stored processing potatoes using high definition accurate mass spectrometry. 2015;2:15002.

55. Lacampagne S, Gagné S, Gény L. Involvement of abscisic acid in controlling the proanthocyanidin biosynthesis pathway in grape skin: new elements regarding the regulation of tannin composition and leucoanthocyanidin reductase (LAR) and anthocyanidin reductase (ANR) activities and expression. Journal of Plant Growth Regulation. 2010;29(1):81-90.

56. Mullen W, Edwards CA, Crozier A. Absorption, excretion and metabolite profiling of methyl-, glucuronyl-, glucosyl-and sulpho-conjugates of quercetin in human plasma and urine after ingestion of onions. British Journal of Nutrition. 2006;96(1):107-16.

57. Passamonti S, Vrhovsek U, Vanzo A, Mattivi F. The stomach as a site for anthocyanins absorption from food11In memory of Livia Mattivi, who died on 15th March 2003. FEBS Letters. 2003;544(1):210-3.

58. Hidalgo M, Oruna-Concha MJ, Kolida S, Walton GE, Kallithraka S, Spencer JPE, et al. Metabolism of Anthocyanins by Human Gut Microflora and Their Influence on Gut Bacterial Growth. Journal of Agricultural and Food Chemistry. 2012;60(15):3882-90.

59. de Ferrars RM, Czank C, Saha S, Needs PW, Zhang Q, Raheem KS, et al. Methods for isolating, identifying, and quantifying anthocyanin metabolites in clinical samples. Analytical chemistry. 2014;86(20):10052-8.

60. Del Rio D, Rodriguez-Mateos A, Spencer JP, Tognolini M, Borges G, Crozier A. Dietary (poly) phenolics in human health: structures, bioavailability, and evidence of protective effects against chronic diseases. Antioxidants & redox signaling. 2013;18(14):1818-92.

61. Stalmach A, Mullen W, Barron D, Uchida K, Yokota T, Cavin C, et al. Metabolite profiling of hydroxycinnamate derivatives in plasma and urine after the ingestion of coffee by humans: identification of biomarkers of coffee consumption. Drug Metabolism and Disposition. 2009;37(8):1749-58.

62. Aura A-M, Mattila I, Seppänen-Laakso T, Miettinen J, Oksman-Caldentey K-M, Orešič M. Microbial metabolism of catechin stereoisomers by human faecal microbiota: Comparison of targeted analysis and a non-targeted metabolomics method. Phytochemistry Letters. 2008;1(1):18-22.

63. Stoupi S, Williamson G, Drynan JW, Barron D, Clifford MN. A comparison of the in vitro biotransformation of (–)-epicatechin and procyanidin B2 by human faecal microbiota. Molecular nutrition & food research. 2010;54(6):747-59.

64. Erlund I, Kosonen T, Alfthan G, Mäenpää J, Perttunen K, Kenraali J, et al. Pharmacokinetics of quercetin from quercetin aglycone and rutin in healthy volunteers. European journal of clinical pharmacology. 2000;56(8):545-53.

Supplementary material

Table S1 – Groups used for statistical comparison both for urine and serum samples.

Group Name	Sampling Time	Berry type
VM 0min	Baseline	*V. myrtillus*
VM 30min	After 30 minutes from assumption	*V. myrtillus*
VM 60min	After 60 minutes from assumption	*V. myrtillus*
VM 120min	After 120 minutes from assumption	*V. myrtillus*
VM 240min	After 240 minutes from assumption	*V. myrtillus*
VM 360min	After 360 minutes from assumption	*V. myrtillus*
VC 0min	Baseline	*V. corymbosum*
VC 30min	After 30 minutes from assumption	*V. corymbosum*
VC 60min	After 60 minutes from assumption	*V. corymbosum*
VC 120min	After 120 minutes from assumption	*V. corymbosum*
VC 240min	After 240 minutes from assumption	*V. corymbosum*
VC 360min	After 360 minutes from assumption	*V. corymbosum*

Chapter 6

Conclusions

In the work comprised in this PhD thesis, LC-MS and LC-MS/MS methods for the analysis of polyphenols in different matrix (i.e. plant tissues, fruits and biofluids) have been developed and applied using both targeted and untargeted metabolomics approaches.

Firstly, the targeted analysis of polyphenols in vegetal matrixes confirmed that the influence of genetic and environmental factors on plant polyphenol biosynthesis can result in an important tool both for environmental and food sciences (Chapters 2 and 3).

In detail, Chapter 2 described a study in which a set of selected sugars and polyphenols were investigated in the plant model *Nicotiana langsdorfii*, wild type and genetically modified, after the exposure to water deficit and heat stress. The insertion of *rolC* and above all *gr* genes induced an upregulation of the phenolic secondary metabolism that may contribute to a better plant response against free radicals produced in consequence of exposure to abiotic stress. Actually, *gr* and *rolC* plants were more tolerant than wild-type organisms to water and heat stress. Interestingly, the metabolic shift of polyphenols belonging to shikimate pathway resulted more informative in respect to the concentration of total polyphenols of the stress condition suffered by the plant, particularly for the long-term effects due to heat shock treatment. This results confirmed the role of metabolomics, and especially of metabolomics analysis of phenols, to understand some important effects of plant exposure to stress factors.

Then, Chapter 3 described the development and application of LC-MS/MS targeted method for polyphenol analysis in food science. In detail, the polyphenolic composition of *V. myrtillus* (bilberry) and *V. uliginosum* L. subsp. *gaultherioides* (false bilberry) fruits was investigated in order to

quantify the most abundant anthocyanins and polyphenols of these two berries species. The importance of this research was related the high nutraceutical value of *V. myrtillus* fruits considered as a functional food and used for production of many transformed product, such as juice and supplement. On the contrary, the lack of information about *V. gaultherioides* polyphenolic profile, as well as the very similar phenotypes of these two species and the coexistence in the same growing area, have made the polyphenolic investigation essential for food quality assessment. An interesting metabolic profile complementarity between *V. myrtillus* and *V. gaultherioides* fruits have been highlighted. Therefore, the very different concentration of the most abundant anthocyanins and polyphenols in the two berry species suggested the possibility of using the ratio of some specific polyphenol concentration as diagnostic ratio. This feature could make feasible the chemotaxonomic discrimination of *V. myrtillus* and *V. gaultherioides* species, with the purpose of discovering possible contaminations of the bilberry commercial chain by ‘‘false bilberry”.

In Chapters 4 and 5, the untargeted metabolomics approach was applied to food science and clinical research in order to perform a comprehensive investigation of polyphenolic profile of fruits and biological fluids, respectively.

Firstly, LC-ESI-TOF and LC-ESI-Q/TOF analysis, performed both in positive and negative modes, allowed to obtain a comprehensive picture of the polyphenolic composition of *V. myrtillus*, *V. corymbosum*, and *V. gaultherioides* berries (Chapter 4). The high potentiality of untargeted approach coupled with the use of a high resolution mass spectrometer resulted in the identification of more than two hundreds of polyphenols, some of which reported for the first time in the investigated *Vaccinium* berries. The identified polyphenols belong to different classes, i.e. anthocyanins, flavonol, flavanol and phenolic acids, and for some of these a

high species-specificity was observed. In fact, anthocyanins glucuronides, dihexosides and coumaroyl-hexosides were highly related to *V. myrtillus* fruits whereas acetyl and malonyl derivatives were more representative of *V. corymbosum* berries. Finally, *V. gaultherioides* fruits, even though generally poorer in the number of identified anthocyanins, were characterized by xyloside derivatives of petunidin, peonidin and malvidin. Analogously, the identified flavonols, flavanols and phenolic acids, detected under negative ionization exhibited a specific relation with the three *Vaccinium* species. For example, flavonol acetyl-hexosides, flavonol aldopentosides, a number of B-type proanthocyanidins and some chlorogenic acids was highly representative of *V. corymbosum* berries.
The comprehensive investigation performed, which evidenced phenolic metabolites exclusively detected in one species or characterized by extremely different intensities in the three berries, can be useful for future developments of methods aiming at evaluating the quality of *Vaccinium* berry transformation products and to avoid frauds. These products, in fact, are not only fruit juices or jams that are not subjected to any particular regulation concerning their phenolic content but also supplements or actual drugs, which must conversely respect what is written in the label, both in terms of plant material used for its preparation and amount of active ingredients contained in the product.

Finally, LC-HRMS and LC-HRMS/MS analysis, performed both in positive and negative modes, allowed to identify the most relevant serum and urinary polyphenol metabolites after the assumption of *V. myrtillus* and *V. corymbosum* supplements. This study represents the first untargeted metabolomics analysis of biofluids after bilberry and blueberry assumption. In detail, compounds putatively attributed to conjugates of benzoic acids, hydroxyhippuric acids, cinnamic acids, phenylpropionic acids, phenylvaleric acids, phenylpentenoic acids and abscisic acid together with

two native anthocyanins, one flavonol metabolite and two catechol derivatives, were in-depth characterized (Chapter 5). Moreover, some specific biomarkers of *V. corymbosum* and *V. myrtillus* assumption were evidenced. Indeed, the much higher concentration of cyanidin and delphinidin glycoside in bilberry resulted in specific metabolites, such as hydroxy-methoxy benzoic acid and hydroxyhippuric acid derivatives. Conversely, the exclusive presence or greater abundance of hydroxy-dimethoxy benzoic and hydroxy-methoxy cinnamic acid conjugated was observed in serum or urine after blueberry assumption due to its high content of phenolic acids and malvidin glycosides.

Interestingly, the application of the untargeted metabolomics approach allowed to identify compounds never reported as polyphenol metabolites after the ingestion of *V. myrtillus* fruits. In detail, some glucuronide and sulphate of hydroxy-(dihydroxyphenyl) valeric acid and hydroxyl-(hydroxyphenyl) pentenoic acid were evidenced with an increasing trend up to 6 hours after *V. myrtillus* supplement administration. These compounds supposed to be flavanol monomer and oligomer metabolite could derive from the different proanthocyanidin profile of *V. myrtillus* in respect to *V. corymbosum* berries. In addition, the cinnamic acid conjugated characterized by a high methylation degree and observed for the first time as specific metabolites of bilberry assumption could derive from different polyphenol classes (anthocyanins, flavonol, flavanol and phenolic acids) after many conjugation steps according to their increasing trend 360 minutes after the assumption.

These new identified metabolites could be biologically active and might partially explain the healthy properties of *V. myrtillus* berries evidenced in clinical trials. For this reason, further studies focusing on the undoubted identification and accurate quantification of these compounds should be carried out together with *in vitro* studies in order to evaluate their potential efficiency against specific pathologies.

Concluding the power of LC-MS technique was demonstrated through the development of targeted and untargeted methods useful in different field of application. The two approaches have shown different advantages that are mainly represented by the high sensitivity and robustness of targeted LC-MS/MS method and the possibility to discover new metabolites with the untargeted LC-HRMS platform.